eman ta zabal zazu
Universidad del País Vasco
Euskal Herriko Unibertsitatea

DESIGN AND VALIDATION OF DECISION AND CONTROL SYSTEMS IN AUTOMATED DRIVING

JOSE ANGEL MATUTE PEASPAN

2021

DESIGN AND VALIDATION OF DECISION AND CONTROL SYSTEMS IN AUTOMATED DRIVING

JOSE ANGEL MATUTE PEASPAN

2021

Thesis Advisors:
Asier Zubizarreta, Ph.D., UPV/EHU
Joshue Perez, Ph.D., Tecnalia RI

To Cecilia and Miriam,
my beloved mothers

AGRADECIMIENTO

Durante el desarrollo de esta Tesis Doctoral, me dí cuenta que alcanzar terminarla resultó ser similar al proceso de construcción de una *casa* propia (metafóricamente hablando, por supuesto). Construir una *casa* propia, no es lo mismo que construir cualquier *casa*. Al ser propia, usualmente surgen indecisiones en busqueda del perfeccionamiento (¿es el *terreno* adecuado para *construir*? ¿la ténica que pienso utilizar es la correcta? ¿Estaré *construyendo* bien? ¿podría vivir en ella el resto de mi vida?). Sin embargo, también me di cuenta que al estar rodeado de buenos *asesores*, la vacilación se convierte en certidumbre y la tarea se simplifica enormemente. La *casa* que he logrado construir y que les presento en este libro, ha sido posible gracias a distintos *asesores* que de una u otra manera han contribuído a su elaboración, de la forma en que describo a continuación:

A mis tutores (*Constructores* expertos y propietarios de *casas* modelo): Asier Zubizarreta y Joshué Pérez. Ustedes me ayudaron a decidir el tipo de *casa* que quería, a aterrizar mis pensamientos e inspiraciones, y definir una estrategia clara para evitar problemas. Me siento muy afortunado de haberles conocido y trabajar junto a ustedes.

A los Directores de Proyecto (Directores de obras): Lucia Isasi y Jesus Murgoitio. Ustedes me ayudaron a tener claros los plazos de ejecución, las metas y expectativas del proyecto. He valorado mucho sus consejos y experiencia.

A mis amigos y compañeros (Los buenos técnicos): Leonardo Gonzalez, Ray Lattarulo, Mauricio Marcano, Sergio Diaz, Gerardo Fernandez, Joseba Sarabia, Carlos Hidalgo, Myriam Vaca y Pedro Lopez. Ustedes también me asesoraron directa o indirectamente, fue de quienes más aprendí, y he aplicado aquí muchas de las técnicas que utilizan (o utilizaron) para *construir* sus respectivas *casas*.

A mi familia (Agentes motivadores del proceso de fabricación): Michiko Horie, Miriam Peaspan y Noel Sulbaran, quienes empujaron mi espíritu para seguir *construyendo*, sobretodo cuando el sol estaba en lo más alto.

Finalmente, como toda buena casa merece un buen perro, agradezco a Mambo quien fielmente estuvo a mi lado durante (todos) los duros días de *construcción*.

DESIGN AND VALIDATION OF DECISION AND CONTROL SYSTEMS IN AUTOMATED DRIVING

Abstract

by Jose Angel Matute Peaspan, Ph.D.
Universidad del Pais Vasco | Euskal Herriko Unibertsitatea
2021

Thesis Advisors:
Asier Zubizarreta, Ph.D.
Joshue Perez, Ph.D.

Nowadays specific solutions for high driving automation in urban areas require low vehicle speed with dedicated infrastructure. Therefore, new types of mobility vehicles are foreseen for advanced urban applications, from city cars as smaller mobility vehicles to city buses with various types of automated functionalities, capable to be implemented regardless of the driving scenario (e.g. confined, dedicated, and open roads).
Currently, the most commercially labored automated driving functionalities are represented by Advanced Driving Assistance Systems (ADAS), which not only enable automated features that make possible a more efficient and easier driving operation for monotonous tasks (e.g. maintain the desired speed on highways), but also include warning and response features that positively impact on the safety of road actors. In this sense, the improvement of current ADAS allows the development of Automated Driving Systems (ADS) for even safer roads, more productive businesses, and more environmentally efficient driving.
One relevant aspect of actual ADAS is the capability to efficiently perform specific automated driving tasks in an isolated way. On one hand, Automatic Emergency Braking (AEB), Cruise Control (CC), and Adaptive CC (ACC) are some driving features that intervene in the longitudinal vehicle motion which have been successfully tested in real environments. In the intervention on the lateral vehicle motion, the Lane-Keeping Assist (LKA) is an essential feature. On other hand, these systems operate under a restricted Operational Design Domain (ODD), most of them designed for highways at speeds higher than 60 km/h, making these driving features unsuitable for urban and suburban applications. Consequently, the combination of previous ADAS may represent a good starting point to develop more complex systems enhancing their current ODD. Also, scalability is a key aspect, which allows covering a broad range of vehicle platforms, from two-seated cars up to full-size transit buses.
Considering the mentioned premises, this Ph.D. Thesis employs a system development life cycle procedure to design, verify, code, validate and implement ADS considering crucial

aspects, such as real-time capability, robustness, operating range, and easy parameter tuning. To develop the contributions, a study of the current state of the art in validation testing, vehicle motion planning and control, and Dynamic Driving Task (DDT) fallback strategies is carried out.

From an ADS development and testing review, it is noted that the interest in ADS validation procedures based on trustworthy vehicle simulation models is a trend that grows and spreads continuously both in the automotive industry and the academy. Additionally, as safety and comfortability are concepts of opposite nature, unbalanced strategies may lead to infeasible solutions in trajectory planning and tracking performances. Moreover, the automated achievement of a minimal risk condition after relevant-performance failures is either partially or entirely ignored in current real-world applications, and fail-operational systems must be developed relying both on hardware and software redundancies.

Taking into account the aforementioned issues, in this Ph.D. Thesis, three main contributions are proposed. First, a two-step method is presented to address the validation of both simulation vehicle models and ADS. Second, novel model-based predictive formulations are implemented to improve safety and comfort in both trajectory planning and tracking processes. Finally, a fallback strategy is proposed, based on dead-reckoning to minimize risk conditions, to improve safety in urban settings in case of malfunction. For the aforementioned contributions, a Renault Twizy and an Irizar i2e bus are selected as research platforms in both virtual and real testing environments.

To demonstrate the effectiveness of the proposed contributions a total of six case studies are introduced in both virtual and real scenarios, validating the approaches. First, to illustrate the application of the two-step validation methodology proposed, an automated Renault Twizy is employed to obtain a vehicle simulation model and tune a Traffic Jam Assist (TJA) driving functionality as a Low-Speed High Automation (LSHA) development. Second, to illustrate the scalability of the previous validation methodology an automated Irizar i2e is used to verify and validate a TJA considering hilly roads for city-urban LSHA application. Third, the proposed trajectory planning approach is presented using a city-urban bus considering the complexity when maneuvering under narrow and challenging roads due to its large dimensions. Fourth, the proposed model-blending procedure based on lateral accelerations is verified by employing model predictive control and assessing the improvement of trajectory tracking. Fifth, the proposed algorithms for object and event detection and response are verified considering traffic-lights and dynamic objects located along the driving path. Sixth, the proposed fail-operational control architecture and decision-based dynamic driving task fallback are evaluated under three different scenarios to achieve a minimal risk condition after a relevant-performance positioning failure.

As the contributions of this Ph.D. Thesis provide verified and validated systems to drive and follow traffic flows in urban environments, future developments must enhance the current ODD, including more conditional and highly automated driving features such as lane-change and overtaking maneuvers, accurate docking or parking, and lane-center positioning redundance.

Summary

Below is a summary of this Ph.D. Thesis in Spanish.

En la última década ha surgido una tendencia creciente hacia la automatización de los vehículos, generando un cambio significativo en la movilidad, que afectará profundamente el modo de vida de las personas, la logística de mercancías y otros sectores dependientes del transporte. El desarrollo de nuevas tecnologías pronto tendrá un gran impacto en los servicios de transporte, afectando notablemente el entorno económico, natural y social.

En el desarrollo de la conducción automatizada en entornos estructurados, la seguridad y el confort, como parte de las nuevas funcionalidades de la conducción, aún no se describen de forma estandarizada [15]. Dado que los métodos de prueba utilizan cada vez más las técnicas de simulación, los desarrollos existentes deben adaptarse a este proceso. Por ejemplo, dado que las tecnologías de seguimiento de trayectorias son habilitadores esenciales, se deben aplicar verificaciones exhaustivas en aplicaciones relacionadas como el control de movimiento del vehículo y la estimación de parámetros. Además, las tecnologías en el vehículo deben ser lo suficientemente robustas para cumplir con los requisitos de seguridad, mejorando la redundancia y respaldar una operación a prueba de fallos.

Considerando las premisas mencionadas, esta Tesis Doctoral tiene como objetivo el diseño y la implementación de un marco para lograr Sistemas de Conducción Automatizados (ADS) considerando aspectos cruciales, como la ejecución en tiempo real, la robustez, el rango operativo y el ajuste sencillo de parámetros. Además, la escalabilidad es un aspecto clave, que permite cubrir una amplia gama de plataformas de vehículos, desde automóviles de dos asientos hasta autobuses de tránsito de tamaño completo, como los que se muestran en la Figura 1.1. Para desarrollar las aportaciones relacionadas con este trabajo, se lleva a cabo un estudio del estado del arte actual en tecnologías de alta automatización de conducción. Luego, se propone un método de dos pasos que aborda la validación de ambos modelos de vehículos de simulación y ADS. Se introducen nuevas formulaciones predictivas basadas en modelos para mejorar la seguridad y la confort en el proceso de seguimiento de trayectorias. Por último, se evalúan escenarios de mal funcionamiento para mejorar la seguridad en entornos urbanos, proponiendo una estrategia alternativa de estimación de posicionamiento para minimizar las condiciones de riesgo.

Motivación y Antecedentes

En los últimos años, el interés en los vehículos automatizados y sus tecnologías relacionadas se ha disparado debido a las múltiples ventajas que brindan en términos de seguridad, medio ambiente y economía.

En cuanto a *seguridad*, aproximadamente 1,35 millones de personas fallecen cada año en accidentes de tráfico en todo el mundo, y entre 20 y 50 millones más sufren lesiones no mortales, muchas de las cuales incurren en una discapacidad según la Organización Mundial de la Salud [16]. En entornos urbanos, entre 8 de cada 10 personas atropelladas son ciclistas y otros usuarios vulnerables, según la base de datos internacional de accidentes y tráfico vial [17]. Un alto porcentaje de estos accidentes, el 94 %, ocurren debido a la incidencia de factores humanos, como la mala toma de decisiones, el incumplimiento de las normas de circulación, una conducción inadecuada y el mal comportamiento de otros vehículos [18]. Así, los vehículos automatizados presentan una solución al problema del transporte en entornos urbanos, reduciendo los accidentes causados por el error del conductor como fallo final en la cadena causal de eventos.

Por otro lado, *el cambio climático y la degradación ambiental* son una amenaza existencial, y se espera una economía moderna, eficiente en el uso de recursos y competitiva sin emisiones contaminantes para 2050. El Acuerdo Verde de la Comisión Europea [19] está abordando las emisiones, congestión urbana y mejora del transporte público. Para 2025, se necesitarán alrededor de 1 millón de estaciones públicas de recarga y reabastecimiento de combustible para los 13 millones de vehículos de cero y bajas emisiones que se esperan en las carreteras europeas. Un cambio a vehículos automatizados también podría provocar el cambio a vehículos eléctricos, ya que los dispositivos de actuación (sistemas *drive-by-wire*) pueden ser controlados centralizadamente, y hace que el sistema sea más eficiente para permitir el uso de Unidades de Control Electrónico (ECU) [20]. La implementación amplia de sistemas de gestión de tráfico inteligente y movilidad automatizada puede ser un punto de inflexión para disminuir el consumo de energía y las emisiones contaminantes [21], fomentando la eficiencia del sistema de transporte y la reducción del tiempo en el tráfico congestionado [15].

Finalmente, los ADS pueden generar amplios *beneficios macroeconómicos* tanto en la creación de empleo como en los operadores. También permitirán eliminar las barreras para los no conductores en el mercado laboral e impulsar su participación [22]. Surgirían nuevas oportunidades laborales en varias áreas de ingeniería e investigación como diseño de vehículos, fabricación, análisis de datos, mantenimiento de vehículos, diseño de redes, redimensionamiento de vehículos, redireccionamiento de servicios de rutas de pasajeros convencionales, entre otros [23, 24]. Se espera que los beneficios en la reducción de los costos de operación actuales oscilen entre 50-60 % [25], además de ahorrar costos en la demanda de transporte relacionada a niños y ancianos [26]. A diferencia de los vehículos privados automatizados, la movilidad automatizada para colectivos influiría positivamente en el consumo energético [23].

Lograr los beneficios antes mencionados requiere más desarrollos en la tecnología de conducción automatizada, que en [1] se describe detalladamente como *el hardware y el software que pueden realizar colectivamente toda la Tarea Dinámica de Conducción (DDT) de forma sostenida, independientemente de si se limita o no a un Diseño de Dominio Operacional (ODD) específico.* El DDT cubre el control de movimiento longitudinal y lateral del vehículo, así como también la Detección y Respuesta de Objetos y Eventos (OEDR). Las definiciones detalladas para los niveles de automatización SAE son en el contexto de los vehículos de motor y su funcionamiento en las carreteras, que van desde la ausencia (nivel 0) hasta la automatización total (nivel 5) de conducción.

Objetivos

En base a la necesidad de desarrollar la tecnología de conducción automatizada, esta Tesis Doctoral tiene como objetivo un desarrollo de ciclo de vida hacia sistemas de conducción altamente automatizados para aplicaciones urbanas, lo que contribuye al desarrollo de una arquitectura de control escalable que abarca desde pequeños turismos individuales hasta vehículos comerciales pesados.

El objetivo principal de esta Tesis Doctoral debe lograrse mediante los siguientes objetivos parciales:

- Desarrollo de una metodología de validación para modelos de vehículos y ADS que complementa las pruebas de pista con simulaciones, asegurando plataformas de prueba virtuales confiables para impulsar el desarrollo de ADS en escenarios urbanos.

- Diseño y validación de formulaciones de Control Predictivo basado en Modelo (MPC) para asegurar el desempeño deseado en términos de seguimiento de trayectorias y velocidad, considerando las especificaciones contrapuestas de seguridad y confort.

- Concepción de una estrategia de toma de decisiones para que el ADS logre una condición de riesgo mínimo después de que ocurra un fallo relevante del sistema para el desempeño de la DDT.

Organización del Manuscrito

Para desarrollar los objetivos mencionados, esta Tesis Doctoral está estructurada en 6 capítulos. A continuación se detallará brevemente el contenido de cada uno.

Capítulo 1. Introducción

En este capítulo se detalla la necesidad de impulsar la automatización, realizando una descripción histórica de las soluciones propuestas, y analizando los desafíos y aplicaciones. En primer lugar, se definen los objetivos y contribuciones de esta Tesis Doctoral. En segundo lugar, se presenta la organización del manuscrito junto con una breve descripción de cada capítulo. Finalmente, se muestra una lista con las publicaciones derivadas de esta Tesis Doctoral.

Capítulo 2. Estado del arte

En este capítulo, se detallan los antecedentes de la conducción automatizada y los trabajos relacionados, divididos principalmente en tres áreas principales. En primer lugar, se presenta la revisión de los métodos actuales de verificación y validación para modelos de simulación de vehículos y ADS. En segundo lugar, se ofrece una revisión de las técnicas de seguimiento de trayectorias, que detalla los diferentes enfoques utilizados en la literatura y compara su desempeño para aplicaciones de conducción automatizada. Por último, se presenta un estudio de las estrategias actuales de toma de decisiones para lograr sistemas operativos a prueba de fallos en la conducción altamente automatizada.

Se observa que el interés en los procedimientos de validación de ADS basados en modelos de simulación de vehículos confiables es una tendencia que crece y se extiende continuamente tanto en la industria automotriz como en la academia. Además, como la seguridad y el confort son conceptos de naturaleza opuesta, estrategias desequilibradas pueden conducir a soluciones inviables en el rendimiento del seguimiento de trayectorias, siendo este el principal problema para ADS cuando se consideran aplicaciones urbanas. Además, la eficiencia y la confiabilidad en ADS se ignoran parcial o totalmente en las aplicaciones actuales del mundo real, donde las soluciones a prueba de fallos no son suficientes y los sistemas operativos deben desarrollarse basándose tanto en redundancias de hardware como de software. En base a esta problemática, se introducen las tres aportaciones principales de la tesis, que se analizarán en los capítulos siguientes.

Capítulo 3. Validación en conducción automatizada

En este capítulo, se presentan las técnicas de obtención de modelos de vehículos que pueden ser usados tanto para sistemas de seguimiento de trayectorias como para plataformas de prueba virtuales. Cuanto más precisos y fiables sean los modelos de vehículos, más se podrá reducir el número de pruebas en la vida real. En este sentido, se introduce un método de validación de dos pasos. En primer lugar, un conjunto de pruebas en lazo abierto intenta ajustar los modelos de simulación utilizando datos experimentales. A diferencia de otras aproximaciones, la propuesta de esta tesis incluye la dinámica de los dispositivos de actuación requeridos para la automatización de vehículos. En segundo lugar, se definen un conjunto de pruebas en lazo cerrado para validar la seguridad técnica del sistema de conducción automatizado seleccionado basado en planes de prueba, mejorando también la respuesta dinámica del vehículo. Para ilustrar la metodología, se proponen casos prácticos utilizando dos vehículos automatizados: un Renault Twizy y un autobús Irizar i2e. En el primer paso, se modela el comportamiento del pedal de freno y los actuadores del volante, así como la dinámica longitudinal y capacidad de giro del vehículo. Luego, en un segundo paso, se valida un sistema automatizado para la asistencia en atascos.

El procedimiento de validación propuesto permite ajustar plataformas de prueba simuladas confiables y estrategias de conducción automatizadas en entornos de simulación, reduciendo el tiempo de desarrollo y la necesidad de pruebas reales. Los algoritmos ADS empleados para obtener resultados de verificación y validación presentados en este capítulo se describen detalladamente en el Capítulo 4. Además, el procedimiento propuesto se evalúa considerando escenarios y casos de uso de conducción automatizada sin fallos, como una práctica estandarizada presentada en la normativa ISO/PAS 21448. Sin embargo, la inyección de fallos eléctricas/electrónicas aún se consideraría en la fase de desarrollo mediante simulaciones, considerando el proceso de verificación de seguridad mencionado en la normativa ISO 26262. La evaluación sistemas de respaldo y estrategias de decisión en caso de fallo es un aspecto que se trata en el Capítulo 5.

Capítulo 4. Seguridad y confort en el control de movimiento

En este capítulo, se presentan técnicas de seguimiento de trayectorias para un control de movimiento del vehículo preciso y cómodo. La precisión suele estar relacionada con la velocidad, la posición y la orientación del vehículo. Por otro lado, el confort se asocia comúnmente con la aceleración y *jerk* tanto en los ejes laterales como longitudinales del

vehículo. La naturaleza opuesta de la seguridad y el confort en la conducción automatizada requiere de un análisis exhaustivo para concebir un control de movimiento del vehículo adecuado. Las formulaciones de MPC se emplean principalmente para contrastar este tipo de enfoques.

Se proponen en tres casos de estudio para la planificación y seguimiento de trayectorias utilizando un autobús que circula a varias velocidades en una ruta con diferentes curvaturas. En primer lugar, el enfoque de planificación de trayectorias propuesto se presenta utilizando un autobús urbano en el que hay que tener en cuenta la complejidad al maniobrar en carreteras estrechas y desafiantes debido a sus grandes dimensiones. En segundo lugar, se propone y testea una estrategia MPC que usa una combinación de modelos en base a la aceleración lateral. En tercer lugar, los algoritmos propuestos para la detección y respuesta de objetos y eventos se verifican considerando semáforos y objetos dinámicos ubicados a lo largo de la ruta de conducción.

Capítulo 5. Respaldo de la tarea de conducción dinámica (DDT)

En este capítulo, se introduce una estrategia de respaldo en caso de fallos que permite aplicar técnicas de *dead-reckoning* en caso de fallo de posicionamiento. El sistema propuesto puede detectar fallos en base a los últimos datos viables conocidos, advirtiendo a la etapa de decisión que establezca una estrategia de respaldo y planificando nuevas trayectorias en tiempo real. Los objetos circundantes y los bordes de la carretera se consideran durante el control de movimiento del vehículo después de un fallo, para evitar colisiones y para mantener el carril. Se simula un caso de estudio basado en un escenario urbano realista con el fin de verificar el sistema.

El sistema de posicionamiento comprende un filtro Kalman para mejorar la ubicación del vehículo cuando la calidad del receptor GPS de posición no es adecuada. Éste es un problema muy común en escenarios urbanos donde la línea de visión del satélite estaría constantemente obstruida. Un sensor virtual se activa en caso de que se detecte un fallo total en el sensor de posición. Este sensor implementa una estrategia de respaldo, realizando el cálculo de posicionamiento usando estrategias de *dead-reckoning*. Con el fin de implementar el sensor virtual anterior, se usa un modelo de vehículo que requiere de los datos de los coeficientes de rigidez de las ruedas, que son estimados mediante pruebas en circuito abierto. El planificador de trayectorias en tiempo real es capaz de reducir el perfil de velocidad después del fallo, esperando un espacio disponible y permitido para realizar una maniobra de cambio de carril y ubicar de manera segura el vehículo en el arcén. En el algoritmo se considera la distancia a objetos que se encuentren ya estacionados, por lo que el espacio disponible para iniciar la maniobra de estacionamiento se contrasta constantemente con un cálculo de espacio requerido. Un sistema para evitar colisiones se activa en todo momento adaptando el perfil de velocidad para mantenerse a una distancia segura de los objetos que se encuentran delante.

Capítulo 6. Conclusiones y trabajo futuro

Este capítulo se centra en los hallazgos más importantes del trabajo y hace recomendaciones respecto a futuras invetigaciones en conducción altamente automatizada.

TABLE OF CONTENTS

LIST OF TABLES

LIST OF FIGURES

LIST OF NOMENCLATURES

$\vec{u}$ Orientation vector of Bezier's control points. 79

$\boldsymbol{A_f}$ Frontal area of the vehicle. 89

$\boldsymbol{B}$ Bernstein polynomial. 78

$\boldsymbol{C_{\alpha f}}$ Cornering stiffness on front tires. 86

$\boldsymbol{C_{\alpha r}}$ Cornering stiffness on rear tires. 86

$\boldsymbol{C_d}$ Aerodynamic drag force. 89

$\boldsymbol{D_{coast}}$ Deceleration during coast-down test maneuver. 93

$\boldsymbol{F_{aero}}$ Equivalent longitudinal aerodynamic drag force. 89

$\boldsymbol{F_{xf}}$ Longitudinal tire force on front tires. 89

$\boldsymbol{F_{xr}}$ Longitudinal tire force on rear tires. 89

$\boldsymbol{F_{yf}}$ Lateral tire force on front tires. 86

$\boldsymbol{F_{yr}}$ Lateral tire force on rear tires. 86

$\boldsymbol{G_e}$ Transfer function (electro-mechanical actuator). 56

$\boldsymbol{I_z}$ Yaw moment of inertia of vehicle. 86

$\boldsymbol{J_e}$ Rotor's inertia (electro-mechanical actuator). 56

$\boldsymbol{K_e}$ Back electromotive force (electro-mechanical actuator). 56

$\boldsymbol{K_t}$ Back electromotive torque (electro-mechanical actuator). 56

$\boldsymbol{L_e}$ Inductance force (electro-mechanical actuator). 56

$\boldsymbol{L}$ Total wheelbase ($l_f + l_r$). 85

$\boldsymbol{N_s}$ Prediction horizon. 82

$\boldsymbol{N_u}$ Control horizon. 82

$\boldsymbol{P}$ Bezier's control points. 78

$\boldsymbol{Q_n}$ Process noise covariance matrix. 123

$\boldsymbol{Q_w}$ Differential states weight matrix. 98

$\boldsymbol{R_e}$ Resistance (electro-mechanical actuator). 56

$\boldsymbol{R_n}$ Measurement noise covariance matrix. 123

$\boldsymbol{R_w}$ Control inputs weight matrix. 98

$\boldsymbol{R_{xf}}$ Force due rolling resistance at the front tires. 89

$\boldsymbol{R_{xr}}$ Force due rolling resistance at the rear tires. 89

$\boldsymbol{R}$ Radius of path ($1/k$). 79

$\boldsymbol{T_w}$ Torque transmitted to the wheels. 89

$\boldsymbol{V_e}$ Voltage (electro-mechanical actuator). 56

$\boldsymbol{V}$ Total velocity at CG of vehicle. 85

$\boldsymbol{W_e}$ Angular velocity (electro-mechanical actuator). 56

$\boldsymbol{X}$ Global cartesian ordinate axis. 78

$\boldsymbol{Y}$ Global cartesian abscissa axis. 78

$\Delta\delta$ Front wheel steering rate. 85

$\Delta\psi$ Heading of target object relative to heading of the vehicle. 90

$\Delta\boldsymbol{v_x}$ Longitudinal velocity of the target object relative to the vehicle. 90

$\Delta\boldsymbol{v_y}$ Lateral velocity of the target object relative to the vehicle. 90

$\Delta\boldsymbol{x}$ Longitudinal distance from the front of the vehicle to the target object. 90

$\Delta\boldsymbol{y}$ Lateral distance from the front of the vehicle to the target object. 90

$\alpha_{\boldsymbol{f}}$ Slip angle at front tires. 86

$\alpha_{\boldsymbol{r}}$ Slip angle at rear tires. 86

β Slip angle at CG of vehicle. 85

δ Front wheel steering angle. 84

$\dot{v}_{\boldsymbol{y}}$ Lateral acceleration at CG of vehicle. 88

λ Switching parameter for vehicle model blending. 87

ψ Heading angle of vehicle. 78

ρ Mass density of air. 89

$\tau_{\boldsymbol{e}}$ Electrical time constant (electro-mechanical actuator). 56

τ_m Mechanical time constant (electro-mechanical actuator). 56

θ Road gradient. 78

ζ Distance on path's segment. 83

a_w Desired comfort level. 80

a_x^{degr} Longitudinal deceleration on degraded mode. 118

a_x^{target} Longitudinal acceleration of target object. 92

a_x Longitudinal acceleration. 76

a_y Lateral acceleration. 80

a_z Vertical acceleration. 80

d_{ey} Lateral displacement of center-lane of planned path. 119

d_p Accelerator and brake pedals position. 89

d_r^{max} Maximum range of sensor. 93

d_r^{min} Desired minimum distance to ensure safety. 93

d_r^{req} Relative distance required to perform a safe-parking. 122

d_r^{ttl} Relative travel distance from the front of the vehicle to the traffic light. 91

d_r Relative travel distance to the target object. 91

d_r Relative travel velocity to the target object. 91

d_{start} Travel distance after failure to reduce speed. 118

d_x Travel distance. 78

e_ψ Heading deviation. 83

e_y Lateral deviation. 83

g Acceleration due to gravity. 89

j_x Longitudinal jerk. 89

k Curvature of path. 79

l_f Longitudinal distance from CG to front tires. 85

l_r Longitudinal distance from CG to rear tires. 85

l_t Length of target object. 90

m Total mass of vehicle. 86

n_w Weight index. 80

r_{eff} Effective radius of rotating tire. 89

r Heading rate of vehicle. 86

s Differential state. 82

t_e Mechanical time (electro-mechanical actuator). 56

t^{delay} Time delay of actuation system. 123

t^{out} Time required on emergency shoulder before totally stop the vehicle. 123

t^{trl} Remaining time before the traffic light status switchs to red light. 91

t^{ttl} Remainig time before reach the traffic light location. 91

t Time. 56

u Control input. 82

v_{ey} Lateral velocity of center-lane of planned path. 119

$v_x{}^{degr}$ Longitudinal velocity on degraded mode. 118

$v_x{}^{ref}$ Longitudinal velocity reference. 80

$v_x{}^{target}$ Longitudinal velocity of target object. 92

v_x Longitudinal velocity. 78

v_y Lateral velocity at CG of vehicle. 86

w_p Width of driving path. 90

w_t Width of target object. 90

z Algebraic state. 82

LIST OF ABBREVIATIONS

ABS Anti-lock Brake System. 23

ACC Adaptive Cruise Control. 3

ADAS Advanced Driving Assistance System. 3

ADS Automated Driving System. 1

AEB Automatic Emergency Braking. 28

AV Automated Vehicle. 23

CC Cruise Control. 26

CG Center of Gravity. 85

DDT Dynamic Driving Task. 3

ECU Electronic Control Unit. 2

EPS Electric Power Steering. 40

ESC Electronic Stability Control. 23

FA Fail-Aware. 37

FCW Forward Collision Warning. 3

FO Fail-Operational. 37

FS Fail-Safe. 37

GNSS Global Navigation Satellite System. 24

GPS Global Positioning System. 5

GVT Global Vehicle Target. 67

HiL Hardware-in-the-Loop. 27

HW Hardware. 37

IMU Inertial Measurement Unit. 23

LDW Lane Departure Warning. 3

LKA Lane Keeping Assist. 3

MPC Model Predictive Control. 11

NMPC Nonlinear Model Predictive Control. 81

ODD Operational Design Domain. 3

OEDR Object and Event Detection and Response. 3

RECA Rear-End Collision Avoidance. 91

RTK Real-Time Kinematic. 5

SAE Society of Automotive Engineers. 3

SC Supply Chain. 10

SiL Software-in-the-Loop. 28

SoA State-of-the-Art. 15

SRQ System Response Quantity. 21

STM Standardized Test Maneuvers. 20

SW Software. 37

TCS Traction Control System. 23

TTC Time To Collision. 76

UKF Unscented Kalman Filter. 111

V2I Vehicle-to-Infrastructure. 24

V2P Vehicle-to-Pedestrian. 24

V2V Vehicle-to-Vehicle. 24

V2X Vehicle-to-X. 24

ViL Vehicle-in-the-Loop. 28

VUT Vehicle Under Test. 64

VV Verification and Validation. 16

XiL X-in-the-Loop. 27

Chapter One

Introduction

In the last decade, an increasing trend towards automation of vehicles has arisen, creating a significant change in mobility, which will profoundly affect the people's way of life, the logistics of goods, and other sectors dependent on transportation. The development of new driving technologies will cause a great impact on transportation services soon, having a remarkable effect on the economic, natural, and social environment.

In the development of high driving automation in structured environments, both safety and comfort, as part of new driving functionalities, are not yet described in a standardized way [15]. As testing methods are using more and more simulation techniques, the existing developments must be adapted to this process. For instance, as trajectory tracking technologies are essential enablers for highly automated vehicles, thorough verifications must be applied in related applications such as vehicle motion control and parameter estimation. Moreover, in-vehicle technologies must be robust enough to meet high safety requirements, improving redundancy to support a fail-safe operation.

Considering the mentioned premises, this Ph.D. Thesis targets the design and implementation of a framework to achieve highly Automated Driving Systems (ADS) considering crucial aspects, such as real-time capability, robustness, operating range, and easy parameter tuning. Also, scalability is a key aspect, which allows covering a broad range of vehicle platforms, from two-seated cars up to full-size transit buses, like those depicted in Figure 1.1. To develop the contributions related to this work, a study of the current state of the art in high driving automation technologies is carried out. Then, a two-step method is proposed addressing the validation of both simulation vehicle models and ADS. Novel model-based predictive formulations are introduced to improve safety and comfort in the trajectory tracking process. Finally, malfunction scenarios are assessed to improve safety in urban settings, proposing a fallback strategy based on dead-reckoning to minimize risk conditions.

The rest of this chapter is organized as follows. In Section 1.1, the need for driving automation is detailed, pointing out a historical overview, challenges, and applications. In Section 1.2, the objectives and contributions of this Ph.D. Thesis are defined. In Section 1.3, the manuscript organization along with a brief description for each chapter is provided. Finally, in Section 1.4 a list of the publications, related to the work in this Ph.D. Thesis is presented.

Figure 1.1 Irizar i2e and Renault Twizy used as research platforms for vehicle models and ADS development (courtesy of Tecnalia R&I and Irizar e-mobility)

1.1 Motivation and Background

In recent years, interest in automated vehicles and their related technologies has exploded because of the multiple advantages they theoretically provide in terms of safety, environment, and economy.

Regarding *safety*, approximately 1.35 million fatal accidents each year in traffic accidents around the world, and between 20 and 50 million more suffer non-fatal injuries, many incurring a disability according to the World Health Organization [16]. In city traffic, among 8 out of 10 people killed are cyclists and other vulnerable road users according to the International Road Traffic and Accidents Database [17]. A high percentage of these accidents, 94%, occur because of the incidence of human factors such as poor decision-making behind traffic law adherence, inappropriate vehicle control and misjudging behavior of other vehicles [18]. Thus, automated vehicles present a solution to the transportation problem in urban environments, reducing accidents caused by driver error as the ultimate failure in the causal chain of events.

On the other hand, *climate change and environmental degradation* are an existential threat, and a modern, resource-efficient, and competitive economy without pollutant emissions is expected by 2050. The EU Green Deal [19] is addressing emissions, urban congestion, and the improvement of public transport. By 2025, about 1 million public recharging and refueling stations will be needed for the 13 million zero- and low-emission vehicles expected on European roads. A shift to automated vehicles could also provoke the shift to electric vehicles, as the actuation devices (drive-by-wire systems) can be controlled by a single source, and it makes the system more efficient to enable the use of centralized Electronic Control Units (ECU) [20]. Broad implementation of automated mobility and smart traffic management systems can be a turning point to decrease energy consumption and pollutant emissions [21], fostering the transport system efficiency and the time reduction in congested traffic [15].

Finally, ADS can prompt extensive *macroeconomic benefits* both in job creation and operators. It will also allow removing barriers for non-drivers in the labor market and boosting their participation [22]. New job opportunities would arise in several engineering and research areas such as vehicle design, manufacturing, data analysis, vehicle mainte-

Table 1.1 SAE driving automation levels [1]

	Level 0	Level 1	Level 2	Level 3	Level 4	Level 5
	No Driving Automation	**Driver Assistance**	**Partial Driving Assistance**	**Conditional Driving Automation**	**High Driving Automation**	**Full Driving Automation**
Control	Driver	Driver	ADS	ADS	ADS	ADS
OEDR	Driver	Driver	Driver	ADS	ADS	ADS
Fallback	Driver	Driver	Driver	Driver	ADS	ADS
ODD	Limited	Limited	Limited	Limited	Limited	Unlimited
Function example	FCW LDW	ACC LKA	Traffic Jam Assistant	Traffic Jam Chauffeur	(Sub)Urban Autopilot	Robot Vehicle
	ADAS			**ADS**		

nance, network design, re-sizing vehicles, re-routing conventional passenger route services, among others [23, 24]. Benefits in the reduction of current operations costs are expected to range between 50-60% [25], besides saving cost in demand-responsive transportation-related with children and the elderly population [26]. In contrast to private automated vehicles, automated mobility for collectives would positively influence the energy consumption [23].

1.1.1 Driving Automation SAE Levels

Achieving the aforementioned benefits requires further developments on high driving automation technology, which is thoroughly described by [1] as *the hardware and software that can collectively perform the entire Dynamic Driving Task (DDT) on a sustained basis, regardless of whether it is limited to a specific Operational Design Domain (ODD).* The DDT covers the longitudinal and lateral vehicle motion control, as well as the Object and Event Detection and Response (OEDR). Detailed definitions for the SAE levels are defined in the context of motor vehicles and their operation of roadways, ranging from no driving automation (level 0) to full driving automation (level 5). The roles of the human driver and ADS along engaged SAE Levels are described in Table 1.1.

1.1.2 Historical Background

Although the number of technological developments has increased in recent years, driving automation technology has been in development for the last 100 years. In the first half of the twentieth century, several technological milestones were achieved in ADS development. Firstly, remotely driven vehicles merely conceived as feature attractions contributed to envision the future of mobility (the middle 1920s to 1950s). Secondly, cooperative driving systems focused on adapted infrastructure were developed (in the 1980s). Thirdly, early developments and large-scale demonstration of automated driving and intelligent transportation systems were proposed (up to the late 1990s). Finally, since the early 2000s, the number of contributions has increased, with real deployments on dedicated, mixed, and open traffic situations. Next, the most important milestones achieved from the historical point of view are summarized in chronological order.

1.1.2.1 Envisioning the Future of Mobility (from 1920s to 1930s)

The *Linriccan Wonder* by Houdina Radio Control was the first registered step towards driving automation, a 1926 Chandler equipped with small electric motors, and a transmitting antenna was radio-controlled across the streets of New York City. Later, an enhanced version of this invention, the *Phantom Auto* by Achen Motors, was demonstrated on the streets of Milwaukee and Fredericksburg in 1926. Probably the first depiction of driving automation in future society is the Futurama exhibit in the World Fair 1939 sponsored by General Motors (GM), which showed radio-controlled electric vehicles through embedded-circuits in roadways, promoting advances in highway design and transportation [27].

1.1.2.2 Electronic Railing (from 1950s to 1970s)

Vehicles guided through electronic railing using grounded cables were proposed since the mid-1950s. RCA Labs, after several experiments with a scale model guided by wires on a laboratory floor, tested this idea using GM's standard models in Nebraska and New Jersey. Confidence in this technology motivated GM to display the Firebird II at Motorama auto shows, a vehicle equipped with an electronic guide system for automatic highways [28]. Experiments in the United Kingdom and Japan showed that the automated steering system guided vehicles accurately over 100km/h on test tracks [29, 30]. In the 1970s, early attempts of automated buses occurred in Sweden and West Germany for precision docking near bus stop platforms. Although electronic railing seemed to be useful for an accurate lateral vehicle guidance task, it resulted to be economically justified only in restricted areas due to installation, electric consumption, and maintenance costs.

1.1.2.3 Vision Guidance (in 1980s)

Vision-based automated vehicles represent a remarkable milestone in safety. In the 1980s, the Mechanical Engineering Laboratory in Japan equipped a vehicle with a stereo-vision system capable of detecting guard rails for lateral control execution at 30km/h and avoiding stationary objects at 10km/h [31]. The Bundeswehr University Munich in Germany, traveled at 63km/h on streets without traffic on an automated Mercedes-Benz van equipped with a vision-guided system [27]. The Carnegie Mellon University in the USA, drove continuously on roads at low speeds while avoiding obstacles using the NavLab, a minibus developed as a self-contained laboratory for navigational and vision system research [32].

1.1.2.4 Automatic Highways (from 1980s to 1990s)

The development of automated driving functionalities, oriented to safety and efficiency results, was supported after the middle 1980s by important funding projects in the USA, Japan, and Europe. Automated vehicles under test included passenger cars, transit buses, trucks, and construction vehicles [31]. In the USA, automatic highway system solutions promoted in the Intermodal Surface Transportation Efficiency Act (ISTEA) included technologies for lateral (magnetic markers) and longitudinal (radar, machine vision, and vehicle-to-vehicle communications) vehicle motion control. California PATH performed the platooning of eight passenger cars at 96km/h with 6.3m of gap between vehicles [33]. In Japan, advances in inter-vehicle communications (100ms of real-time transmission) permitted the

performance of flexible platoons, changing lanes and merging into other platoons at 50-60km/h. The vision-based sensor fusion with Real-Time Kinematic Global Positioning System (RTK-GPS) was an essential development for the lateral and longitudinal motion control of a 5-vehicle platoon [34]. In Europe, advances in traveler information, vehicle control, and safety (e.g. machine vision algorithms and Kalman filters) were fostered by the PROMETHEUS program stimulated by Daimler-Benz Research [35].

1.1.2.5 A New Century (from 2000s to 2010s)

In contrast to earlier times, developments in automated driving buses and trucks became an actual research trend after the early 2000s. Besides safety and efficiency, the possible introduction of intelligent transportation systems and automated urban mobility increased the interest in additional aspects, such as energy-saving, environment, and convenience [31]. **In USA**, California PATH sponsored by Caltrans performed demonstrations of automated transit buses and trucks. The automated buses featured full-speed highway driving, precision docking and narrow lane driving using magnetic markers, and a realistic driver-vehicle interface. Also, automated trucks presented a coupled longitudinal control of tractor-trailer rigs with 3m of separation using radar and lidar [33, 31].

Applications as platooning, cooperative-adaptive cruise control, lateral guidance, and precision docking in automated buses reached full demonstration in 2009 under the Vehicle Assist and Automation (VAA) [36]. **In Japan**, Toyota developed the Intelligent Multimodal Transit System (IMTS) performing automated platoon of transit buses along dedicated lanes from 2002 to 2008. The Ministry of Economy, Trade, and Industry sponsored the Energy ITS project for truck automation between 2008 and 2012. Automated driving solutions included both the automation of heavy trucks for highway platooning and light trucks for urban streets under mixed traffic. By 2012 a lane-changing platoon of three fully automated both heavy and light trucks drove at 80km/h with a 4m gap along an expressway without traffic. The lateral control used vision for lane marker detections, and the longitudinal control used vehicle-to-vehicle communications, radar, and lidar for gap and obstacle detection [37].

In Europe, Phileas program presented a fully electric articulated bus capable of lateral motion control and precision docking using magnetic markers, also with speed control for smooth parking and departure at bus stops. The KONVOI initiative performed research on truck platooning driving the lead vehicle manually, and the demonstration with four tractor-semitrailer combinations took place in 2009 [38]. The CityMobil2 project is the largest demonstrator related to low-speed automated shuttle buses, considering a broad range of topics such as user acceptance, security, safety, technology, costs, and legal issues [24].

1.1.2.6 Current Efforts and New Applications

Future automated vehicles are expected to operate transport services efficiently and flexibly in smart and connected infrastructures. The advancements are currently pursued intensely by the technological and automobile industries, being the latter split between traditional manufacturers and newer entrants as startups. Some developments and prototypes being developed are detailed in Figure 1.2. Next, the most significant efforts are detailed in three of the most relevant application areas: cars, trucks, and buses.

Ford Fusion Hybrid (USA)[8]

EasyMile Shuttle Pod (Germany)[3]

Volvo Refuse Truck (Sweden)[12]

UD Heavy-Duty Truck (Japan)[10]

Yutong Interurban Bus (China)[19]

ADL Full-Sized Bus (UK)[26]

Figure 1.2 Examples of current efforts and new applications

Automated Cars The main developments towards driving automation address primarily the car market, enabling the manufacturers to afford the research and development costs among many vehicles, and increase the current driving automation levels considering the scalability to medium- and heavy-duty markets (e.g., automated trucks and buses). Advanced Driving Assistance Systems (ADAS) at SAE Level 2 and below are currently on the market, such as Traffic-Jam Assist, Parking Assist, Adaptive Cruise Control, and Stop&Go. Furthermore, a long development path still expects further advancements in ADS at SAE Level 3 and above, including Traffic-Jam Chauffeur, Highway Chauffeur, Urban and Suburban Pilot, Highway Autopilot and Highway Convoy [15]. However, in recent years new entrants in the automotive market have more recently become involved in developing technologies, offering shared rides in low-speed SAE Level 4 automated shuttles in worldwide demonstration sites, including 2getthere[1], Coast Autonomous[2], EasyMile[3], Local Motors[4], May Mobility[5], Navya[6], Ridecell[7], among others. Technology firms are considering partnerships with transportation network companies to augment shared rides services in passenger vehicles, such as Uber, Lyft[8], and Waymo[9]. Among the aforementioned initiatives in mobility services, deployments include automated ridesharing services for big cities by General Motors and Ford, automated shuttle services in Silicon Valley by Daimler and Bosch, automated ride-hailing service by Waymo [39].

Automated Trucks Today most driving functionalities for heavy-duty vehicles aim at on-highway applications rather than slow urban environments, considering warnings and actuation for following distance and collisions [40]. High automation in commercial platforms from simple to more and more complex environments could be employed, such as confined (port and terminals), hub-to-hub (from factories to hub or terminals), open roads (highways or roads) and urban environments (cities) [41]. Connected automated commercial vehicles could enable the logistics sector by the progressive deployment towards a higher level of automated heavy commercial vehicles depending on the application domains and the ODDs. Some initiatives are currently under early testing from several manufacturers such as UD Trucks[10], Kenworth Truck Co.[11], Volvo[12], and Daimler[13]. Examples of advanced and partial automated driving functions already introduced are cooperative adaptive cruise control, multi-brand truck platooning, traffic-jam chauffeur, and highway chauffeur. Ongoing research and developments on this application include Platooning Ensemble Project[14], Aeroflex Project[15] and Falcon Project [42].

[1] video: Autonomous Shuttle Demonstration | Sendai International Airport https://rb.gy/3ha6gi
[2] report: USF Hosts Its First-Ever Autonomous Vehicle Demonstration https://rb.gy/z0uoh6
[3] report: German autonomous shuttle fleet awarded innovation prize https://rb.gy/mxjffy
[4] report: Robotic Research Helps Olli Shuttle Bring Autonomous Vehicle https://rb.gy/bbsmk7
[5] report: May Mobility Restarts Autonomous Shuttle Service in Grand Rapids https://rb.gy/smlmrr
[6] report: Self-Driving Shuttle for Passenger Transportation https://rb.gy/e10twm
[7] report: Ridecell Introduces the First Complete Autonomous New Mobility https://rb.gy/8dvmil
[8] report: Where to find self-driving cars on the road right now https://rb.gy/3wia1q
[9] report: Partnering with Valley Metro to explore public transportation solutions https://rb.gy/qkddme
[10] video: The first L4 autonomous driving trial by a heavy-duty truck in Japan https://rb.gy/9fxt2o
[11] report: Kenworth Truck Co. displays Level 4 autonomous T680 at CES https://rb.gy/w4lhqw
[12] video: Volvo pioneers autonomous, self-driving refuse truck https://rb.gy/7cjldq
[13] video: Testing of the first series-production autonomous truck on public roads https://rb.gy/dq4xdz
[14] webpage: Platooning Ensemble Project https://platooningensemble.eu/
[15] webpage: Aeroflex Project https://aeroflex-project.eu/

Automated Buses High automation solutions in transited areas are focused on low vehicle speeds and dedicated infrastructure applications. The automated, smart, and seamlessly connected mobility includes 24/7 business models such as booking, sharing, and networking platforms, docking and charging services, and software solutions for managing and maintaining vehicles. The Personal Rapid Transit (PRT) as a transportation model includes urban shuttles for collective and individual users on confined, dedicated, or open roads as possible site deployments [15]. Automated city-buses and coaches solutions integrated with traditional public transport services rely on developments from Advanced Driver Assistance Systems (ADAS) solutions such as following and bus-stop automation, bus-platooning, and traffic-jam assistance. Ongoing international research projects on this application include; Daimler Future Bus City Pilot[16], Connected & Automated Public Transport Innovation project[17] and Singapore Autonomous Vehicle Initiative[18].

The field of automated full-size buses is a nascent market. Hence, research development and pilot activities primarily show proof-of-concept, gather data, and represent an early stage in the development of future products, including; Vehicle Assist and Automation Demonstration [40], Active Safety-Collision Warning Pilot [43], Automated Bus Research [44], Yutong Automated Bus Demonstration[19], Alphaba Bus Demonstration[20], Automated Driving for Universal Services [45], Haneda Airport Automated Bus Demonstration[21], Volvo Automated Bus Projects[22], LILEE Systems Automated Bus Demonstration[23], Baidu Apolong Buses[24], Automated Bus Demonstrations at Singapore[25] and Scotland[26], Scania and Nobina Automated Bus Demonstration[27], and AutoDrive Project[28].

1.1.3 Challenges

New technologies and services enabled by ADS seem to highly contribute to several societal challenges of road transportation, including; shared mobility, public transport, accessibility, logistics, vehicle and infrastructure technologies, and regulatory adaptations. Therefore, unique challenges arise in essential areas such as *users and society*, *systems and services*, and *vehicles and technologies* [15].

1.1.3.1 Users and Society

Many countries and jurisdictions now have some appropriate legislation and regulations in place to enable driving automation, although work on implementation is still lacking [46]. High uncertainty regarding several issues still exists, for instance, safety, insurance and liability, and user and operator acceptance are some issues that demand more research

[16]report: The Mercedes-Benz Future Bushttps://rb.gy/q9xj4a
[17]report: Connected & Automated Public Transport Innovation Project https://rb.gy/ruixmp
[18]report: Singapore Autonomous Vehicle Initiative https://rb.gy/gf417e
[19]report: Yutong completes world's first trial operation of unmanned bus https://rb.gy/rkmsl8
[20]report: Self-driving buses are being tested in China https://rb.gy/cruumq
[21]report: Driverless terminal bus goes on test run at Tokyo's Haneda airport https://rb.gy/lnn9zw
[22]report: Volvo demonstrates autonomous bus https://rb.gy/8mfp3m
[23]report: LILEE Systems Presents Major Advances in Autonomous Rapid Transit https://rb.gy/w21bb4
[24]report: Baidu just made its 100th autonomous bus ahead of commercial launch https://rb.gy/l5okmb
[25]report: NTU Singapore and Volvo unveil worlds first full size autonomous bus https://rb.gy/utdi5e
[26]report: Scotland to trial first autonomous full-sized bus fleet in passenger service https://rb.gy/n5v5hn
[27]report: Nobina and Scania pioneer full length autonomous buses in Sweden https://rb.gy/kuetob
[28]webpage: AutoDrive Project https://autodrive-project.eu/

[40]. In safety, the *Vision Zero* in EU aims to halve road casualties by 2020 and eliminate traffic fatalities and injuries by 2050 [47]. Operational, functional, and perceived safety and comfort as part of the development of new functionalities of a whole automation level are not yet standardized [15]. In insurance and liability, concerning implications are carried out as the driver can no longer be accountable for accidents because of driving automation, so relevant laws must be analyzed [48]. In user and operator acceptance, people seem to be more comfortable using automation technologies in cities where pilots are under deployment. In this sense, demonstration programs are essential for continuous technological progress, also contributing to answering questions regarding the feasibility of driving automation in urban mobility vehicles [24, 46]. Shifting the workload of operators from manual driving to a continuous monitoring task may negatively affect acceptance, as little or no intervention requests are preferred by driving operators [49].

1.1.3.2 System and Services

Conventional analytical procedures for infrastructure detection present limits in complex urban scenarios. Consequently, a particular challenge is the development of automotive-compatible safety, which release methods based on big data and artificial intelligence for functional components. Understanding physical and digital infrastructure and connectivity will help to understand deployment opportunities, especially in areas like crossings, road-work zones, tunnels, urban environments, special events, and natural disasters [15]. Regarding automated driving services, shared automated vans and buses may be at least as important as private driverless cars. Many localities are prioritizing driverless minibusses, for instance, to extend the range of existing public transport, provide on-demand services, and to transfer tourists. There are also further opportunities to expand the use for freight in closed environments such as industrial, port, and mining areas. [46]. More product-oriented (advice and services of maintenance), user-oriented (leasing and sharing), result-oriented (Outsourcing and functional results), and new business models must require studies in the coming years given the impressive development of technologies [50].

1.1.3.3 Vehicle and Technologies

Many of the lower-level automation systems used in heavy-duty vehicles operate at high-speeds on highways, whereas urban buses operate at low-speeds on urban roads. Additionally, current sensing technology has false positives to be implemented in transit operations [40]. It is of importance to understand and design the interaction between humans and automated vehicles at different levels of automation without induced negative consequences. Moreover, systems must fulfill several requirements which increase the complexity of vehicle technologies; Firstly, be scalable enough to cover different vehicle platforms, models, and markets. Secondly, be robust enough to meet improved redundancy to support a fail-safe operation. Finally, highly secured against cyber-attacks to ensure system integrity [15].

The challenges in tracking systems for automated passenger vehicles in urban environments are focused on the rapid increase of the current technology readiness level. Nowadays, many of the capabilities to complete safe and comfortable automated shuttling services are developed scatter by different projects, using specific scenarios which consider very controlled conditions (some examples in Figure 1.2). To achieve the deployment of this technology in complex environments, a research effort to define and implement a reli-

able and modular solution for automated vehicles in different driving scenarios is required, especially in structured environments as seaports, airports, urban and inter-urban zones.

To provide solutions to current challenges of automated driving, especially those related to urban scenarios, the AutoDrive Project [28] was proposed.

1.1.4 AutoDrive Project

The AutoDrive Project [28] targets fail-aware, fail-safe, and fail-operational integrated electronic components, Electrical/Electronic architectures, as well as embedded software systems for highly and fully automated driving to make future mobility safer, more efficient, affordable, and end-user acceptable. The goal is to make driving as safe as flying.

To achieve the target, the multidisciplinary consortium of AutoDrive composed of 60 partners collaborates into three groups of Supply Chains (SCs). A SC is centered on common research topics, demonstrators, and defines the interfaces between the necessary work packages of the project. Figure 1.3 depicts the three groups of SC in the AutoDrive Project.

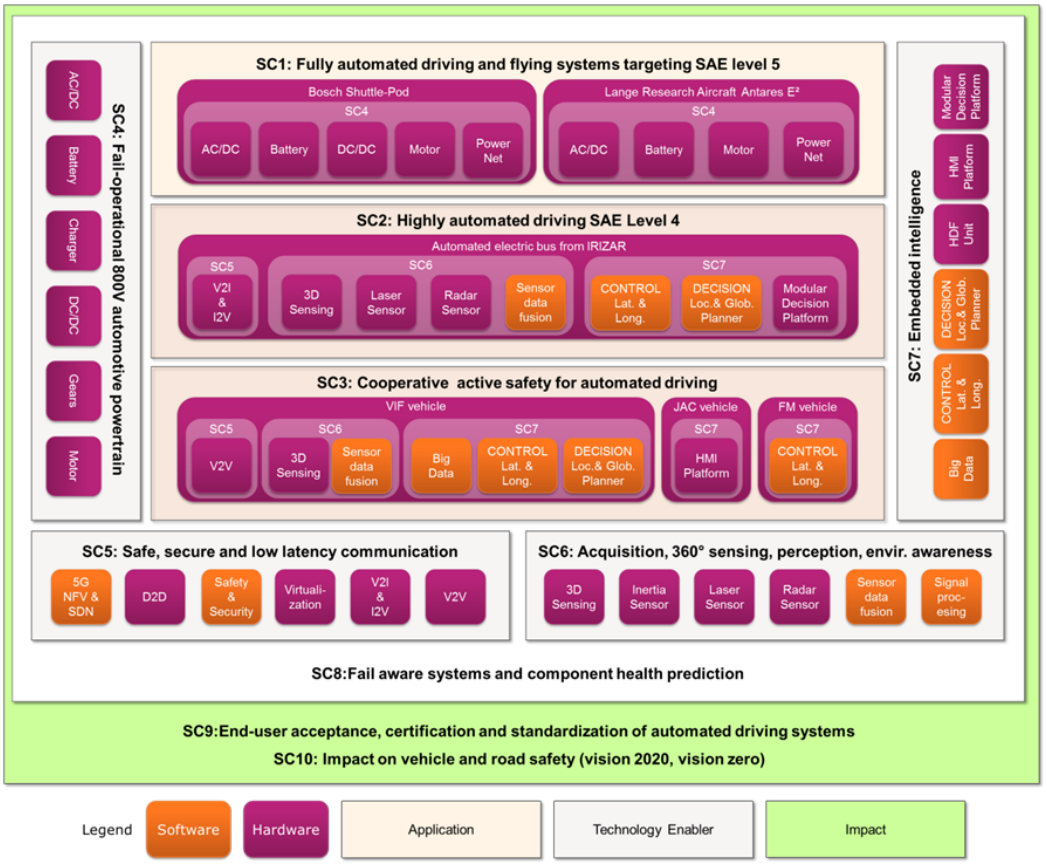

Figure 1.3 Supply Chains in AutoDrive Project[28]

The core of the project is the *Technology Enabler* SCs, which shows the outcome of ver-

tical research. It covers semiconductor components, embedded systems, power-train components, and integration aspects. This cluster includes; Fail-operational 800V automotive power-train (SC4), Safe, secure and low latency communication (SC5), Acquisition, 360° sensing, perception, environmental awareness (SC6), Embedded intelligence and systems for automated driving (SC7), and Fail aware components and health prediction (SC8).

Results achieved by the technology enablers will be validated in the horizontal *Application* SCs to build products. This cluster includes fully automated driving and flying systems targeting SAE level 5 (SC1), Highly automated driving - SAE level 4 (SC2), Cooperative active safety for automated driving - SAE level 3 (SC3).

These innovative products will form the basis to generate European values to be quantified and reflect the economic, societal, and pan-European *Impact* of AutoDrive. Two *Impacts* are considered in AutoDrive, namely End-user acceptance to robust and affordable systems standardization (SC9) and Impact on vehicle and road safety (SC10).

The work of this Ph.D. Thesis is aligned with the goals of the SC2: Highly Automated Driving - SAE Level 4 [1]. This SC is focused on developing automated driving technologies applied to urban environments, targeting SAE Level 4. A case study based on an Irizar electrical bus in Malaga city is proposed as a demonstrator for this SC, which is also detailed in this PhD thesis.

The project has received funding from ECSEL Joint Undertaking under grant agreement No. 737469 and support from the European union's Horizon 2020 Research and Innovation Programme. The development covers 2017-2020 spanning the advancement of this Ph.D. Thesis.

1.2 Objectives

Influenced by the motivation and background statements, this Ph.D. Thesis targets the design and validation of systems towards high driving automation for urban applications, which contributes to the development of a scalable control architecture covering from small individual passenger cars to heavy-duty commercial vehicles.

The primary goal of this Ph.D. Thesis is to be achieved by the next partial objectives:

- Development of a well-defined validation method for vehicle models which complements track testings with simulations, assuring trustworthy virtual test platforms to boost the development of reliable ADS in urban scenarios.
- Design and validation of Model Predictive Control (MPC) formulations to ensure the desired performance in terms of path and speed tracking, despite the opposite nature of both safety and comfort.
- Conception of a decision-making strategy for the ADS to achieve a minimal risk condition after a DDT performance-relevant system failure occurs.

1.3 Manuscript Organization

To develop the mentioned objectives, this Ph.D. Thesis is structured into 6-chapters, including the present one. A brief explanation summarizes the most relevant content.

Chapter 2. State of the Art In this chapter, automated driving background and related works are detailed, divided mainly into three major areas. Firstly, the revision of current verification and validation methods for vehicle simulation models and ADS is presented. Secondly, a review of trajectory tracking techniques is given, which details the different approaches used in the literature and compares their performance for automated driving applications. Lastly, a survey of current decision-making strategies to achieve fail-operational systems in high driving automation is introduced.

Chapter 3. Validation in Automated Driving In this chapter, vehicle models useful both for trajectory tracking systems and virtual test platforms are presented. The more accurate and reliable the vehicle models are, the more the number of real-life tests can be decreased. In this sense, a two-step validation method is introduced. Firstly, an open-loop test set attempts to tune the required vehicle simulation models using experimental data considering also the dynamics of the actuation devices required for vehicle automation. Secondly, a closed-loop test strives to validate the technical safety of selected automated driving system based on test plans, also improving the vehicle dynamics response. To illustrate the methodology, case studies are proposed using automated vehicles such as a Renault Twizy and an Irizar i2e bus. In the first step, the brake pedal and steering wheel actuators' behavior is modeled, as well as its longitudinal dynamics and turning capacity. Then, in a second step, a low-speed high automation functionality for traffic-jam assistance is validated.

Chapter 4. Safety and Comfort in Motion Control In this chapter, trajectory tracking techniques for accurate and comfortable vehicle motion control are presented. Accuracy is usually related to the velocity, position, and orientation of the vehicle. On the other hand, comfort is commonly associated with the acceleration and jerk both in the lateral and longitudinal axes of the vehicle. The opposite nature of safety and comfort in driving automation deems necessary a thorough analysis to conceive proper vehicle motion control. MPC formulations are mainly employed to contrast several approaches. Also, a procedure that blends vehicle models using MPC for trajectory tracking is presented. A full-size bus driving at several speeds on a route with different curvatures is proposed as a case study.

Chapter 5. Dynamic Driving Task Fallback In this chapter, a fail-operational approach for dead-reckoning in case of positioning failures is introduced. The proposed system can detect failures in the last available positioning source, warning the decision stage to set up a fallback strategy, and planning a new trajectory in real-time. The surrounding objects and road borders are considered during the vehicle motion control after failure, to avoid collisions, and for lane-keeping purposes. A case study based on a realistic urban scenario is simulated for testing and system verification.

Chapter 6. Conclusions and Future Work This chapter focuses on the most important findings of the work and recommends regarding future research in high driving automation.

1.4 Publications

The publications derived from this Ph.D. Thesis are presented in Table 1.2.

Table 1.2 List of journal and conference publications

Chapter	Publication
3	• Matute, J. A., Marcano, M., Diaz, S., and Perez, J. (2019). Experimental Validation of a Kinematic Bicycle Model Predictive Control with Lateral Acceleration Consideration. IFAC-PapersOnLine, 52(8), 289-294. • Matute-Peaspan, J. A., Zubizarreta-Pico, A., and Diaz-Briceno, S.E. (2020). A Vehicle Simulation Model and Automated Driving Features Validation for Low-Speed High Automation Applications. IEEE Transactions on Intelligent Transportation Systems: 1–10. doi:10.1109/tits.2020.3008318.
4	• Marcano, M., Matute, J. A., Lattarulo, R., Martí, E., & Pérez, J. (2018). Low-speed longitudinal control algorithms for automated vehicles in simulation and real platforms. Complexity, 2018. • Matute, J. A., Marcano, M., Zubizarreta, A., and Perez, J. (2018). Longitudinal model predictive control with a comfortable speed planner. IEEE International Conference on Autonomous Robot Systems and Competitions (pp. 60-64). IEEE. • Matute-Peaspan, J. A., Gonzalez, L., and Zubizarreta, A. (2019). A study of a comfortable vehicle motion predictive control with no speed limit reference. 6th International Conference on Models and Technologies for Intelligent Transportation Systems (pp. 1-6). IEEE. • Matute, J. A., Lattarulo, R., Zubizarreta, A., and Perez, J. (2019). A Comparison Between Coupled and Decoupled Vehicle Motion Controllers Based on Prediction Models. IEEE Intelligent Vehicles Symposium (IV) (pp. 1843-1848). IEEE. • Matute-Peaspan, J. A., Marcano, M., Diaz, S., Zubizarreta, A., Perez, J. (2020). Lateral-Acceleration-Based Vehicle-Models-Blending for Automated Driving Controllers. Electronics, 9(10), 1674.
5	• Matute-Peaspan, J. A., Perez, J., and Zubizarreta, A. (2020). A Fail-Operational Control Architecture Approach and Dead-Reckoning Strategy in Case of Positioning Failures. Sensors, 20(2), 442.

Chapter Two
State of the Art

To develop contributions of this Ph.D. Thesis, a study of current *State-of-the-Art* (SoA) is carried out in this section, which considers three main areas: 1) Virtual testing in Automated Driving Systems (ADS), 2) Safety and comfort in vehicle motion, and 3) Dynamic driving task fallbacks. As this Ph.D. Thesis is focused on industrial components advancements, research is oriented as a system development life cycle. This way, the first section of this survey is strongly related to the entire development process, while the next two sections are intrinsically connected with verification of systems as shown in Figure 2.1.

The organization of this chapter is as follows. In Section 2.1, the literature on the validation process for vehicle simulation models and high driving automation systems using virtual environments is examined. In addition, related works on test-based modeling and applications are briefly described. In Section 2.2, research on vehicle motion control for high driving automation are explored. Trajectory planning and tracking techniques are presented, along with the basic notions in Model Predictive Control (MPC) as the key tool in the development of this work. In Section 2.3, advances on Dynamic Driving Task (DDT) fallback strategies for ADS are described. The relationship between system failures and fail-operational strategies is particularly emphasized. Finally, the main conclusions are summarized in Section 2.4.

2.1 Virtual Testing in Automated Driving

The advances in computing capacity have increased at an outstanding pace, fostering the use of modeling methods and numerical solution techniques to replicate and predict a broad spectrum of real-world processes. The assessment of future manufactured products or research projects using mathematical models avoids unnecessary redesigns and costly experiments once needed to meet reliability or safety requirements. Consequently, for manageable sub-systems and even entire systems, *virtual testing* plays a leading role in supplementing test-based engineering, helping to understand specific performance issues, flaws, or sensitivities (e.g. automobiles crash-worthiness testing). Moreover, impractical, expensive, or restricted tests are eliminated from high-consequence systems in fully representative environments and scenarios (e.g. catastrophic transportation accidents).

In the process to obtain higher readiness levels in driving automation technology, formal and forefront verification methodologies for sub-systems must be combined to increase the success rate when validations of entire systems take place. In this regard, reliable driving simulators allow the exhaustive assessment of vehicle models and advanced system responses mainly through scenario-based *virtual testing*, time-boosting improvements

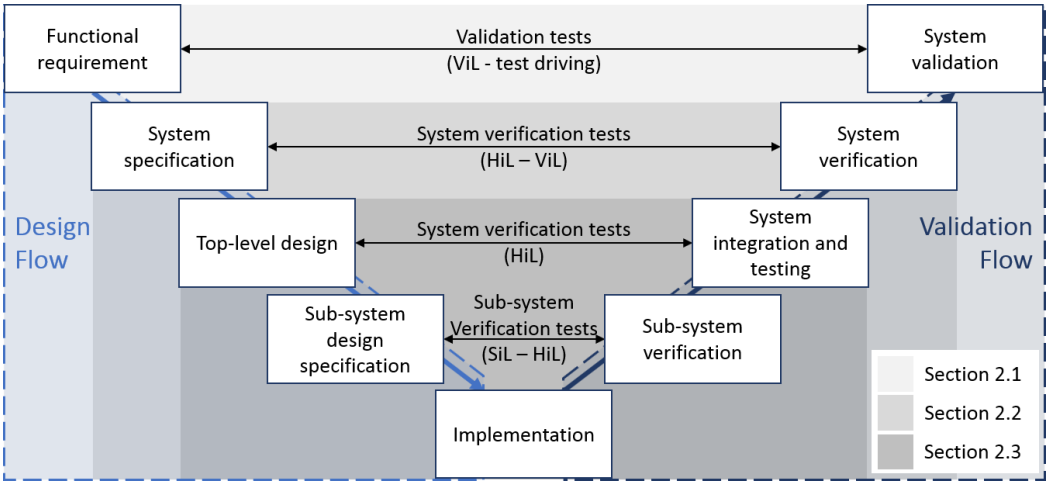

Figure 2.1 System development life cycle (V-model) and its relation with SoA

regarding the designer's particular perspective.

The trustworthiness of simulations is of great concern for the scientific and engineering community, as a lack of credibility and confidence in results provides little value because of differences with physical reality. Therefore, methods and techniques must be developed and implemented to increase the level of credibility in the vehicle simulation model, which is the base for *virtual testing* of driving systems. Generally, validation processes target the accuracy quantification inferred from the comparison of simulation (solution) and experimental (data) results, claiming that validation requires data with which to compare solutions [51]. In this regard, Verification and Validation (VV) emerged as a fundamental research field.

The main goal of VV is ensuring that models and simulations are correct and reliable enough [52] to predict the behavior of the real-world system that it represents [53]. **Verification** is a term commonly related to the question *Did I build the thing right?*, this means the assurance that a developed system fulfills the pre-defined specifications [51] bearing in mind two aspects: design (includes all specifications and nothing else in the model or simulation design) and implementation (includes all specifications and nothing else in the model or simulation as built) [52]. **Validation** is a term usually associated with the question *Did I build the right thing?*, it targets to determine the accomplishment of the developed system in the real-world [51] considering two aspects: concept (when assessing the expected fidelity of the model or simulation conceptual model) and the result (when comparing results from the implemented model or simulation with an appropriate referent to show that the model or simulation can support the intended use) [52].

The main findings for virtual testing emphasize validation procedures for ADS and vehicle simulation models as virtual test platforms for ADS research. The entire process is based on a system development life cycle, which starts with the definition of functional requirements, ending with system validations through test-driving or Vehicle-in-the-Loop simulations (ViL) as depicted in Figure 2.1.

2.1.1 Validation of Vehicle Simulation Models

A clear distinction among validation studies is defined between those focused on driver responses within simulators and others on the accuracy of dynamic model predictions within simulators [54, 55]. The second group of studies, also known as *physical validation* [54], is the focus of this Ph.D. Thesis. These studies assess the degree to which the vehicle dynamics simulation reproduces real vehicle behavior. In this regard, a complete *physical validation* assessment would be formally discretized in several approaches such as absolute, relative, and external validations [56]. Absolute and relative approaches validate the scales and trends correspondence between simulated and real responses, respectively. The external approach validates that those simulation results at a certain time and place can be generalized to other situations. In order to perform these validations, several simulators for vehicle dynamics are currently available including CarMaker[29], CarSim[30], veDyna[31], VDMS[32], and Dynacar[33].

2.1.1.1 Design of Vehicle Simulation Models

Vehicle dynamics is a branch of vehicle mechanics that studies the motion of ground vehicles and their resultant forces according to the natural laws [11]. The performance, handling, and ride of a vehicle are characterized by the forces and moments developed by the tire-ground interaction and environmental conditions, generated over the range of operating conditions [57]. These driving characteristics are influenced by several factors such as: wheel locations, the geometry of the suspension system, elastic bearings in the wheel suspensions, etc. In this sense, the prototype and actual testing of complex vehicle systems is traduced into a considerable economical effort by automakers. The use of mathematical vehicle models contributes to contain the development costs of control and their applications, resulting also in an increased functional range, product quality, and cost-efficient solutions by integrating mechanical, electrical, and electronic hardware into modules [11].

Simulation in vehicle dynamics allows the assessment of integrated systems and components using vehicle models. The fields of application for the development of vehicle systems include, kinematics and dynamics of the chassis and the steering, vehicle dynamics of the entire vehicle, ride comfort of the entire vehicle, and analysis of accidents [11]. As an advantage, different or critical maneuvers can be performed repeatedly under predefined parameters and conditions which is difficult in actual testing. However, great care is necessary for vehicle dynamics modeling as numerical simulations are only approximations of real events. The level of accuracy and computation time contrast with the modeling effort, which determines the complexity of both the vehicle model and simulation environment.

A complex vehicle simulation model comprises the modules depicted in Figure 2.2. Virtual testing scenarios usually consider entire multi-body models for dynamics assessment, nonetheless, some subsystems can be considered to construct simpler vehicle models when real-time applications are required as model-based motion control. Aspects related to handling, performance, electromechanical actuator, tire dynamics design, and different kinds of vehicle models for real-time purposes are covered next.

[29] webpage: IPG automotive https://ipg-automotive.com/
[30] webpage: Mechanical simulation https://www.carsim.com/
[31] webpage: Real-Time Simulation of Vehicle Dynamics https://www.tesis.de/en/vedyna/
[32] webpage: Vehicle Dynamics for use with MATLAB/Simulink https://millikenresearch.com/vdms.html
[33] webpage: Dynacar by Tecnalia http://dynacar.es/en/home.php

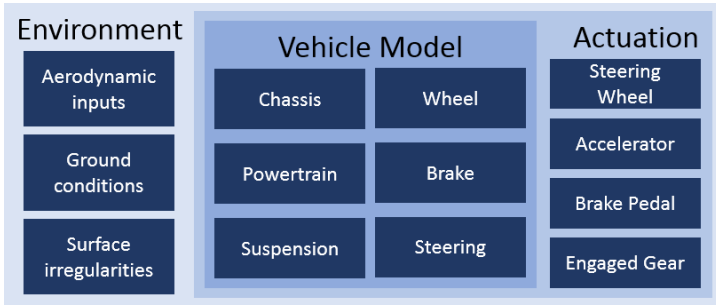

Figure 2.2 Vehicle simulation model systems

Handling Dynamics The handling requirements for vehicle simulations depend on the intended application. To simulate the longitudinal dynamics, just one degree of freedom may be sufficient. However, for the description of the lateral dynamics two or more are necessary [11]. In this sense, five techniques can be found for vehicle simulation modeling: point-mass, geometric, single-track kinematic and dynamic, twin-track, multi-body, finite-element, and hybrid vehicle models [58, 59]. A brief description of each modeling method is pointed next and are summarized in Table 2.1.

- **Point-mass model:** It considers the vehicle as a particle and it is commonly used in motion planning [60]. Even though it considers accelerations, it ignores the turning capacity of the vehicle [59].
- **Geometric model:** It considers the basic geometry of the vehicle and uses its geometric relationships for path tracking [61, 62]. Although it offers good robustness in most low-speed maneuvers, it ignores the velocity and forces on the vehicle which causes poor tracking performance at high speeds and transitional maneuvers [63].
- **Single-track models:** Allow a plausible description of vehicle behavior without major parametrization effort. Single-track models can be grouped into two approaches: kinematic or dynamic models. On one hand, **kinematic model** is a simplified representation that, besides geometry, considers the orientation, velocity, and acceleration of the vehicle [64]. It provides appropriate performance at low-speed (less than 5m/s) when tire deformations are small and slip-angles on the wheels can be neglected [65]. However, when the lateral forces on tires increase (e.g., while turning at high speeds), its accuracy is compromised [66, 67]. On other hand, **dynamic model** is a more complex vehicle representation that, besides geometry and kinematics, considers the internal forces and the inertia of the vehicle, providing accurate results in high-speed applications and extreme handling maneuvers [68, 69, 70]. Its implementation requires a tire model to estimate the longitudinal and lateral tire forces. For this purpose, a linear tire model is typically used, as it represents a good trade-off between computational efficiency and accuracy [71, 72, 73].
- **Twin-track model:** It is characterized by no kinematic wheel suspension as the wheels are assumed to be simply connected to the chassis being springs and dampers applied forces. It is sufficient for initial principle investigations or basic vehicle simulation models, however is not possible to investigate spatial motions of the wheels.

Table 2.1 Comparison of models in terms of performance and applications

Model	Strength(s)	Weakness(es)	Applications
Point-Mass	- Simplest model - Easiest implementation	- Ignores minimum turning	- Motion planning
Geometric	- Considers minimum turn - Robust in most maneuvers	- Ignores internal forces - Ignores acceleration - Not suitable at high speeds	- Motion planning/tracking - Low speeds - Constant speed/curvature
Single-track, kinematic	- Simple motion description - Considers chassis slip	- No wheel's slip/skid - Speed range is limited	- Motion planning/tracking - Low speeds (<5m/s) - Varying speed/curvature
Single-track, dynamic	- Accurate motion estimate - Handling dynamics - Stability at handling limit	- Tire forces calculation - Less numerical efficiency	- Motion planning/tracking - High speeds (>5m/s) - Varying speed/curvature - Chassis slip angles <5deg
Twin-track	- More accuracy	- No suspension model - No wheel spatial motion	- Motion tracking - Basic virtual platform
Multi-body	- Best accuracy - All suspension forces	- Low numerical efficiency - Complex implementation	- Motion planning - Virtual test platform
Finite-element	- Structural deformations	- No real-time use	- Examine chassis forces
Hybrid	- Rigid and elastic model	- No real-time use	- Examine tire forces

- **Multi-body model:** It is the most accurate representation of vehicle dynamics, which is mainly employed as a virtual test platform for driving automation developments. Its high complexity and low computational efficiency make it difficult to implement this method today for real-time applications, therefore it is barely used for motion planning [74].

- **Finite-element model:** It is primarily used to give a mathematical description of elastic and plastic characteristics of mechanical components, being not suitable for vehicle motion on real-time applications.

- **Hybrid model:** It combines multi-body and finite-element to model both rigid and elastic mechanical systems [11].

Performance Dynamics The two major components of longitudinal models are the vehicle dynamics (e.g. longitudinal tire forces, aerodynamic drag forces, rolling resistance forces, and gravitational forces) and powertrain dynamics (e.g. internal combustion engine, the torque converter, the transmission, and the wheels) [65]. A thorough description of these systems dynamics and how to model them can be found in [57, 9, 65, 64, 11]

Tire Dynamics A high influence in the vehicle dynamics is due to the forces and moments from the ground acting on each tire of the vehicle. The tire behavior depends on the geometric disposition of the layers of rubber-coated cords, which are commonly defined as *bias-ply* or *radial-ply* [9]. A brief description of each modeling method is described next.

- **Linear model:** As previously mentioned, it is typically used, as it represents a good trade-off between computational efficiency and accuracy [71, 72, 73].

- **Brush model:** It allows the estimation of longitudinal tire force at small slip ratios describing the tire as a series of independent springs that undergo longitudinal deformation [75, 76]. Although, good approximations for small slip ratio and angle are estimated through linear tire models [65], more sophisticated methods for large slip ratio and slip angle are required.

- **Elastic Foundation model:** For lateral force generation on tires enables the use of this simplification when large side-slip angles are present [77]. In the presence of both large slip ratio and slip angle, the combined lateral and longitudinal tire forces can be described using a parabolic normal force distribution [75].

- **The Magic Formula model:** It provides an accurate mathematical model based on empirical expressions, useful in broad operational conditions including both large slip ratio and slip angle and combined longitudinal and lateral forces calculation[78].

- **Dugoff's model:** An also complete alternative tire model which in contrast to the Magic Formula model can be analytically derived from lateral and longitudinal forces equations [79].

Actuation Dynamics The automation of a vehicle includes electromechanical systems attached to control devices (steering wheel, accelerator, and brake pedals) allowing the execution of commands from the control system. Two alternatives are often available in AVs: a) adapted external actuators or b) integrated internal actuators. Methodologies to obtain actuator models include system identification, real test characterization, and electromechanical properties consideration [80, 81].

2.1.1.2 Validation Methods for Vehicle Simulation Models

Most of the validation methodologies for vehicle simulation models coincide in contrasting simulation results with full-size vehicle experiments. Generally, a driving event is deconstructed and simplified to define a Standardized Test Maneuver (STM), which is employed as a validation assessment being is useful to predict the outcome driving events. An STMs can be performed by a steering robot or a human driver being classified in [82] according to response type (stochastic, periodic, transient, or steady-state), the application (fundamental or purpose dependent), the domain of analysis (frequency or time domain), and the input type (open or closed-loop). Regarding the required validation tests, the fundamental maneuvers[34],[35] are highly reproducible and are performed to determine the primary vehicle's dynamical characteristics. On the other hand, the purpose dependent maneuvers [36] are oddly reproducible but can approximate real-life behaviors. A combination of STMs in terms of response type, application, the domain of analysis, and input type is recommended for validation assessment as it covers as many aspects of vehicle dynamics as possible.

The validity of a vehicle simulation model is accepted under certain conditions according to [83, 84]: 1) In some portion of the operational range (e.g. low or high lateral acceleration maneuvers, small or large steer angle values, or input frequencies within a specified range), 2) For a specified group of inputs and outputs (e.g. valid simulation of lateral sprung

[34]standard: ISO 4138 https://www.iso.org/standard/54143.html
[35]standard: ISO 7401 https://www.iso.org/standard/54144.html
[36]standard: ISO 3888-1 https://www.iso.org/standard/67973.html

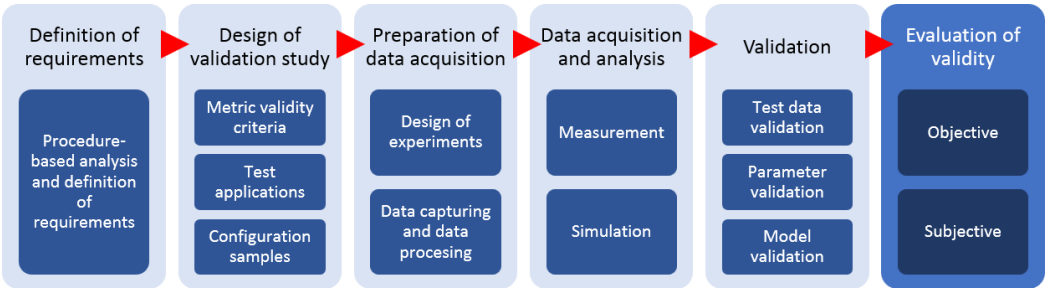

Figure 2.3 Vehicle simulation model validation process overview [2]

mass acceleration might not predict vertical sprung mass acceleration), and 3) Within the experimental random error level at a given operational point.

Figure 2.3 comprises most of the basic steps in the validation methodologies proposed in the literature ending with different *evaluation of validity* methods such as *objective* and *subjective* validation approaches, which are detailed next.

Objective Validation This strategy asserts that error and uncertainty estimation must occur both in experimental and computational results, as a necessary step in a validation assessment's judge [85]. Validation metrics rely on the statistical concept of *confidence intervals* and how many metrics are compared between *System Response Quantity* of interest from the computational model (SRQ^p) and physical experiment (SRQ^m).

In general, [86] presents a three-step statistical method incorporating experimental uncertainties into the computational analysis; 1) characterize the source of uncertainty, 2) ensemble of calculations and 3) uncertainty quantification of the output. This methodology concludes that taking the mean value of all input parameters does not lead to a mean value of the output, and the ensemble of calculations contributes to a better estimation of the output in the simulation model. Given the importance of predictions for *virtual prototyping*, [87] develop frameworks for assessing the predictive uncertainty of computing applications.

Focused on vehicle simulation models, [83] presents arguably the first objective approach defining two development branches for experimental and simulation tasks. In experiments, both the SRQ^m and inputs to excite the physical system must be appropriately measured and recorded. The data reduction includes analogic-digital conversion, digital filtering, and Fourier transformation. In simulations, the same inputs employed in the experiments consider the obtention of SRQ^p, including an assembling process. The simulation data includes Fourier transformation or data file size reduction. The quantitative study considers time-domain and frequency-domain metrics. At the end of this procedure, both qualitative and quantitative comparisons are recommended from experiments and simulation data sets.

In [88], a methodology aims to validate a specific application to be simulated, allowing the definition of fewer parameters, repetitions, and maneuvers. Also, the proposed method does not require driving robots or dedicated test areas. This validation method targets 4-steps: 1) Parametrization, 2) Isolated lateral vehicle dynamics validation, 3) Isolated longitudinal dynamics validation, and 4) Combined lateral and longitudinal dynamics validation. The calibration and validation processes are separated, using a set of experimental data for vehicle model calibration different from the one used for simulation model

validations.

In [2], a novel concept proposes statistical measurements considering the SRQ^m from more than one experimental vehicle and contrast them with SRQ^p from different model parametrizations, instead of the usual 1-to-1 comparison between measurements and simulations. In [89], a contrast of four different statistical methods to construct a confidence band is used to compute an accumulated validation metric. A sine wave lane change maneuver is employed in simulation runs, adjusting the vehicle mass to resemble varying experiments.

Subjective Validation In this approach, the consistency between simulation model results and the perception of how the real system should operate is performed by expert decision-makers. This procedure is also known as *face validity*. Although objective approaches are useful in the judge of simulation models, subjective methods as the *hypothesis test* contribute to a final validation [90, 53, 91]. Moreover, approaches as the *model builder's risk* and *model user's risk* [86] provide concepts of error types to avoid incorrect conclusions.

In general, [92] presents a 7-step approach for conducting a successful simulation study, along with practical techniques for developing valid and credible models. It recommends *sensitivity analyzes* to evaluate those factors with the greatest impact on performance measures. In this case, statistical experimental design [93] is the endorsed approach when two or more factors of interest are considered in the analysis. Additionally, two basic principles and common difficulties are described as guidelines for obtaining good model data.

Focused on vehicle simulation models, [84] lists three primary phases including experimental data collection, vehicle parameter measurement, and comparison of simulation predictions with experimental data. The experimental data collection considers six categories of testing maneuvers and strives to determine the experimental random error level present in the data. The vehicle parameter measurement emphasizes that is an unacceptable practice to employ parameters that are impossible to measure in simulations. It also recommends performing simulation validations using several different vehicles. The parameters which describe the vehicle simulation model must be measured independently without using the data from experimental measurements, as the major goal is the prediction of experiments.

Different approaches for data assessment, reference points definitions, intervals analysis, experimental and simulation data processing are presented in [82] employing a double lane change maneuver as a case study. Two more STM such as step response and sine sweep maneuvers presented in [12] complete the mentioned study developing a general validation methodology considering the V-model for project management, however, the proposed methodology focuses only on lateral vehicle dynamics.

2.1.2 Validation of Automated Driving Systems

After the validation process of vehicle simulation model is completed, a reliable simulation test platform which resembles the actual vehicle dynamics is achieved. Based on this vehicle simulation model, virtual testing is a practical and valuable tool for the developent of ADAS/ADS. Currently, several simulators for ADAS/ADS are currently available including

ANSYS[37], TASS PreScan[38], Gazebo[39], Apollo[40], CARLA[41], VI-grade[42],and AirSim[43].

In the validation of Automated Vehicles (AVs), two approaches are commonly considered. First, that the intended functionality (see Section 2.2) is safe enough in the absence of technical failures (such as random or systematic failures in hardware or software)[44]. Second, that the intended functionality, once its safety is ensured, is robust enough in the presence of technical failures[45] (see Section 2.3). In this section, a brief explanation regarding the design of ADS is given, before the assessment of different ADS validation methodologies.

2.1.2.1 Design of Automated Driving Systems

The design of ADS includes the hardware and software capable of performing the entire DDT on a sustained basis, regardless of whether it is limited or not to a specific Operational Design Domain (ODD) [1]. ADS requires several systems, each one responsible for a different task. Current developments involve the proposal of similar control architectures, whose pioneer approaches were tested on experimental vehicles at DARPA Grand Challenge [62, 94]. Commonly, three tasks covering perception, decision, and control, are considered essential to enable ADS, being also fields where advances are currently required [3, 4, 5].

An abstracted perspective of a control architecture for ADS is depicted in Figure 2.4. Contributions in this Ph.D. Thesis are focused on *Decision*, *Control*, *Actuation*, and *Supervision* systems, with special emphasis in those components highlighted in dark-blue (vehicle and actuation simulation models, behavioral and local planning, trajectory tracking, failure detection and response). The vehicle-driver-environment interaction on the top represents a way to define validation methods for virtual testing, which is an aspect thoroughly considered in Chapter 3. A description of the main systems is developed next.

Acquisition The acquisition senses the in-vehicle states and ego-vehicle surroundings. **In-vehicle sensors** include accelerometer, gyroscope, wheel speed, and steering wheel angle sensors. A combination of accelerometers, gyroscopes, and magnetometers into the same electronic device is known as an Inertial Measurement Unit (IMU). A different combination of in-vehicle sensors enables the implementation of ADAS such as: Anti-lock Brake System (ABS), Traction Control System (TCS), and different Electronic Stability Control (ESC) approaches including differential braking, steer-by-wire, and active torque distribution [65].

Surrounding acquisition devices include RaDAR, LiDAR, and camera. **RaDAR** provides high accuracy direct distance and velocity measurements relative to ego-vehicle [95, 96], being useful for object detection both in short-range (auto parking and blind-spot) and long-range (Adaptive Cruise Control (ACC) and collision avoidance). **LiDAR** offers a high resolution of direct distance measures at medium range for a large field of view

[37] webpage: ANSYS | ADAS and Autonomous Vehicles https://rb.gy/1bzqgp
[38] webpage: PreScan | Simulation of ADAS & active safety https://rb.gy/0swwbc
[39] webpage: Gazebo | Robot simulation made easy http://gazebosim.org/
[40] webpage: Apollo Simulation | A comprehensive solution for the development...https://rb.gy/vk6oud
[41] webpage: CARLA | Open-source simulator for autonomous driving researchhttps://carla.org/
[42] webpage: VI-gradehttps://www.vi-grade.com/
[43] GitHub: Microsoft AirSimhttps://github.com/microsoft/AirSim
[44] standard: ISO/PAS 21448 https://www.iso.org/standard/70939.html
[45] standard: ISO 26262 https://www.iso.org/standard/68383.html

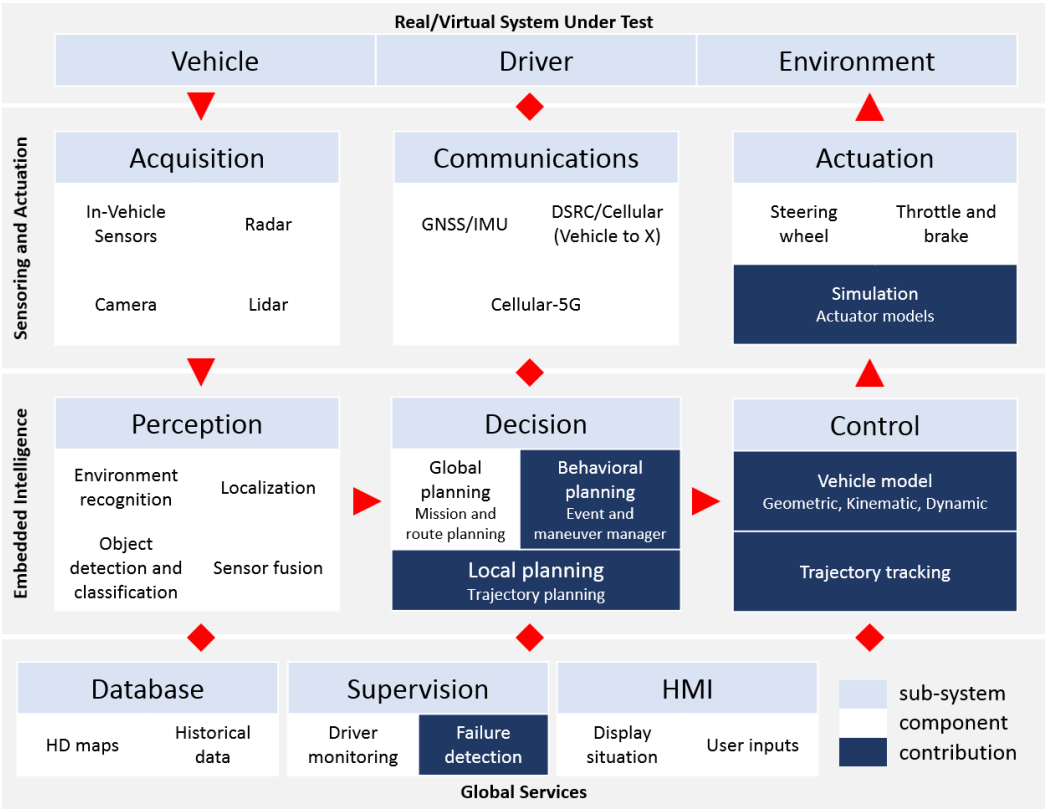

Figure 2.4 Abstracted control architecture for ADS based on [3, 4, 5]

of three-dimensional point clouds around ego-vehicle [96]. Road markings, pedestrians, bicyclists, and cars can be recognized by LiDAR [69]. Single, stereo and infrared **cameras** provide 2D images from the real world used mostly for an on-road vehicle, pedestrian, lane markings, and traffic sign detections [97]. A thorough comparison of different devices is presented in [98].

Communication The communication receives data for Global Navigation Satellite System (GNSS), Dedicated Short-Range Communications (DSRC), and Cellular-5G technologies. **GNSS** is classified under communication sensors instead of acquisition sensors as it triangulates the ego-vehicle global position and velocity using an antenna to communicate with satellites, achieving different accuracy levels such as: Standard Positioning Service (SPS, 3-8m), Differential GPS (DGPS, 1-3m), and Real-Time Kinematic Global Positioning System (RTK-GPS, 2-40cm) [99]. **DSRC** enables vehicle-to-X (V2X) low latency end-to-end wireless communications, being a suitable and relying option for safety applications related to vehicle-to-pedestrian (V2P), vehicle-to-vehicle (V2V), and vehicle-to-infrastructure (V2I) communications [100]. **Cellular-5G** represents several improvements for V2X with respect to DSRC in aspects such as coverage range, scalability, deployed infrastructures, capacity, and throughput. However, 5G still needs development in latency

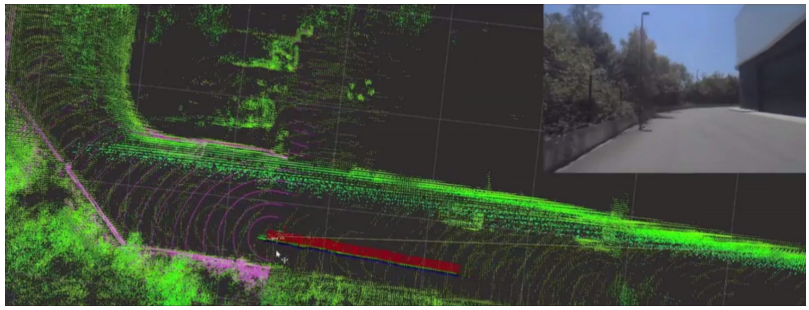

Figure 2.5 LiDAR-based localization through 3D mapping (courtesy of the University of Alcala de Henares, Irizar e-Mobility and AutoDrive Project)

for ADS applications [101].

Perception The perception processes the data from acquisition and communication, building a surrounding model, and performing ego-vehicle **localization**. The surrounding model includes **object detection and classifications**, which are usually improved by combining the strengths of dissimilar sensors using centralized, decentralized, and hybrid sensor fusion architectures [102]. Mathematical methods for **sensor fusion** include probability, artificial intelligence, and theory of evidence techniques [103]. Additionally, the surrounding model allows the **environment recognition** for collision-free driving, building a map from prior or Simultaneous Localization And Mapping (SLAM) methods [104]. In this sense, global ego-vehicle localization based on communication (GNSS/IMU) can be combined with local localization through detecting pedestrians, vehicles, road shapes, road markings, and landmarks [105]. Figure 2.5 shows an example of a LiDAR-based localization.

Decision The decision receives the localization, environment model, and communication data, which is employed for global, behavioral, and local planning. Different planning techniques are classified according to the desired implementation in ADS, such as graph search, sampling, interpolating, and numerical optimization [3]. At the highest decision level, **global planning** (also known as strategic planning) defines the mission or route from the current position to the desired destination considering safety, speed, distance, and energy efficiency [106]. This process is mostly performed offline because both the road network and traffic data are commonly requested in an external database [4]. Examples of route planning algorithms include arc flags, customizable route planning, contraction hierarchies, transfer patterns, and round-based public transit optimized router [107].

After a route is defined, **behavioral planning** (also known as tactical planning) manages real-time events related to other road users, road conditions, and signals from infrastructure, defining the best driving maneuver. One approach described in [62] is to use a finite state machine with transitions governed by the perceived driving context such as relative position concerning the planned route and nearby vehicles. Techniques for uncertain urban settings presented in [108] include gaussian mixture models, gaussian process regression, learning techniques, model-based approaches, and Markov decision processes.

When driving behavior is specified, **local planning** (also known as reactive planning)

calculates a dynamic feasible, comfortable, and collision-free trajectory, considering an estimated ego-vehicle pose and drivable space provided by the perception. Examples of numerical approaches are variational methods, graph-search approaches, and incremental tree-based [3, 108]. Current developments on trajectory planning are showed in Section 2.2.1.

Control The control calculates appropriate actuation commands to correct tracking errors on trajectory reference estimated by decision. The longitudinal and lateral motion control is achieved by correctly selecting the steering wheel, throttle, and braking pedal position. Therefore, **trajectory tracking** comprises path and speed tracking which can be developed in a coupled or decoupled way. ADAS/ADS functionalities for longitudinal and lateral motion control include Cruise Control (CC), Adaptive Cruise Control (ACC), Cooperative-Adaptive Cruise Control (CACC), and lane-keeping assist [109]. As one source of trajectory tracking errors is an inaccurate **vehicle model** [108], this Ph.D. Thesis attempts to contribute to vehicle modeling, aiming for robustness and stability in the motion control task. Important works on trajectory tracking techniques are presented in Section 2.2.2.

Actuation The actuation executes the commands defined by the control. Current automotive systems are developed with drive-by-wire components that integrate electromechanical actuators and signal-based functions to facilitate the implementation of automated functionalities [110]. Examples of these systems are the electronic acceleration pedal and electrically driven **accelerator** or injection pump [111], the electronic **brake** pedal and electrical pneumatic booster, and electrical power **steering** [112].

Advances in solid-state electronics, sensors computer technology, and control are playing an increasing role in the development of automated driving functionalities such as active stability control systems, ride quality, fuel economy, and vehicle emissions [65].

In general, control is ignored among validation procedures as an appropriate response of the actuation devices is assumed. However, control inputs often do not resemble clear signals, and disturbances on electromechanical devices (e.g. time delay, signal amplitude, noises, etc.) are critical for realistic virtual testings and must be considered in **actuation simulation models**.

Database The database contains relevant information related to the alternative routes in the surroundings. The global planning component uses the available information to construct a route according to the mission defined by the user. **Digital maps** can be considered to increase the positioning accuracy based on digital landmarks processed by the *perception* [4]. **Historical data** allows artificial intelligence to use information as inputs to causal reasoning for machine learning algorithms [98].

Supervision The supervision is often represented as a parallel branch in the entire ADS control architecture and connected to specific systems providing at least fail-aware responses. On one hand, non-technical failures provoked by the driver behavior can be covered by **Driver monitoring**, enabling the detection of fatigue or monotony contributing to the prevention of crashes [113]. On the other hand, technical failures provoked by hardware or software devices are covered by **failure detection**, allowing the implementation of

more refined architectures that target fail-safe and (or) fail-operational behavior from the intended driving functionality. Advances on DDT fallback strategies and fail-operational architectures are thoroughly presented in Section 2.3.

Human-Machine-Interface The Human-Machine-Interface (HMI) is the interface between the human driver or passenger and the ADS. **Display situation** describe outputs to the user respect to the ego-vehicle and its surroundings, allowing the driver to have a broad perspective of the current DDT status. **User inputs** allow selecting those ADS tasks defined by the HMI designed such as driving destinations, lane change maneuvers, and road exits allowances [114].

2.1.2.2 Validation Methods for Automated Driving Systems

As a large number of traffic condition combinations are possible during the driving process, different approaches to address safety validation of ADS have been proposed in [115, 6], such as: traffic-simulation-based testing, scenario-based testing, formal verification, function-based testing, real-world testing, shadow mode testing, and staged introduction of AVs. A brief explanation of these approaches is presented next.

Traffic-Simulation-Based Testing This concept targets the simulation of road networks, being suitable for macroscopic assessments. Multi-agent simulators of virtual cities show that lower accidents number can be achieved with higher levels of driving automation [116]. Moreover, the occurrence frequency and damage severity of scenarios [117], and component failures or inaccuracies [118] can affect the overall traffic safety. The efficiency of staged introduction of AVs method can be increased with traffic-simulation-based testing as it is compatible with the Operational Design Domain (ODD) expansions, however, both methods are still not suitable for validation of SAE L5 systems [6].

Scenario-Based Testing Fostered by the rapid market introduction of ADS, scenario-based testing is mostly employed as validation methodology following the process depicted in Figure 2.6. A Driving scenario is defined as a temporal sequence (typically around 10s [6]) in which driving events occur. It can be categorized as functional (verbal description), logical (parameter ranges and distributions) or specific scenarios (exact parameter values) [119, 120]. The parameters which describe logical and specific scenarios are divided into six layers such as 1) surface condition, 2) traffic infrastructure, 3) temporal construction sites, 4) road users and objects, 5) environment conditions, and 6) digital information [121, 122].

In this sense, specific scenarios can be selected using testing-based methods that focus on covering the scenario space, or falsification-based techniques that focus on finding corner case scenarios. The scenario space coverage or ODD must include a large number of possible driving situations, even considering the six-layer model if an ODD expansion is considered. The corner case scenarios are particularly relevant due to safety assessment failures that can be used for both improvement and insight into the performance capabilities of ADS [123].

The scenario execution is usually developed using physical or X-in-the-loop (XiL) testing enabling the modeling and definition of verifiable driving scenarios and functions [124]. The XiL simulation testing includes acquisition and communication (Hardware-in-the-loop, HiL), real-time coding for hardware components or vehicle dynamics (Software-in-the-loop,

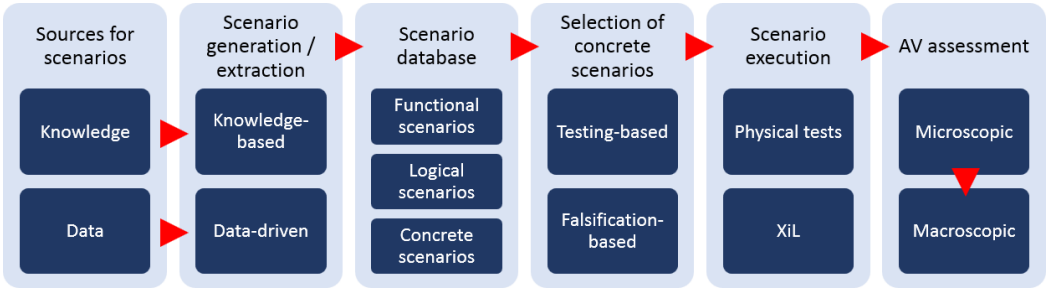

Figure 2.6 Taxonomy of the scenario-based testing [6]

SiL) [125], and full-scale AVs testing in a HiL environment (Vehicle-in-the-loop, ViL). Consequently, hardware components are connected to the virtual environment to test ADS both in real-world and simulations [126].

Scenario-based testing is also differentiated between those concerning ADAS and ADS. While ADAS scenarios bottomed on rating purposes and consider simplified scenarios such as wide test grounds, ADS scenarios set up in a more refined way considering several sources such as accident statistics, field tests, simulation results, brainstorming of experts, experience, and systematic deduction [115]. **This validation method is employed in this Ph.D. Thesis and is described in-depth in Chapter 3.**

Formal Verification Formal verification of safety requires the specifications and traffic rules across an entire ODD, which must be made available in a machine-readable format [6]. Compliance of traffic rules among road participants eliminates the accidents produced by AVs, therefore, a set of traffic rules in a formal language were developed [127]. The theorem proving, reachability analysis, and correct-by-construction synthesis, are distinguished as formal verification methods. Some examples of theorem provers are the responsibility-sensitive safety [128], KeYmaera [129] and Isabelle [130]. The reachability analysis is mainly performed online during run-time and determine that reachable states (from given initial states, inputs, and parameters) do not intersect with the occupancy of other traffic participants [131]. The correct-by-construction synthesis aims to automatically generate controllers from formal specifications such as linear temporal logic [132],

Function-Based Testing The requirements and specifications phase defines the system functions for experiments or simulation. The developed functionality is then tested considering a fixed scenario to confirm its performance. The function-based testing approach is broadly employed in standardized procedures for ADAS functionalities validation such as ACC[46] and Automatic Emergency Braking (AEB)[47]. This approach is difficult to implement in ADS functionalities validation as the definition of every conceivable situation is nearly impossible. The assessment result (even from a predefined standardized test set) might not correspond to possible real-world scenarios, therefore it should not be used in future regulations [6].

[46]test protocol: Euro NCAP - Lane Support Systems https://rb.gy/sfjzok
[47]test protocol: Euro NCAP - VRU AEB https://rb.gy/xwgwil

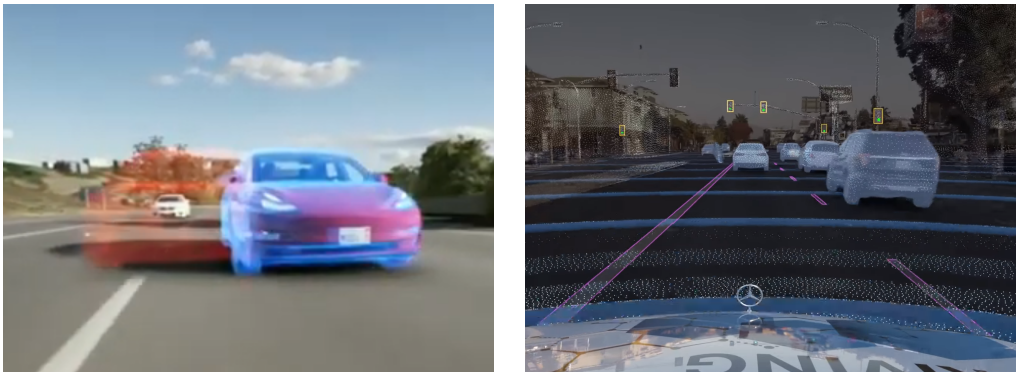

(a) (b)

Figure 2.7 ADS testing on (a) shadow mode with faster car overtaking at right side from Tesla[48] and (b) staged introduction of AVs from Mercedes-Benz[49]

Real-World Testing Although this method is the standard for SAE levels 2 or below, it is economically unfeasible for ADS [6]. In real-world testing, the entire system is assessed in realistic scenarios. Affirming with enough confidence that ADS outperform human drivers requires 11 billion miles driven with fewer fatal accidents [133]. Nonetheless, easy driving situations are handled most of the time, and rare or challenging events are difficult to trigger. A residual risk without an uncertainty cannot be determined as even the most comprehensive statistical proof does not guarantee a full test approach [134, 135].

Shadow Mode Testing In this validation method, the vehicle is being driven by a human or an ADS, meanwhile, other ADS is passively executed receiving real data from the acquisition devices but having no access to real actuators on the vehicle. This procedure permits the evaluation of the safety level of new decision-making algorithms before real implementation [136]. A relevant aspect is a comparison between road user behaviors in simulation and reality, as considerable differences represent a drawback due to only limited validity is provided [6]. This method is employed by automakers to test versions of ADS [48] (See Figure 2.7a).

Staged Introduction of AVs This method aims to limit the occurrence of traffic events, making economically feasible the safety assessment based on a real-world approach. The limited ODD safety concept includes a trained driver to react if necessary. When safety validation is ensured, the ODD can be gradually expanded and even the safety driver be omitted. This approach is currently applied in pilot projects for the introduction of SAE L4 vehicle in urban areas [49] (See Figure 2.7b). Although this procedure seems promising, some authors believe that it is not suitable for validation of SAE L5 systems [6].

[48] video: What is Shadow Mode Tesla Autonomy https://rb.gy/raozcj
[49] video: Mercedes-Benz Pilot Project | Automated Ridesharing Service https://rb.gy/75hhw3

2.1.3 Credibility in Virtual Testing

The literature survey considers different methods of vehicle simulation model validation, including confidence intervals and face validity. Most of the validation approaches rely almost exclusively on one or another method, without taking advantage of each method's strengths. For example, face validity is predominantly applied as a validation approach, although is biased by individual opinions and experts would reach different conclusions. In this regard, an appropriate quantification assessment would contribute to the final judge of decision-makers.

A compromise between objective and subjective assessments into a same procedure would represent an improvement. Although objective approaches as *error*, *uncertainty*, and *confidence intervals*, are suggested for the overall simulation model validation, subjective methods as the *hypothesis test* contribute to a final validation [90, 53, 91], as even though they do not contribute in quantification, these approaches provided concepts of error types to avoid incorrect conclusions such as: *model builder's risk* and *model user's risk* [86].

A direct relationship between vehicle dynamics and ADS is not evident in current validation procedures, being this essential for virtual testing in automated driving. Consequently, vehicle dynamics validation methods should consider the behavior of the actuation, which most of the cited works ignore and is present in all ADS. Moreover, available STM are not representative of traffic-based driving scenarios, where safety and comfort in both lateral and longitudinal motion control are crucial in urban environments. Finally, test cases, data handling, and metrics must be effectively described in validation projects, trying to obtain the best balance between effort to gain model confidence and value to the final user.

Based on the previous analysis, this Ph.D. Thesis proposes a novel approach for both vehicle dynamics model and ADS validations in Chapter 3. The credibility in virtual testing increases when modeling techniques target both actuation and vehicle dynamics using simulation environments flexible enough to allow road actors and scenario-based testing for AV microscopic assessment.

2.2 Safety and Comfort in Vehicle Motion

The vehicle motion contains a series of tasks for trajectory planning and tracking that allow reaching destinations while avoiding obstacles safely and efficiently. Based on a previously built environment map, the vehicle trajectory generation comprises global and local approaches combined with the capability to perceive situations that might represent a risk. To properly track trajectories, actuation commands are estimated to minimize lateral deviation distance from the center-path, heading, and speed references.

Safety and comfort are design constraints to be considered when designing novel ADS features. Hence, they must be considered in the whole validation process depicted in Figure 2.1, especially in complex ADS which handle highly unpredictable environments [137]. As safety and comfort are important design constraints in these subsystems, an analysis will also be carried out considering these.

2.2.1 Trajectory Planning

Trajectory generation is an essential task concerned with the real-time planning of a vehicle's state feasible transition. For that purpose, kinematic limits based on vehicle dynamics

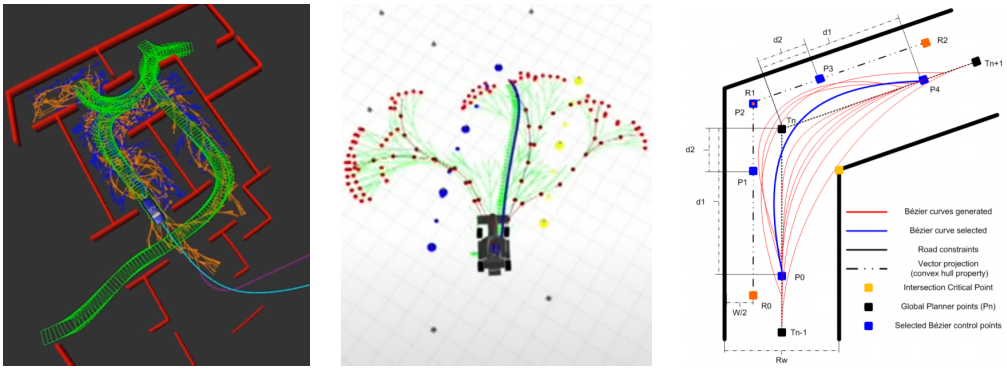

(a) (b) (c)

Figure 2.8 (a) A*[50], (b) RRT[51], and (c) Bézier [7] path planning techniques

have to be considered, along with the constraints imposed by different driving situations, such as navigation comfort, lane boundaries, traffic rules, road users avoidance, ground roughness, and ditches [138]. Several techniques oriented to road networks and driving rules are presented in this section, are classified into four groups regarding the intended implementation: graph search, sampling, interpolating, and numerical optimization [3].

2.2.1.1 Graph Search Methods

The graph search algorithms enable the solution of path planning in discrete configuration spaces, often represented as an occupancy grid map or lattice [139], depicting where the neighbor objects are in the surrounding cells while considering the vehicle's evolution over the time [140]. **Dijkstra Algorithm** continuously examines possible neighbors on closest node not yet examined and stopping when the goal node is achieved [141]. It has been employed to construct paths for self-driving cars [142] navigating forwards and backwards in a parking lot [143], and urban implementations [144]. **A* Algorithm**[50] implement heuristic for faster node searching using cost functions to define node weights [145]. Several authors have achieved improvements using **A* Algorithm** as a development basis such as **Anytime Dynamic A*** [146], **Anytime D*** [94], and **Hybrid-State A*** [147]. In another approach, **State Lattice Algorithm** performs the motion planning search over a hyper-dimensional grid of states [148], where time and speed dimensions are mostly considered for developments [149]. It has been employed to define the driving centerline path [150], iterative optimization [151], tactical reasoning [152], and candidate paths along a route [153]. However, graph search algorithms present some drawbacks such as relying highly on grid map resolutions, vehicle dynamics is ignored [4], as well as a high computational cost when vast and unknown search areas [154] with large objects number are considered [3].

2.2.1.2 Sampling Methods

The sampling-based algorithms randomly sample the state space for collision-checking, dealing with the problems faced by graph search methods. **Rapidly exploring Random**

[50] video: A* in Action - Artificial Intelligence for Robotics https://rb.gy/hhb0bq

Tree Algorithm (RRT)[51] is the most influential sampling method for the trajectory planning of AVs [155]. It is suitable for unknown environments as nodes are constructed in the state space evolution [156], allowing fast planning in semi-structured spaces executing a random searching tree navigation. Available differential constraints can be associated with vehicle dynamics and path curvatures [4], guaranteeing kinematic feasibility and enabling reactive generation use [156]. However, suboptimal path solutions (jerkiness and curvature continuity lack) have been demonstrated with RRT [157]. In this regard, several improvements are proposed such as **Optimal RRT (RRT*)** for asymptotic optimality [158], **Linear Quadratic Regulator-RRT* (LQR-RRT*)** for complicated dynamic problems [159], and **Informed RRT*** for convergence rate and final solution quality improvements [160]. In another approach, RRT variants have been employed to reuse trajectories built in previous planning cycles [161], and generate smooth, continuous, and feasible trajectories based on B-splines in the post-processing phase [162]. Some drawbacks of RRT family techniques are, the resulting jerkiness due to non-continuous trajectories, as well as the path's optimality depends strongly on the execution time frame [3].

2.2.1.3 Interpolating Methods

The interpolating methods use a previously known set of waypoints (e.g. those obtained from graph search and sampling methods) to generate new ones that can be employed for smooth path and speed planning. **Line and circle** focus on minimal length paths with both curvature and start/end position constraints. Despite simplicity is not realistic for curvature continuity of vehicle models [163, 156]. **Clothoid** offer a continuous curvature function according to road designs. However, due to its iterative construction process, the computational effort is high [164]. **Sigmoid** provides a solution to trajectory candidates generation in lane changes useful for highway geometries [165]. Point-based curves subfamily as **polynomial functions** [151], **spline curves** [149], and **Bézier curves** [166] are suitable for geometrically constrained environments and ego-vehicle dynamic constraints assurance [156]. Some authors claim that **spline curves** results might not be optimal as it focuses more on achieving continuity instead of meeting road constraints [167]. In contrast to sampling methods, interpolating techniques enable a continuous curvature path suitable for comfortable driving, in addition to a low computational cost. A comprehensive review of the pros and cons of these methods is presented in [3].

2.2.1.4 Numerical Optimization

The numerical optimization methods minimize or maximize a function with constrained variables. It is broadly used in motion planning, either to decrease graph exploration solving times or to exploit problem mathematical properties [156]. **Linear programming (LP)** is the simplest algorithm which solves a linear cost function under linear inequalities or equalities [151]. The Levenberg-Marquardt algorithm is useful as a special case for non-linear problems optimization [168]. **Quadratic programing (QP)** consists on a convex approximation solution to the original problem using an iterative search [169]. **Dynamic programing (DP)** breaks complex computational problems into simpler interdependent subproblems that combined achieve the global problem solution [170]. Finally, **MPC** is the most popular predictive application solution. It solves the problem at each time step

[51] video: Autonomous Racing | AMZ Driverless with flüela https://rb.gy/48ajk5

over a horizon time, applying the first sequence of control actions [171]. Although its replanning ability is the main advantage, it is not suitable for non-convex and high complex problems [156]. Several solving packages for numerical optimization are currently available including CVX[52], CVXGEN[53], Gurobi[54], YALMIP[55], MATLAB Optimization Toolbox[56], NPSOL[57], and ACADO Toolkit[58].

2.2.2 Trajectory Tracking

The trajectory tracking task is essential in the design of ADS as it is responsible for the guidance of the vehicle. It receives a feasible obstacle-free path and speed references from the trajectory planning task. Additionally, it considers the vehicle states estimated by the perception and decision. Consequently, it deals with the vehicle motion control using the steering wheel, accelerator, and brake pedal as control actions in an appropriate manner, ensuring control stability and avoiding both delays and overshoots. Several control strategies oriented to perform trajectory tracking are presented in this section, being classified into five groups: linear, nonlinear, optimal, adaptive, and robust control.

2.2.2.1 Linear Control

This approach is governed by linear differential equations applied under the assumption that the outputs of systems are roughly proportional to their inputs. A **proportional-integral-derivative (PID)** control is a widely used linear technique for both longitudinal and lateral vehicle motion control[59]. Although it is simple and effective, even a well-designed PID control (which would be a time-consuming task due to parameter tuning) still has low robustness. A **full-state feedback** control allows modeling the vehicle as a linear dynamical system, contributing to the tuning procedure via pole placement [172], although look-ahead distances can reduce the noise in offset measurements, noticeable overshoots and degraded performance can occur during maneuver transitions [173]. A **feedforward** control is suitable for handling rapid maneuver variations, allowing the anticipation of future changes in road's curvature [174]. The feedback and feedforward combination increase the robustness of control [175]. From a comparative study, a **lead-lag** control also offers a good performance in path tracking contributing also with the reduction of undesirable frequency responses [173]. Although linear methods are of simple applicability and low computational cost, they are sensitive to measurement noises and provide poor responses at sudden transitions.

2.2.2.2 Nonlinear Control

This approach is governed by nonlinear differential equations applied more on real-world control that do not obey the superposition principle. Several nonlinear controllers are based on the kinematic bicycle model due to its advantages for trajectory tracking [108].

[52] webpage: MATLAB Software for Disciplined Convex Programming http://cvxr.com/cvx/
[53] webpage: Code Generation for Convex Optimization https://cvxgen.com/
[54] webpage: Gurobi Optimizer https://rb.gy/pu97de
[55] webpage: YALMIP | Solvers https://rb.gy/idxccs
[56] webpage: MathWorks | Optimization Toolbox https://rb.gy/klvkam
[57] webpage: User guide for NPSOL 5.0: Fortran package for nonlinear programming https://rb.gy/hgnerc
[58] webpage: ACADO Toolkit https://acado.github.io/
[59] video: Controlling Self Driving Cars https://rb.gy/al0hdc

The **Lyapunov stability-based** control is used to avoid undesired lateral behaviors as collisions and lane departures [176], nonetheless, the speed is assumed constant as the system is time-invariant [177]. To overcome this issue, a **backstepping** control can be used to achieve uniform local exponential stability for a finite domain with time-varying references [178]. If higher speeds are required (e.g. highway applications), a **feedback linearization** control can be used to constrain the steering angle and perform a continuous lateral vehicle motion [179]. However, to cover a broader speed range (e.g. from urban to highway applications) a **gain scheduling technique** is required to avoid oscillatory responses [173]. The last method is a category of control design for **Linear Parameter Varying (LPV)** models [180]. Although these methods deal with nonlinear models or uncertain parameters, they are also sensitive to parameter variations, and the proof of stability is problematic. Moreover, nonlinear observers are required if all state variables are not measurable.

2.2.2.3 Intelligent control

This approach integrates several techniques and concepts from different disciplines including computer science, control theory, fuzzy logic, genetic algorithms, and neural networks. Fuzzy control transforms inputs into linguistic variables using membership functions, and outputs are chosen based on if-then-like form rules [181]. **Fuzzy logic** cover a wide range of driving functionalities such as steering and angular speed for lateral control [182], human-like driving behavior in CACC [183], and single lane change for overtaking maneuvers [184]. However, tuning of membership functions is not straightforward, stability analysis is not possible, and rules would become unmanageable depending on variables number. **Genetic algorithms** are for general-purpose searching on population candidates to evolve the problem solution. This technique has been applied to automatically tune membership functions on fuzzy logic control [185]. **Neural networks** assigns weights to each connection of an adaptive net capable of learning, the weights tuning is performed using training data to imitate driver reaction. Nonetheless, the need for training data and no explanation in case of failures are the main drawbacks [181]. In general, intelligent control methods allow abstraction from the plant and the model, but some may imply high computational cost (Genetic Algorithms), and their stability is still an open research area.

2.2.2.4 Optimal Control

This approach is governed by a set of differential equations describing the paths of control variables that minimize cost functions. The most popular optimal technique in path tracking is the Linear Quadratic Regulator (LQR) [186]. The LQR feedback control combined with an external feedforward control provides both robustness and tracking accuracy [187], nonetheless, a great effort in tuning the weighting matrixes to increase robustness is required [4]. Indirect methods have the advantage of reducing the optimization dimensionality to the state space, as the **Pontryagin's minimum principle** [188] which is defined by a two-point boundary value problem solved by the **shooting method** [189]. Optimal control methods have the advantage that they allow multiple terms to be weighted to obtain optimal trajectories, however, most of the approaches are based on linear models (such as the LQR-based ones), and their computational cost may be high due to the required optimization process.

2.2.2.5 Adaptive Control

This approach adapts the control parameters to the controlled system. Unknow parameters, time-varying parameters, and unknown disturbances can be solved by adaptive controllers for automatic guided vehicle applications such as trajectory tracking [190, 191] and skidding ratio estimation [192]. One drawback of this technique is the difficulty of tuning adaptive parameters, being often defined using trial-and-error or simulation [193]. A combination of adaptive controllers with nonlinear techniques such as **Inversion and Immersion (I&I)** control and **Proportional-Integral (PI)** control have been used for trajectory tracking. Although both approaches offer good performance, I&I showed to be sensitive to uncertainties [71], and PI have a detrimental effect on the actuators due to high gains when operated in the nonlinear region of vehicle dynamics [71].

2.2.2.6 Robust Control

This approach explicitly deals with uncertainty achieving robust performance and stability within a modeled error bound. The **Sliding Mode Control (SMC)** is a robust technique that with a simple structure can deal with driving disturbances such as crosswinds, varying vehicle parameters, and changing road friction [194]. As in SMC, the control power is unnecessary large due to chattering issues [195], this phenomenon is reduced using saturation functions, switching functions, and high order SMC techniques [196]. **H_∞ loop-shaping** control is another robust technique that motivates the path tracking of ground vehicles such as tractor-semitrailer-combination in the presence of slip [197]. A comprehensive design and comparison of robust nonlinear controllers for the lateral dynamics are described in [71]. Note, however, that robust controllers may present chattering problems (e.g. in the SMC controller), which may damage the actuators if not considered in the design.

2.2.2.7 Model Predictive Control

Advances in programming algorithms and computing power enable the implementation of predictive control on real-time applications of automated driving. In contrast to the moderate driving conditions that can be solved by simpler control laws described before, Model Predictive Control (MPC) can handle high fidelity models to execute moderate, aggressive, or emergency maneuvers [108]. Its attractiveness comes from the capacity to include system constraints, including those related to safety and comfort, both in the current state and future ones [198]. This technique has been implemented in several automated driving applications such as ACC [199, 200], active front steering [201], vehicle handling [202, 68], and closed-loop stability [203]. The successful implementation of MPC is dependent on a proper model and an appropriate solver to ensure real-time performance. Due to the advantages of MPC, this control approach is the main focus of this Ph.D. Thesis contributing to trajectory tracking solutions as those described as follows.

Linear MPC It mostly solves convex quadratic programs exactly at each sampling time [204]. Several studies in the last decade determined that acceptable computation times are possible after a single linearization of the vehicle's state at the current time step [205], and by providing conditions for the uniform local-asymptotic stability of a *Linear Time-Varying Nonlinear MPC (LTV-NMPC)* recast into a quadratic problem [203]. A linear vehicle model and dynamic tire model combination have the efficacy to bound the vehicle

motion within this stable region of the state space, controlling the vehicle at the limits of handling [70].

Unconstrained MPC approaches resulted in minimal computational requirements [206] using a linearized kinematic model and time-varying linear quadratic programming [207]. However, constrained MPC methods also achieve high-speed performance [208] using vehicle's center of mass, constant velocity assumption, and steering model estimation [209].

Nonlinear MPC It faces convergence and high online computational complexity issues [108] based on the dilemma of either fulfill a convergence criterion or give an approximate solution in a limited computation time [204]. This is demonstrated in [210] by simulating a nonlinear vehicle and tire models to perform an emergency maneuver in icy condition, showing a computational time not suitable for real-time implementation.

Less computationally expensive solutions with accuracy improvements have been achieved studying the lateral and longitudinal motion control in a coupled way, generating grid points to build nodal state parameter vectors in the state space where optimal solutions are computed off-line [211], and using a single optimization problem in the absence of tire models [212]. However, when different objective functions compete (e.g. increase tracking performance, reach a speed setpoint, and reduce steering rate) the optimization problem may be unfeasible, producing unexpected behaviors on the vehicle motion and compromising safety. In this sense, state that keeping the lateral acceleration under a threshold of 0.5g guarantees a feasible solution when a kinematic single-track model is used [213].

2.2.3 Compromise Between Safety and Comfort

The relation between planning and tracking tasks for driving is fundamental in the performance of automated vehicle motion. A valid interaction between decision and control improves the overall ADS architecture execution along with the decrement of any computational effort which targets real-time implementations. Smooth and efficient trajectories are often the responsibility of planning systems. However, an active affinity must exist with both the tracking system's capabilities and vehicle dynamics of testing platforms, which is often avoided if decision and control solutions are developed separately. Consequently, if more importance is given to accuracy in planning systems, less comfortable and even unfeasible trajectories appear and robust solutions in control are required to deal with this kind of issue. Moreover, safety becomes mandatory when DDT fallback strategies are requested even in unexpected circumstances, as will be detailed after in Section 2.3.

To increase robustness in trajectory tracking solutions, comfort should not be considered in the decision alone (e.g. trajectory planning) as it would assume that the control will follow references perfectly. If an appropriate affinity between planning and tracking systems is not satisfied, a poor response will prevail on the overall behavior. In this regard, a balance of safety and comfortability must be assured while developing control designs scalable to platforms of different size and intended application. Moreover, the increment of application range on vehicle motion control is a crucial task that contributes to enlarge the ODD of ADS implementations. Hence, solutions for both ease and emergency maneuvers in both urban and inter-urban scenarios are also a poorly developed field in the surveyed literature.

Based on the previous analysis, in Chapter 4 this Ph.D. Thesis verifies compatible driving functionalities for both trajectory planning and tracking, achieving appropriate compromises between safety and comfort. An interpolating method as the Bezier curve is

employed to assure safety and comfort in path planning, as its capability to concatenate continuous local paths and intuitive manipulation enable feasible curvatures related to the steering capacity of automated vehicles within the road boundaries. Moreover, both safety and comfort are considered using Model Predictive Control for trajectory tracking, due to its capability to constrain the driving execution related to state measurements and control parameters, even during the execution of moderate and emergency maneuvers.

2.3 Dynamic Driving Task Fallback

The current and most advanced driving automation technologies are not able to surpass human driving abilities, particularly in the road awareness context. AVs would face different kinds of malfunctions while driving, from technical ones related to hardware (HW) and software (SW) devices to functional failures related to intended driving applications. Any of these scenarios prevent the ADS to properly ensure safety while performing Dynamic Driving Task (DDT), particularly among SAE Levels 3 to 5. In this regard, the design of fail-aware (FA, e.g. self-diagnostics), fail-safe (FS, e.g. active safety), and fail-operational (FO, redundancy in both HW and SW) components and systems ensure the appropriate performance of DDT in both regular and challenging scenarios.

In this Section, a literature review on DDT fallback strategies and fail-operational architectures is described. A relationship between failures in susceptible systems (e.g. acquisition, communication, and actuation) and fallback strategies among top-level design systems (e.g. perception, decision, and control) is also covered. The successful verification process includes SiL and HiL testing techniques, fitting with the initial specifications as part of a whole validation process depicted in Figure 2.1.

2.3.1 DDT Fallback Strategies

As DDT and *DDT fallback* are different functionalities, the achievement of one does not guarantee the other's performance. Particularly, the *DDT fallback* is defined as the response to either perform the DDT or achieve a minimal risk condition after the occurrence of a performance-relevant system failure or upon an ODD exit. In this regard, the ODD is defined by [1] as *operating conditions under which a given driving automation system or feature thereof is specifically designed to function, including, but not limited to, environmental, geographical, and time-of-day restrictions, and/or the requisite presence or absence of certain traffic or roadway characteristics.*

Successful implementation of DDT Fallback strategies are focused on both conditional driving automation or above (SAE levels 3-5), and one of the main tasks in ADS design (perception, decision, or control), in case of failures in sensing or acting systems (acquisition, communication or actuation). This is one of the main focuses of this Ph.D. Thesis, being analyzed in Chapter 5. A summary of the different DDT fallback strategies related to SAE levels and ADS design is detailed next.

2.3.1.1 Regarding SAE Levels

As mentioned in Section 1.1.1 the SAE levels describe the driving automation grade of developed systems. SAE Level 3 ADS is capable to perform the entire DDT within its ODD and may not be able to perform DDT fallback. In this sense, FA systems are

required to detect failures or ODD exits, performing the DDT for at least several seconds while requesting a takeover, as human drivers must deal with these situations. On the contrary, for SAE Level 4 and above the DDT transition to a human driver is not allowed, hence ADS must able to perform both DDT and DDT fallback having FS systems that achieve a minimal risk condition when DDT is compromised. Moreover, the presence of FO systems minimizes failures or ODD exits occurrence, allowing ADS to drive up to a global destination.

Next, a brief summary detailing the most representative DDT fallback strategies according to SAE Levels is presented.

Conditional driving automation (SAE Level 3) After and ADS failure or when approaching the ODD exit, a receptive fallback ready user responds to FA system requests to intervene resuming the DDT performance [1]. Studies have been conducted to understand at which point in time inattentive drivers must be directed back to the DDT from non-driving related tasks, showing that takeover requests (e.g. visual or auditive) need at least 5-7s in advance to ensures collision avoidance by drivers upon stationary objects [214], or that people driving manually are 2.5s faster to press the brakes in response to red traffic lights in contrast to other driving AVs [215]. In the meantime, the takeover request issue remains a complex process that needs further investigations [216], also expecting that it hopefully remains as an exception in safety-critical events [217]. In this regard, results show that safety would be compromised as some drivers (with whom all responsibility lies) are unaware of ADS actual capabilities and limitations [218].

High driving automation and above (SAE Levels 4-5) ADS would prompt passengers to perform DDT (if available) after the occurrence of an ADS failure or approaching an ODD exit and automatically achieves a minimal risk condition in the absence of a response from passenger [1]. Current DDT fallback systems often perform a simple emergency stop maneuver on the current lane in case of malfunction events, and regarding the circumstance, this may be both unsafe and uncomfortable for other road actors involved (e.g. inside tunnels or on highways) [218, 219]. Hence, more extensive strategies must be developed that handle failures and allow ADS to reach the driving destination or remove the vehicle from traffic to a safe space and parking it, if necessary.

2.3.1.2 Regarding ADS Design

Currently, several FS and FO DDT fallback strategies focused on high driving automation level or above are proposed in the literature. Strategies for acquisition, communication, and actuation that rely on FO schemes for electronic hardware are classified according to ADS design in Section 2.1.2.1. A summary of DDT fallback strategies according to a system failure is presented in Table 2.2, and are detailed next.

Perception-Based Strategies These strategies attempt to ensure the status availability of the vehicle and its surroundings despite failures in the acquisition, communication, or actuation sub-systems.

In [220], a strategy is proposed which focuses on very narrow curve scenarios to improve the road classifier performance using sensor fusion techniques. Three different features such as shape extracted from digital maps, geometry, and appearance of urban roads are

Table 2.2 DDT fallback strategy vs system failure

DDT fallback	System failure: Acquisition	Communication	Actuation
Perception	Fernandez et al. [220] Emzivat et al. [218] Xue et al. [221, 222] Grubmuller et al. [223]	Kabzan et al. [224]	
Decision	Yu and Luo [219] Ruf et al. [225] Svensson et al. [226]	Lee et al. [227]	Tengg and Stolz [228]
Control	Venkita et al. [229]	Mugalide [230] An et al. [231]	Venkita et al. [229] Isermann et al. [110]

implemented to mitigate failures from grayscale cameras used to calculate the vanishing point to create a set of radial rays that fits the road limits such as lane markings or curbs.

In [218], a case study simulates both embedded map and localization components to correctly locate the ego-vehicle on the right lane if the front camera fails, slowing down speed enough to mitigate rear-end collisions from precedent vehicles. Missing vehicles would be replaced by ghost ones with the last perceived condition, being this claimed as valid for 1s. The proposed strategy showed that collisions cannot be totally avoided, focusing more on accident reduction than achieve a minimal risk condition.

In [221], a virtual lead vehicle is also considered within a strategy triggered by front sensor failure which produces a coned blind area, then removing the vehicle from active lane to a designated parking zone safely and immediately. Location module, side, and rear sensors are considered to still active to position the ego-vehicle, detect road boundaries and objects, respectively. Although two DDT fallback scenarios simulated emergency parking from lane-change maneuvers, vehicles parked on designated zones are not considered. In [222] an improved strategy comprises lane-keeping and lane-change maneuvers, as two of three phases proposed for a simulation study on a straight left-hand expressway section. The method includes numerical analysis of four fallback scenarios under real-time consideration such as car-following, overtaking, and overtaken cases. Nonetheless, pulling-over to a road shoulder is a missing maneuver assessment in the improved fallback strategy.

Decision-Based Strategies These strategies attempt to define a sequence of actions to ensure safety, modifying the original trajectory of the vehicle as a response to failures in the acquisition, communication, or actuation sub-systems.

In [225], an FS trajectory allows to terminate at zero speed on the slowest lane or shoulder as the safest achievable state, if any failure exists in ADS architecture including acquisition, perception, or decision. Planning options from both intra-lane and inter-lane states are proposed, requiring just an additional fraction of the Hidden Markov Model total computation time, by using the same goals and constraints but different weighting on the final state. Several real traffic situations from aerial footage are compared to human maneuvers as ground truth.

In [226], a two-step maneuver to achieve a minimal risk condition if internal system fault exists. The strategy consists of slowing down the velocity on the same lane after failure, then a stopping trajectory to the safest reachable area is planned and executed. A

safety monitor architecture concept is claimed to be capable of detect errors and mitigate hazardous situations as a separated high integrity sub-system. Nonetheless, static environment scenarios are considered only, hence moving objects are not contemplated in the strategy.

In [219], a strategy comprising 3-degraded levels with 7-different fallback scenarios are proposed if conventional vehicle failures or ADS functional failure exists. The 3-degraded levels include fallback, minimal risk condition, and failure mitigation strategy modes. A 6-degree polynomial to re-plan trajectories for the motion control module. The study focuses on two test scenarios such as *no obstacles in lane* and *leading car in lane*, showing feasible results in simulations bringing the vehicle to a safe state without driver takeover.

Control-Based Strategies These strategies try to guarantee the controllability objective in case of failures in the acquisition, communication, or actuation sub-systems.

In [230], an FS speed profile for cooperative driving provides reaction if failure is detected in communication. A programming functionality enables FS dynamic platoon for formation and management, and reactions are possible if the dynamically changing obstacle fails to follow the predicted behavior. After a Campus Area Network (CAN) communication failure, control messages slow down the vehicle to stop regarding the current and future speed commands.

In [231], rear-end collision avoidance strategy purely based on IEEE 802.11p claim to ensure fail-safety allowing automatic braking if unreliable wireless communication failure exists. Results showed higher traffic densities can be achieved if control is delegated to ADS. The automatic braking uses the maximum physically possible intensity using stronger decelerations without considering the driver's reaction time. Evaluated pre-crash scenarios include lead vehicle stopped, decelerating, and moving.

In [227], a lane-centering (LC) FS control strategy is performed switching to differential braking controller if Electric Power Steering (EPS) system fails (e.g. communication failure, control processor crash, a mechanical problem in the steering system, etc.). After failure, brake commands apply forces at each wheel of the vehicle to follow the desired path performing LC operation. A supervisory function operates in conjunction with an LC steering controller monitoring the status of EPS.

In [229], experiments on a Range Rover Evoque test vehicle show that an active reconfiguration is capable of switching to a fallback lateral controller if the yaw-rate sensor fails, using a smooth approach to damp undesired dynamic transients. Moreover, an actuation failure on one of the four in-wheel drive motors is assessed, using a re-allocation of torque commands among healthy motors. In this regard, failure detection and isolation methods allow completing a double lane change maneuver safely under fault injections.

2.3.2 Fail-Operational Architectures

Current automotive FS approaches to target a safe state achievement through deactivation or degradation of driving functionalities in case of detected non-tolerable failures. Common automotive FS solutions that provide a degraded mode (sometimes in a limited time) are Anti-lock Braking System (ABS), ESC, and AEB. However, fail functions must consider additional measures that contemplate fault tolerance [232].

In contrast to FS methods, FO function deactivation is not allowed as critical safety goals cannot be accomplished, and alternatives for safe execution becomes mandatory. In

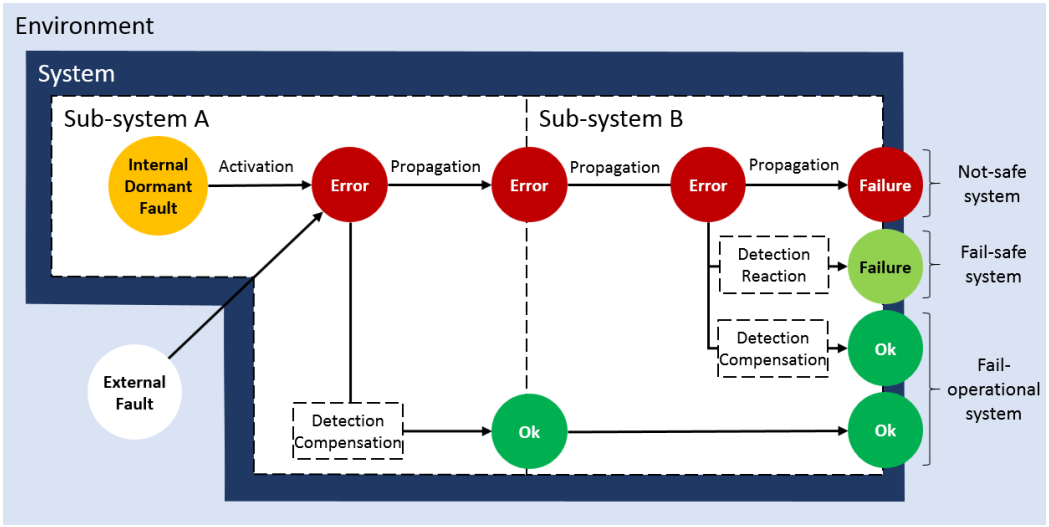

Figure 2.9 Failure propagation in systems[60] inspired in [8]

this regard, FO architectures comprises either *design diversity* that focuses on two or more dissimilar implementations that are functionally equivalent, or *redundancy* that achieves parallel estimations with two or more equal implementations (e.g. 2-out-of-3 or 2-out-of-2 diagnosis-FS architectures) [232].

The events in FS and FO systems[60] such as faults, errors, and failures are depicted in Figure 2.9. An error is produced either by the activation of an *internal dormant failure* or an *external fault* (e.g. vulnerability to an external attack). An error propagation within a given sub-system is delivered to the following sub-system which would: a) propagate the same error causing a permanent failure by an *not-safe system* design, b) the error is detected by a *fail-safe system* which respond (e.g. degraded mode) achieving a minimal risk condition before an accident occurs, and c) the error is detected by a *fail-operational system* which compensates the intended functionality [8].

Successful implementation of fail-operational architectures is focused on sensing or acting systems that are most susceptible to failures (acquisition, communication, or actuation). This is the main focus of this Ph.D. Thesis, being analyzed in Chapter 5. A summary of the fail-operational architectures related to sensing and acting systems is detailed next.

2.3.2.1 Acquisition-Based Architecture

These architectures are focused on assuring the acquisition components' availability to avoid the propagation of errors due to the activation of internal dormant or external faults within the acquisition sub-system.

An example of this architecture is depicted in [223], where an arrangement of one long-range RaDAR and two cameras comprises a proposed 3-sensors architecture overlapping field-of-view (FoV). It provides an object tracking with fault-masking data fusion techniques, detecting and excluding one signal failure from both HW (highly distorted mea-

[60] slides: Autonomous Driving | From Fail-Safe to Fail-Operational Systems https://rb.gy/6kgjky

surement) or SW (faulty Kalman filtering model). Simulations showed that failure-free object tracking can be provided by masking faulty sensors. Moreover, active landmarks in the overlapping FoV allows failure detection as fast as possible.

2.3.2.2 Communication-Based Architecture

These architectures are focused on maintaining the communication devices' availability to avoid the propagation of errors due to the activation of internal dormant or external faults within the communication.

An example can be found in [224], where disturbed positioning state estimation due to temporary or permanent sensor failures are classified as *outlier*, *drift* and *null*. As null failures are addressed by updating the measurement using the respective callback, a couple of implementations address both outliers and drift detections, using the Chi-squared approach and variance-based sensor isolation, respectively. Observability results were obtained from this strategy using a 4-kind arrangement of positioning sensors.

2.3.2.3 Actuation-Based Architecture

These architectures are focused on assuring the actuation components' availability to avoid the propagation of errors due to the activation of internal dormant or external faults in the actuation.

In [228], a safety-gateway for AVs allows limiting steering wheel angles and brake pedal to avoid critical situations if potentially harmful values are received from the ADS. Limitations in actuation devices' location are dependent on the selected speed. Four different failure modes are implemented overriding both together and separately the three actuation signals (e.g. steering wheel angle, acceleration, and brake pedals). This study targets to increase safety mitigating the reaction time impact due to sudden failures at high speeds.

In [110], basic redundant structures for fault tolerance in drive-by-wire systems are presented and thoroughly described, being classified into static and dynamic redundancies. Meanwhile, static redundancy requires three or more parallel modules and compare and mask output signals using a voter, the dynamic redundancy requires fewer modules at the cost of more information processing by *hot-standby* and *cold-standby* methods.

2.3.3 The Challenge of Urban Environments

Positioning in dynamic urban environments is one of the challenges of the current ADS. In this regard, although communication devices (e.g. GNSS) are capable to provide around 2cm of positioning accuracy in ideal open-sky conditions, multipath and non-line-of-sight issues can arise from obstacle interference (e.g. tall buildings and trees) in urban scenarios. Moreover, a low-frequency update is another limitation that has been solved by fusing GNSS with in-vehicle sensors (e.g. GNSS with IMU and in-vehicle sensors), however, this is still a short-term solution due to sensor noises and slowly drifted integration error. Consequently, digital maps and perception data fusion seems like one opportunity to solve the long-term GNSS outage [4], nonetheless further investigation is still necessary for digital mapping and techniques to deal with dynamic environments.

A fail-operational architecture allows ADS to remain operative in case of relevant performance failures. Here, top-level design systems are integrated and must consider both

HW and SW redundancies to increase the trustworthiness of the entire control architecture. Hence, further investigations and developments are required, especially in positioning functionalities as the reviewed strategies focus mostly on acquisition sub-system failures for object detection, ignoring the ego-vehicle localization performance. Moreover, a planned DDT fallback strategy requires to be developed in case of positioning failures in urban scenarios, defining more general use cases instead of specific applications on straight roads in inter-urban scenarios.

Based on the previous analysis, in Chapter 5 DDT fallback strategies are combined with fail-operational architectures, verifying technical safety approaches for urban environments. A fail-operational architecture improves localization accuracy provoked by poor signal reception due to obstacle interferences in urban environments. An unscented Kalman filter contributes to fuse noisy states from the communication with acquisition devices such as odometry and accelerators. Moreover, a decision-based strategy allows for achieving a minimal risk condition when permanent localization failures are present. A virtual positioning sensor keeps available the ego-vehicle status, while re-planning trajectory to reach safe areas in the route relying on digital maps from the database, and considering road actor for rear-end collision avoidance, all of these, in a degraded mode for driving execution.

2.4 Conclusion

In this chapter a survey on three main areas related to ADS development have been covered: 1) Virtual testing techniques for vehicle dynamics and automated driving; 2) Advances in planning and tracking solutions for vehicle motion control; and 3) DDT fallback strategies based on system failures and fail-operational architectures (SAE Level 4-5). Several remarks on each aspect are given next.

Firstly, a direct relationship between vehicle dynamics and ADS is not evident in current validation procedures, being this essential for virtual testing in automated driving. Consequently, vehicle dynamics validation techniques should consider the behavior of the actuation present in automated vehicles, which most of the cited works ignore. Moreover, available STMs are not representative of traffic-based driving scenarios, where safety and comfort in both lateral and longitudinal motion control are crucial in urban environments. In this regard, test cases, data handling, and metrics must be effectively described in validation projects, trying to obtain the best balance between effort to gain model confidence and value to the final user. Taking into account these ideas, in Chapter 3 a novel validation procedure of both vehicle simulation models and driving automation systems is presented.

Secondly, comfort should not be considered in the decision alone (e.g. trajectory planning) if robustness in trajectory tracking solutions is considered as a target. In some circumstances, control would not follow references perfectly, then deteriorating the overall driving behavior due to an inappropriate affinity between planning and tracking systems. In this regard, a balance of safety and comfortability must be assured while developing control designs scalable to platforms of different size and intended application. Moreover, the increment of application range on vehicle motion control is a crucial task that contributes to enlarge the ODD of ADS implementations. Hence, solutions for both ease and emergency maneuvers in both urban and inter-urban scenarios are also a poorly developed field in the surveyed literature. In order to give more insight into this issue, in Chapter 4 compatible driving functionalities for both trajectory planning and tracking are verified,

achieving appropriate compromises between safety and comfort.

Finally, a fail-operational architecture is required to maintain the ADS operative in case of relevant-performance failures. Here, top-level design systems are integrated and must consider redundancies both HW and SW to increment the entire control architecture's trustworthiness. Therefore, further investigations and developments in positioning systems are necessary as current strategies focus mostly on acquisition failures for object detection, ignoring the localization performance. Moreover, a planned DDT fallback strategy requires to be developed in case of positioning failures in urban scenarios, defining more general use cases instead of specific applications on straight roads in inter-urban scenarios. This area is covered in Chapter 5, in which a novel DDT fallback strategy is combined with fail-operational architecture, verifying technical safety approaches for urban environments.

As a conclusion of the present review for high driving automation systems development and testing, it is noted that the interest in ADS validation procedures based on trustworthy vehicle simulation models is a trend that grows and spreads continuously both in the automotive industry and academy. Additionally, as safety and comfortability are concepts of opposite nature, unbalanced strategies may lead to infeasible solutions in trajectory tracking performance, being this the main issue for ADS when urban applications are considered. Moreover, efficiency and reliability in ADS are either partially or entirely ignored in current real-world applications, where fail-safe solutions are not enough, and fail-operational systems must be developed relying both on hardware and software redundancies.

Chapter Three

Validation in Automated Driving

The development of driving automation functionalities has increased over the last decades, increasing their complexity while pushing to adequate available validation procedures to this breakthrough technology [15]. Nowadays, ADAS requires a significant amount of track testing hours before reaches the market. Hence, an increased testing effort is expected for higher levels of automation, such as ADS. To validate ADS, track testing is often complemented with trials in simulation considering scenario-based testing. In this regard, and as analyzed in the previous chapter, well-defined validation methods and trustworthy virtual test platforms must be assured to reduce development time and costs [233].

A particular combination of current ADAS is expected in future ADS features. Current ADAS include speed assist systems (e.g. speed limitation function, intelligent speed assist, and adaptive cruise control), lane support systems (e.g. lane-keeping assist and emergency lane keeping), and Automatic Emergency Brake (AEB) systems (car-to-car and Vulnerable Road User, VRU). The spectrum of possible traffic scenarios is reduced to a clear Operative Design Domain (ODD) which permits an easier evaluation of their performance using simulation and track testing.

To make use of simulation-based validation approaches, both vehicle dynamics and traffic-scenarios must be properly modeled. Generic *virtual prototyping* methods have been defined in [234], depicting aspects to consider through validation processes and possible issues related to prediction and model calibration. The classic approach relies on the comparison of experimental and simulation results. As the absolute validation of simulations is impossible, it only can be defined as *not invalid* if the difference between experiments and simulations fulfills a defined validity criterion [233]. In addition, when considering simulation-based testing, on one hand, Standardized Test Maneuvers (STM) are generally employed for vehicle dynamics model validation [235]. On the other hand, scenario-based testing is mostly employed for technical safety validation, as driving actions and events occur in a defined temporal sequence [6].

Taking into account the previous issues, in this chapter, a novel approach for both vehicle dynamics model and ADS validations, including a complete framework to develop these is proposed. In order to fully explain the procedure, this chapter is structured as follows. Section 3.1 motivates the methodology's development making contrast with current perspectives. Section 3.2 describes the validation approach for vehicle simulation models and driving automation features. Section 3.3 describes the virtual and real test circuits and scenarios employed in the present chapter, as well as the rest of the Ph.D. Thesis. Sections 3.4 and 3.5 describe the application of the methodology in two case studies. Finally, Section 3.6 summarizes the main ideas and results.

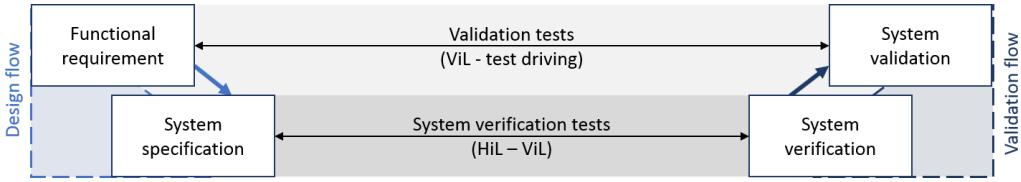

Figure 3.1 Requirement and specifications for system verification and validation

3.1 Motivation

Addressing the need for models and proper validation as analyzed in Chapter 2, several studies have been focused on the vehicle dynamics model validation through the so-called *validation triangle* between STM, simulation models, and real-world [82]. Transient response, fundamental application, and time-domain analysis are part of the common methodology. Based on these, some authors have validated the lateral and longitudinal vehicle motions separately [236], and some others assessed the combined response of the entire system through unique tests saving time and effort [88]. Moreover, note that when considering driving automation features, the required actuation system should also be considered in the vehicle simulation model, which most of the cited works ignore [6, 235]. Moreover, classic test maneuvers may not be representative of conventional driving scenarios in which both lateral and longitudinal motion evaluation is important [83]. Consequently, test cases, data handling, and metrics must be effectively described in validation projects, trying to obtain the best balance between the effort to gain model confidence and the value to the final user.

In this chapter, a novel two-step validation methodology is presented, which is based on the top of the system development life cycle showed in Figure 2.1 (which is an excerpt of the validation cycle detailed in Figure 3.1). Firstly, an open-loop test procedure allows tuning vehicle simulation models, including the actuation devices required for implementing both driving automation applications. Secondly, a closed-loop test procedure is proposed for technical safety testing of automated driving features, which also would contribute to the assessment of both the vehicle simulation model tuning and vehicle dynamics status of the actual vehicle. To illustrate the modularity and scalability of the approach, two case studies based on real automated vehicles including a Renault Twizy and an Irizar i2e bus are detailed. Functional requirements and systems specifications are considered to develop a Traffic Jam Assist (TJA) functionality, contributing to the verification and validation of Low-Speed High Automation (LSHA), as one development path for urban mobility vehicles in Europe [15].

3.2 A Validation Approach for AD features

In this section the proposed validation approach for AD features is detailed. In order to better explain the approach, Section 3.2.1 assesses the vehicle dynamics model testing which increases the fidelity level of the virtual test platform. Section 3.2.2 evaluates technical safety testing in the absence of any malfunction[44]. Finally, Section 3.2.3 describes an integrated validation procedure using simulations in the assessment of technical safety.

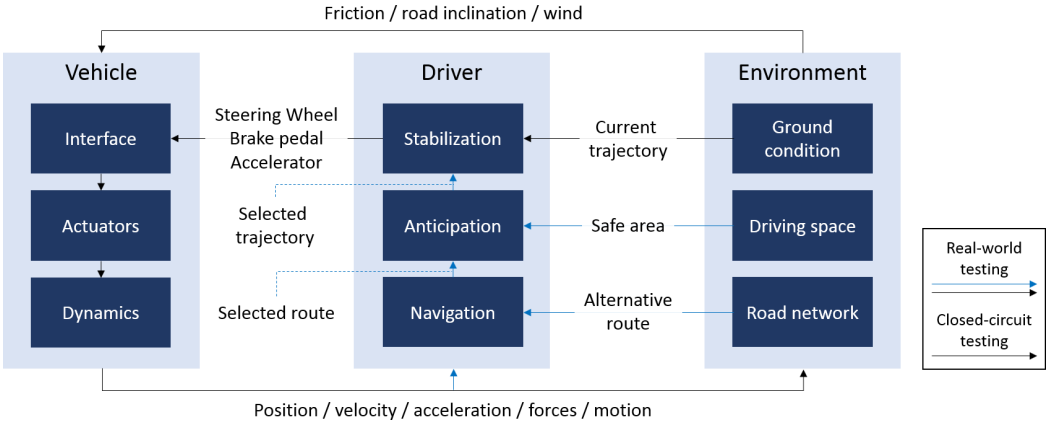

Figure 3.2 Vehicle-driver-environment interaction inspired in [9, 10, 11, 12]

3.2.1 Vehicle Dynamics Model Testing

The virtual test driving using realistic vehicle simulation models significantly increases the efficiency of the entire ADS development process. However, the simulation models used to reproduce the vehicle dynamics highly affect ADS performance in virtual environments, as the more the simulation model resembles the real vehicle, the more realistic simulations will be obtained. The value of a simulation model (or confidence that it is *not invalid*) comes from a trade-off between the model's confidence and its computational cost [237]. Therefore, as simulations are approximations of the physical nature, it is highly costly and time-consuming to determine the *absolute validity* of models [91]. Instead, *not invalid* results are conceivable within the boundaries of a predetermined operation, which requires conducting tests and evaluations until the model achieves a sufficient confidence level.

A minimum fidelity in the vehicle dynamics model is generally determined performing driving maneuvers, which regarding the intended use, would resemble or not real-world driving events. In this regard, a direct comparison between the response given by a simulation and the real vehicle (e.g. Position, velocity, acceleration, forces, etc.) can be carried out if the control inputs from the driver (e.g. Steering wheel, brake pedal, accelerator, and/or gear position) and the disturbance inputs from the environment (e.g. Tire-road friction, road inclination, wind, etc.) are known.

This comparison can be carried out considering two approaches: Real-world testing and closed-circuit testing. These approaches will be detailed next, and the scheme of the driver-vehicle-ground interaction for both is depicted in Figure 3.2.

3.2.1.1 Real-world Testing

Real-world testing is the result of vehicle-driver-environment interaction when the road network and driving space affect the subjective perception and skills of the driver to complete the desired maneuver. The *road network* and *driving space* represent any environmental element affecting the vehicle dynamics through the driver's perception (e.g. other vehicles, Vulnerable Road Users (VRU), traffic lights or signs, etc.), this is also defined as *passive environment* [82]. The *navigation* and *anticipation* decide a trajectory according to the

available route and safe area to perform the driving test maneuvers.

Test maneuvers acquired from the previous process result in an ambiguous validation task for the vehicle simulation model. Note that the definition of testing scenarios involve an unpredictable number of variables, whose repeatability and comparability is reduced due to the difficulty to obtain the same inputs and outputs in different experiments. Moreover, the response from complex environments is a difficult task to analyze when the vehicle dynamics correspond to coupled behaviors resulting from performance, handling, and ride characteristics, which are easier to assess in an isolated way. In this regard, the most important aspects of vehicle dynamics can be assessed and reproduced in virtual testing using simpler maneuvers under controlled environments such as *closed-circuit testing*, as detailed next.

3.2.1.2 Closed-Circuit Testing

Closed-circuit testing reproduces driving situations that exhibit a general dynamic response of vehicles as an approximation to real-world testing. Here, real events are divided into simpler ones allowing the execution of specific driving situations without affecting the driver's intention nor original trajectory due to unpredicted elements on the road. Furthermore, as control inputs from the driver and environment disturbances are the only aspects present during the driving test, repeatable and comparable data can be obtained, which can be used for a comprehensive assessment of the tested model or feature. In fact, the importance of repeatability is fostering the continuous introduction of robotized actuators (e.g. double lane change test [61]), as some critical tests heavily depend on the driver's skills.

Performing driving maneuvers is the most accepted procedure to validate vehicle simulation models, consequently, real driving events are deconstructed into Standardized Test Maneuvers (STM) for closed-circuit testing. In this regard, STM provides several advantages such as cost and time effort economy, along with the obtention of high confidence models contrasted with repeated and comparable experiments. Moreover, STM allows the assessment of a vehicle dynamics simulation considering: 1) a limited operating range (e.g. low lateral accelerations, or small steering wheel angles); 2) and a specific group of inputs and outputs (e.g. braking while steering maneuver differs from a bump in the road disturbance, or lateral sprung mass acceleration differs from vertical one); as two main aspects for validation[84].

As presented in [82], specific STMs can be related to the dynamic response (e.g. steady-state, transient, periodic, and stochastic), the domain of analysis (e.g. time or frequency domain), input method (e.g. open-loop and close-loop testing), or scope of application (e.g. fundamental and purpose-dependent maneuvers). Therefore, any of these approaches would enable an accuracy assessment at a given operating point, and the obtained results must be as good as the intended driving functionality demand (e.g. trend of responses over difference among values). In practice, predefined strategies to validate vehicle simulation models have been made available by some specialized standardization institutions such as the *International Organization of Standards* [62]-[63], and the *Federal Highway Administration* [64]. Selected STM and examples of validity methods are depicted in Table 3.1.

[61] webpage: ISO double lane change by VEHICO https://rb.gy/dmy2al
[62] standard: ISO/DIS 22140 https://www.iso.org/standard/72680.html
[63] standard: ISO/DIS 11010-1 https://www.iso.org/standard/75910.html
[64] standard: FHWA-JPO-16-405 https://rosap.ntl.bts.gov/view/dot/34271

Table 3.1 Selected standardized test maneuvers and examples of validity method

Test maneuver	Characterization Aim	Validity method	
		Objective	Subjective
Acceleration	Powertrain performance	[238]	[239]
Coast-down	Aerodynamic and rolling resistance	[88]	[239]
Low-speed	Powertrain braking	[240]	[84]
Braking	Braking performance	[238]	[241]
Steady-state turning[34]	Lateral steady-state response		[242]
Step input[35]	Lateral transient response	[83]	[82]
Double lane-change[36]	Emergency lateral response	[88]	[12]

In this Ph.D. Thesis, the entire system (e.g. vehicle model) and sub-systems (e.g. chassis, wheels, powertrain, brake, suspension, and steering) are considered and detailed in this chapter. Based on the results from STMs, objective (confidence intervals) and subjective (face-validity) validation techniques described in Section 2.1.1.2, are combined to achieve an improved assessment. The level of accuracy required for the simulation model targets LSHA driving functionalities as described in Section 3.4.

3.2.2 Technical Safety Testing

Once the vehicle simulation model is validated, virtual testing allows the understanding of possible responses and outcomes more efficiently and safely than real-world maneuvers. This is particularly interesting for testing new driving functionalities, as virtual testing provides two main advantages. Firstly, they provide development assistance, as structured tests during development helps to determine safety failures, corner cases, and capability boundaries. Secondly, they allow increasing the qualitative or statistical confidence in the safety and performance of the full system, subsystems, and/or components. This is, virtual testing allows the validation of the approach before real implementation. However, as the accuracy of simulations is limited and numerical uncertainties are still present, an assessment based on simulations requires a final contrast with real-world driving.

Although several types of simulation exists for driving functionalities testing and each implementation contributes towards different goals, two types of virtual testing are mostly employed: 1) functional safety testing[45] and 2) technical safety testing[44]. Functional safety testing focuses on detecting failures in software and hardware, and in the development of safety concepts to ensure controllability while avoiding driving risks. Similar to functional safety, the simulation can include testing on different platforms such as Software-in-the-Loop (SiL), Hardware-in-the-Loop (HiL), and Vehicle-in-the-Loop (ViL) in the full system, sub-systems, and (or) components [122]. On the other hand, technical safety testing focuses on demonstrating safety in the absence of any failure, increasing confidence across known and (or) un-known driving scenarios. Technical safety simulation is the main scope of this Chapter, while functional safety will be thoroughly covered after in Chapter 5.

Scenario generation for technical safety testing mostly derives from real-world driving events including those of continuous occurrence, crash or pre-crash scenarios, variations in ODD, or ADS weaknesses focus. Simulation allows variation in a high number of variables to construct driving scenarios tailored to validate the Safety of the Intended Functionality (SOTIF). For SAE L0-L2 systems, the current SOTIF validation approach relies on driving

Table 3.2 Selected Standardized Test Functions

Safety Assist System	Functionality	Scenarios
Speed Assist System[46]	- Speed Limitation Function - Intelligent Speed Assist - Intelligent ACC	- Activation/Deactivation - Setting Adjustable Speed - Speed Control
Lane Support System[46]	- Lane Keeping Assist - Emergency Lane Keeping	- Dashed/Solid Line - Road Edge - Solid Line - Oncoming/Overtaking Vehicle
AEB System[47]	- Car-to-Car - Vulnerable Road User	- Rear stationary/moving/braking - Front Turn-Across-Path - Pedestrian - Cyclist

events as those presented in Table 3.2, constructed from statistical data of accidents[46] and crashes[47]. For SAE L3-L5, the validation of previous functionalities combined with maps and infrastructure must follow a similar scenario-based testing approach.

The approach proposed in this Ph.D. Thesis employs specific scenarios for technical safety testing related to three-of-six-layers of the scenario-based testing method described in Section 2.1.2.2, including surface condition (vehicle dynamics model), road users and objects (static and dynamic), and digital information (vehicle-to-traffic-light data). The performance of scenario space coverage assessment through testing-based methods includes a combination of driving situations described in Table 3.2. Moreover, the scenario execution considers SiL and HiL verification tests for SOTIF of ADS before performing ViL validation tests.

3.2.3 Integrated Validation Procedure

A summary of the proposed validation test methodology is detailed in Figure 3.3. The proposed approach is based on two steps, assessing both the vehicle dynamics model and technical safety testings as an integrated validation procedure. Firstly, an *open-loop validation testing* is proposed to identify useful parameters of the automated vehicle and assure reliability during simulations, such as time delay, rate limit, and control gains of real actuation, as well as the vehicle's capacity, to accelerate, brake, and turn. Secondly, a *closed-loop validation testing* is proposed which allows to test and tune vehicle motion control algorithms based on the dynamic model defined in the first step. Moreover, a refinement of the vehicle dynamics model is also possible in this step.

In both approaches, the difference between System Response Quantity from the computational model (SRQ^p) and physical experiment (SRQ^m), as a measurement agreement which will be used to validate both the vehicle simulation model and ADS technical safety. Examples of SRQ in validation methodologies of vehicle simulation models were previously covered in Section 2.1.1.2. In this Ph.D. Thesis, special emphasis on decision-making and motion control algorithms is made, however, this approach is generic enough to include also the perception system validation. Uncertainty and error calculations are considered, as a good practice for SRQ difference [82]. Accuracy requisites define the adequacy of validation metrics for the vehicle simulation model and ADS technical safety.

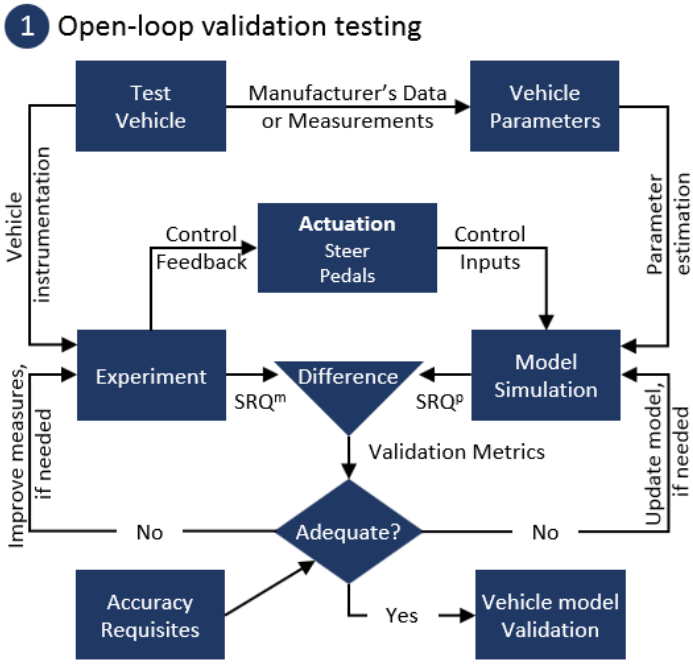

(a)

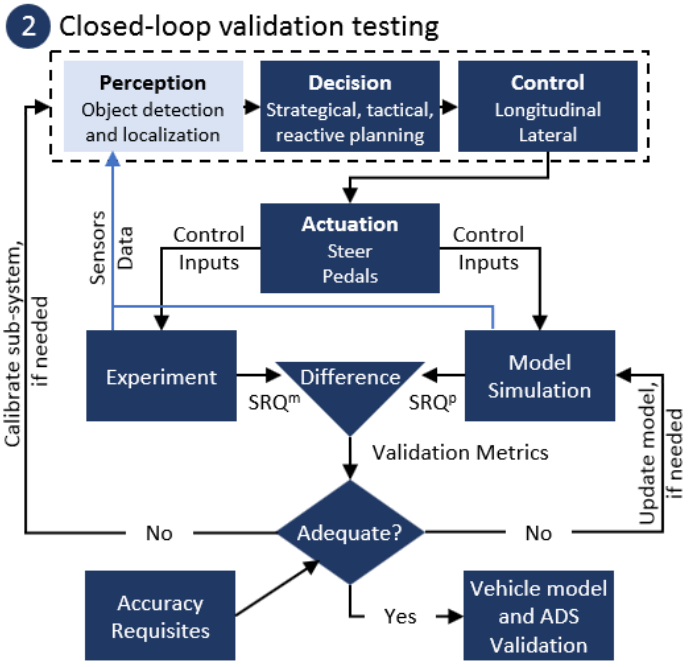

(b)

Figure 3.3 (a) Open-loop and (b) closed-loop validation testing procedures

3.2.3.1 Open-Loop Validation Testing

The open-loop validation testing aims to determine the dynamic model of both the vehicle and its internal actuation system so that this model is feasible enough to time-boost the development of ADAS/ADS functionalities through simulations. In this regard, the proposed procedure is depicted in Figure 3.3a.

The first step in the open-loop validation testing is to gather the *vehicle parameters* of interest associated with the *test vehicle* that is useful to define both vehicle's model and the experiment's scope. Typical parameters identified in vehicle dynamics modeling are: frontal area, coefficient of drag and rolling resistance, the Center of Gravity (CG) location (longitudinal and vertical), wheel inertia, and tire model parameters [243]. Depending on the intended application, vehicle model complexity, and desired accuracy more or fewer parameters are required.

In contrast with other methodologies proposed for vehicle simulation model validation [83, 84, 88, 89, 235], the *actuation* behavior on the inputs of the vehicle (steering wheel, throttle, and brake pedals) has a remarkable importance in the proposed approach. As pointed in Figure 2.4, when considering vehicles with ADAS/ADS functionalities, a low-level control layer (actuation system) receives the position commands from the high-level control (control system). Hence, as this low-level control layer influences the dynamics of the inputs and the vehicle dynamics, a proper actuation system parametrization is proposed to ensure accuracy in the vehicle simulation model.

Once the actuation behavior and vehicle dynamics are modeled, the SRQ difference is evaluated to conclude whether the model satisfies the accuracy requirements. If the simulation model is considered not valid, either experimental measurements need to be added/improved or the simulation model updated/calibrated [86].

3.2.3.2 Closed-Loop Validation Testing

Once models with feasible dynamics for both vehicle and actuation systems have been defined, they can be used to time-boost the development of ADAS/ADS functionalities, by their integration on a simulation framework that enables the evaluation of perception, decision-making, and/or motion control algorithms.

In this sense, if an ADAS/ADS feature of a certain level of driving automation is to be tested, the steps defined in Figure 3.3b are necessary. The object detection and ego-vehicle localization are gathered from *sensor data* (acquisition and communication systems) and processed by the *Perception* system. The *Decision* system uses the obtained information from the ego-vehicle and its surroundings to define comfortable driving, considering safe distances from road borders and objects ahead on-route. Then, the *Control* system tracks the path and speed references, delivering position commands to the *Actuation* system.

As in the open-loop tests, the same surrounding behavior needs to be defined both in *experiment* and *model simulation* to compare their SRQ when evaluating their performance within the entire driving automation system. Moreover, tuning the developed simulation model is possible by comparing dynamic responses from the performed tests to assess the achieved accuracy level.

Table 3.3 Technical specifications of test vehicles


Make and Model	Renault Twizy 80	Irizar i2e bus	Unit
Weight (f - r)	265 - 346	6193 - 9749	kg
Total Weight	611	15942	kg
Yaw Inertia	243.18	115062.60	kg-m^2
Track Width	1.09	2.55	m
Wheel Base	1.69	5.77	m
Overhang (f - r)	0.31 - 0.34	2.81 - 3.40	m
Dimensions (l - w - h)	2.34 - 1.24 - 1.45	12.16 - 2.55 - 3.30	m
Drag Coefficient	0.64	2	
Max. Power	8kW (Electric)	250kW (Electric)	
Max. Torque	57	3000	N-m
Transmission Ratio	1:9.23 (Single reduction)	(Single reduction)	-
Braking Torque	360	12000	N-m
Front/Steering Ratio	38:1	31:1	
Suspension (f - r)	Macpherson strut	ZF RL82EC - ZF A132	
Stiffness (f - r)	5840 - 8100	140000 - 228000	N-m
Damping (f - r)	660 - 1400	11900 - 3240	N-s/m
Tires (f - r)	P125/80R13 - P145/80R13	275/70R22.5	
Wheel Radius (f - r)	0.27 - 0.28	0.45	m

3.3 Testing Framework for Validation

In this section, the testing framework developed to implement the aforementioned validation approach is detailed. This framework includes the different elements (test vehicles and test fields, virtual validation environment, and control architecture design) that will be used in this Ph.D. Thesis to apply the methodology detailed in Section 3.2.3 to the different driving functionalities proposed.

For that purpose, first, specifications of the two real vehicles used in the different developments will be detailed in Section 3.3.1. Second, the virtual environment and its elements will be detailed in Section 3.3.2. Finally, the control framework considered to test the different functionalities on both real and virtual environments will be analyzed in Section 3.3.3.

3.3.1 Test Vehicles and Test Fields

Two test vehicles are considered for the different developments proposed in this Ph.D. Thesis: a Renault Twizy 80 and an Irizar i2e bus. The first is a single-seater vehicle for urban mobility, and the second is an urban bus of 80-passenger capacity. Both vehicles are electric and originally conceived as non-automated vehicles, so electro-mechanical actuators had to be attached to driving devices. Table 3.3 presents the technical specifications of both vehicles.

In-vehicle sensors provided by respective OEMs offer useful data from CAN bus gateways including, wheel velocity from odometry, transmission gear position (Park, Reverse,

(a) (b) (c)

Figure 3.4 Test fields: (a) Tecnalia, (b) Irizar, (c) Malaga (Courtesy of Google)

Neutral and Drive), steering wheel, accelerator, and brake pedals position. Main computers send command signals to different actuation controllers. In both vehicles, electrical motor-based systems control the steering wheel and brake pedal. Also, the accelerator position commands are possible by-passing pedal sending signals directly to Electronic Control Units (ECUs). Different arrangements of sensors ensure real-time localization and object detection in the surroundings. A description of each vehicle instrumentation is described in Section 3.3.3.

Three different test fields were available to perform verification and validation of driving automation systems. The first two were closed-test circuits that were employed for testing and development of driving functionalities, and are presented in Figures 3.4a-b. These test fields of 370m and 600m of travel distance, respectively, are located in the facilities of Tecnalia and Irizar e-mobility (Basque Country-Spain). Both are part of AutoDrive Consortium[28]. The final scenario is a touristic seaport (Malaga - Spain), an urban circuit of 2.2km of travel distance as depicted in Figure 3.4c.

3.3.2 Virtual Validation Environment

The virtual validation environment is based on the simulation software Dynacar [244]. Dynacar features a vehicle physical model with a multi-body formulation, which makes use of relative coordinates and semi-recursive equations of motion based on velocity transformation. Therefore, as a tool for vehicle simulation model development, it allows the change of numerous parameters and variables to test different driving conditions. Moreover, actuation parameters such as steering wheel position and torque on wheels enable the research and development of both simulation models and ADAS/ADS functionalities.

The required models to perform virtual testing (analyzed in Section 2.1.1.1) such as a vehicle, actuation, and environment (sub-systems included) are described next.

3.3.2.1 Vehicle Model

The vehicle simulation models employed are based on ready templates from Dynacar Vehicle Dynamics Simulation software [244]. In the required sub-systems, the parameter values

were replaced with those of the Renault Twizy 80 and an Irizar i2e bus, both electric vehicles conceived for urban environments and with a considerable difference in passenger capacity. The vehicle simulation model comprises the components showed in Figure 2.2, which are detailed as follows.

Chassis Dynacar enables two or more chassis selection if articulated vehicles are going to be modeled. In this Ph.D. Thesis, the vehicles consist of one chassis. The information regarding the weight distribution, CG location, and moments of inertia are obtained from static load measurements. The drag force is the main aerodynamic parameter acting over the CG of both models, being provided by OEMs. In *Renault Twizy*, the vertical CG position is calculated through the axle lift method[65]. In *Irizar i2e*, this position is assumed at half of the overall height due to the difficulty to perform the same test.

Suspension Dynacar considers independent suspensions types as macro-joints, and their behavior is modeled using lookup tables. In *Renault Twizy*, steering-knuckle-type suspensions at the front and rear axles are linked to the chassis. The stiffness and damping characteristics are taken from [245]. In *Irizar i2e*, a steering-knuckle-type suspension at the front axle and a rigid-axle-type suspension at the rear axle is linked to the chassis. The stiffness and damping characteristics are provided by the OEM of the bus.

Wheel Dynacar allows the modeling of vehicles with two or more axles, and two or more wheels per axle. Moreover, it enables the selection of two different tire models such as the Pacejka Magic Formula and a simplified model with a spherical single-point-contact. In this Ph.D. Thesis, the Pacejka Magic Formula tire model of a standard tire defined in [78] has been used. In *Renault Twizy*, two wheels at the front and rear axles are linked to the suspension system. In *Irizar i2e*, two wheels on the front and four wheels at the rear are linked to the suspension system.

Steering Dynacar considers one steerable axis for computing the steering feedback forces, and the behavior is modeled using lookup tables. In this Ph.D. Thesis, both vehicles have a front steerable axis. In *Renault Twizy*, the steering characteristics are taken from [245]. In *Irizar i2e*, the steering characteristics are provided by the OEM of the bus.

Powertrain Dynacar does not feature any powertrain system, as the vehicle dynamics is based on a rolling chassis model. Therefore, each wheel needs to be provided with its traction torque. This allows users to fully develop or integrate their own powertrains and control algorithms. In this Ph.D. Thesis, simplified powertrain dynamics including motor, torque converter, and transmission is implemented as described in [65].

The powertrain modeling targets those devices onboard the real test platforms, which are similar both in *Renault Twizy* and *Irizar i2e*. The transmission consists of a single gear, and the torque converter transmits the motor power to the axle shaft, and hence, to the wheels. The powertrain type is rear-wheel-drive with a spool differential, meaning that it acts like a locked axle rotating both rear wheels at the same speed. The propulsive power is provided by an electric synchronous motor which also is capable to provide regenerative braking.

[65]standard: ISO 19380 https://www.iso.org/standard/64761.html

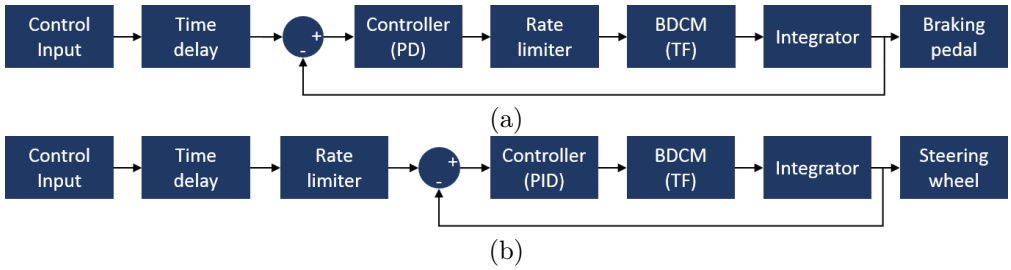

Figure 3.5 Actuation models for (a) brake and (b) steering wheel

Brake Similar to the powertrain, Dynacar does not feature any brake system. In this Ph.D. Thesis, a simplified brake model consisting of a simple hydraulic circuit was implemented. In this regard, a force applied over the braking pedal is transmitted to the master cylinder's push-rod, displacing a volume into the brake line finally affecting the wheel cylinder's pressure located in calipers. No antilock system or vacuum booster is part of the circuit. This brake system design, implemented in both vehicle simulation models, is described in [246].

The hydraulic braking torque is an input to the vehicle model, which principle is similar both in *Renault Twizy* and *Irizar i2e*. This value is obtained by defining the relationship between the brake pedal location and the friction torque generated due to the contact of pads and brake discs. A limitation valve was simulated to restrict the brake pressure to the rear wheels considering a permissible braking percentage.

3.3.2.2 Actuation Model

On the contrary to vehicles with an integrated actuation system conceived by manufacturers, non-automated vehicles require the attachment of electro-mechanical actuators on the brake pedal and steering wheel. This is the case of the vehicles considered in this Ph.D. Thesis, the *Renault Twizy* and *Irizar i2e*. A brand controller is often included to ensure that motors follow the position commands given by high-level control. The elements that usually compose the actuation model are detailed in Figure 3.5.

As an electro-mechanical actuator is commonly a Brushless Direct Current Motor (BDCM), it can be modeled as a second-order transfer function, as in [247], defining Equations 3.1a-c.

$$G_e(t) = (1/K_e)/(\tau_m\,\tau_e t^2 + \tau_m\,t + 1) = W_e(t)/V_e(t) \tag{3.1a}$$
$$\tau_m = R\,J/(K_e\,K_t) \tag{3.1b}$$
$$\tau_e = L_e/R \tag{3.1c}$$
$$\theta(t) = W(t)/t \tag{3.1d}$$

where G_e, W_e, and V_e are the transfer function, angular velocity, and the source voltage in a continuous-time (t). τ_m and τ_e are the mechanical and electrical time constants, K_e and K_t are the back electromotive force and torque constants, R_e is the resistance, L_e is the inductance, J_e is the rotor inertia, and t_e is the mechanical time.

(a)

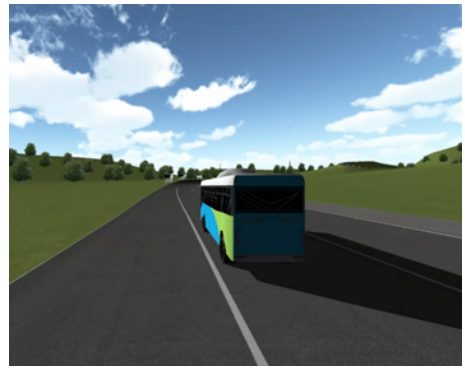

(b)

Figure 3.6 (a) Renault Twizy and (b) Irizar i2e bus in Dynacar environment

The parameters of the electro-mechanical motors are provided by manufacturers. Additionally, as in real implementations, a controller is employed to position the motors in the desired value with an error near zero. Moreover, the *time delay* of the vehicle's internal communications, the *rate limit* of actuators and the gains for the *PID controllers* can be optimized by-hand through experiments, as shown in the case study in Section 3.4.

3.3.2.3 Environment Model

Dynacar's *Road Editor* allows the user to create new or modify existing scenarios, in which the vehicles can be driven. There are two main options to generate driving scenarios: 1) Straight roads with altitude changes and 2) Realistic 3D scenarios (called *stages*) [244]. Moreover, the friction coefficients of driving surfaces (which are related to the wheel model described previously) can be defined, hence the wheel-road interaction is contemplated.

One of the attributes of Dynacar refers to the 3D representation of test vehicles, using files that contain the information regarding all the objects that are part of the 3D vehicles such as objects (chassis, wheels, steering wheel, and forces, as .obj files), lights (front, reverse and indicators, as .png files), sounds (engine, gear change, ignition, wind, and tire skid, as .wav files) and cameras (tire skid marks and smoke). A 3D representation of test vehicles in Dynacar environment is depicted in Figure 3.6.

3.3.3 Control Architecture Design

Matlab/Simulink is proposed as the key tool for implementing the different ADAS/ADS functionalities (lane-keeping assist, cruise control, adaptive cruise control, rear-end collision avoidance, and fallback strategies in case of technical failures) in the proposed testing framework for validation.

The use of this software allows rapid prototyping, modularity, and scalability, which are key aspects for applying the methodology proposed in Section 3.2.

Next, the control software and hardware architectures proposed will be detailed. Note that these will be used for real and virtual environments.

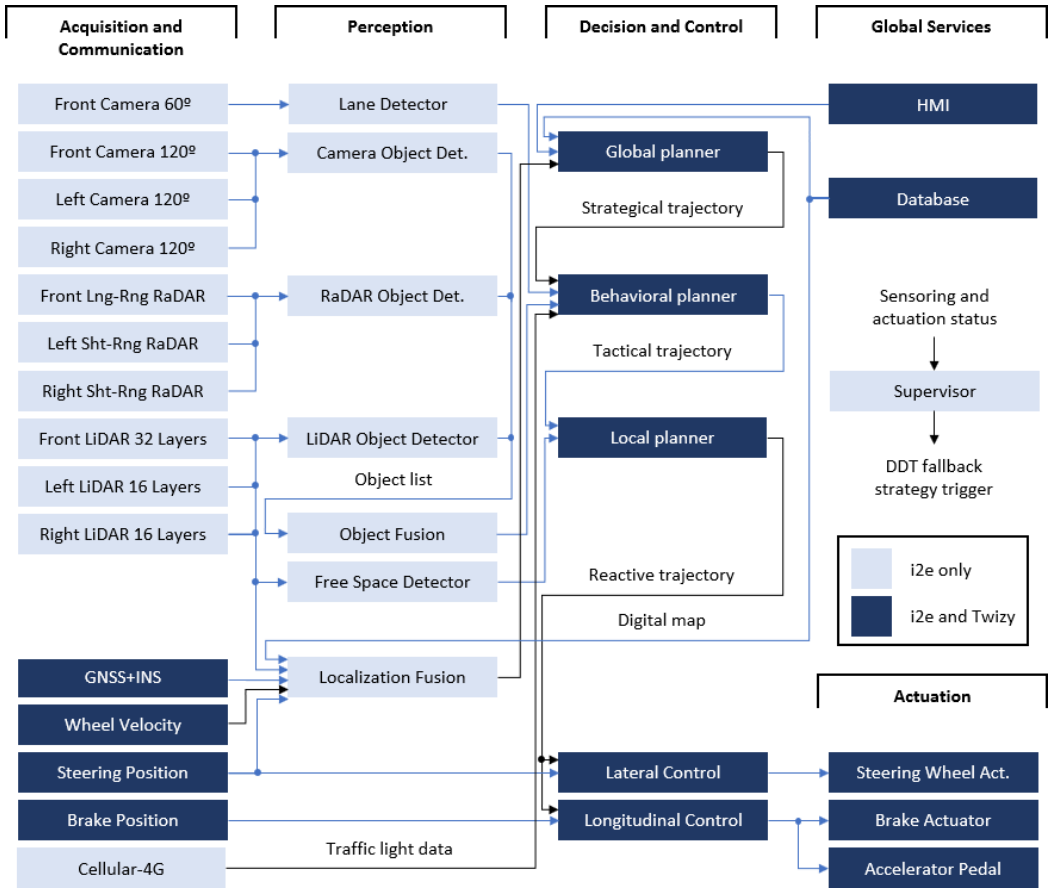

Figure 3.7 Software architecture designs proposed in this Ph.D. Thesis

3.3.3.1 Software Architecture

The software architecture design developed in this Ph.D. Thesis containing the main systems (acquisition, communication, perception, decision, control, actuation, HMI, database, and supervision) is depicted in Figure 3.7 including the elements detailed in Section 2.1.2.1.

Acquisition The acquisition provides information received through different devices in real or virtual test platforms. In *Irizar i2e*, acquisition devices include four cameras, three LiDARs, and three RaDARs. Additionally, in-vehicle sensors provide information on wheel velocity, steering wheel, and brake pedal position. In *Renault Twizy*, besides the in-vehicle sensors, virtual devices are considered for *object detection and recognition* even in real testing as detailed in the case study in Section 3.4.

Communication Communication provides information to decision, specifically, ego-vehicle localization from GNSS+INS fusion. The surrounding condition is also considered from intelligent infrastructure using Cellular technology, performing a link with virtual traffic

lights through a mesh-network over Wireless Fidelity (WiFi) with Ad-Hoc network using Optimized Link State Routing Protocol (OLSR) [248, 249].

Perception Perception uses Intempora/RTMaps running under the Linux environment to process the information from acquisition and perform both environment recognition, and object detection and classification. **Lane detector** uses a frontal camera and deep learning techniques to give information about the number, type, and waypoints of road lanes [250]. **Free space detector**, uses the merge point cloud from LiDARS and calculates a free space polygon representing the boundaries of a driveable area [220]. **Object fusion** uses detections from cameras, RaDARs, and LiDARs to provide information about object detection such as type, size, relative distance, and speed. First, 2D object detection is performed separately by cameras and RaDARs using deep learning techniques to achieve a 360^{o} covering. Second, data from LiDARs is merged in a unique point cloud, and 3D object detection estimates objects in surroundings employing deep learning. Finally, the data is fused in two ways to increase precision and accuracy, as well as redundancy in detection systems: using cameras with 1) RaDARs and 2) LiDARs [251, 252]. **Localization fusion** uses information from LiDARs, GNSS+INS, in-vehicle sensors, and digital maps from the database to give the ego-vehicle status such as a global position, velocity, acceleration, and orientation. A 3D match between recorded point clouds from digital maps and current ones from LiDARs allows a positioning estimation with high fidelity at some locations where the reception of satellites is not good enough such as tunnels and urban canyons [253]. This Ph.D. Thesis contributes to this last aspect, which is thoroughly described in Chapter 5.

Decision Decision uses Matlab/Simulink to process information mainly from perception, communication, HMI, and database to provide a safe and comfortable route to be followed and generate new trajectories in real-time, if necessary. **Global planner** uses information from the user (HMI), digital maps (database), and current ego-vehicle position (localization fusion) to construct a strategical trajectory locating hard-points along the route considering typical urban maneuvers (e.g. straight or curve paths, intersections, roundabouts, and merging). **Behavioral planner** uses information from the previous strategical trajectory, lane detector, object fusion, and intelligent infrastructure data (Cellular-4G) to modify (if necessary) the original driving maneuver developing a tactical trajectory locating new hard-points due to real-time events such as dynamic objects and traffic signal status. **Local planning**, uses the information from the previous tactical trajectory and driveable area (free space detector) to calculate a reactive trajectory considering both safety and comfort for passengers. This Ph.D. Thesis contributes in these aspects, which are described in Chapters 4 and 5.

Control Control uses Matlab/Simulink to track the reactive trajectory from the decision, and estimate position commands for actuation. The control is based on predictive strategies considering simplified models that resemble the vehicle behavior. Lateral control uses path reference variables (such as cross-track and orientation errors), current ego-vehicle status, and steering wheel position to calculate a new one. Longitudinal control uses speed reference, current ego-vehicle status, and brake position to estimate the new position of pedals. Physical constraints such as longitudinal jerk and steering wheel change rate are considered as control parameters, which allows specifying directly the comfort level. This Ph.D. Thesis contributes to these aspects, which are thoroughly described in Chapter 4.

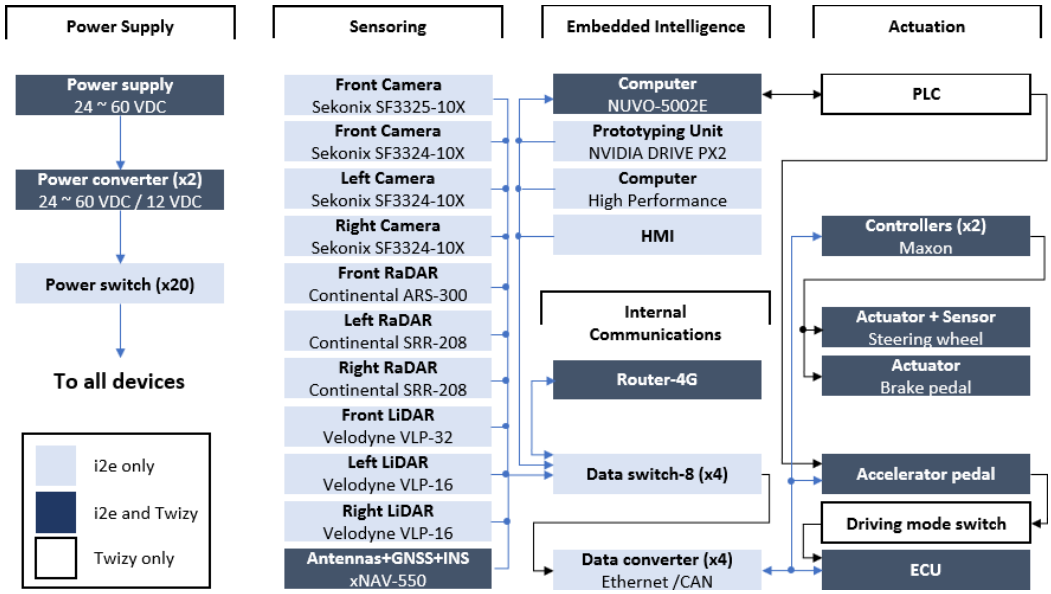

Figure 3.8 Hardware architecture designs proposed in this Ph.D. Thesis

Actuation Actuation receives information from control, moving the electro-mechanical actuators on the steering wheel and brake pedal in an accurate and reliable manner. Action commands in both virtual and real test platforms have been normalized between [-1, 1], from left to right turn for the steering wheel, and from braking to accelerating for the pedals. Actuation feed-back is available in order to return from automatic to a manual driving mode in case of driver requests.

Global Services World information from **Database** contains digital maps (roads, lanes, traffic signals, and static infrastructure) which can be accessed at any time by the perception and decision for localization or create trajectories according to current ego-vehicle status. **Supervision** is monitoring the acquisition, communication, and actuation systems status in case of technical failures. It can trigger appropriate trajectories to perform DDT fallback strategies and achieve a minimal risk condition. Moreover, driver requests by physical means (touching an emergency button, steering wheel, accelerator, or brake pedals) allow changing from automated to manual driving mode. This data is processed by decision. **HMI** defines the destination point and possible alternative to reach it. Additionally, the users are allowed to change driving parameters such as maximum speed, comfort level, and stops requests. This information is processed by the decision system.

3.3.3.2 Hardware Architecture

The proposed hardware architecture is based on development platforms, since the focus of AutoDrive Project[28] is the initial buildup of an automated vehicle demonstrator. The main elements in the hardware architecture design and their location on test platforms are respectively presented in Figures 3.8-3.9 and are detailed next.

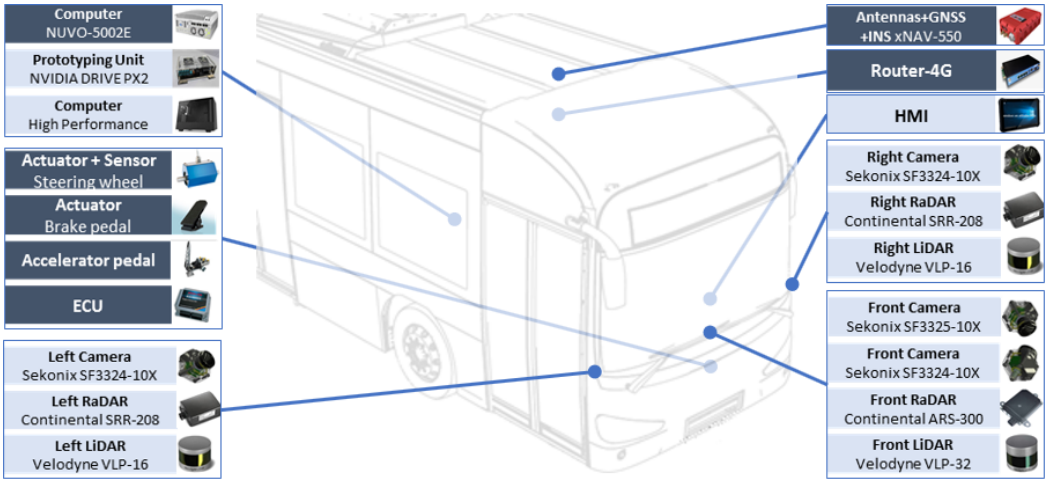

(a)

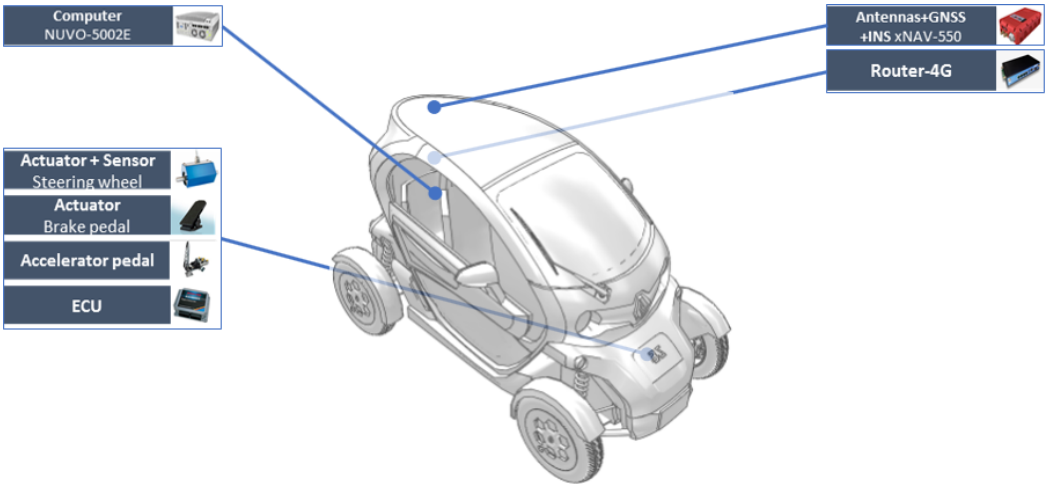

(b)

Figure 3.9 Hardware location on (a) Irizar i2e and (b) Renault Twizy

Power Supply The power supply is provided by test vehicle batteries from 24 to 60 VDC. Power converters to 12 VDC allow the energy supply to all hardware devices. In *Irizar i2e*, failure injection testing is feasible due to a power switch arrangement. In this regard, it is possible to cut off the energy source in the acquisition, embedded intelligence, actuation, and internal communication devices to test the ADS behavior in case of selected malfunctioning.

Sensoring Several sensors are installed in test platforms. In *Irizar i2e*, a group of cameras, RaDARs, and LiDARs are located at each front corner of the body. Additionally, one LiDAR and RaDAR are installed on the front side of the body. This arrangement is capable to acquire information from ahead, sides, and rear directions. A couple of high definition cameras for long and short view distances are installed at the center front side of the bus fixed both to the dashboard and windshield. In both *Irizar i2e and Renault Twizy*, the precise location of the vehicle along the route is possible with a GNSS+INS fusion, this is performed by the OXTS xNAV-550. The GNSS+INS is connected to one (*Renault Twizy*) or a couple (*Irizar i2e*) of antennas fixed to the top of the vehicle. A torque sensor is attached to the steering wheel, being useful to auto-manual driving mode switching from driver requests.

Embedded Intelligence In *Irizar i2e*, the information received by acquisition devices is processed in parallel by a rapid prototyping unit (NVIDIA DRIVE PX2) and a high-performance computer. In these, the data from surroundings is converted into objects and/or events, which are processed by an industrial computer (NUVO-5002E).

Actuation The actuation reference signal calculated by the embedded intelligence is executed by electro-mechanical motors fixed to the steering wheel and brake pedal. As both test vehicles are provided with a throttle-by-wire system, a by-pass in the electrical connection is enough to deliver the actuation signals from the control system.

Internal Communications Internal communications are managed mainly by ethernet, where data switches centralized the data transference from most devices including a wireless router-4G. In *Irizar i2e*, CAN/ethernet converters are connected with Actuation and ECU. In *Renault Twizy*, a Programmable Logic Controller (PLC) converts the data from NUVO-5002E to Actuation, considering also a driving mode switch which energizes electro-mechanical actuators and by-passes the accelerator pedal to receive commands from PLC.

3.3.3.3 X-in-the-Loop Testing

In this Ph.D. Thesis, simulations, and experiments were performed considering Model-in-the-Loop (MiL), Hardware-in-the-Loop (HiL) and Vehicle-in-the-Loop (ViL) approaches as shown in Figure 3.10, fulfilling the system Validation and Verification (VV) phases depicted in Figure 2.1. In particular, this chapter focuses on early and late development phases as pointed in Figure 3.1.

The XiL testing consists of two computers, one containing the ADS algorithms and the other the virtual validation environment described in Section 3.3.2. An ethernet connection allows emulating communications as in ViL testing on real vehicles.

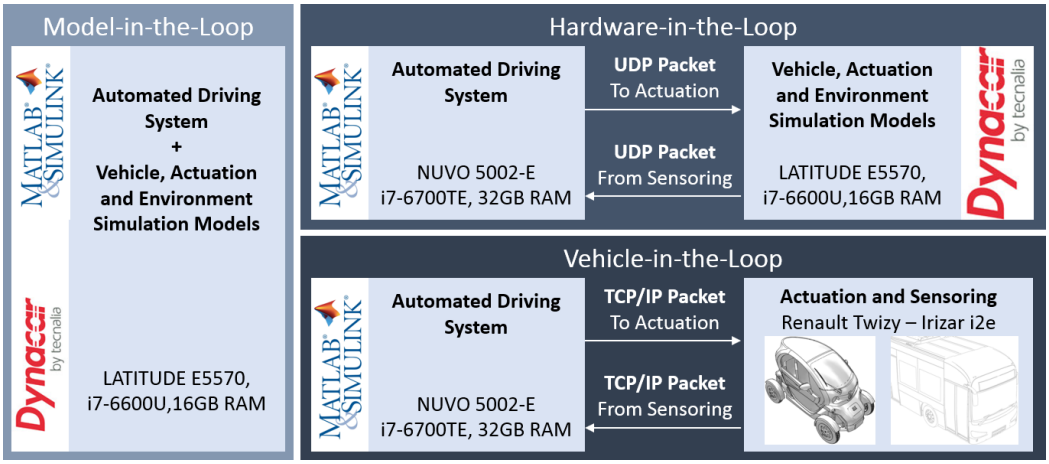

Figure 3.10 X-in-the-Loop testing architectures

3.4 Case Study: Renault Twizy

To illustrate the application of the methodology proposed in Section 3.2.3, a particular case study is presented using the *Renault Twizy* and the testing framework proposed in Section 3.3. The aim is to obtain a feasible vehicle simulation model of an automated *Renault Twizy* (see Figure 1.1) and use it to simulate and tune a Traffic Jam Assist (TJA) driving functionality as an LSHA development.

The selected vehicle detailed in Section 3.3.1 has been adapted for automated driving. For that purpose, an industrial computer (NUVO-5002E) pointed in Section 3.3.3.2 has been employed both in the real vehicle and MiL testing, running the ADS on MATLAB/Simulink. Figures 3.7-3.8 summarizes the software and hardware architecture designs. Figure 3.10 points to the MiL arrangement to perform virtual testing.

3.4.1 Requirements and Specifications

As detailed in Section 3.2.2, the requirements and specifications for technical safety testing[44] describe driving scenario-based use-cases considering *functional range*, *desired behavior*, *fuctional system boundaries*, and *driving scenario* [254].

The use-case definition for Traffic Jam Assist (TJA) is shown in Table 3.4, based on the standard ISO/PAS-21448[44].

3.4.2 Open-Loop Validation: Obtaining a Simulation Model

As defined in the proposed methodology (Figure 3.3a), the first step is to obtain a simulation model of the test vehicle, the Renault Twizy. The main technical parameters are detailed in Table 3.3, which are used to implement a multibody formulation-based dynamics model using Dynacar as detailed in Section 3.3.2.1.

Table 3.4 Use-case for Traffic Jam Assist based on ISO/PAS-21448[44]

Functional range			Traffic Jam Assist
Desired behavior			The system keep vehicle on driving lane and avoid collisions with objects ahead considering passenger's safety and comfort
System boundaries			Virtual acquisition and perception systems, GNSS+INS positioning, virtual (MiL) and real (Renault Twizy) testing
Scenario	**Action and events**		- The Vehicle Under Test (VUT) is tracking a planned trajectory - A moving object exists on the VUT's path without a hazardous distance (Time-to-Collision > 2s)
	Goals and values		Goal: Keep driving on path, no lane nor heading change Safety: Lateral (<0.5m) and heading (<20deg) deviation, longitudinal velocity (<5m/s), relative distance VUT to GVT (>5m) Comfort: Lateral (<2m/s^2) and Long. (<1m/s^2) acceleration
	Scene	**Dynamic elements**	Moving object ahead on the road with variable velocity
		Scenery	Closed-circuit testing
		Self-representation	The VUT is for passenger transfer use

Table 3.5 Actuation parameters of Renault Twizy

Device	**Brake**	**Steering**	**Unit**	**Device**	**Brake**	**Steering**	**Unit**
Actuator Model	408057	136210	-	**Time Delay**	8.00e-2	8.00e-2	s
Resistance	3.07e-1	1.43e-1	ohm	**Rate Limiter**	2	4.85e-1	rad/s
Inductance	1.88e-4	5.65e-5	H	**Proportional**	1	8.00e-1	-
Rotor inertia	1.21e-4	2.09e-3	kg-m^2	**Integral**	0	6.00e-1	-
Torque Constant	5.34e-2	3.28e-2	N-m/A	**Derivative**	1.20e-2	2.00e-1	-
Mechanical time	1.30e-2	3.99e-1	s	**Filter Coeff.**	100	100	-

3.4.2.1 Actuation Parameters

As defined in Figure 3.8, two electro-mechanical actuator systems are introduced in the brake pedal and steering wheel of the real test vehicle. Both actuation systems have low-level controllers to ensure that motors follow the position command given by the high-level controller. The elements that compose the low-level actuation system model are detailed in Section 3.3.2.2. Specifically, parameters for actuation modeling have been extracted from manufacturer data (Maxon), and their values are contained on the left side of Table 3.5.

Additionally, as in real implementations, a controller is employed to position the device in the desired value with zero error. Moreover, the time delay of the vehicle's internal communications, the rate limit of actuators, and the gains for the PID controllers are optimized by-hand through experiments. The right side of Table 3.5 shows the tuned parameters.

3.4.2.2 Validation of the Vehicle Model

Once the models for actuation and vehicle dynamics have been defined, the overall simulation model needs to be validated using experimental data. In addition to the blocks previously mentioned, the parameters associated with the powertrain and braking performance, as well as steering wheel and front wheels angle ratio, are obtained from the manufacturer specifications of these elements.

A series of tests are proposed to validate the simulation model including brake and

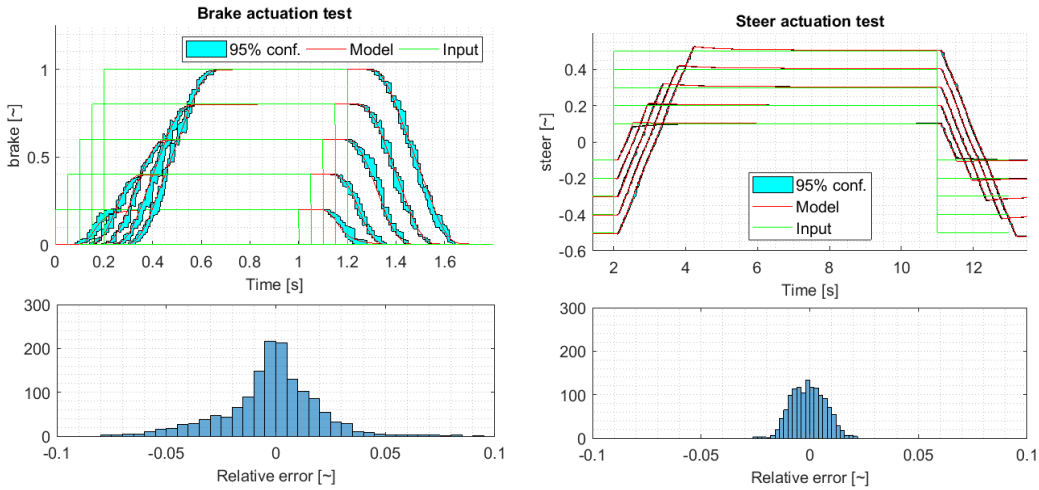

(a) (b)

Figure 3.11 (a) Brake and (b) steering actuation response

steering actuation, longitudinal, and lateral dynamics. Note that this is an iterative process in which several tests are required to optimize some parameters to fit experimental data, as some phenomena (as time delays or nonlinear effects) are difficult to model otherwise. The results of the tests mentioned previously are thoroughly analyzed as follows.

Brake and Steering Actuation A series of step input commands of different amplitudes are used to identify the maximum speed and displacement range of each actuator. Additionally, the PID parameters are extracted from the motor controller to simulate them and optimize the proposed actuation models using experimental tests. The motor positioning is used as a validation metric to compare SRQ from measurements and predictions.

Figure 3.11 shows comparisons between open-loop model predictions and experimental measurements for the brake pedal and steering wheel actuators, which are normalized between [0,1] and [-1,1], respectively. As the SRQ (positions) accuracy of the predictions is within 95% of model confidence, the actuation models of Figure 3.5 (including low-level controllers and mechanical actuators) are considered validated for both brake pedal and steering wheel. Results evidence the significant effect of the actuation dynamics on the inputs of the vehicle dynamics. Moreover, histograms containing the relative error in position between model predictions and means of experimental measurements, show that in most cases the positioning differences are below 5%.

Longitudinal Dynamics Straight-line *acceleration* and *braking* STM are usually employed to characterize longitudinal performance in vehicle dynamics (see Table 3.1). In this Ph.D. Thesis, instead of making different isolated tests, a combined acceleration-braking test is proposed, in which a series of step input commands with similar magnitudes for acceleration and braking is executed, together with intervals of zero input commands (*Coast-down* and *Low-speed* STMs). This allows optimizing the powertrain, braking, aerodynamic

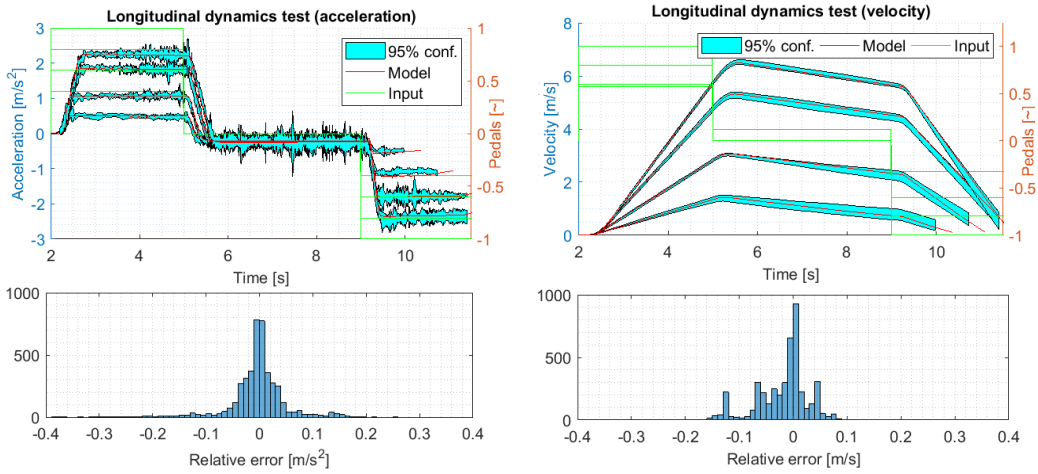

(a) (b)

Figure 3.12 Longitudinal (a) acceleration and (b) velocity from pedals input

drag, and rolling resistance constants with the same test results. The acceleration and velocity are used as validation metrics to compare SRQ from measurements and predictions.

Following the scheme of Figure 3.3a, open-loop tests are performed by the application of a sequence of the accelerator and brake pedal step inputs, covering acceleration, coasting, and braking, from a starting standing still to a final full stop. Figure 3.12a shows experimental and predicted longitudinal acceleration for four individual tests ranging from 30% to 100% pedal step inputs. The longitudinal dynamics, modeled in Dynacar as detailed in Section 3.3.2.1, is shown to predict well the delays, ramps, and acceleration levels obtained in the vehicle. It is noted that, after performing the tests, it was established that the brake pedal was not fully released for a zero input. This fact was considered in the simulations. Figure 3.12b shows the corresponding speed profiles, averaged over eight tests for each pedal step size, with their corresponding uncertainty intervals. As differences between the two SRQs selected (longitudinal acceleration and velocity) are well within 95% of model confidence, the longitudinal dynamics modeling, coupling vehicle dynamics, and actuators, is considered validated. Moreover, histograms show relative error between real and virtual vehicles in accelerations and velocities below 0.1m/s^2 and 0.1m/s, respectively.

Lateral Dynamics To define the relationship between the steering wheel and front wheel angles, tests with different turning angles at a low constant speed will be executed (*steady-state turning*). This allows comparing the circular paths described by the real vehicle and the simulation model. A localization device is necessary for carrying out this test. The path radius is used as a validation metric to compare SRQ from measurements and models.

Figure 3.13 shows steady-state paths for four steering wheel positions (40, 60, 80, and 100%) at a constant speed of 1m/s. Confidence bands from experimental trajectories correspond to 3 repetitions of both left and right turning. Note that only half of the circular trajectories are being plotted so experimental uncertainties and model predictions can be observed. These open-loop results, comparing measured and predicted path ra-

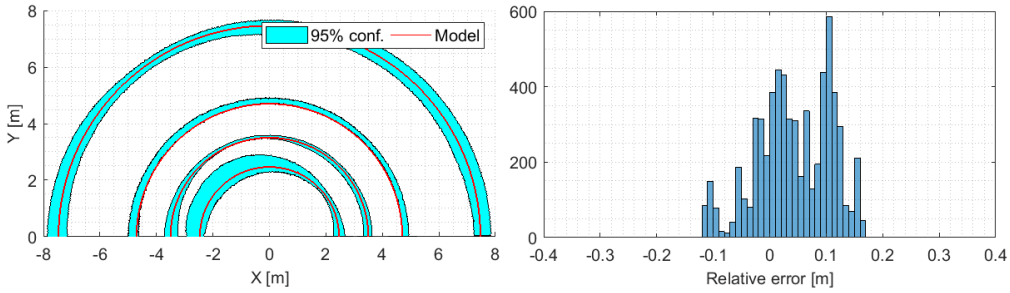

Figure 3.13 Steady-state turning at constant velocity

diuses, validate the steady-state lateral dynamics behavior of the model, allowing tuning of the corresponding parameters, such as the steering wheel/front-wheel angle gain at 31/1. Moreover, histograms show a relative error between real and virtual turning radius below 0.2m.

3.4.3 Closed-Loop Validation: LSHA Feature Simulation

The proposed methodology allows the testing of LSHA functionalities based on the simulation model obtained previously. As stated earlier, a proper simulation model can be used to time-boost the development of automated driving functionalities, and even further optimize the developed model by a proper choice of closed-loop testing.

In this section, an ADAS feature has been selected as a case study. The developed LSHA functionality is a Traffic Jam Assist, which combines Lane Support System (LSS) and Speed Assist System (SAS) (see Table 3.2) to follow a traffic flow at low speeds (<30km/h) without lane change support [15]. To implement this functionality, lateral and longitudinal vehicle motion controllers are employed. The lateral control allows the vehicle to remain within its lane, while the longitudinal control either maintains the required speed (Cruise Control-CC) or adapts its longitudinal speed to maintain a safe distance from an obstacle or a preceding vehicle (Adaptive Cruise Control-ACC). The implementation of this trajectory tracking approach is detailed in Chapter 4.

In this case study, relative distances and velocities concerning the VUT are defined with a virtualized *Acquisition and Perception systems*, mimicking a traffic jam situation locating a virtual Global Vehicle Target (GVT) ahead. The GVT represents a vehicle, whose purpose is to activate sensor systems, representing a vehicle having the necessary features to be recognized from any direction (3D vehicle target)[66]. The closed test circuit presented in Figure 3.4a is employed for real and virtual scenario-based testing. The lateral and heading deviations from test paths, lateral acceleration, steering wheel position, longitudinal velocity and acceleration, pedals position, relative distance VUT to GVT are used as validation metrics to compare SRQ from experimental measurements and model predictions.

[66]Technical Bulletin: Euro NCAP - Global Vehicle Target Specification https://rb.gy/igid4z

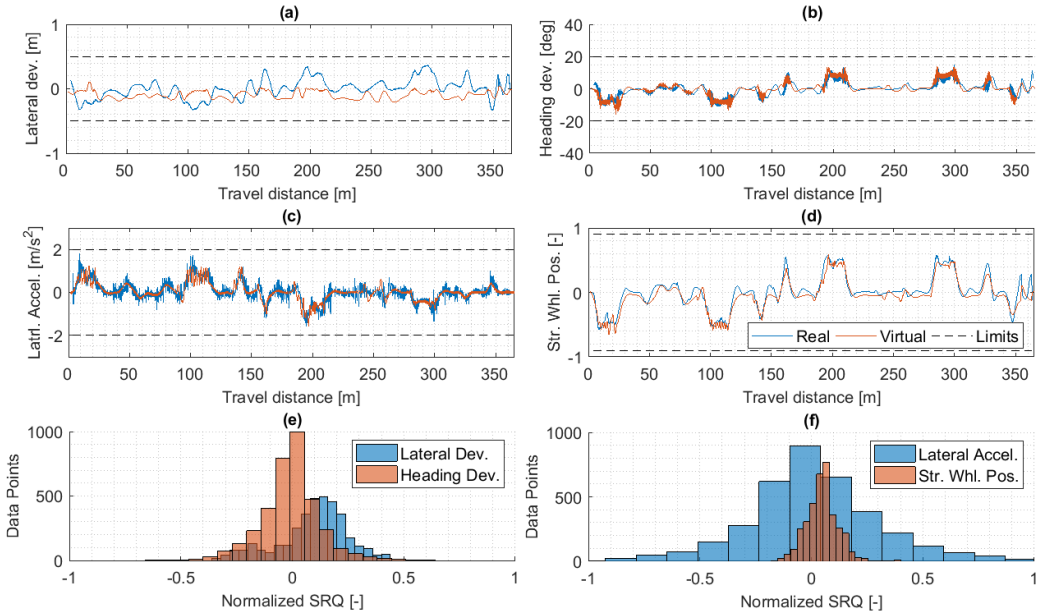

Figure 3.14 LSS VV in Renault Twizy: (a) Lateral and (b) Heading Deviations, (c) Lateral Acceleration, (d) Steering Wheel Position, and (e-f) Error Distribution of Normalized SRQs

3.4.3.1 System Verification and Validation

Real and virtual executions were performed using MiL and ViL testing platforms, as shown in Figures 3.8 (Renault Twizy) and 3.10, respectively. The VV assessments are based on both *face-validity* (subjective approach) and *statistical validity* (objective validation) similar to the open-loop validation process to obtain a simulation model. Both LSS and SAS are considered, as both combined result in TJA driving functionality.

Regarding the LSS, the assessment is performed through face-validity and statistical analysis between real and virtual testings as portrayed in Figure 3.14. Here, the SRQs focus on lateral and heading deviations, lateral acceleration, and steering wheel position. The lateral and heading deviations compiled in Figures 3.14a-b evaluate the ability to follow the predefined path. As the same LSS is applied to both experiments and simulations, the analysis of these errors supports the feasibility of the dynamic model to evaluate or develop control schemes. Tracking errors in real and virtual environments show similar behaviors, with the same frequency components, though, as expected, the experiments evidence slightly higher amplitudes due to positioning uncertainties typical of the GNSS+INS device. Further simulation analysis showed that an important component of the tracking errors corresponds to a frequency of around 0.13Hz, which has been directly related to the LSS performing compensations to the suspension misalignment. Yet, the model can simulate the actual system even in this condition. The lateral acceleration and steering wheel position in virtual testing follows an overall behavior of the experimental measurements along the route as shown in Figures 3.14c-d. Error distributions between real and virtual SRQs are presented in Figures 3.14e-f. Each SRQ is normalized considering its respective

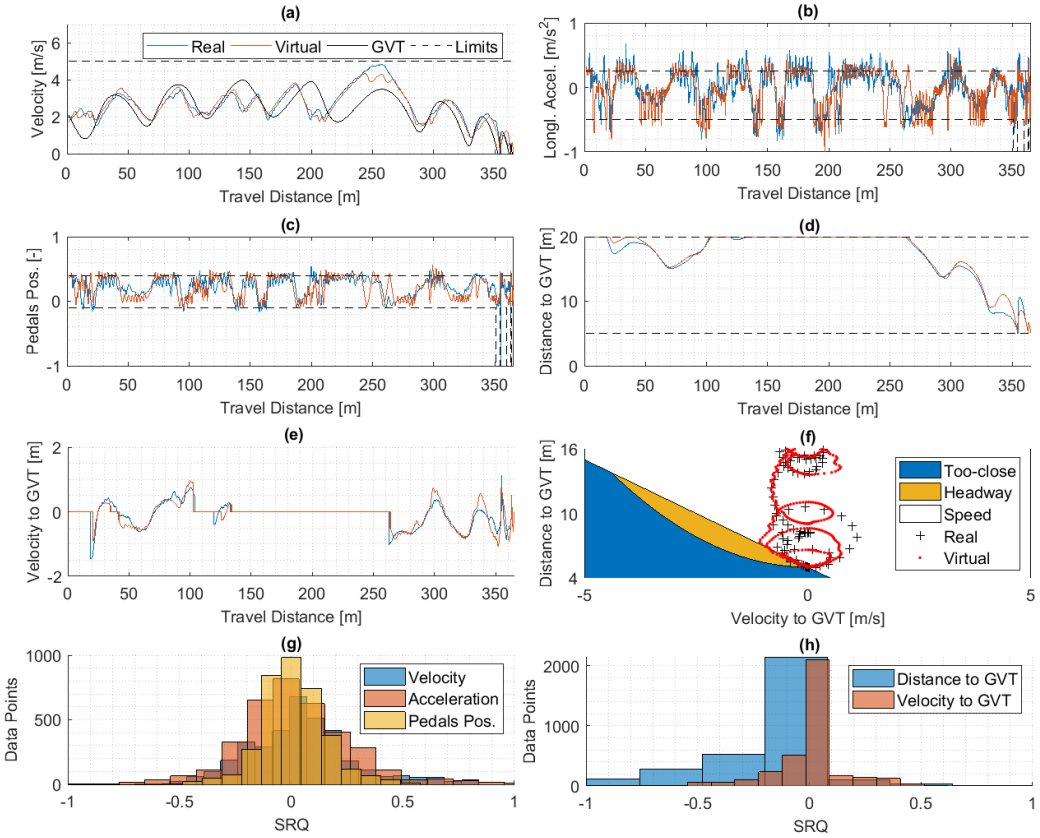

Figure 3.15 SAS VV in Renault Twizy: Longitudinal (a) Velocity and (b) Acceleration, (c) Pedals Position, Relative (d) Distance and (e) Velocity to GVT, (f) Range vs. Range-Rate Diagram, and (g-h) Error Distribution of SRQs

comfort or safety threshold limit magnitude (dashed black lines). Slight tails in most SRQs represent a good match between the real environment and simulations. The heavy tail of the lateral deviation constitutes a poor match being mostly affected by the previously mentioned positioning uncertainties of real measurements, moreover, the bimodal distribution (two peaks) also evidence the suspension misalignment mentioned before. LSS safety and comfort goals are achieved at each SRQs assessment.

Regarding the SAS, the assessment is performed through face-validity and statistical analysis between real and virtual testings as depicted in Figure 3.15. Here, the SRQs focus on longitudinal velocity and acceleration, pedals position, relative distance, and velocity from VUT to GVT. The longitudinal velocity of VTU is decreased either the magnitude of the lateral acceleration increases (comfort) or the relative distance to GVT decreases (safety), performing an ACC considering the velocity of the GVT as shown in Figure 3.15a. The longitudinal acceleration and pedals position shows a dynamic response of real and virtual testings very similar while accelerating and braking validating a proper longitudinal dynamics modeling as depicted in Figures 3.15b-c. At the end of the test, deceleration

limits are increased to keep a safe distance to GVT. The relative distance and velocity from VUT to GVT, as recorded by the virtualized *Acquisition and Perception systems*, evidence how a small-time difference on the detection time can affect the SAS and VUT's ensuing motion as pointed in Figure 3.15d-e. Moreover, the SAS combines both comfort and safety performing *speed*, *headway* or *too-close* longitudinal control related to the zone location of the relative distance-velocity relationship as presented in the range vs. range-rate diagram in Figure 3.15f. The safety minimum distance of 5m is remained at all times, even in a Stop and Go event, which makes this SAS suitable for urban driving scenarios. Error distributions between real and virtual SRQs are presented in Figures 3.15g-h. This time the normalization was not considered as the SRQs have a similar magnitude, allowing the analysis with raw data. Slight tails in most SRQs represent a good match between the real environment and simulations. SAS safety and comfort goals are achieved at each SRQs assessment as the threshold limits are respected.

3.5 Case Study: Irizar i2e

To illustrate the scalability of the methodology proposed in Section 3.2.3, a second case study is presented using the *Irizar i2e* and the testing framework proposed in Section 3.3. In this case, the aim is to verify and validate a TJA driving functionality, considering hilly roads and heavy-duty commercial vehicles in a city-urban LSHA development.

As in the previous case study, the selected vehicle detailed in Section 3.3.1 has been adapted for automated driving. For that purpose, an industrial computer (NUVO-5002E) (Section 3.3.3.2) has been employed for both HiL and road testings, running the ADS on MATLAB/Simulink. Figures 3.7-3.8 summarizes the software and hardware architecture designs. Figure 3.10 illustrates the HiL arrangement to perform virtual testing.

3.5.1 Requirements and Specifications

The use-case definition for TJA is similar to the previous case study, presented in Section 3.4.1 and specified in Table 3.4. Nonetheless, some remarks are pointed next.

The **system boudaries** consider real perception devices to perform object detection. Regarding the **scenario**, although objects in the surroundings must be detected as part of **action and events**, those may be, or not, contained on the Vehicle Under Test's (VUT) path. This is due to the fact that road testing has been performed in a confined area with an uncontrolled environment (Irizar facilities depicted in Figure 3.4b). In addition, **goals and values** thresholds are adjusted to assure: 1) **Safety**, by defining a variable limit for longitudinal velocity which must be enforced even on road gradients (10%); and 2) **comfort**, by constraining lateral and longitudinal accelerations ($<0.315 \mathrm{m/s^2}$)[64]. Regarding the **scene**, random objects in the surroundings are allowed as mentioned previously in system boundaries (pedestrians, bicycles, cars, motorbikes, bus, and generic objects).

3.5.2 Open-Loop Validation: Obtaining a Simulation Model

The procedure to obtain a reliable simulation model for the *Irizar i2e* bus also considers the methodology specified in Figure 3.3a. The main technical parameters for actuation devices, longitudinal and lateral dynamics, were obtained performing identical procedures as the ones described previously in Section 3.4.2. The validation results were also assessed

following subjective and objective approaches, obtaining a vehicle simulation model that fulfills confidence intervals in the same way as in Renault Twizy.

As most of the open-loop validation results are sensible for the bus manufacturer, the most relevant technical data obtained from these testings will remain confidential except those already detailed in Table 3.3.

3.5.3 Closed-Loop Validation: LSHA on Hilly Roads

The proposed methodology allows the testing of LSHA on Hilly Roads based on the simulation model obtained from the open-loop procedure. As stated before, a proper simulation model time-boost the development of ADS, optimizing the vehicle simulation model through closed-loop testing.

As in the previous case study, a TJA functionality has been selected to test the scalability of the ADS tracking a trajectory at low speeds (<30km/h) without lane change support. To implement this functionality, lateral and longitudinal vehicle motion controllers are employed. The lateral control allows the vehicle to remain within its lane, while the longitudinal control either maintains the required speed (Cruise Control-CC) even at considerable road gradients (± 10deg). The implementation of this trajectory tracking approach is thoroughly explained in Chapter 4.

The closed test circuit presented in Figure 3.4b is employed for real and virtual scenario-based testing, the implementation of this trajectory planning approach is detailed in-depth with a case study in Chapter 4. The lateral and heading deviation from test paths, lateral acceleration, steering wheel position, longitudinal velocity and acceleration, and pedals position of VUT is used as validation metrics to compare SRQ from experimental measurements and model predictions.

3.5.3.1 System Verification and Validation

Real and virtual executions were performed using HiL and ViL testing platforms, as shown in Figures 3.8 (Irizar i2e) and 3.10, respectively. The VV assessments are based on both *face-validity* (subjective approach) and *statistical validity* (objective validation). Both LSS and SAS are considered, as both combined result in TJA driving functionality.

Regarding the LSS, the assessment is performed through face-validity and statistical analysis between real and virtual testings as portrayed in Figure 3.16. Here, the SRQs focus on lateral and heading deviations, lateral acceleration, and steering wheel position. The lateral and heading deviations compiled in Figures 3.16a-b evaluate the ability to follow the predefined path. As the same LSS is applied to both experiments and simulations, the analysis of these errors supports the feasibility of the dynamic model to evaluate or develop control schemes. Tracking errors in real and virtual environments show similar behaviors, with the same frequency components, though, similar to the previous case study (Renault Twizy), the experiments evidence slightly higher amplitudes due to positioning uncertainties of the GNSS+INS device which have been included in this time, presenting a poor positioning reception of near 1m at some locations of the route. Yet, the model can simulate the actual system even in this condition. The lateral acceleration and steering wheel position in virtual testing follows an overall behavior of the experimental measurements along the route as shown in Figures 3.16c-d. Error distributions between real and virtual SRQs are presented in Figures 3.16e-f. Some SRQs are normalized considering their

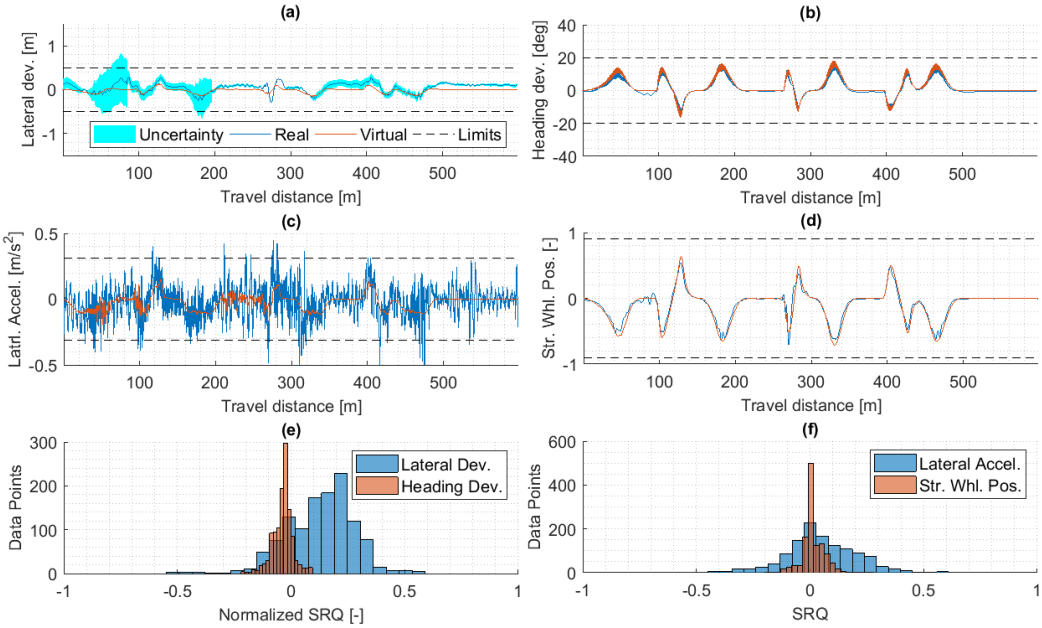

Figure 3.16 LSS VV in Irizar i2e: (a) Lateral and (b) Heading Deviation, (c) Lateral Acceleration, (d) Steering Wheel Position, (e-f) Error Distribution

respective comfort or safety threshold limit magnitude (dashed black lines). Slight tails in heading deviation and steering wheel position represent a good match between the real environment and simulations. However, the heavy tails on lateral deviation and acceleration constitute a poor match being mostly affected first, by positioning uncertainties, and second, by noisy data acquisition. LSS safety and comfort goals are achieved at each SRQs assessment.

Regarding the SAS, the assessment is performed through face-validity and statistical analysis between real and virtual testings as depicted in Figure 3.17. Here, the SRQs focus on longitudinal velocity and acceleration, and pedal position. The longitudinal velocity of VTU properly respects the threshold limits along the route, even at uphill or downhill circumstances as shown in Figure 3.17a. The longitudinal acceleration and pedals position shows a dynamic response of real and virtual testings very similar while accelerating and braking validating a proper longitudinal dynamics modeling as depicted in Figures 3.17b-c. Error distributions between real and virtual SRQs are presented in Figures 3.17d-f. Slight tails in all SRQs represent a good match between the real environment and simulations resulting in a high fidelity virtual testing environment. SAS safety and comfort goals are achieved at each SRQs assessment as the threshold limits are respected.

Regarding object detection, the perception system on-board allows sensing the surroundings as depicted in Figure 3.18. A sequence of pictures shows the object detection on the uphill zone of the route. The surroundings correspond with the ADS environment (blue background squares), perceiving the surroundings from LiDARs (white point clouds) and detecting, classifying, tracking, and fusing objects (green squares). None object obstructed the driving path in the present case study.

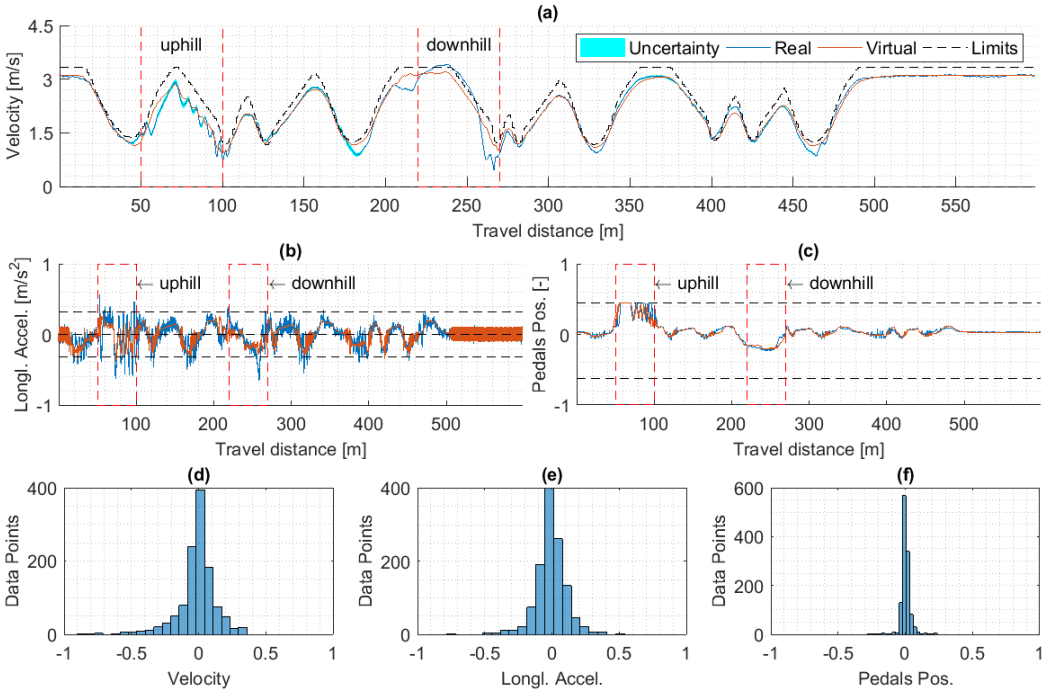

Figure 3.17 SAS VV in Irizar i2e: Longitudinal (a) Velocity and (b) Acceleration, (c) Pedals Position, and (d-f) Error Distribution of SRQs

3.6 Conclusion

In this chapter, a two-step methodology is proposed to validate not only the vehicle and its actuation models under simulation environments but also automated driving functionalities through technical safety testings. For that purpose, first, a set of open-loop tests are proposed, which allow tuning models for the actuation devices, longitudinal and lateral dynamics. Second, the developed model allows testing ADS functionalities in a set of closed-loop tests based on driving scenarios.

In order to apply the integrated validation procedure, a Testing Framework for Validation is proposed. It allows scenario-based testing both in virtual and real environments in a progressive manner, following the best engineering practices in the system development life cycle of systems such as MiL, HiL, ViL, and road testings. Moreover, the actuation dynamics and modeling are thoroughly described, thinking on conventional vehicles expected to be modified and originally not conceived with the automated actuation system (drive-by-wire). Furthermore, the modularity of the testing framework for validation has the capability of handling vehicles of different characteristics, from a Renault Twizy 80 to an Irizar i2e bus.

To illustrate the approach, two case studies based on automated vehicles of considerable dissimilar sizes are proposed. In both case studies, the vehicle models and actuation systems are firstly validated using real data. Results show that actuation dynamics have a significant effect that must be considered, as they could importantly affect the development

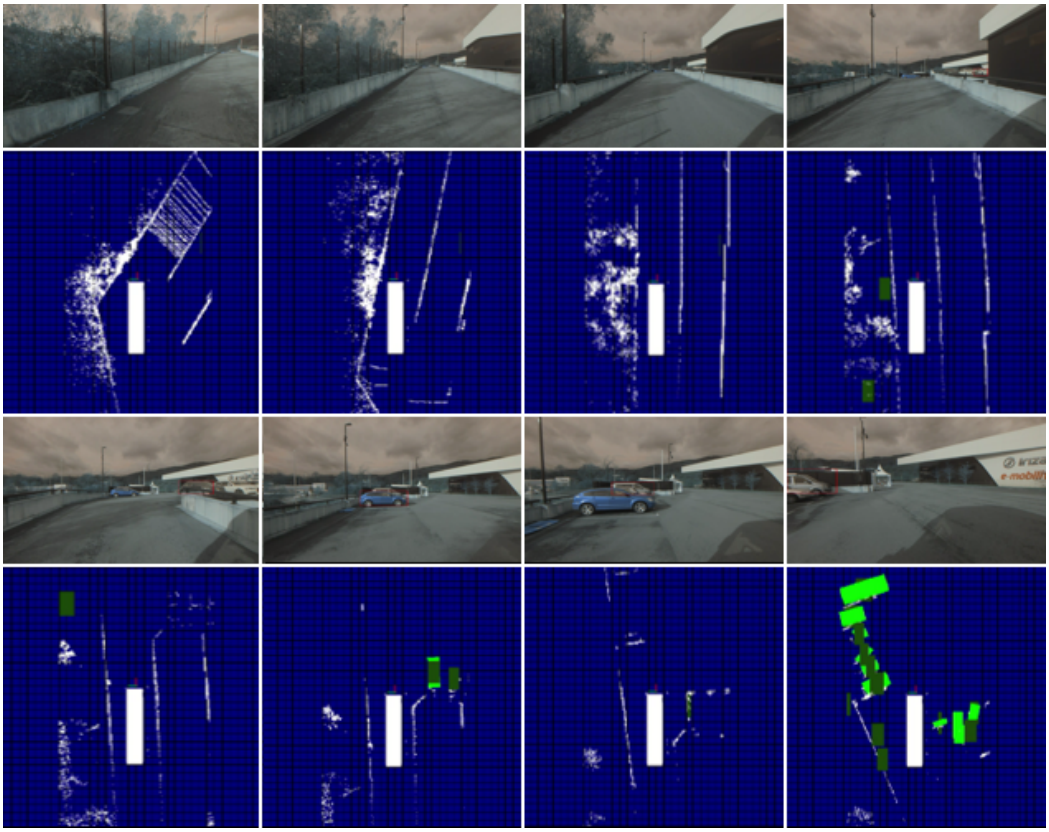

Figure 3.18 Object detections during uphill zone (courtesy of Vicomtech, Irizar e-Mobility and AutoDrive Project)

using virtual testings. Secondly, TJA functionality is tested. The LSS keeps the vehicle on lane along the tests ensuring safety. Regarding Renault Twizy's case study, the consideration of lateral acceleration allows the SAS to adapt the longitudinal velocity while avoiding collisions with GVT ensuring safety and comfort. Regarding the Irizar i2e's case study, the consideration of road gradients allows testing the SAS on critical driving scenarios for heavy-duty passenger vehicles. Subjective (face-validity analysis) and objective (statistical analysis) validation approaches assess the behavior between experiments and simulations.

In conclusion, the proposed validation procedure enables to tune reliable simulated test platforms and automated driving strategies in simulation environments, reducing the time on real test implementations. The ADS algorithms employed to obtain the VV results presented in this chapter are thoroughly described as follows in Chapter 4. Moreover, the proposed procedure is evaluated considering non-faulted automated driving scenarios and use cases, as a standardized practice presented in ISO/PAS 21448[44]. However, the injection of electric/electronic malfunctions would be still considered in the development phase using simulations, considering the safety verification process mentioned in the standard ISO 26262[45]. The evaluation of fail-operational systems is an aspect covered in Chapter 5.

Chapter Four

Safety and Comfort in Vehicle Motion

Safety and comfort are major influences in driving behavior. The physical capabilities of vehicles in terms of acceleration and jerkiness, as passengers' comfortability threshold levels, must be considered for vehicle modeling. When safety maneuvers are not required comfort must determine the driving behavior, hence, decision and control systems are essential for the development and testing of trajectory planning and tracking algorithms. Successful results from system verification testings mostly rely on the next aspects:

- In-vehicle modeling, the knowledge of handling, performance, and tire characteristics become necessary when model-based control techniques are employed. On one hand, handling describes the direction of motion of the vehicle in response to a steering control parameter. On the other hand, performance defines the straight-line motion of the vehicle due to acceleration and braking control parameters.
- In trajectory planning, usual strategies consist of two stages; the estimation of a path and then the definition of a speed profile related to the previously defined path. However, both the path and velocity would be independently modified when objects or events arise while the Dynamic Driving Task (DDT) is executed. Normally, the combination of both path and velocity estimations is also known as trajectory planning.
- In trajectory tracking, proper control methods must be designed to safely follow the desired reference path and velocity. Model Predictive Control (MPC) is one of the most popular advanced model-based control techniques for this purpose. MPC approaches use the vehicle and tire models to predict the future behavior of the vehicle and compute the optimum control sequence to be applied. Moreover, this latter calculation is carried out considering explicitly the physical constraints of the system and its actuators.

This chapter investigates novel trajectory planning and tracking procedures where vehicle modeling plays an important role, based on the middle of the system development life cycle showed in Figure 4.1. Section 4.1 explain motivations behind the use of specific techniques for proper vehicle motion control. Section 4.2 describes the required specifications to ensure safety and comfort during the DDT execution, along with typical vehicle models as useful tools. Section 4.3 details the strategies for trajectory planning and tracking employed for verification testing. Sections 4.4-4.6 describe the application of proposed approaches in three case studies considering an automated Irizar i2e bus. Finally, Section 4.7 summarizes the main ideas and contributions of this chapter.

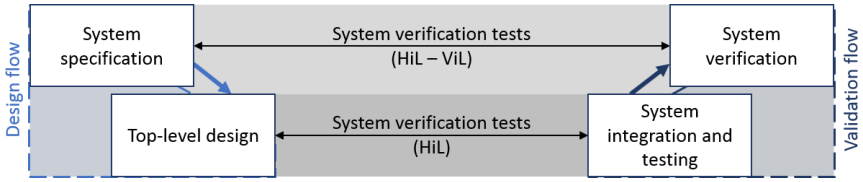

Figure 4.1 System verification testing

4.1 Motivation

Verification and Validation (VV) methods to ensure the technical safety of an Automated Driving System (ADS) using virtual testings have been covered in Chapter 3. In this chapter, statistical grey box testings were employed in real-world tests to assess the performance of a particular ADS system on a variety of driving scenarios. This is considered an appropriate test design technique[44][122], useful to demonstrate the Safety Of The Intended Functionality (SOTIF) and the positive impact of the ADS approach without driver interaction. Moreover, the employed procedures helped to answer the question *Did I build the right thing?* mentioned in Section 2.1. However, the algorithms contained in the ADS core were not contemplated, which are responsible to perform longitudinal and lateral vehicle motion control on a sustained basis[1], laying the foundations to achieve the SAE Level 2 of driving automation.

In this chapter, algorithms for vehicle motion in automated driving are presented, which are based on the middle of the system development life cycle showed in Figure 2.1 (which is an excerpt of the validation cycle detailed in Figure 4.1). The relationship among concepts of safety, vehicle limits, and driver comfort is entirely considered at each stage of development. Firstly, passenger's safety and comfort play a role in the definition of path and Speed Trackings, which are conceived using interpolating methods for trajectory planning. Secondly, MPC is employed to track the previously mentioned trajectory references, bearing in mind the ability of this optimal control approach to take into account constraints that are related to the physical vehicle limits, safety, and comfortability. Finally, to illustrate and verify the technical feasibility of the developed algorithms, two case studies based on virtual testings that include the Irizar i2e bus are considered. This testing platform has a more challenging dynamics response and dimensions in contrast to Renault Twizy as described in previous chapters.

4.2 Safety and Comfort Influence on Vehicle Motion

Safety and comfort, which are related to each other, are two major application areas when considering the development of controllers for vehicle motion. In the evolution of control approaches for automated vehicles, comfortability must influence primarily the vehicle handling and performance when safety maneuvers are not engaged. In this latter case, however, safety will have to be prioritized. Hence, if model-based control approaches are considered, considering the physical capabilities of vehicles in the model is as important as comfort levels suitable for human mobility[64].

Regarding safety, the primary measures of driver collision risk in the literature are the longitudinal acceleration (a_x) and Time-To-Collision (TTC), the latter one is the time it

Table 4.1 Acceleration and jerk threshold values

x-Accel.[64]	m/s^2	Uncomfort[68]	m/s^2	x-Jerk[64]	m/s^3
↑ **Max.**	5.49	**Not**	<0.32	**Comfort**	0.98
↑ **Comfort**	3.66	**A little**	0.32 to 0.63		
↓ **Comfort**	-3.66	**Fairly**	0.5 to 0.1	**Uncomfort**	>3.92
↓ **Uncomfort**	-4.57	**Yes**	0.8 to 1.6		
↓ **Min.**	-4.57 to -6.10	**Very**	1.25 to 2.5	**Crash**	>14.72
↓ **Min.**$^{\text{Standard}}$	-9.81	**Extreme**	>2		

takes for both vehicle and object to collide if they continue on their current path with their present kinematic characteristics held constant. The distribution of TTC values can be used for safety improvement assessment and compare observed field and simulated trajectories [255]. In this sense, quantitative criteria from safety events per miles provide statistics that are easy to interpret and compare, such as *crash* (relative distance equal or less than zero), *near-crash* (a_x>0.5g and TTC<2s) and *Forward Collision Warning* (FCW, TTC<2.4s).

When considering driver comfort, acceleration and jerk are useful parameters to ensure comfortability, being also convenient to convey information about the feasible vehicle limits. Drivers rarely engage in unsafe or uncomfortable driving maneuvers, hence most of the time a fraction of the handling and performance capabilities of the vehicle are used due to a variety of reasons including safety, comfort, and fuel consumption. Probabilistic[64] and experimental[256] threshold values for driving acceleration and jerk are pointed in Table 4.1. These values have been used as System Response Quantity (SRQ) in two case studies presented in Chapter 3.

4.3 Vehicle Motion Planning and Tracking

The vehicle motion comprises the DDT subtasks necessary for real-time planning and control of lateral and longitudinal components of vehicle motion. On one hand, lateral control includes detection of the vehicle's position relative to the lane boundaries and the application of steering and/or differential braking inputs to maintain an appropriate lateral positioning. On the other hand, longitudinal control includes maintaining the reference speed as well as detecting a preceding vehicle on the driving path, maintaining an appropriate gap to preceding object, and applying propulsion or braking inputs [1].

In this section, methods to generate and track the desired driving trajectory focusing on urban environments and considering both safety and comfort are proposed. Furthermore, techniques to respond appropriately in case of object or event detections are also covered.

4.3.1 Trajectory Planning

The trajectory planning for road vehicles consists of two stages; the estimation of a path and then the definition of a speed profile related to the previous path. Normally, the combination of path and velocity planners is also known as trajectory planning.

In this section, a method for trajectory planning is proposed, which is composed of two steps. First, a path planning procedure is proposed consisting of an interpolating method

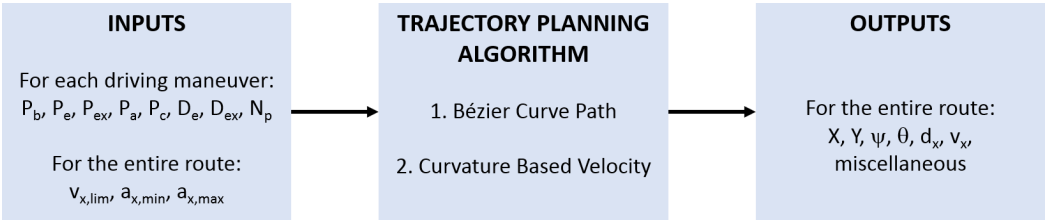

Figure 4.2 Inputs and outputs of trajectory planning algorithm

based on Bézier curves, as this method allows to generate with low computational cost a continuous curvature path which can be compatible with comfortable driving (see Section 2.2.1.3). Once the path has been defined, a method for speed planning is proposed, which estimates a comfortable speed profile by considering both the path's curvature and the physical thresholds of the vehicle, actuation devices, and driving road.

The flowchart presented in Figure 4.2 describes the steps for the trajectory planning procedure proposed in this Ph.D. Thesis. The global cartesian coordinates (X, Y), orientation angle (ψ), road gradient (θ), travel distance (d_x), and velocity (v_x) are considered as the most important parameters to define a driving trajectory which is defined by waypoints. Moreover, additional 'miscellaneous' data can be included for a better definition of the path according to the Operational Design Domain (ODD) such as infrastructure location (traffic signals, traffic lights, speed bumps, crosswalks, bus stops, etc.), consequently, contributing to enhancing the knowledge of trajectory planning developed on previous works [171].

4.3.1.1 Path Planning

As previously stated, the method selected for path planning is the generation of Bézier curves due to its pliability to use location on the road to defining inputs, while assuring continuity is the curvatures of the estimated path. A general mathematical representation is shown in Equation 4.1

$$[X(\tau), Y(\tau)] = \sum_{i=0}^{n} B_i^n P_i \quad \tau \in [0, 1] \tag{4.1}$$

where n is the polynomial order of the curve, i is an order counter, B is the Bernstein Polynomial related to the order of the curve, and P are the control points selected, which goes from 0 to 1. Finally, $X(t)$ and $Y(t)$ define a path in the XY plane in the time domain.

As most of the urban and interurban driving maneuvers can be reduced to a typical set, in this Ph.D. Thesis the most common ones have been considered (intersections, lane-changes, and roundabouts) (see Figure 4.3).

The path generation of driving maneuvers depends only on the input parameters defined by the user. Considering these parameters, the path planning algorithm is capable to estimate the position of the Bézier points which define both orientation and waypoints of the path.

In this sense, the next input parameters are essential in the path planning procedure (see Figure 4.3):

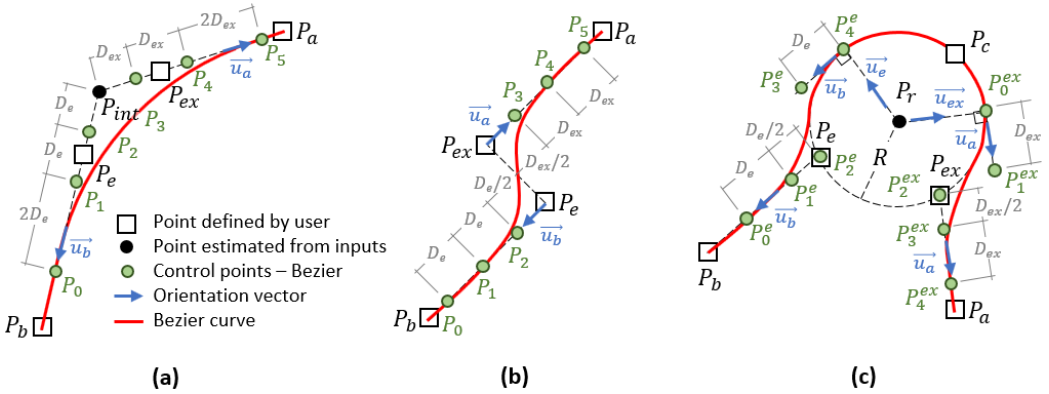

Figure 4.3 Path planning based on Bézier curves for typical driving maneuvers such as: (a) intersection, (b) lane change and (c) roundabout

- The pre-entrance (P_b), entrance (P_e), exit (P_{ex}) and post-exit (P_a) points. In the roundabout maneuver, an additional point located on the perimeter (P_c) is required.
- The entrance (D_e) and exit (D_{ex}) distances among the control points.
- The number of points (N_p) to define the Bézier curves at the entrance and exit of driving maneuvers, which is used to obtain an even value of τ.

From the previous inputs, the next parameters are estimated by the algorithm:

- Orientation vectors at entrance ($\vec{u_b}$) and exit ($\vec{u_a}$). For roundabouts, these vectors are suggested as tangent to the perimeter for calculation simplicity.
- For intersections, crossing $\vec{u_b}$ and $\vec{u_a}$ gives an intersection point (P_{int}). In roundabouts, a center point (P_r) is obtained from circle with P_e, P_c and P_{ex}, as in [166].
- Control points (P) are located over $\vec{u_b}$ and $\vec{u_a}$ as described in Table 4.2. In roundabouts, orientation vectors $\vec{u_e}$ and $\vec{u_{ex}}$, are perpendicular to $\vec{u_b}$ and $\vec{u_a}$, respectively.
- Points describing the Bézier curves using Equation 4.1 and Table 4.3. In roundabouts, the perimeter of a circle must be described to link the entrance and exit paths.

To obtain feasible results from the path planning generation process, the maximum steering angle of the testing vehicle must be considered so that its physical capabilities are not surpassed. Moreover, the area covered by the testing vehicle's body when executing the planned path must be supervised to avoid possible collisions (mostly while turning) with static infrastructure. In Section 4.4, several techniques to obtain successful path planning are analyzed applied to a particular study case.

4.3.1.2 Speed Planning

The speed planning considers the path geometry estimated previously in Section 4.3.1.1. The path curvature (k), also defined as the inverse of the path's radius ($k = 1/R$), is

Table 4.2 Bézier control points equations for typical maneuvers

Point	Intersection	Lane change	Roundabout^{e}	Roundabout^{ex}
P_0	$4Du_b + P_i$	$5Du_b/2 + P_e$	$3D_e u_b/2 + P_e$	$Ru_{ex} + P_r$
P_1	$2Du_b + P_i$	$3Du_b/2 + P_e$	$D_e u_b/2 + P_e$	$D_{ex} u_{ex} + P_0^{ex}$
P_2	$Du_b + P_i$	$Du_b/2 + P_e$	P_e	P_{ex}
P_3	$Du_a + P_i$	$Du_a/2 + P_{ex}$	$D_e u_e + P_4^e$	$D_{ex} u_a/2 + P_{ex}$
P_4	$2Du_a + P_i$	$3Du_a/2 + P_{ex}$	$Ru_e + P_r$	$3D_{ex} u_a/2 + P_{ex}$
P_5	$4Du_a + P_i$	$5Du_a/2 + P_{ex}$	-	-

Table 4.3 Bézier polynomial coefficient equations for typical maneuvers

Coeff.	Intersection/Lane change	Roundabout
K_0	P_0	P_0
K_1	$-5P_0 + 5P_1$	$-4P_0 + 4P_1$
K_2	$10P_0 - 20P_1 + 10P_2$	$6P_0 - 12P_1 + 6P_2$
K_3	$-20P_0 + 30P_1 - 30P_2 + 10P_3$	$-4P_0 + 12P_1 - 12P_2 + 4P_3$
K_4	$5P_0 - 20P_1 + 30P_2 - 20P_3 + 5P_4$	$P_0 - 4P_1 + 6P_2 - 4P_3 + P_4$
K_5	$-P_0 + 5P_1 - 10P_2 + 10P_3 - 5P_4 + P_5$	-

the result of a planar differential geometry[67] calculated analytically considering the global cartesian coordinates X and Y as described in Equation 4.2.

$$k = \frac{||X'Y'' - X''Y'||}{(X'^2 + Y'^2)^{3/2}} \tag{4.2}$$

To measure human comfort, the acceleration is frequently used in driving environments as is related to vibrations[64]. This measure captures useful information to classify the driving actions as comfortable or not (e.g. intensive back-and-forth car-following behavior, extreme turning at high-speed, or uncomfortable ride due to the irregular road). In this sense, the comfort prediction is defined as the resultant of a three-dimensional vector which combines longitudinal (a_x), lateral (a_y) and vertical (a_z) accelerations as described in Equation 4.3

$$a_w = (a_x^2 + a_y^2 + a_z^2)^{1/2} \tag{4.3}$$

where a_w represents the desired comfort level during the driving task. In most cases, as the vehicle motion is assumed to be on a flat surface, the a_x and a_z are usually neglected and a_y is only considered as the maximum desired value. Consequently, the speed reference ($v_x{}^{ref}$) is calculated as described in Equation 4.4

$$v_x^{ref} = (\frac{a_w}{n_w|k|})^{1/2} \tag{4.4}$$

where a_w goes from a_w<0.315m/s^2 (not uncomfortable) to a_w>2m/s^2 (extremely uncomfortable), and the weight index (n_w) is a recommended constant at 1.4[68]. The absolute value of k is considered to avoid negative values into the square root.

[67] Kroon, D. J. (2011). 2D Line curvature and normals. Mathworks File Exchange. https://rb.gy/tpidwe
[68] standard: ISO 2631-1 https://www.iso.org/standard/7612.html

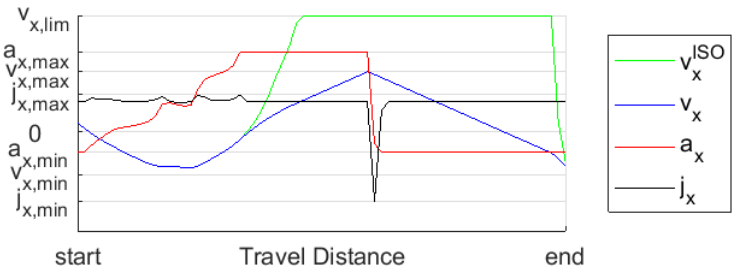

Figure 4.4 Speed Planning Based on ISO 2631-1[68] and FHWA-JPO-16-405[64]

The previous estimation is capable of reducing the value of v_x^{ref} according to k, being this mainly related to a maximum permissible value for a_y while turning. However, sudden acceleration and braking result from this procedure at the exit and entrance of curves, respectively. Consequently, longitudinal acceleration thresholds must also be considered to avoid uncomfortable driving executions. Furthermore, the longitudinal jerk is also a key comfort requirement for vehicle passengers which must be contemplated. A graphic representation of this issue is depicted in Figure 4.4.

The obtained v_x^{ref} results suitable for trajectory tracking, especially for feedback controllers where the system is reactive and not capable to make adjustments due to future references in the longitudinal velocity. However, together with the trajectory tracking response, smooth transitions defined in the planning phase highly contribute to more safe and comfortable driving.

4.3.2 Trajectory Tracking

Once the driving trajectory has been planned, path and speed references must be tracked to perform the vehicle motion control in road vehicles.

To perform trajectory tracking, the most popular approach is Model-based Predictive Control (MPC), which has been analyzed in Section 2.2.2.4. MPC approaches require a proper dynamic model to predict the system behavior in a defined sliding-horizon and allow to compute optimal inputs to consider the system constraints explicitly.

As vehicle dynamics are nonlinear by nature, the proposed approaches are based on Nonlinear MPC (NMPC), whose formulation is detailed first, before detailing the proposed tracking approaches.

4.3.2.1 Model Predictive Control Problem Formulation

A finite-horizon constrained NMPC problem solved at each time step has the form described in Equations 4.5a-f.

$$\min_{s,z,u} \quad \sum_{k=0}^{N_s-1} \|s_i(z_i,u_i) - s_i^{ref}\|^2_{Q_w} + \sum_{k=0}^{N_u-1} \|u_i - u_i^{ref}\|^2_{R_w} \tag{4.5a}$$

$$\text{s.t.} \quad s_0 - \overline{s}_0 = 0, \tag{4.5b}$$

$$s_{i+1} - f_i(s_i, z_i, u_i) = 0, \quad i = 0, ..., N_s - 1 \tag{4.5c}$$

$$s_{i+1}^{min} \leq s_{i+1} \leq s_{i+1}^{max}, \quad i = 0, ..., N_s - 1 \tag{4.5d}$$

$$u_i^{min} \leq u_i \leq u_i^{max}, \quad i = 0, ..., N_u - 1 \tag{4.5e}$$

$$u_i = 0, \quad N_u \leq i \leq N_s. \tag{4.5f}$$

where $s_i \in \mathbb{R}^{N_s}$ is the differential state, $z_i \in \mathbb{R}^{N_s}$ is the algebraic state, and $u_i \in \mathbb{R}^{N_u}$ is the control input. The N_s and N_u are the prediction and control horizons, respectively ($N_u \leq N_s$). The $[s_{i+1}, u_i]^{min,max}$ are the differential states and control constraints, respectively. The subscript $k+1$ denotes variable value at $k+1$ steps ahead of the current time.

The NMPC control law is defined by Equation 4.5a. The problem relies on the initial value constraint defined in Equation 4.5b, where $\overline{s}_0 \in \mathbb{R}^{N_s}$ can be time dependent. An implicit system of *differential algebraic equations* is described by the nonlinear dynamics in Equation 4.5c. The constraints for differential states and control inputs, are denoted by Equations 4.5d and 4.5e, respectively. According to N_s and N_u values, values for u_i can be neglected as in Equation 4.5f. In this regard, the solution of the NMPC problem from Equations 4.5a-f provides a model-based feedback strategy based on the current state and time.

Equations 4.5 define an Optimal Control Problem (OCP) to be solved at each time step [13]. In this regard, OCP solver packages have been developed and are currently available both in open-source such as IPOPT[69] and DSOA [257], as well as proprietary-source such as PROPT[70] and MUSCOD-II[71]. At the same time, NMPC software packages based on multiple shooting are available such as OptCon [258] and NEWCON [259].

[69] GitHub: COIN-OR Foundation/IPOPT https://github.com/coin-or/Ipopt
[70] webpage: PROPT - MATLAB Optimal Control Software (DAE, ODE) http://tomdyn.com/
[71] webpage: NEOS Server/MUSCOD-II https://rb.gy/qok16q

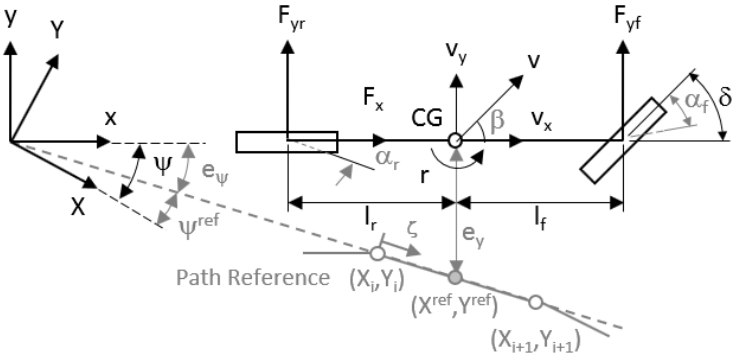

Figure 4.5 Single track model for vehicle lateral dynamics

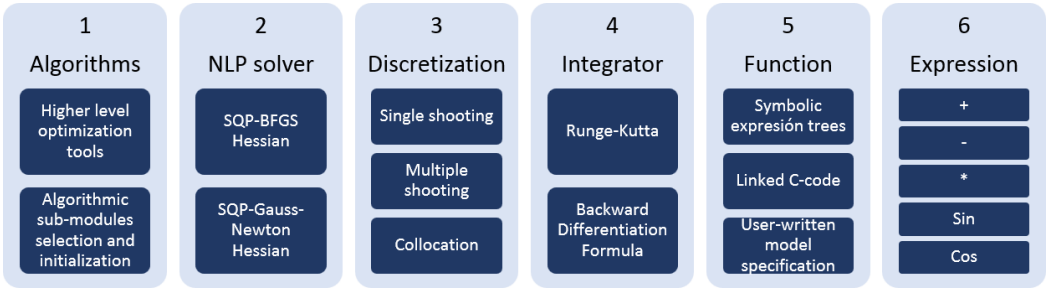

Figure 4.6 ACADO Toolkit's 6-main algorithmic base classes [13]

In this Ph.D. Thesis, ACADO is selected for feedback control based on real-time optimization (NMPC), considering that most of the other existing packages are either not open-source or limited in their user-friendliness, difficult to install (especially on embedded hardware), not designed for closed-loop NMPC applications, and hard to extend with specialized algorithms. The basic structure of ACADO is depicted in Figure 4.6 [13].

4.3.2.2 Lateral and Heading Deviations

MPC approaches require to operate the knowledge of the future reference to be followed. In this particular case, this is provided by the trajectory planning proposed in Section 4.3.1. In addition, the difference between the vehicle's location and the planned path must be estimated to properly perform the trajectory tracking. As shown in Figure 4.5, the path reference is divided in consecutive straight segments, so if the projection of the vehicle onto one segment is out-of-bounds ($0>\zeta>1$), the previous or next segment must be selected to make a new projection. Equation 4.6 is useful to know if the projection is on the segment:

$$\zeta = \frac{(X - X_i)(X_{i+1} - X_i) + (Y - Y_i)(Y_{i+1} - Y_i)}{(X_{i+1} - X_i)^2 + (Y_{i+1} - Y_i)^2} \tag{4.6}$$

where X and Y are the global axis coordinates, i defines the location of the items into an array, and the value of ζ must be in the 0-1 interval for a correct projection of the vehicle's location on the segment of the path to be considered in-bounds. A previous or next segment will be selected, decreasing ($j = -1$) or increasing ($j = 1$) the value of i, in the case that ζ is negative or higher than 1, respectively. In the latter case, it means that the projection is out-of-bounds.

Once the proper segment of the path has been found ($0<\zeta<1$), the perpendicular distance from the vehicle's location to the driving path, together with the difference in their orientation are calculated. These variables are known as *lateral and heading deviations* or *lateral and angular errors*. A flow diagram of this process is shown in Figure 4.7.

Parameters from the trajectory planning procedure such as $X_{i,i+1}$ and $Y_{i,i+1}$ (see Figure 4.5) are taken from each segment of the path as references for the trajectory tracking task. Equations 4.7a-b show the calculations for lateral (e_y) and heading (e_ψ) deviations respect to a segment of the path.

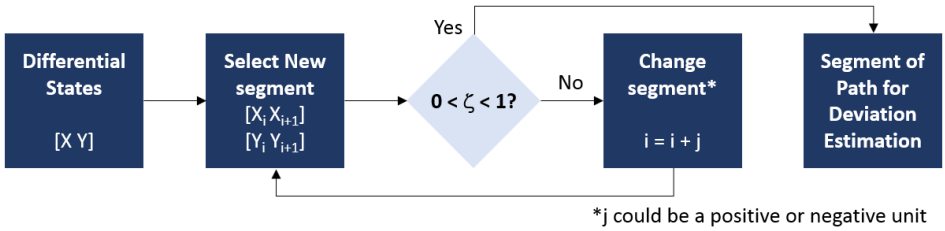

Figure 4.7 Segment of the path selection

$$e_y = \frac{(Y - Y_i)(Y_{i+1} - Y_i) - (X - X_i)(X_{i+1} - X_i)}{(X_{i+1} - X_i)^2 + (Y_{i+1} - Y_i)^2} \tag{4.7a}$$

$$e_\psi = \psi - \psi_i \tag{4.7b}$$

where ψ is the orientation angle of the vehicle to global X axis and ψ_i is the orientation angle reference from the path's segment.

4.3.2.3 Internal MPC Models for Path Tracking

To perform path tracking using an MPC approach, accurate models that define the handling dynamics of the vehicle are required. However, at the same time, these need to be as simple as possible, so the proposed path tracking MPCs can be implemented in real-time platforms.

As mentioned in Section 2.1.1.1, the single-track vehicle model is a well-known simplification used in vehicle control approaches [9, 65, 260], where the front and rear wheels are defined as single wheels at each axle, and the vehicle is assumed to have a planar motion. The notation usually employed in the literature for a front-steered-only vehicle model is depicted in Figure 4.5. As also described in Section 2.1.1.1, the single-track vehicle model can be defined considering the vehicle kinematics or dynamics. Hence, depending on the used model, two main approaches arise: the kinematic and dynamic model-based methods. Also, both can be blended to increase the operational range of the MPC.

Kinematic Model-Based Approach In this approach, the major assumption is that the velocity vectors at front and rear wheels are in the direction of their orientations. Consequently, the velocity vector at front wheel and the front wheel steering angle (δ), make the same angle with respect to the longitudinal axis of the vehicle. In this sense, the slip angle of front and rear wheels is neglected. This is a reasonable assumtion at low speeds (less than 5m/s), as the lateral forces at tires are small [65]. The vehicle motion is described by Equations 4.8a-e:

$$\dot{X} = v_x \cos(\psi + \beta)/\cos\beta \tag{4.8a}$$
$$\dot{Y} = v_x \sin(\psi + \beta)/\cos\beta \tag{4.8b}$$
$$\dot{\psi} = v_x \tan\delta/L \tag{4.8c}$$
$$\dot{\delta} = \Delta\delta \tag{4.8d}$$
$$\beta = \tan^{-1}(l_r \tan\delta/L) \tag{4.8e}$$

where β is the vehicle's slip angle, located between the velocity (V) of the center of gravity of the vehicle (CG) and its longitudinal axis. The estimation of β depends only on geometric relationships as is described in [65]. The L is the wheelbase distance, which results from the sum of distances from the CG to the front (l_f) and rear (l_r) axles, respectively.

When implementing the lateral path tracking using this model, the front steer angle rate ($\Delta\delta$) is considered as the control input to define handling limits instead of δ, as an aggressive steering results in higher wear of mechanical components and lead to unpredictable driving. On the other hand, the longitudinal velocity (v_x) is considered as the external variable instead of V as it is easier to measure in real implementations, hence $V = v_x \cos\beta$ must be included in Equations 4.8a-b. This basic formulation can be further enhanced if different phenomena are considered, as analyzed below.

- **Lateral Jerk:** Considering small time steps for the computation of the vehicle's motion, its lateral acceleration can be approximated as a uniform circular motion. From previous *slip angle approach* which considers a front wheel steered vehicle, it is possible to approximate the path radius as $R = L/\delta$ ($\tan\delta \approx \delta$) for small values of β ([65]). Therefore, the lateral motion behavior can be also described by $a_y = v_x^2\delta/L$. Furthermore, a_y would be derived as depicted in Equation 4.9.

$$\dot{a_y} = (2a_x\delta + v_x\Delta\delta)v_x/L \tag{4.9}$$

  This allows to include a_y as a state variable in the MPC formulation, allowing to impose comfort-related constraints on it. Moreover, the current v_x can be reduced if a_y is used as driving constraints, providing safety from relating speed limits and comfort feeling in DDT execution. This latter approach has been implemented in the case study of Section 3.5.

- **Lateral and Heading Deviation Rates:** From previous *slip angle approach* which considers a front wheel steered vehicle, it is possible to derivate e_y and e_ψ rates as described in Equations 4.10.

$$\dot{e_y} = v_x \sin(e_\psi) \tag{4.10a}$$
$$\dot{e_\psi} = v_x \tan\delta/L \tag{4.10b}$$

  where e_ψ is the heading deviation described in Equation 4.7b.

  These equations redefine the vehicle's position and orientation from a global coordinates system (X, Y, ψ) to a local one (e_y, e_ψ), simplifying the development of lane

support systems as the lateral and heading deviations concerning the driving lane can be used instead of global coordinates [261]. Moreover, this allows to consider these variables in the states vector of the MPC, allowing to predict their time-evolution and impose safety-related constraints on them. This implementation is used in the case study of Section 5.5.

Dynamic Model-Based Approach This approach allows to consider higher speeds (>5 m/s) than the aforementioned one (Kinematic Model-Based Approach), as it takes into account the effects of tire forces and slips angles. Hence, the dynamics of both the vehicle and tire are considered.

As the lateral force on the tires increases, the slip angles at the wheels are no longer considered negligible and a dynamic approach becomes necessary [65]. The vehicle motion from this method is described by Equations 4.11a-b:

$$\dot{v_y} = (F_{yf}\cos\delta + F_{yr} - mv_x r)/m \tag{4.11a}$$
$$\dot{r} = (l_f F_{yf}\cos\delta - l_r F_{yr})/I_z \tag{4.11b}$$

where v_y is the lateral velocity at CG, r is the heading rate, m is the total mass and I_z is the yaw axis inertia of the vehicle. The external lateral forces on the front (F_{yf}) and rear (F_{yr}) axles are in Equations 4.12a-b:

$$F_{yf} = C_{\alpha f}\alpha_f \tag{4.12a}$$
$$F_{yr} = C_{\alpha r}\alpha_r \tag{4.12b}$$

where $C_{\alpha f}$ and $C_{\alpha r}$ are the cornering stiffness on the front and rear axles, respectively; and α_f and α_r are the slip angles associated with those axles, defined in Equations 4.13a-b.

$$\alpha_f = \delta - \tan^{-1}((l_f r + v_y)/v_x) \tag{4.13a}$$
$$\alpha_r = \tan^{-1}((l_r r - v_y)/v_x) \tag{4.13b}$$

The estimation of $C_{\alpha f}$ and $C_{\alpha r}$ is a complex task in a real scenario, as these coefficients represent the interactions between tires and road surface, which may not be linear. Hence, in this Ph.D. Thesis, a procedure for a real-time identification of these parameters is thoroughly described in Chapter 5.

Model Blending Approach The aforementioned two approaches (kinematic and dynamic) can be blended in a single one that combines the benefits of both. This allows to increase the operating range of the MPC. To implement this approach, both models have to be combined considering the same differential states. In this sense, to the dynamic model Equations 4.11a-b, the kinematic model Equations 4.14a-b must be added:

$$\dot{v_y} = (F_x\tan\delta/m + v_x\Delta\delta/\cos^2\delta)l_r/(l_f + l_r) \tag{4.14a}$$
$$\dot{r} = (F_x\tan\delta/m + v_x\Delta\delta/\cos^2\delta)/(l_f + l_r) \tag{4.14b}$$

The lateral velocity (v_y), and yaw rate (r) are calculated with respect to the reference system attached to the CG (see Figure 4.5). Furthermore, v_y can be approximated to $v_y = l_r\, r$ considering $r = v_x \tan\delta/(l_f + l_r)$ [224]. As the *kinematic model-based approach*, v_x is an external variable that can be assumed as a time varying function (from *Acquisition* or *Perception* systems), or can be obtained from a longitudinal vehicle model [65].

Thus, when lateral tire forces can be neglected, the kinematic model provides appropriate and fast results, while the dynamic model is used when tire slip is significant. This way, considering the previous set of equations, the vehicle motion is described by Equations 4.15a-f:

$$\dot{X} = v_x \cos\psi - v_y \sin\psi \tag{4.15a}$$

$$\dot{Y} = v_x \sin\psi + v_y \cos\psi \tag{4.15b}$$

$$\dot{\psi} = r \tag{4.15c}$$

$$\dot{\delta} = \Delta\delta \tag{4.15d}$$

$$\dot{v_y} = (1-\lambda)\dot{v_y}^{kin} + \lambda\dot{v_y}^{dyn} \tag{4.15e}$$

$$\dot{r} = (1-\lambda)\dot{r}^{kin} + \lambda\dot{r}^{dyn} \tag{4.15f}$$

where $[X, Y, \psi, \delta, v_y, r]^T$ are the states related to the CG.

The superscripts $(.)^{kin}$ and $(.)^{dyn}$ specify the relation of v_y and r with the kinematic and dynamic models defined in previous sections. The parameter λ is selected to switch or blend the two proposed vehicle models. If $\lambda = 0$, then a full kinematic model is applied. On the contrary, if $\lambda = 1$, then a fully dynamic model is engaged. An intermediate value of λ defines a model blended circumstance. The definition of λ along with different strategies selected for model blending are described in the case study analyzed in Section 4.5 for better clarity, although a brief analysis is carried at the end of this subsection.

Similar to the *kinematic model-based approach*, $\Delta\delta$ is considered as control parameter. The use of incremental variables as $\Delta\delta$ (used in Equations 4.14a-b and 4.15d) allows handling limitation for safe and comfortable driving. On the other hand, v_x, $C_{\alpha f}$, $C_{\alpha r}$ and λ are considered as external variables which can be measured or identified during the DDT execution.

Tuning Procedure for Model Blending The blending of vehicle models is based on two aspects: 1) the switching condition, and 2) the switching method.

The switching condition is based on a physical measure usually available on the vehicle's acquisition, v_x being the most used [262]. However, this value is typically defined by the designer by a rule of thumb based on several tests. A clear reference for this value is defined by [65] as 5m/s, this being the recommended limit to employ the kinematic vehicle model. Nonetheless, this limit does not apply to all cases. For instance, in straight-line motion, lateral forces can be neglected, and the kinematic vehicle model could be considered valid in this condition even after 5m/s.

The switching method is defined as how the switching condition occurs. Two main approaches have been proposed: a sudden or *step* change and a progressive one, in which a *linear* blending is proposed. According to [224], a progressive transition between models offers a better response in the vehicle motion control in contrast to sudden switching

Table 4.4 Tuning procedure for model blending

Steps	Procedure
1.	Plan a route for trajectory-tracking at constants v_x^{ref}
2.	Execute motion control using kinematic vehicle model
3.	Execute motion control using dynamic vehicle model
4.	Average $e_y^{kin,dyn}$ values in a grid of v_x^{ref} vs $\dot{v_y}$
5.	Create surface plots from **4**
6.	For *step* switching method:
6.a.	Make Linear Regressions (LR) of $e_y^{kin,dyn}$ vs $\dot{v_y}$
6.b.	Intersect LRs to find a $\dot{v_y}$
6.c.	The *step* switch is defined by **6b**
7.	For *linear* switching method:
7.a.	Identify lowest $\dot{v_y}$ in surfaces intersection from **5**
7.b.	Estimate difference between **6b** and **7a**
7.c.	Use **6b** as point symmetry distance to **7a**
7.d.	The *linear* switch is defined by **7c**

conditions. However, the obtainment of v_x values for this progressive blending is a complex task, as more than one reference for the switching condition is necessary and no more than *trial-and-error* methods are defined to achieve it.

In this work, a novel approach is proposed. The lateral acceleration $\dot{v}_y$ is considered as the switching condition parameter as it can be directly related to the current lateral forces on tires in any condition. The use of this variable is more consistent with the theoretical assumptions referred by [65] for the kinematic and dynamic vehicle models.

Based on this switching condition, the procedure proposed in Table 4.4 selects the best switching value of $\dot{v_y}$ for model blending in *step* and *linear* methods. The lateral and heading deviations (see Equations 4.7) are considered as key metrics. This procedure is further illustrated in the case study of Section 4.5.

4.3.2.4 Internal MPC Models for Speed Tracking

Similar to path approaches, the speed tracking based on MPC highly relies on both accurate and simple models to be suitable for real-time implementations.

The longitudinal vehicle dynamics contemplates several external forces acting on a vehicle such as aerodynamic drag, gravitational, rolling resistance, traction and braking forces. The left side of Figure 4.8 shows these external longitudinal forces acting on a vehicle moving on an inclined road of angle θ.

The point-mass model is a well-known simplification broadly used in vehicle control approaches [263], where the longitudinal vehicle dynamics is defined as an integration chain as pointed in Equations 4.16a-b.

$$\dot{v_x} = (F_{xf} + F_{xr} - F_{aero} - R_{xf} - R_{xr} - mg\sin\theta)/m \tag{4.16a}$$

$$\dot{a_x} = j_x \tag{4.16b}$$

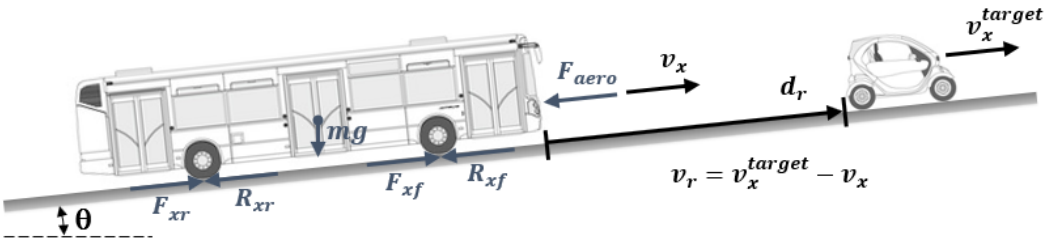

Figure 4.8 Longitudinal forces on an inclined road and range-rate definition

where the F_{xf} and F_{xr} are the longitudinal tire forces at the front and rear tires, the R_{xf} and R_{xr} are the forces due to rolling resistance at the front and rear tires, F_{aero} is the equivalent longitudinal aerodynamic drag force, and g is the acceleration of gravity.

Similar to the handling limitation using $\Delta\delta$ in *path tracking*, the performance can be limited using the jerk (j_x) as control parameter in *speed tracking*. The definition of threshold values for a_x and j_x assure both safety and comfort according specific driving scenarios as mentioned in Section 4.2 and developed next in Section 4.3.3.4.

The primary longitudinal vehicle dynamic equation is described in Equation 4.16a. In cases where a characterization effort on powertrain and braking systems is made, $F_{xf}+F_{xr}$ would be substituted by $T_w d_p / r_{eff}$, where T_w represents the torque on the tractive and braking wheel, d_p is the accelerator ($0<d_p<1$) and brake ($-1<d_p<0$) pedals position, and r_{eff} is the effective tire radius. However, as many real testing systems are difficult to characterize, $F_{xf} + F_{xr} = ma_x$ is a simplification that works for most practical purposes.

The rolling resistance force for radial-ply truck tires ($R_{xf}+R_{xr}$) is empirically described by [9] as in Equation 4.17:

$$R_{xf} + R_{xr} = (6\mathrm{e}^{-3} \tanh v_x + 0.23\mathrm{e}^{-6} v_x^2) mg \cos\theta \tag{4.17}$$

where $\tanh v_x$ is included to avoid numerical inconsistencies in MPC formulation when $v_x \approx 0$. Here, v_x is defined in km/h.

Finally, F_aero is defined by [65] as in Equation 4.18:

$$F_{aero} = \rho C_d A_f v_x^2 / 2 \tag{4.18}$$

where ρ is the air density, C_d is the drag coefficient, and A_f is the frontal area.

The equations previously presented are useful for speed tracking and would be employed to perform the basic Advanced Driving Assistance System (ADAS) features such as *Cruise Control* (CC) system. However, additional considerations are necessary for safety assurance if static or dynamic objects appear on the driving path. These will be considered separately in the following section.

4.3.3 Object and Event Detection and Response

The Object and Event Detection and Response (OEDR) comprises the DDT subtask that includes monitoring the driving environment and executing an appropriate response[1].

In this section, algorithms developed to estimate the existence of objects and(or) events on the driving path are described. In this sense, other functionalities are activated to

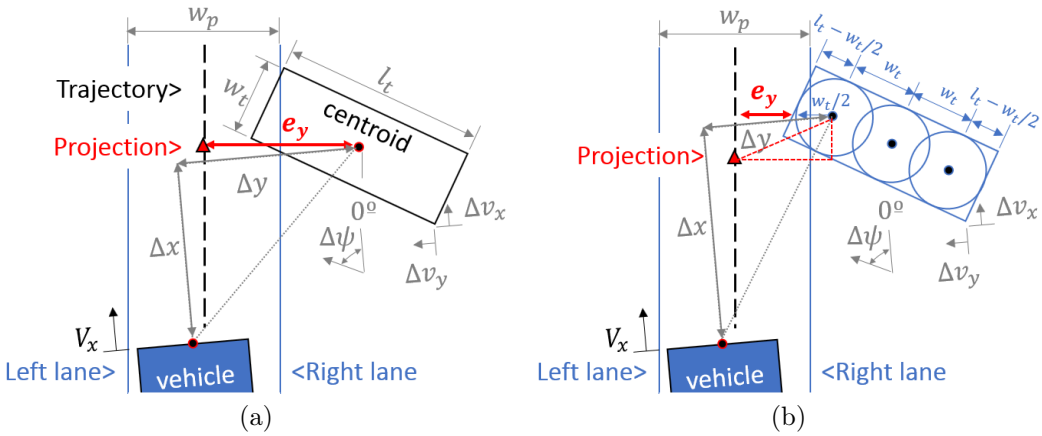

Figure 4.9 Object detection (a) off-path with centroid, (b) on-path with circles

execute appropriate responses considering both safety and comfort bearing in mind those aspects covered in Section 4.2.

4.3.3.1 Detection of Objects on Driving Path

The response to objects depends on the location of the road actors in the surroundings. The perception system is constantly monitoring the environment detecting, recognizing, and classifying objects. Meanwhile, the decision system estimates if an appropriate response to such objects is necessary or not based on the Operative Design Domain (ODD) defined for the desired application.

In this Ph.D. Thesis, the ODD defined for the AutoDrive Project is focused on a bus driving on dedicated lanes in urban environments. In this sense, different kinds of road actors such as pedestrians, cyclists, and vehicles would obstruct the driving path during the DDT execution and an appropriate response must be performed. As no lane changes are conceived for traffic in dedicated lanes, the speed tracking systems supported by collision avoidance described in previous sections (e.g. CC, ACC, and ABS) become necessary. The condition for object response during the DDT execution is defined by geometric relationships depicted in a generic form in Figure 4.9.

In general, a three-dimensional object detection is interpreted by perception systems in form of bounding boxes with relevant data such as, width (w_t), length (l_t), relative heading ($\Delta\psi$), distances (Δx, Δy) and velocities (Δv_x, Δv_y) with respect to the ADS-dedicated vehicle. However, as relative distances of objects are commonly associated with the centroid of bounding boxes, the use of distances relative to the centroid for driving path obstruction verification would result in unsafe behaviors due to objects would partly obstruct the way as shown in Figure 4.9a.

In this Ph.D. Thesis, each bounding box is transformed into several circles with diameter equal to their width (w_t) distributed along their length (l_t) as shown in Figure 4.9b. Consequently, the lateral deviation of each object (e_y) is calculated considering their circles in same way as for vehicle as described in Section 4.3.2.2. If e_y is bigger than path's half-width ($w_p/2$) the target object is considered off-path, otherwise ($e_y < w_p/2$) the target

object is considered on-path and object response algorithm must be activated.

The quantity of circles contained within the bounding box depends on l_t. However, the use of 7-circles covers most typical objects in urban environments. The case study presented in Section 3.4 detects a dynamic object moving forwards along the driving path to perform ACC. Moreover, the detection and response to path-crossing objects are analyzed in one case study of this chapter presented in Section 4.6.

4.3.3.2 Detection of Events on Driving Path

External events are situations in the driving environment that require a response by the driver or ADS, such as other vehicles, lane markings, and traffic signs. In ADS categorized as SAE Level 2 or below, the ADS is not capable of recognizing or respond to some events and the driver must complete the OEDR subtask of the DDT. In ADS categorized as SAE Level 3 or above, the ADS must at least issue a request to intervene with enough time for a typical driver to respond appropriately, including performance-relevant system failure and ODD-exit [1].

In this Ph.D. Thesis, the developed ADS is capable to respond to some events considering the ODD defined in the AutoDrive Project's (passenger transference driving on dedicated lanes through urban environments with mixed traffic) such as traffic light status and bus stops. The detection of traffic lights is defined by Equation 4.19.

$$t^{ttl} < t^{trl} \tag{4.19}$$

where the remaining time before reach the traffic light location (t^{ttl}) can be estimated as $t^{ttl} = d_r^{ttl}/v_x$ (where ${d_r}^{ttl}$ is the relative distance to-traffic-light along the driving path), and t^{trl} is the remaining time before the traffic light status switches to red light. If $t^{trl} > t^{ttl}$, the vehicle can continue as there is enough time before the red light switch. Otherwise, the traffic light location along the route is considered to stop at a safe distance as there is not enough time before the red light switch.

The detection and response to traffic lights are analyzed in one case study of this chapter presented in Section 4.6. On other hand, considering ADS with SAE Level 3 and higher, events related to performance-relevant system failures and the achievement of minimal risk conditions using automated DDT fallback strategies are covered in Chapter 5.

4.3.3.3 Steady-State Response

The point-mass model presented in Section 4.3.2.4 can be expanded to perform complex ADAS features, such as Adaptive Cruise Control (ACC), Rear-End Collision Avoidance (RECA) or Automatic Emergency Braking (AEB) systems. These features adapt the speed tracking system behavior if an object is detected ahead on the driving path. In this sense, the primary vehicle motion described in Equations 4.16a-b would be enriched with additional considerations as those presented in Equations 4.20a-b.

$$\dot{d_r} = v_x^{target} - v_x \tag{4.20a}$$

$$\dot{v_r} = a_x^{target} - a_x \tag{4.20b}$$

where d_r and d_r are the relative travel distance and velocity to a target object in front of the vehicle, respectively. This strategy strongly depends on sensors' capability to measure

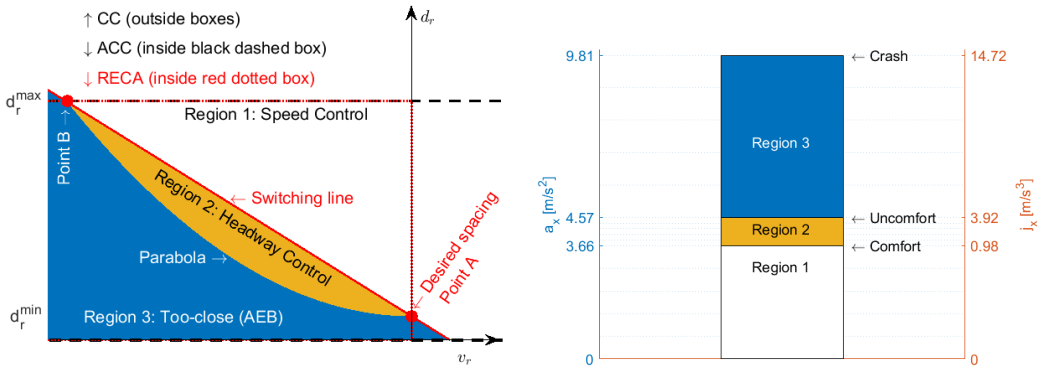

Figure 4.10 (a) Range vs range-rate diagram [14] and (b) threshold levels [64]

relative parameters. As real sensor devices (e.g. RaDAR, LiDAR and cameras) commonly provide only d_r and v_r measurements, the longitudinal velocity of a target object (v_x^{target}) is estimated from Equation 4.20a, and the acceleration of a target object (a_x^{target}) is neglected and assumed as zero.

The major difference between ACC and RECA/AEB systems rely on the operative range based on v_r. While RECA/AEB is activated only when $v_r < 0$ and manipulates only the brake pedal (d_r is continuously reduced), ACC remains active even if $v_r > 0$ and considers the actuation on both accelerator and brake pedals, to follow a preceding object while maintains a desired d_r. On one hand, the case studies presented in Sections 4.6 and 5.5 evaluate RECA/AEB applications. On the other hand, the case study described in Section 3.4 assessed an ACC implementation.

It is important to note that this procedure for steady-state object following can be implemented as planning (e.g. using *Numerical Optimization*) or tracking (e.g. using *Model Predictive Control*) algorithms as mentioned in Sections 2.2.1.4 and 2.2.2.4, to generate or follow a speed profile as described previously in Sections 4.3.1 and 4.3.2.

4.3.3.4 Transitional Tracking Design

A complete speed tracking algorithm must cover the entire operating range, not only maintaining a safe distance with a preceding object ahead on the road when it appears but also performing CC tracking the speed profile defined by trajectory planning. When a new target object is encountered, a range vs. range-rate ($d_r - v_r$) diagram [14] becomes useful to decide whether the vehicle should: 1) use speed control, 2) use spacing control, 3) brake as hard as possible to avoid a collision.

The $d_r - v_r$ diagram is defined as shown in the right side of Figure 4.10, and the inertial positions and velocities for both the preceding object and vehicle are defined as in Equations 4.20a-b. A typical $d_r - v_r$ diagram, as developed by [14] is shown in Figure 4.10a. The relationship of the $d_r - v_r$ diagram with the threshold values described in Table 4.1 are presented in Figure 4.10b. This approach was used in case studies of Sections 3.5, 4.6 and 5.5.

From measured v_r and d_r values and $d_r - v_r$ diagram, a speed tracking system deter-

mines the control mode in which it should operate. For instance, CC mode is activated while a target object does not exist or it is beyond the sensor's maximum range (${d_r}^{max}$). When a target object appears, ACC/RECA mode is activated operating in *Region 1* under speed control, operates in *Region 2* under spacing control, or decelerates at maximum allowable deceleration to avoid collisions in *Region 3*. The last region's behavior is commonly employed for AEB systems.

The method to estimate the slope of the *switching line* is presented in [65]. The deceleration during coasting (D_{coast}) which depends of each vehicle dynamics as mentioned in Section 3.2.1.2, serves to calculate a parabola with deceleration D_{coast} that passes through Point A and the desired minimum distance to ensure safety (${d_r}^{min}$) at $v_r = 0$ would be used to determine the slope using Equation 4.21.

$$d_r = d_r^{min} + v_r^2/(2D_{coast}) \tag{4.21}$$

Once the *parabola* is constructed, the maximum measurable d_r of the sensor (d_r^{max} at Point B) is considered to calculate the slope of *switching line*, obtaining a straight line from Points A to B. Alternatively, sensor's maximum measurable v_r define Point A [65].

4.4 Case Study: Trajectory Planning for Heavy-Duty Vehicles

Heavy-duty vehicles such as buses are considerably affected by their large dimensions when maneuvering under dynamically changing environments (e.g. drive in narrow urban roads while performing sharp turns). In this sense, the development of an effective trajectory planning approach is highly required.

In the present case study, the proposed trajectory planning methods described in Section 4.3.1 are employed to properly generate a feasible reference to track based on *Bézier curves* as *interpolating method*. The selected driving environment is a confined area located at Irizar facilities depicted in Figure 3.4b. This trajectory planning approach is the one used in the case study for Verification and Validation (VV) detailed in Section 3.5.

4.4.1 Data from Digital Maps

The trajectory planning procedure begins with gathering the most reliable data available from the desired driving environment. In this sense, digital maps provide content to support sensor data increasing the driver's safety and comfort, knowing in advance several road attributes such as road altitude, traffic signs, speed restrictions, lanes, etc.

The first step in trajectory planning consists of the definition of a driveable area. Consequently, raw data is gathered from the map editor[72] defining road borders limited by non-driveable spaces including parking spots and infrastructure as shown in Figure 4.11.

4.4.2 Path Planning

Once a driveable area free of static objects is defined, path planning algorithms described in Section 4.3.1.1 can be employed. The obtained result is depicted in Figure 4.12.

[72] Java Open Street Map: https://josm.openstreetmap.de/

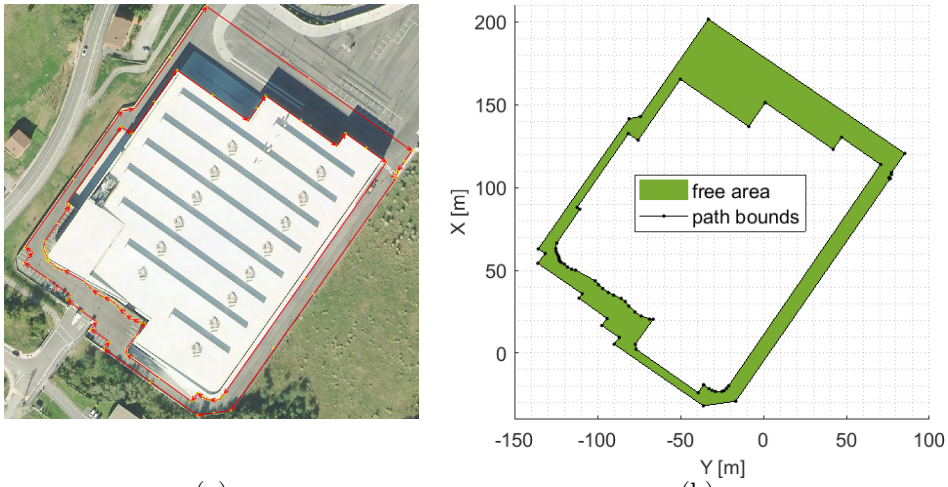

(a) (b)

Figure 4.11 Road borders gathered from (a) JOSM and scattered on (b) layout

For the selected testing scenario, 4-intersection and 3-lane-change maneuvers were enough to plan the path of the entire driving route based on Bézier curves (see Figures 4.3a-b). The path's waypoints correspond to the vehicle's CG location as it is used for path tracking development. Furthermore, collision checks among the vehicle's path area and boundaries were performed for each maneuver along the entire route to ensure driving safety. The path areas placed at each waypoint were estimated considering the width, length, and CG location of the Irizar i2e bus described in Table 3.3.

Please, observe that the planned path for the different driving maneuvers respects the road borders at all times, which is mandatory to ensure safety during the DDT execution. Moreover, the curvature is an essential parameter that can be obtained from here to plan a comfortable speed profile as detailed in the next section.

4.4.3 Speed Planning

Once the driving path is planned, the speed planning algorithms described in Section 4.3.1.2 can be employed. The obtained result is depicted in Figure 4.13.

The speed planning was estimated using Equation 4.4 and a_w=0.158 as a comfortable value. It is obtained that v_x^{ref} decreases as the absolute value of the curvature (k) increases, ensuring comfortable a_y levels while turning.

Performance limits for v_x and a_x were considered in the speed planning. Meanwhile, v_x limits are defined by the legal top speed from the driving route (5 m/s), a_x limits were defined by comfort thresholds for acceleration and braking ($\pm$ 0.315 m/s^2). The threshold limits employed here were taken from the ISO standard values depicted in Table 4.1.

4.4.4 Road Gradient Planning

Most trajectory planning executions assume nearly flat surfaces on which altitude changes do not affect considerably the trajectory tracking. However, when heavy-duty vehicles

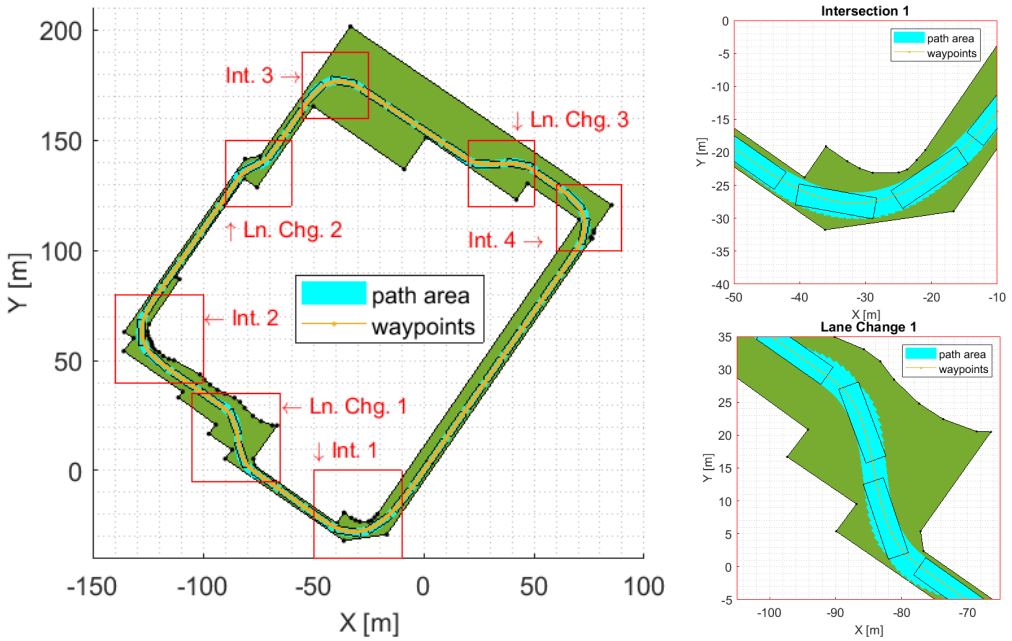

Figure 4.12 Path planning and driving maneuvers

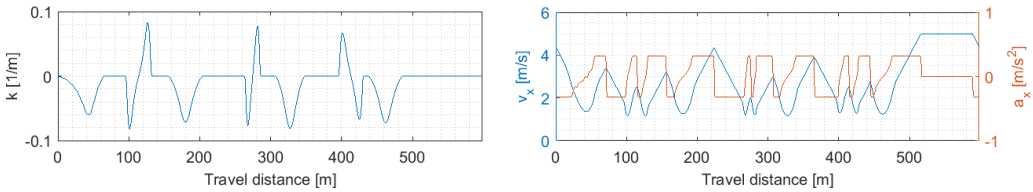

(a) (b)

Figure 4.13 Speed planning with (a) path curvature and (b) performance limits

are considered to perform automated trajectory tracking, information related to the road gradient of the driving path plays an important role in the speed tracking performance.

The road gradient information is estimated considering the road altitude gathered from digital maps, CG location, and wheelbase distance of the vehicle. The obtained result is depicted in Figure 4.14. Successful speed tracking results from this road gradient planning have been analyzed in the case study of the previous chapter (see Section 3.5).

4.5 Case Study: Trajectory Tracking Based on Vehicle-Models-Blending

The proposed vehicle model blending procedure described in Section 4.3.2.3 is applied to a particular case study for trajectory tracking based on MPC. A simulated Irizar i2e bus is employed as a test vehicle for this case study, whose parameters are detailed in 3.3.1. The

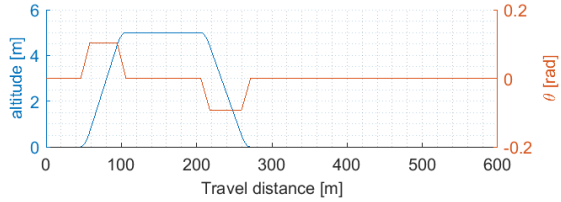

Figure 4.14 Road gradient planning from altitude

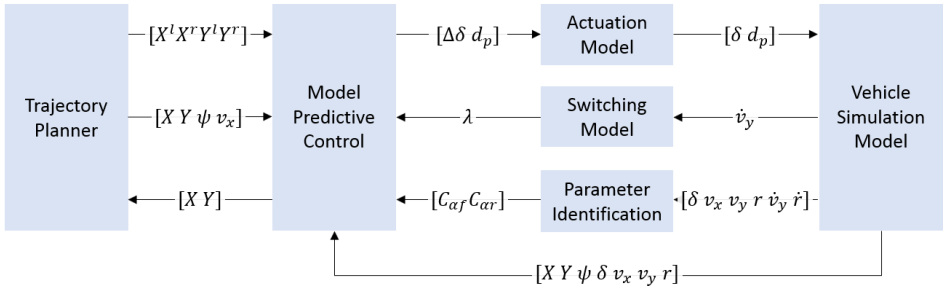

Figure 4.15 Control architecture of trajectory tracking case study

overall control architecture of the proposed case study (which is an excerpt of the entire software architecture design detailed in Figure 3.7) is depicted in Figure 4.15.

Virtual executions were performed using the MiL testing platform shown in Figure 3.10. The verification testing assessment is based on both face-verification and statistical approaches.

Next, a thorough description of each subsystem of the control architecture is presented. However, the parameter identification will be covered in Chapter 5 due to its importance for virtual sensors and the performance of DDT fallback strategies.

4.5.1 Model-Blending-Based MPC Controller

The developed MPC is used to implement a trajectory tracking approach that considers certain constraints related to vehicle and actuation limits. Furthermore, the planned trajectory is considered feasible and free of objects.

This case study follows a generic MPC formulation as described in Equations 4.22a-d

$$\begin{aligned} \max \quad & \text{Trajectory tracking} && (4.22a)\\ \text{s.t.} \quad & \text{Vehicle model,} && (4.22b)\\ & \text{Actuation limits,} && (4.22c)\\ & \text{Road limits.} && (4.22d) \end{aligned}$$

Next, the different elements required to implement the MPC will be analyzed.

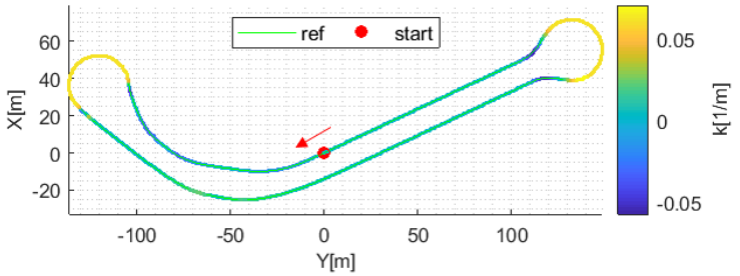

Figure 4.16 Planned trajectory considering the vehicle's maximum turning.

4.5.1.1 Trajectory Planner

The planned trajectory considers a realistic urban scenario with a total travel distance of approximately 680 m, being part of the touristic seaport depicted in Figure 3.4c. It contains a couple of roundabouts with maximum curvatures (k) of around 0.08 m^{-1} connected through an avenue with smoother paths. The motion planner is based on the approach detailed in Section 4.3.1 and implemented in the previous case study in Section 4.4, considering the center-path of the road's right-lane. The starting vehicle's position and orientation, including the curvature segments, are depicted in Figure 4.16.

Considering the MPC's predictions ($[X, Y]$), new positions and orientations are estimated repeatedly at each iteration as new references for trajectory tracking ($[X, Y, \psi, v_x]$). Additionally, the center-lane path's border positions are continuously considered ($[X^l, X^r, Y^l, Y^r]$), using them as path constraints to avoid lane departures.

As this case study is focused on analyzing the effect of model blending in vehicle motion control, the round-about on the right side in Figure 4.16 is planned using non-smooth curvatures provoking high lateral accelerations, which will help to analyze the model blending efficacy in extreme handling maneuvers.

4.5.1.2 Switching Model

As previously stated, the model blending procedure detailed in Section 4.3.2.3 will be implemented in the MPC controller. Two different types of blending methods based on $\dot{v}_y$ are proposed in this work for comparison purposes. Firstly, a *step* switch which causes a sudden change between kinematic and dynamic models. Secondly, a *linear* switch which executes a progressive change between models. The switching parameter λ defined in Equations 4.15e-f is characterized by Equation 4.23:

$$\lambda = \min[\max[\frac{|\dot{v}_y| - \dot{v}_y{}^{min}}{\dot{v}_y{}^{max} - \dot{v}_y{}^{min}}, 0], 1] \tag{4.23}$$

where $\dot{v}_y{}^{min}$ and $\dot{v}_y{}^{max}$ are the minimum and maximum acceleration thresholds defined by the switching designer (see the *tunning procedure for model blending* from Section 4.3.2.3 for more details). On the one hand, for the *step* method, $\dot{v}_y{}^{min}{=}\dot{v}_y{}^{max}$ is employed, where the change between *kin* and *dyn* models is performed when the sign from the estimation $(|\dot{v}_y| - \dot{v}_y{}^{min})/0$ results in $-\infty \vee \infty$, therefore switching λ between $0 \vee 1$, respectively. On the other hand, for the *linear* method, $\dot{v}_y{}^{min}{<}\dot{v}_y{}^{max}$ is applied.

Additionally, a third switching strategy, called *speed* is considered for comparison purposes. This strategy, as proposed by [65], suddenly switches between the kinematic and dynamic models at 5 m/s and will be considered as a benchmarking strategy. Therefore, Equation 4.23 is also employed using v_x as switching condition instead of $\dot{v_y}$.

4.5.1.3 Nonlinear Model Predictive Control

The developed controller make use of the **blended vehicle model** defined in Section 4.3.2.3, requiring an appropriate switching method for model change (i.e., the ones proposed in Section 4.5.1.2). The λ plays an important role in the formulation (see Equations 4.15e-f). In addition to the path-tracking related models, additional equations are considered in the vehicle model for speed tracking as those described in Section 4.3.2.4.

Tire cornering stiffnesses are parameters identified at real-time employing the direct method detailed in [264], however, and as previously mentioned, this will be covered in Chapter 5 due to its importance for virtual sensors and DDT fallback strategies.

As the vehicle models are nonlinear, the proposed approach is a nonlinear MPC, which also includes a set of state and control constraints, designed to guarantee a safe DDT subtask execution. The problem formulation is solved at each time step with a prediction horizon defined as $i, i+1, ..., i+N_{s,u}$ and presented in Section 4.3.2.1 (see Equations 4.5a-f).

Here, the $Q_w = \text{diag}(q_X, q_Y, q_\psi, q_{v_x})$ and $R_w = \text{diag}(q_{\Delta\delta}, q_{d_p})$ are the weight matrices associated with the state tracking and control inputs, respectively (Equation 4.5a). The weights are set to q_X=q_Y=q_ψ=q_{v_x}=1 and $q_{\Delta\delta}$=q_{d_p}=10.

The $x_{i+1} = f_i(x_i, z_i, u_i)$ represents the blended model defined in Section 4.3.2.3. The differential states $x_i = [X, Y, \psi, v_x]_i^T$ are minimized according to the driving route cartesian coordinates, orientation, and speed references (x_i^{ref}). The algebraic states $z_i = [C_{\alpha f}, C_{\alpha r}, \lambda]_i^T$ are online data obtained from parameter identification (see Section 5.3.2) and switching model (see Section 4.5.1.2). The **actuation limits** or control inputs $u_i = [\Delta\delta, d_p]_i^T$ are calculated by minimizing the cost function by the MPC.

Constraints (Equations 4.5c–4.5d) are defined for differential states $x_i = [X, Y, \delta, v_x]_i^T$ as [$\text{X}^{l,r}$,$\text{Y}^{l,r}$, ± 0.68 rad,v_x^{ref}]; and control inputs $u_i = [\Delta\delta, d_p]_i^T$ as ± [0.5 rad/s,1].

Minimizing Equation 4.5a allows for calculating the optimum value of $u = [\Delta\delta, d_p]_i^T$ for the current time step. For that purpose, the nonlinear MPC is solved with the automatic code generator of the open-source ACADO toolkit described in Section 4.3.2.1, using QPOASES as the set solver, the sequential programming technique, and the direct multiple-shooting method for discretization. The prediction horizon is 5 s of look-ahead time considering a fixed time step among predictions of 0.5 s.

Road Limits Keeping the vehicle on the planned path to avoid undesired lane departures is considered through additional constraints [$\text{X}^{l,r}$,$\text{Y}^{l,r}$] as depicted in Figure 4.17. An additional distance (d_w = 0.2 m) is taken into account to avoid unfeasible solutions when results from $|X_i^l - X_i^r|$ or $|Y_i^l - Y_i^r|$ are near to zero.

The path borders are obtained from the planned trajectory considering a continuous lane-width along the route, permitting a maximum lateral displacement from the center-lane path of 0.725 m. The constraint values for path borders are processed in real-time as

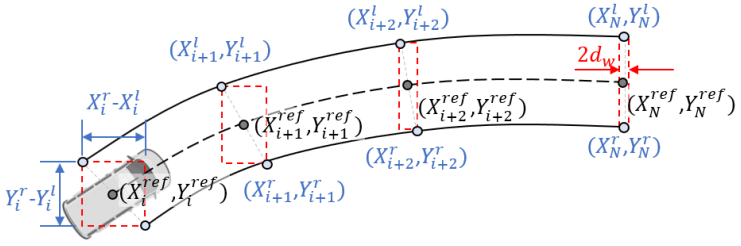

Figure 4.17 Path borders as constraints based on X and Y

described in Equations 4.24a–4.24d:

$$\underline{X_i} = \min([X_i^l, X_i^r, X_i^{ref} - d_w]) \tag{4.24a}$$

$$\overline{X_i} = \max([X_i^l, X_i^r, X_i^{ref} + d_w]) \tag{4.24b}$$

$$\underline{Y_i} = \min([Y_i^l, Y_i^r, Y_i^{ref} - d_w]) \tag{4.24c}$$

$$\overline{Y_i} = \max([Y_i^l, Y_i^r, Y_i^{ref} + d_w]) \tag{4.24d}$$

4.5.1.4 Actuation Model

The control variable $\Delta\delta$ calculated by the MPC is integrated at this stage to obtain a δ normalized between [–1,1] considering a maximum value of $\delta = 0.68$ rad. The control variable d_p is constrained between [–1,1] in the MPC formulation and represents the maximum brake and throttle pedal positions, respectively. Actuation delays of 150 ms for accelerator and 80 ms for both steering wheel and brake pedal were approximated by second-order transfer functions (see Section 3.3.2.2). Also, rate limitations are applied to mimic real actuation behavior.

4.5.2 Tuning Procedure for Model Blending

Considering the tuning procedure defined in Section 4.3.2.3, the parameters to perform the three switching methods introduced in Section 4.5.1.2 (*step*, *linear* and *speed*) are defined and evaluated. In addition, pure kinematic (*kin*) and dynamic (*dyn*) methods are considered for comparison.

In this section, the procedure defined in Section 4.3.2.3 is applied to select the best switching value for $\dot{v_y}$ for model blending in *step* and *linear* methods. Note that the *speed* method is based on the v_x as proposed in [65]. In the latter case, a *step* method is applied, in which a kinematic model is used below 5 m/s, and a dynamic model at higher speeds.

The results of the step-by-step procedure described in Table 4.4 are detailed next.

Steps 1 to 5 (e_y vs v_x vs a_y): Once the planned route for trajectory-tracking of Section 4.5.1.1 is defined, the vehicle motion control is executed using *kin* and *dyn* vehicle models at several v_x^{ref} as described previously. The median is estimated for the absolute values $|e_y|$ and $|e_\psi|$ considering *kin* $(.)^{kin}$ and *dyn* $(.)^{dyn}$ models in a grid of v_x^{ref} vs a_y. In practice, the median provides a better estimation in contrast to mean values for the *cut-off* definition pointed in *Steps 6a–c*. Results are processed through a two-dimensional convolution [265] creating surface plots as depicted in Figure 4.18.

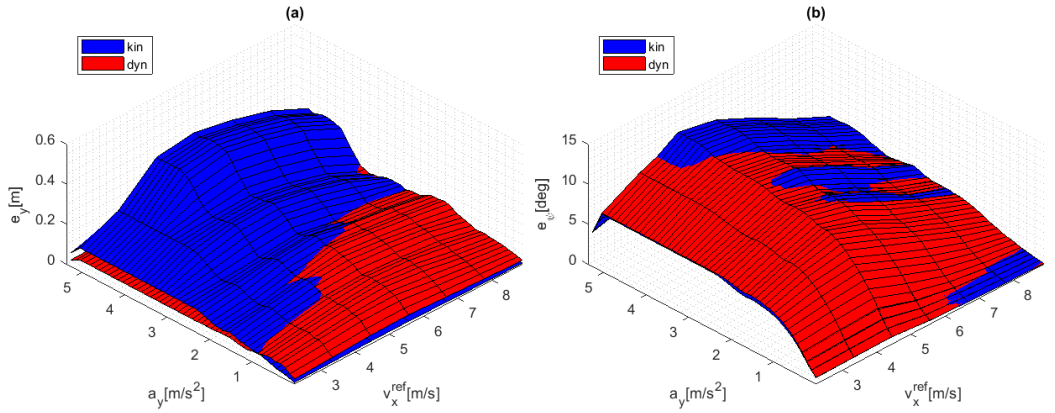

Figure 4.18 (a) e_y and (b) e_ψ for *kin* and *dyn* considering v_x^{ref} and a_y.

The e_y^{kin} and e_y^{dyn} results are depicted in Figure 4.18a, in blue and red, respectively. The influence of a_y is remarkable along several v_x^{ref} tested, having a clear limit from *kin* and *dyn* surface intersections. These surface intersections help to prove the initial hypothesis which presents a_y as a more appropriate switching condition than v_x.

The e_ψ^{kin} and e_ψ^{dyn} results are depicted in Figure 4.18b, in blue and red, respectively. There is no clear influence of a_y or v_x on the improvement of the path-tracking performance in terms of e_ψ, as *kin* and *dyn* models seem to have similar behavior. These findings motivate the idea of selecting e_y over e_ψ as the basis for a switching strategy.

Steps 6a–c (*step* blending): A linear regression is calculated from $e_y^{kin,dyn}$ vs a_y as showed in Figure 4.19a (i.e., considering all the values of $e_y^{kin,dyn}$, associated with a certain a_y and all related v_x^{ref} values). The intersection of LR^{kin} and LR^{dyn} is approximately in 1.5 m/s^2, this being a useful cut-off value to define the switching condition to a_y. This value allows for obtaining the lowest e_y values for *kin* and *dyn* models. As stated previously, if the same procedure is applied to $e_\psi^{kin,dyn}$ (Figure 4.19b), no relevant results can be extracted, as both models have similar performance.

Steps 7a–d (*linear* blending): The a_y becomes relevant around 1 m/s^2 as depicted in Figure 4.18a. This is the lowest a_y value that can be extracted from the surface intersection, which is useful for defining the initial condition of a progressive switching between models. In addition, the *step* switching (defined at 1.5 m/s^2) is considered as the point of symmetry to this initial condition. Therefore, the *linear* switching is determined from 1 m/s^2 to 2 m/s^2 being centered around the *step* switching condition. The switching methods for model blending based on $\lambda \in [0,1]$ are presented in Figure 4.19a.

4.5.3 Trajectory Tracking Verification Tests

The performance evaluation of vehicle models and switching methods employed are detailed in this section. The elements in the control architecture defined in Figure 4.15 and detailed in Section 4.5.1 are implemented in a MATLAB/Simulink setup which is used to perform a simulation-based analysis.

Three complete laps are simulated in the defined scenario (Figure 4.16), the results

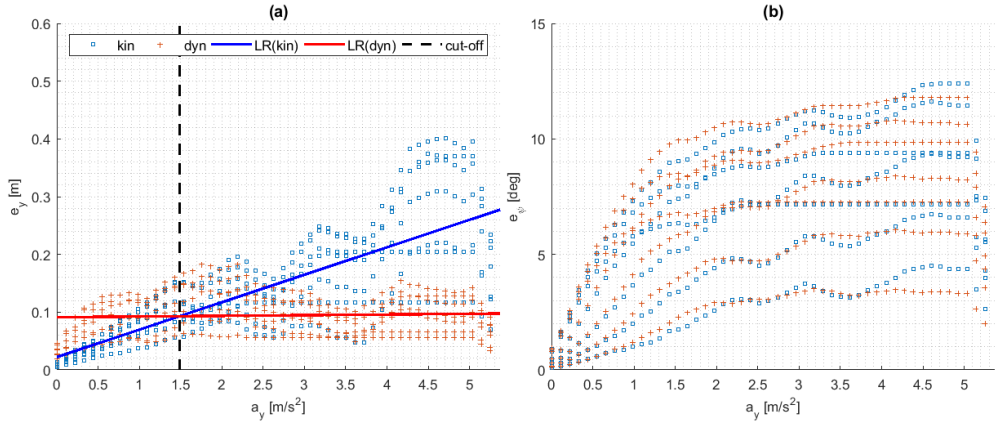

Figure 4.19 Linear regression in (a) e_y finding the a_y "cut-off" and (b) e_ψ.

being recorded and evaluated. Eight values for v_x^{ref} are defined from 1.1 m/s to 8.8 m/s, equally spaced at 1.1 m/s for each simulation test. This will allow for studying the influence of v_x and the lateral acceleration (a_y) in the lateral motion control for the defined route.

4.5.3.1 Trajectory-Tracking Response Analysis

Results for three-of-eight simulation tests at constant v_x^{ref} have been selected for discussion simplicity (2.2 m/s, 5.5 m/s, and 8.8 m/s). The *linear* method has been chosen for Figure 4.20b–d as it presents the best performance compared to other methods. The route values (black line) are located at zero values on z-axis as a reference, and the z-axis limits correspond to minimum and maximum estimation values of v_x, a_y, and e_y, respectively.

Figure 4.20b shows the v_x of the bus for the *linear* method. Although the v_x^{ref} is set as constant, note that the MPC regulates the final speed to avoid lane-departures (e.g., v_x^{ref} = 8.8 m/s) as defined in Section 4.5.1. Hence, this is considered as a proper performance.

Figure 4.20c shows the a_y of the bus. Larger values are obtained while turning as the v_x^{ref} increases. Important transitions are observed mostly on the roundabout at the right-side due to non-smooth planned curvatures. This transitional behavior is observed in a_y results independently of the tested v_x^{ref}, a phenomenon that is not acquired previously in v_x results.

Figure 4.20d shows the e_y of the bus, which is calculated by considering the road's center-lane and the current position at each time step. The transitional effects described in a_y seem to affect the e_y response, and, therefore, the path tracking.

The former results demonstrate that the MPC with the *linear* method provides an appropriate trajectory tracking.

4.5.3.2 Lateral and Angular Error Analysis

Figure 4.21a–b shows the statistical distribution of e_y and e_ψ for five study conditions related to the five analyzed methods, allowing comparison for their trajectory-tracking performance. The boxes span (blue boxes) cover from 2% to 98% of the data, the whiskers

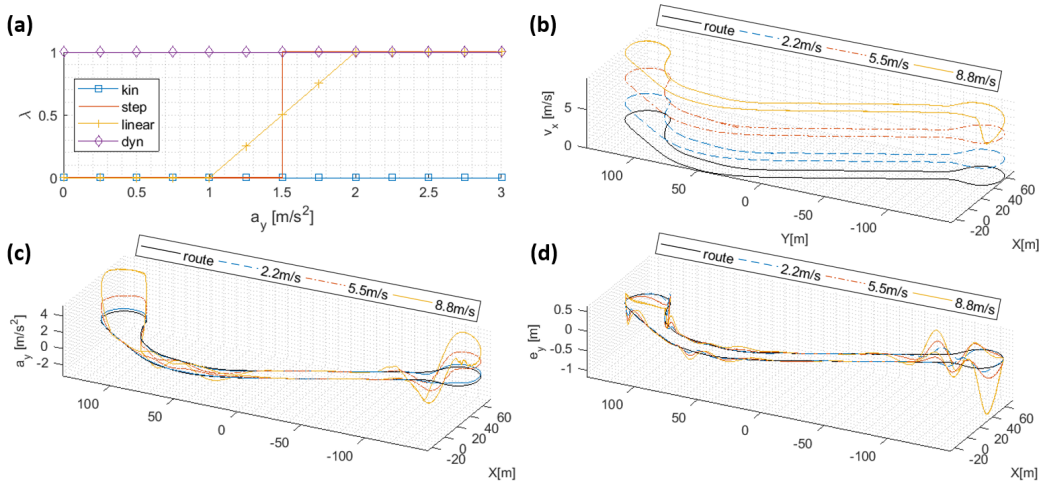

Figure 4.20 Results for: (a) switching methods for model blending; (b) v_x; (c) a_y and (d) e_y for *linear* method

span (black lines) cover from 1% to 99% of the data, the median (red horizontal lines) and mean (μ, red plus signs) values as statistical metrics assessment.

In Figure 4.21a, it can be seen that, for this low speed test track, the kinematic model (*kin*) clearly outperforms the dynamic model (*dyn*) as expected. However, blending these two models can produce better results than either one of them individually. Note that this particular track has the most low speed turns towards the left, whereas right-hand turns are mostly high speed. This allows for exemplifying the limitations of the *speed* method. The positive e_y distribution resembles the kinematic model behavior, while the negative side is much closer to the dynamic model. Since they can be correlated to the left and right-hand turns and thus the predominantly high and predominantly low speeds, it becomes clear that blending based on the speed uses either model in some cases where the other one behaves better (i.e, on the high speed, turns, it uses the dynamic approximation even if the lateral forces are low and the kinematic model behaves better).

On the other hand, the hereby introduced switching strategies (*linear* and *step*), based on lateral acceleration, provide better behavior than the use of either kinematic or dynamic models, or even the aforementioned blending approach based on the *speed method*. This is achieved by actually switching when the lateral forces are significant, thus properly using the best approach in every condition to reduce errors (see Figure 4.18), rather than just avoiding singularities (which is the main motivation for the speed based blending). Since most of the track has low lateral acceleration, most of the error distribution for both a_y-based methods (*linear* and *step*) resembles the kinematic model behavior (see the blue boxes in Figure 4.21a, associated with the 2%–98% data interval). However, the black whiskers do show a significant improvement in reducing the lateral error corresponding to those cases with either high lateral acceleration and low speed or those of high speed and low lateral acceleration, thus proving the advantage of introducing the lateral acceleration as the blending parameter in place of the currently accepted vehicle velocity.

Furthermore, it is noted that the *linear* blending is slightly better than the *step* in

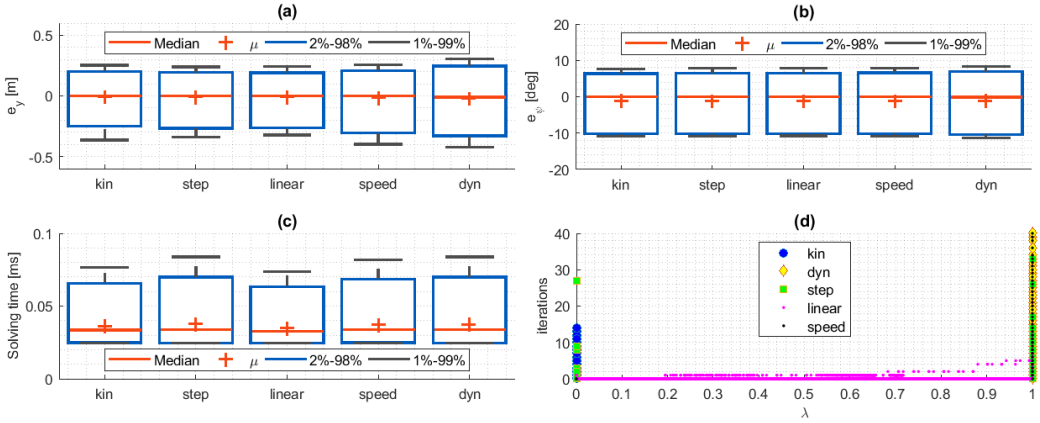

Figure 4.21 Results for: (a) e_y, (b) e_ψ, and (c) solving time statistics; (d) iterations number vs. λ for different methods.

terms of the maximum dispersion (black whiskers), though the actual advantage of this technique relates to the computational cost, as will become evident in the discussion below.

Figure 4.21b shows that the e_ψ behaves very similarly regardless of the implementation of either of the analyzed methods, which fit the results shown in Section 4.5.2 and endorse the decision of considering e_y surfaces for the blending procedure.

4.5.3.3 Computational Cost Analysis

To demonstrate the real-time capability of the presented approach, computational cost analysis has been carried out. The required time to calculate each control cycle of the proposed MPC controllers with the different blending methods has been evaluated. All controllers were executed at 10 ms of time step employing the Model-in-the-Loop testing architecture described in Figure 3.10. The results are depicted in Figure 4.21c, in which the statistical distribution of the solving time is depicted, following the same representation applied to Figure 4.21a–b. It can be seen where the worst-case scenario is for the *step* and *dyn* approaches, with mean values of 0.04 ms and maximums of nearly 0.08 ms. On the contrary, the *linear* method offers the best time efficiency with a mean value of 0.03 ms and a maximum solving time of 0.07 ms. Hence, results demonstrate that computational cost can be reduced by the use of blended models.

Note that all the referred approaches are based on a nonlinear MPC. In this case study, the previously calculated state and input values are used as a seed for the next iteration. Hence, when sudden or abrupt changes are required, the number of iterations required to solve the MPC problem increases significantly as depicted in Figure 4.21d. For instance, this happens when a sudden transition from a kinematic to a dynamic model has carried out in the *step* method. In this sense, the *linear* method reduces the required computational cost by lowering the number of iterations required to solve the optimization problem in the blending procedure to even slightly better values than the simple kinematic model.

4.6 Case Study: OEDR in Urban Environments

Car-to-car and car-to-pedestrian impacts are one of the most frequent accidents on the roads due to driver distraction or misjudgment of traffic in front of him. In urban environments, these accidents normally occur at relatively low speeds where the impacted car is already at standstill[73] or the pedestrian crosses the path of the vehicle[47]. Consequently, driving technology that supports adequate braking and/or ultimately stops the vehicle by itself to avoid tail crashes with other vehicles, or impact with vulnerable road users like pedestrians and cyclists are highly required.

A simulated Irizar i2e bus is employed as a test vehicle for this case study, whose parameters are detailed in Section 3.3.1. Virtual executions were performed using the MiL testing platform shown in Figure 3.10. The verification testing assessment is based on both face-verification and statistical approaches.

The proposed techniques for Object and Event Detection and Response (OEDR) described in Section 4.3.3 are employed to properly keep a safe spacing with any object ahead on the driving path, bearing in mind comfortability when safety is not a primary issue. Moreover, the OEDR algorithms are combined with the speed tracking method detailed in Section 4.3.2.4. Also, the selected driving environment is the one thoroughly described in a previous case study in Section 4.4. Finally, the *kinematic model-based approach* described in Section 4.3.2.3 is employed for path tracking, however, it is not the focus this time as it was assessed in the previous case study in Section 4.5.

4.6.1 OEDR-based MPC Controller

The developed MPC is used to implement a speed tracking approach that considers certain constraints related to safety and comfort. Furthermore, the planned trajectory is considered feasible and dynamic objects and events are present along the route.

This case study follows a generic MPC formulation as described in Equations 4.25a-d

$$\begin{aligned} \max \quad & \text{Speed tracking} && \text{(4.25a)} \\ \text{s.t.} \quad & \text{Vehicle model,} && \text{(4.25b)} \\ & \text{Actuation limits,} && \text{(4.25c)} \\ & \text{Safety limits.} && \text{(4.25d)} \end{aligned}$$

Next, the different elements required to implement the MPC will be analyzed.

4.6.1.1 Objects and Events in Driving Environment

The selected driving environment is the confined area located at Irizar facilities depicted in Figure 3.4b whose planned trajectory was previously described in-depth in Section 4.4. The changing nature of road actors in the surroundings of ADS-dedicated vehicles, allow the performance assessment of the proposed OEDR-based MPC controller. In this sense, several traffic lights (events) and dynamic objects are located along the planned trajectory as shown in Figure 4.22.

[73] test protocol: Euro NCAP - AEB Car-to-Car systems https://rb.gy/lexd8i

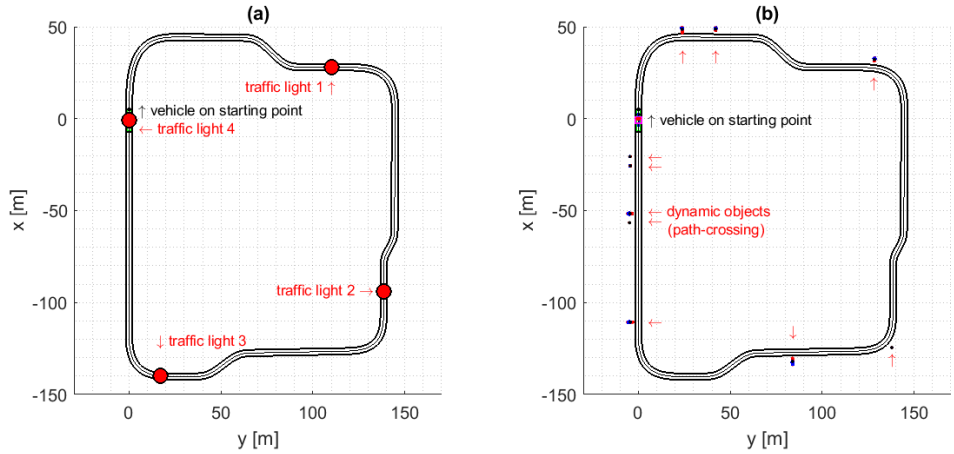

Figure 4.22 OEDR scenarios for: (a) traffic lights and (b) path-crossing objects

Four traffic lights are equally spaced along the driving route as depicted in Figure 4.22a. These traffic lights have a usual changing status mimicking the urban ones comprising green, yellow, and red lights with 15 s, 10 s, and 25 s of time duration, respectively, before switching from one to another light status.

Ten objects are randomly spaced along the driving route as portrayed in Figure 4.22b. These objects have a dynamic behavior consisting of continuously crossing the driving path from one side to the other. For this, a sine wave functions with amplitudes varying between 4-6m and frequency 0.06 rad/s defines their distances to the path. Each object has a different width and length as described in Section 4.3.3.1. All objects have a heading angle perpendicular to their location along with the travel distance of planned trajectory, in the same direction as their crossing vectors.

4.6.1.2 Nonlinear Model Predictive Control

The developed controller makes use of the speed tracking method defined in Section 4.3.2.4, improved by the addition of *steady-state response* equations proposed in Section 4.3.3.3.

As the longitudinal vehicle model is nonlinear, the proposed approach is a nonlinear MPC, which also includes a set of state and control constraints, designed to guarantee a safe and comfortable DDT subtask execution. The problem formulation is solved at each time step with a prediction horizon defined as $i, i+1, ..., i+N_{s,u}$ and presented in Section 4.3.2.1 (see Equations 4.5a-f).

Here, the $Q_w = \text{diag}(q_{v_x}, q_{d_r}, q_{v_r})$ and $R_w = \text{diag}(q_{j_x})$ are the weight matrices associated with the state tracking and control inputs, respectively (Equation 4.5a). The weights for the control inputs remain constant as q_{j_x}=1 during the DDT execution, while the weights for the differential states $[q_{v_x}, q_{d_r}, q_{v_r}]$ vary depending on the transitional tracking mode: *cruise* ([1, 0, 0]), *speed* ([1, 0.5, 0.5]), *headway* and *too-close* ([1, 1, 0]).

The $x_{i+1} = f_i(x_i, z_i, u_i)$ represents the **vehicle model** defined by Equations 4.16-4.20. The differential states $x_i = [v_x, d_r]_i^T$ are minimized according to the speed references, relatives distance and speed with respect to a object ahead on driving path (x_i^{ref}). The relative distance reference (d_r^{ref}) is defined by the switching line of transitional tracking

design described in Section 4.3.3.4. The algebraic states $z_i = [v_x^{target}, a_x^{target}]_i^T$ are online data estimated by the decision system. The **actuation limits** or control inputs $u_i = j_{x,i}^T$ are calculated by minimizing the cost function by the MPC.

Constraints (Equations 4.5c–4.5d) are defined for differential states $x_i = [v_x,\ a_x,\ d_r]_i^T$ between $[0,\ -a_x^{limit},\ d_r^{min}]$ and $[v_x^{ref},\ 1.1\ \text{m/s}^2,\ d_r^{max}]$; and control inputs $u_i = j_{x,i}^T$ as $\pm j_x^{limit}$. The constants $[d_r^{min},\ d_r^{max}]$ represent the desired relative distances for **safety limit** and maximum range of sensor [2 m, 20 m]. The values $[a_x^{limit}, j_x^{limit}]$ depend on the transitional tracking mode explained in Section 4.3.3.4 and considering the safety and comfort thresholds described in Table 4.1 and Figure 4.10b: *cruise* and *speed* ([2.01 m/s^2, 0.98 m/s^3]), *headway* ([2.51 m/s^2, 3.92 m/s^3]) and *too-close* ([5.40 m/s^2, 14.72 m/s^3]).

Minimizing Equation 4.5a allows calculating the optimum value of $u = j_{x,i}^T$ for the current time step. For that purpose, the nonlinear MPC is solved with the automatic code generator of the open-source ACADO toolkit described in Section 4.3.2.1, using QPOASES as the set solver, the sequential programming technique, and the direct multiple-shooting method for discretization. The prediction horizon is 5 s of look-ahead time considering a fixed time step among predictions of 0.5 s.

4.6.2 Actuation Model

The control variable P is constrained between [–1,1] in the MPC formulation and represents the maximum brake and accelerator pedal positions, respectively. To achieve this, the control output j_x from MPC is divided by a_x^{min} = -5.40 m/s^2 and a_x^{max} = 2.5 m/s^2 when brake or accelerator pedals is pushed, respectively. Actuation delays of 80 ms and 150 ms for brake and accelerator pedals, respectively, were approximated by second-order transfer functions (see Section 3.3.2.2). Also, the same rate limitations defined in MPC constraints are applied to mimic real actuation behavior.

4.6.3 OEDR Verification Tests

The performance evaluation of the proposed OEDR methods is detailed in this section. One complete lap is simulated at each one of both defined scenarios (Figure 4.22a-b), and the results are recorded and assessed. Detection and responses to traffic lights or dynamic objects analysis are considered separately. This will allow studying the influence of d_r and v_r in the longitudinal motion control for the defined route.

4.6.3.1 Traffic Lights Detection and Response

Figure 4.23 shows the detection and response to traffic lights on the path. Figure 4.23a shows the driving events defined by the four traffic lights status (*green, yellow and red areas*) changing at the same time, consequently, the time to *red* status of next traffic light (t^{trl}) and time reaching the next traffic light (t^{ttl}) are constantly compared as defined in Equation 4.19.

Figure 4.23b illustrates traffic light detections (*gray areas*) when t^{trl} is lower than t^{ttl}, meaning that next traffic light will change to *red* before reach it at the current speed, therefore, the ADS-dedicated vehicle must stop before the traffic light location to respect the red light status. The first three traffic lights were detected at the maximum distance provided by the sensor (20 m) and the vehicle reduced its speed and even entirely stopped,

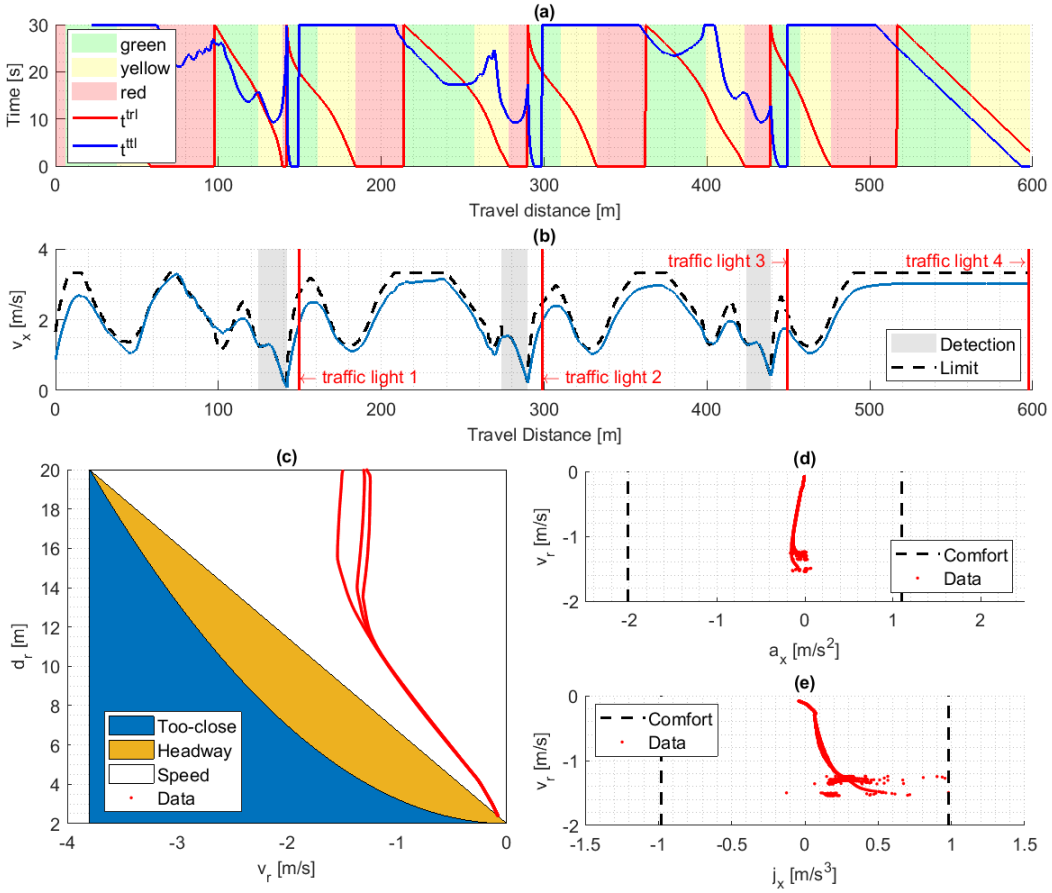

Figure 4.23 Results for traffic lights: (a) time-to-red and time-to-traffic-light, (b) v_x, (c) Range vs. Range-Rate Diagram, d) a_x vs. v_r and e) j_x vs. v_r

while maintaining a safe distance (2 m) to the traffic light. As t^{trl} was higher than t^{ttl} for the fourth traffic light, there was enough time before red light status and the vehicle could continue at *cruise* mode executing speed tracking under the defined speed limit.

Figure 4.23c depicts the results for d_r and v_r in a range vs. range-rate diagram. The transitional tracking was executed in *speed* mode at all times, showing that the previous time comparison estimation avoids sudden braking responses from unexpected *red* switching, therefore, a comfortable braking execution is always possible. Moreover, Figures 4.23d-e show a top view of the previous diagram, having the same data located within comfort thresholds (and actuation limits) for both a_x and j_x when accelerating and braking.

4.6.3.2 Path-Crossing Objects Detection and Response

Figure 4.24 shows the detection and response to dynamic objects transversely crossing on the driving path. Figure 4.24a shows the current speed and limit along the driving route. Seven of ten available objects with different width, length, and crossing behavior

were detected on the driving path (*gray areas*). The speed was reduced comfortably when objects were detected at higher Time-To-Collisions (TTC, $d_r/v_r > 4$ s). On the contrary, speed was reduced abruptly when objects were detected at lower TTC ($d_r/v_r < 4$ s), avoiding frontal impacts and ensuring safety as a primary issue.

Figure 4.24b illustrates same detections (*gray areas*) when objects goes within road limits as described in Section 4.3.3.1, therefore, the ADS-dedicated vehicle must stop before object location avoiding frontal impacts. Three of seven detections occurred suddenly at a relative distance (d_r) lower than the maximum sensor range (20 m). In any case, the vehicle reduced its speed and even entirely stop maintaining a safe distance (2 m) to objects at all times.

Figure 4.24c depicts the results for d_r and v_r in a range vs. range-rate diagram. The transitional tracking was executed in *speed* mode (red points) in most of the detections performing a comfortable braking execution. However, to achieve a safe distance and avoid crashes, *headway* (red circles) and *too-close* (red crosses) executions provoked sudden braking responses when unexpected objects on the path were dected. Moreover, Figures 4.24d-e show a top view of the previous diagram, having the same data located within comfort thresholds (and actuation limits) for both a_x and j_x at acceleration and braking. When safety was a primary issue, threshold limits were increased to uncomfort or maximum values.

Figure 4.25 shows the most critical result from sudden detection and response to the path-crossing object, being located after 40 m of travel distance (d_x). The ADS-dedicated vehicle was traveling at $v_x = 1.14$ m/s before the object entered on road limits. Once located on the driving path, the object is detected at $d_r = 4.5$ m with a TTC ≈ 2.5 s, which is considered as a potentially dangerous situation of vehicle conflict[64], hence, the current speed is abruptly reduced to maintain a safe distance. Once the object is located out of the driving path, the planned speed profile is again tracked as no object is obstructing the driving path.

4.7 Conclusion

In this chapter, safety and comfort on different methods for vehicle motion planning and control in automated driving have been proposed. On one hand, a trajectory planning approach has been proposed to tackle the reference generation problem for both path and velocity considering driving safety (e.g. collision checking with static infrastructure in path planning, and legal limitation in speed planning) and comfort (e.g. lateral and longitudinal acceleration thresholds in trajectory planning). On the other hand, an MPC-based set of trajectory tracking controllers that consider both path and velocity tracking have been proposed. These consider both driving comfort (e.g. acceleration and jerk threshold limits) and safety (e.g. path and speed tracking accuracy, physical limits in both vehicle and actuation systems) by the introduction of related constraints. Moreover, a model blending approach has been proposed to further increase the operational range of the trajectory tracking controllers.

The proposed approaches have been used in the different case studies detailed in this Ph.D. Thesis. In particular, in this Chapter, three case studies have been analyzed.

In a first case study, Bézier curves generation is employed for path planning using information from global planners based on JOSM. First, digital maps were useful to gather

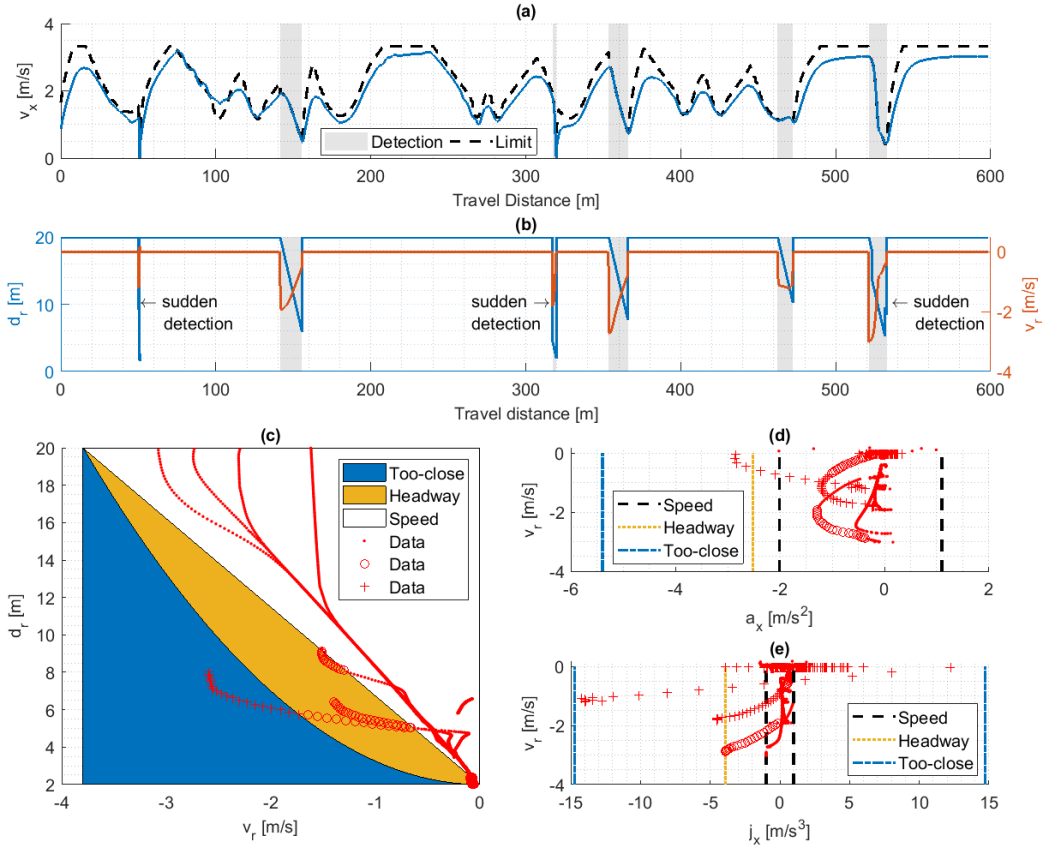

Figure 4.24 Results for path-crossing objects: (a) v_x, (b) d_r and v_r, (c) Range vs. Range-Rate Diagram, d) a_x vs. v_r and e) j_x vs. v_r

essential data from a selected testing circuit such as path boundaries and road elevations. Secondly, the driving area covered by the vehicle allows collision checking using path reference waypoints, vehicle dimensions, and driving area free of static objects. Thirdly, a speed profile is generated considering the path curvatures, and threshold limits for velocity, accelerations bearing in mind both safety and comfort. Lastly, the road gradient planning is based on the altitude information from a digital map.

In a second case study, the use of the a_y as opposed to the v_x is proposed as the switching condition to blend vehicle models within an MPC-based trajectory tracking control. As tire forces are the critical factor for the validity of the kinematic/dynamic models, the a_y is considered as a variable with direct relation to these forces, allowing for increasing the overall performance of the blended approach. Additionally, a formal step-by-step tuning approach is proposed and detailed for two methods: *linear* and *step*. The results of the method presented show that the proposed blending approaches based on a_y provide a relative improvement of 15% in terms of e_y, in contrast to the method based on v_x proposed in the literature. Additionally, it allows for reducing the maximum computational cost by 12% if a linear blending approach is used. Moreover, the validity of the tuning procedure

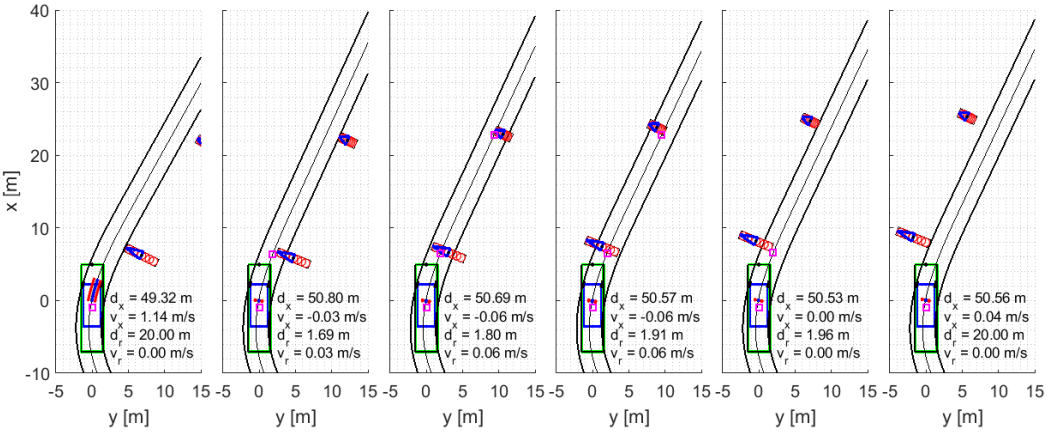

Figure 4.25 Path-crossing object sequence

is demonstrated.

In a third case study, object and event detection and response algorithms were proposed and implemented within an MPC-based speed tracking control. As in urban environments, the compromise between safety and comfort is always present depending on road actors' behavior located on driving surroundings, the changing nature of traffic lights, and dynamic objects were assessed. The comparison between time-to-red-light and time-to-traffic-light values allows a comfort braking or continue at current speed as enough time is available, respecting the red light status at all times. When objects are crossing on the path, comfort braking is performed when safety is not a primary issue. In the latter case, the increase in threshold limits enables emergency brakings to avoid impacts.

In conclusion, the proposed techniques for vehicle motion enables the verification of trajectory planning and tracking strategies in simulation environments. Most of the ADS algorithms employed in this chapter are an essential part of the VV results presented in Chapter 3. Moreover, the integration and verification of different ADS systems are considered bearing in mind non-faulted automated driving scenarios, as a standardized practice presented in ISO/PAS 21448[44]. However, the injection of electric/electronic malfunctions would be still considered in the development phase using simulations, considering the safety verification process mentioned in the standard ISO 26262[45]. The evaluation of fail-operational systems is an aspect covered in the next chapter.

Chapter Five

Dynamic Driving Task Fallback

In the last decade, Automated Driving Systems (ADS) have shown significant advances, mainly from the acquisition, perception, control, and actuation point of view [3]. Several important developments have been achieved and mentioned in the latest European Commission reports [266], where the challenges on communication technologies and cybersecurity, on-board sensors capacities, infrastructure requirements, mobility concepts, and city contexts are playing an active role for sustainable urban transportation developments.

ADS obtain information from the surroundings using different sensors, such as cameras, differential global positioning systems (GPS), Light Detection and Ranging (LiDAR), and Radio Detection and Ranging (RaDAR) [98]. Perception tasks are critical for increasing the level of automation of ADS developments, as environment recognition in any scenario, including lighting and weather conditions, should be assured. Moreover, their Fail-Operational (FO) capacity during autonomous mode is crucial to ensure safety, as sensor and perception errors can be easily propagated to decision and control systems in different maneuvers, causing fatal accidents [267].

Some authors have considered sensor data fusion for more robust performance on different contexts: obstacles detection [268], perception of the environment [269], localization [270], and Traffic Sign Detection and Recognition [271]. A detailed description of the most popular methods and techniques for performing data fusion is presented in [272], where the author concludes that the appropriate technique to be implemented depends on the type of problem. In the automotive field, the Bayesian approach, extended and Unscented Kalman Filter (UKF) are mostly used [62, 273, 274]. However, these techniques depend mainly on the information directly given by onboard sensors without any fallback strategy.

This chapter proposes a novel decision-based Dynamic Driving Task (DDT) fallback method where positioning of an ADS-dedicated vehicle plays an important role, based on the bottom of system development life cycle shown in Figure 5.1. The rest of this chapter is divided as follows. Section 5.1 further details the motivation behind the use of DDT fallback strategies to achieve higher driving automation levels. Section 5.2 details a FO control architecture proposal describing each system. Section 5.3 provides an overview of the FO positioning system proposal where, vehicle model, cornering stiffness estimation and the adaptive UKF are the main contributions. Section 5.4 describes the DDT fallback strategy proposed for the decision system, considering a real-time trajectory generation, Rear-End Collision Avoidance (RECA), and trajectory tracking. Section 5.5 develops a case study describing the driving scenario and test platform for virtual testing, including results and discussion. Finally, Section 5.6 presents some remarks and conclusions.

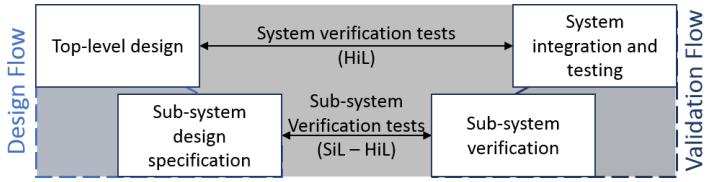

Figure 5.1 System and sub-system verification testing

5.1 Motivation

Currently, the most widely used global localization approaches involve Global Navigation Satellite Systems (GNSS) such as GPS and Galileo [275]. The implemented devices even can implement differential GPS approaches, which have become affordable in recent years, or Inertial Navigation System (INS) [270], which may be fused with GNSS data to provide more reliable data. Although this approach works properly in open scenarios such as highways, in urban environments, their localization accuracy is not guaranteed for ADS [275]. Hence, a FO positioning system, which also uses the dynamic model of the vehicle, is required to increase the accuracy. Moreover, ADS must have DDT fallback strategies to be executed when the positioning system fails [276]. As mentioned in Section 2.3, Table 2.2 summarizes some of the most important DDT fallback strategies.

A better assessment of FO strategies for DDT fallback functions is needed to achieve higher levels of automation on ADS [1]. This Ph.D. Thesis is focused on this area, and its main contribution is a FO strategy approach considering positioning failures, implemented within a general control architecture for automated vehicles.

In brief, the proposed improvements presented in this chapter are related to a FO positioning system that comprises an Unscented Kalman Filter (UKF), a virtual sensor, and a monitor system, capable of remaining operative from degraded to total failure of the position reception and warns for fallback triggering. Moreover, a case study is proposed which resembles a real urban scenario in which a DDT fallback strategy is required to cope with a major positioning failure.

5.2 Fail-Operational Control Architecture

As mentioned in Section 1.1.4, the driving functionalities proposed in this Ph.D. Thesis aims the fulfillment the requirements of AutoDrive Project[28] by developing SAE Level 4 [1] automated driving capabilities. More precisely, the case study proposed is a highly automated driving bus to carry passengers in an urban scenario with mixed traffic conditions.

The required automation level must include the lateral and longitudinal vehicle motion control, a complete Object and Event Detection and Response (OEDR) system, and the capability to be robust enough to support FO operation [15].

The control architecture proposed to achieve this goal is depicted in Figure 5.2, covering seven systems of those suggested by [3] required for ADS developments (Database, Acquisition, Perception, Supervisor, Decision, Control, and Actuation). This architecture allows the verification of a DDT fallback strategy after the occurrence of a positioning system failure.

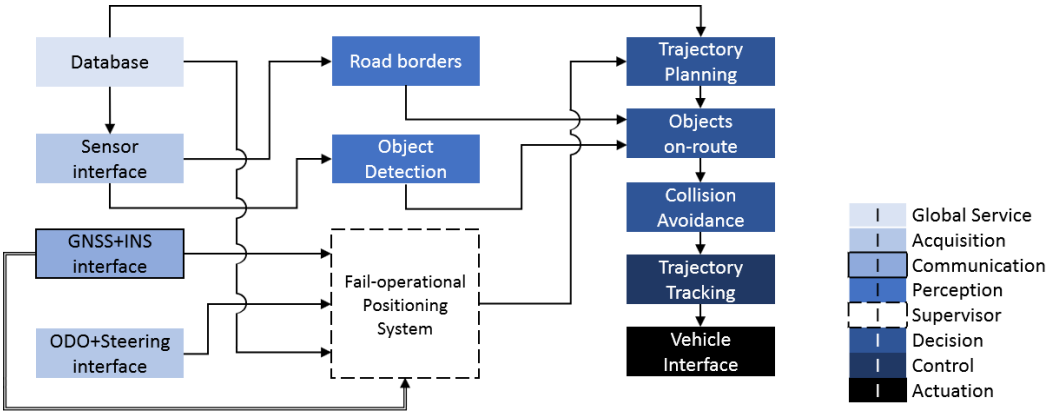

Figure 5.2 Fail-Operational Control Architecture

Aligned with those descriptions given in Section 2.1.2.1, the different systems which compose the proposed FO control architecture are detailed next.

5.2.1 Database

The database is composed of a list of waypoints that contain relevant information of the fixed route, such as global axis coordinates (X, Y), orientation angles (ψ), and velocity limits (v_x). Additionally, information related to safe-parking places is included, considering three different cases: stop not allowed, stop on-lane permitted, and stop on-shoulder available. These waypoints will be illustrated in the case study in Section 5.5.

5.2.2 Acquisition

The acquisition system interface provides two features: the vehicle surrounding recognition, and the vehicle's global position on the route.

For the first feature, a sensor interface will be used, which provides relevant information about the surroundings. This will be processed by the perception system, which will detect features such as road borders and objects.

To estimate the vehicle position, a GNSS+INS, odometer, and steering sensors will be considered. These devices provide the vehicle position (X, Y), front-wheel angle (δ) and inertial parameters as orientation (ψ), acceleration (a_x) and velocity (v_x).

Commercial GNSS+INS interfaces present noise and signal quality reductions, and are common on-board sensors in commercial vehicles. Hence, the failure of this sensor must be handled by the proposed FO positioning system and fallback strategy.

5.2.3 Perception

The information provided by the acquisition system will be used to detect the road borders and objects within the sensor range. These will be estimated in coordinates relative to the vehicle. On the other hand, an object list will be provided considering relative distances

and velocities. This system comprises environment recognition, localization, and object detection and classification.

5.2.4 Supervisor: Fail-Operational Positioning System

The supervisory system will be continuously monitoring the positioning accuracy and the status of sensor devices (GNSS+INS) of the acquisition system.

When the vehicle performance is highly compromised or a relevant sensor failure is detected, a FO strategy will be activated. Using the data from positioning sensors (GNSS+INS, odometer, and steering sensors), a virtual positioning sensor will be switched on and employed to perform the fallback strategy that leads the test platform to a safe state. This is one of the contributions of this Ph.D. Thesis and its development are broadly detailed in Section 5.3.

5.2.5 Decision

The decision system will create the trajectory reference to be followed by the automated vehicle and will be integrated by a trajectory planning and a collision-avoidance system.

The trajectory planning, in the case of normal operation, will generate optimum trajectories for a specified scenario. However, in the case of system failure, such as the case study analyzed in Section 5.5, the trajectory planner will adjust the original route. Using the information of safe-parking places from the database, the proposed trajectory planning will modify the route to achieve the nearest safe state. This is an important contribution to this Ph.D. Thesis and will be covered in Section 5.4.1.

On the other hand, the collision-avoidance system will be focused on avoiding rear-end collisions with target objects. The perception system detections will be first analyzed to evaluate if they are within the trajectory to be followed. Therefore, objects located outside the road borders won't represent a collision risk and adjustments won't be required over the original trajectory, while objects on the driving path will require adjustment of the trajectory by maintaining a safe distance to the objects ahead. The proposed approach, which will be detailed in Section 5.4.2, can work not only in normal operation but also when there exists a degraded condition due to failure in positioning sensors.

5.2.6 Control

The references estimated by the decision system will be followed by the trajectory tracking controller, providing reliable inputs to the vehicle interface. Velocity (v_x), acceleration (a_x), and jerk (j_x) will be considered the main state parameters to control the longitudinal vehicle motion behavior, employing the *internal MPC models for speed tracking* described in Section 4.3.2.4. The position in global coordinates (X, Y) and the yaw angle of the vehicle (ψ) will be used to estimate lateral and angular deviations, respectively, employing the *internal MPC models for path tracking* described in Section 4.3.2.3. The lateral deviation concerning the path's center-lane (e_y) will also be considered as a state parameter. A detailed explanation of this system is presented in Section 5.4.3.

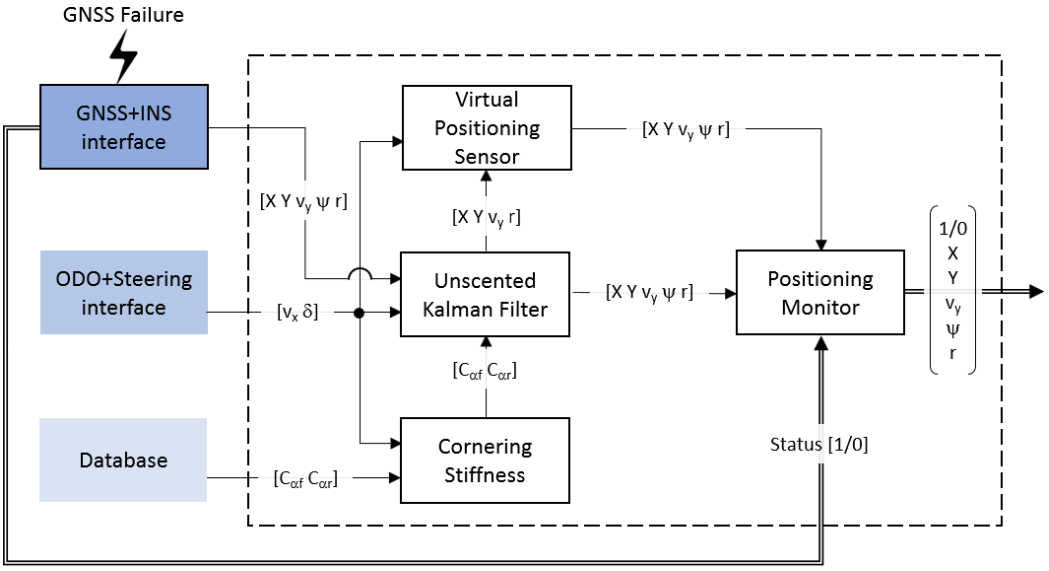

Figure 5.3 Flowchart of the fail-operational positioning system

5.2.7 Actuation

The actuation system will receive information from the control system. Its task is to act on the inputs of the automated vehicle, this is, the steering wheel and the pedals. Note that the procedure to characterize the actuators and include them in the control model has been presented in Section 3.4.2.

5.3 Fail-Operational Positioning System

In this section, the supervision system of Figure 5.2 is thoroughly detailed. The proposed approach uses a sensor fusion strategy that combines the information of GNSS+INS, odometer, and steering sensor to provide positioning data even in degraded circumstances. Moreover, it integrates a quality monitor that allows detecting sensor failures. The overall architecture of the proposed FO positioning system is depicted in Figure 5.3.

This strategy first uses the current values of velocity (v_x) and front-wheel angle (δ) to estimate the front ($C_{\alpha f}$) and rear ($C_{\alpha r}$) cornering stiffness from database values. This data will be used in a second step, where an adaptive UKF is employed to attenuate the accuracy lacking on the GNSS-INS positioning measurement. This is a problem regularly faced in urban environments due to obstructions in the line-of-sight of satellites [274].

When a relevant performance failure is detected, a virtual positioning sensor is activated. It makes use of the last position estimated by the UKF, the estimation of the cornering stiffness, and the data provided by the odometer sensors and steering wheel sensors to estimate the position of the vehicle by performing dead reckoning.

The detection of a degraded condition and critical failure is carried out by a monitor, which selects the positioning source data to provide a FO response, and informs to decision about the failure. Next, the main functional systems depicted in Figure 5.3 are analyzed.

5.3.1 Vehicle Model for Positioning Estimation

The proposed FO positioning system requires a vehicle model to implement both the lateral motion control and UKF.

The lateral motion of a vehicle can be estimated and controlled by employing simplified models, being this a technique that reduces the computational effort for real-time implementations while providing enough accuracy for control purposes [212]. As mentioned in Section 4.3.2.3, for velocities at less than 5 m/s the lateral forces on the tires can be neglected, and the vehicle motion can be calculated entirely on geometric relationships of X, Y and ψ [65]. Above 5 m/s, the assumption of no lateral forces on the tires begins to be compromised, as the lateral vehicle motion is affected by its dynamics being necessary to take into consideration a more complex model to improve results [224]. In these cases, a mix of simplified single-track models for lateral vehicle dynamics (Figure 4.5) provides a good accuracy vs complexity relationship.

5.3.2 Cornering Stiffness Identification

Using the simplified single-track dynamic model (which has been defined in Section 4.3.2.3; Equations 4.11a-b), it is possible to estimate the cornering stiffness coefficients $C_{\alpha f}$ and $C_{\alpha r}$. As the identification of these parameters is complex, an approach based on the *direct method* described by [264] is proposed. This way, a state-space representation is described in Equation 5.1.

$$\begin{bmatrix} C_{\alpha f} \\ C_{\alpha r} \end{bmatrix} = \begin{bmatrix} 2\alpha_f & -2\alpha_r \\ 2l_f\alpha_f & 2l_r\alpha_r \end{bmatrix}^{-1} \begin{bmatrix} m(\dot{v_y} + v_x r) \\ I_z \dot{r} \end{bmatrix} \tag{5.1}$$

where l_f and l_r are the longitudinal distance from Center of Gravity (CG) to front and rear tires, $\dot{v_y}$ is the lateral acceleration, r is the yaw rate, $\dot{r}$ is the yaw acceleration, m is the total mass of the vehicle, I_z is the moment balance around the yaw axis of the vehicle, and α_f and α_r are the slip angles on the front and rear tires defined in Equations 4.13.

The implementation for cornering stiffness identification can be made using off-line or on-line approaches as detailed next.

5.3.2.1 Off-line Identification

An open-loop test method for determining the steady-state circular driving behavior[34] is employed for the cornering stiffness estimation at constant steering wheel angles and velocities. Using this procedure, a cornering stiffness map can be generated and integrated into the control architecture. This allows to implement a cornering stiffness estimator as input to the UKF (Figure 5.3), so that for any v_x and δ the coefficients $C_{\alpha f}$ and $C_{\alpha r}$ can be derived.

The use of an off-line cornering stiffness estimator implies that the open-loop tests must cover the whole range of v_x and δ to be performed by the test vehicle within the Operative Design Domain (ODD). Although this can be implemented for on-line estimations, this procedure helps to fix values when necessary avoiding some singularities in circumstances, as no lateral accelerations [277].

This procedure was employed in the case study of this chapter in Section 5.5.

5.3.2.2 On-line Identification

The estimation of cornering stiffnesses is performed in real-time introducing the current vehicle states in Equation 5.1. After this, two separate one-dimensional Kalman filters reduce peak values from numerical inconsistencies in both $C_{\alpha f}$ and $C_{\alpha r}$. The filters are evaluated in the discrete-time domain, no control input is considered, and gain matrices related to states and measurement are constants valued as 1 [264, 278].

In contrast to [264], the use of a linear Kalman filter avoids the definition of a threshold limit for αf and αr, as the slip angles would approach zero when the vehicle is driving straight or during transient steering maneuvers, affecting the cornering stiffness calculation.

This procedure was employed in one case study of the previous chapter described in Section 4.5. The process and measurement noise covariances were settled to 0.01 N/rad and 1 N/rad, respectively. Moreover, a Kalman Filter block from MATLAB/Simulink was employed for this purpose.

5.3.3 Adaptive Unscented Kalman Filter

An adaptive Unscented Kalman Filter (UKF) will be used to attenuate the errors introduced in the GNSS-INS positioning measurement when the satellite signal quality is reduced. In contrast to other Kalman filtering techniques, the UKF frequently provides a lower estimation error and is preferable for implementations in automated driving applications [62]. In this sense, a UKF-based approach capable of adapting the measurement noise covariance matrix is presented here, this is an adaptive UKF.

The development of UKF requires space-state transition model of the vehicle detailed previously, the dynamic single-track model, detailed in Section 5.3.1, which can be defined in state-space form as in Equation 5.2.

$$\begin{bmatrix} \dot{X} \\ \dot{Y} \\ \dot{y} \\ \dot{v}_y \\ r \\ \ddot{\psi} \end{bmatrix} = \begin{bmatrix} 0 & 0 & 0 & -\sin\psi & \frac{v_x \cos\psi}{\psi} & 0 \\ 0 & 0 & 0 & \cos\psi & \frac{v_x \sin\psi}{\psi} & 0 \\ 0 & 0 & 0 & 1 & 0 & 0 \\ 0 & 0 & 0 & -\frac{2C_{\alpha f}+2C_{\alpha r}}{m v_x} & 0 & -v_x - \frac{2C_{\alpha f} l_f - 2C_{\alpha r} l_r}{m v_x} \\ 0 & 0 & 0 & 0 & 0 & 1 \\ 0 & 0 & 0 & -\frac{2{l_f}C_{\alpha f} - 2{l_r}C_{\alpha r}}{I_z v_x} & 0 & -\frac{2{l_f}^2 C_{\alpha f} + 2{l_r}^2 C_{\alpha r}}{I_z v_x} \end{bmatrix} \begin{bmatrix} X \\ Y \\ y \\ v_y \\ \psi \\ r \end{bmatrix} + \begin{bmatrix} 0 \\ 0 \\ 0 \\ \frac{2C_{\alpha f}}{m} \\ 0 \\ \frac{2{l_f}C_{\alpha f}}{I_z} \end{bmatrix} \delta \quad (5.2)$$

where X, Y, v_y, ψ and r are parameters obtained from the GNSS-INS interface. v_x and δ are parameters received from the odometer and steering angle sensor interface. A linear relationship between the steering angle and the front-wheel angle is employed to obtain the current value of δ. The stiffness coefficients C_{α_f} and C_{α_r} are obtained through the procedure described in Section 5.3.2.

The process noise covariance matrix in a vehicle model is suggested to be calculated as the propagation of each value per time step [273], in this sense, gathering the standard deviation of parameters from the test vehicle circulating in normal conditions helps to determine the process noise.

The measurement noise covariance matrix is mainly associated with the accuracy of the acquisition devices. These can be extracted from commercial GNSS devices data-sheet.

5.3.4 Virtual Positioning Sensor

When a GNSS failure event occurs (lower signal quality or total disconnection), a virtual positioning sensor will be used to provide an indirect position measurement by combining information from the remaining physical sensors.

The velocity from the odometer (v_x^{odo}), the lateral velocity from the filter (v_y^{ukf}), and the yaw angle obtained due to a discrete integration from the filter yaw rate measure (ψ^{int}), are considered to estimate the vehicle velocities in global coordinates ($\dot{X}$,$\dot{Y}$). A state-space representation is described as,

$$\begin{bmatrix} \dot{X} \\ \dot{Y} \end{bmatrix} = \begin{bmatrix} \cos\psi^{int} & -\sin\psi^{int} \\ \sin\psi^{int} & \cos\psi^{int} \end{bmatrix} \begin{bmatrix} {v_x}^{odo} \\ {v_y}^{ukf} \end{bmatrix} \tag{5.3}$$

The obtained velocities are consequently integrated to obtain X and Y. The last available values before the failure for X, Y, and ψ are considered to be the initial values for the newly integrated parameters. The remaining available parameters as v_y and r are combined with the indirect estimations to maintain the same structure information sent by the UKF.

5.3.5 Positioning Monitor

The monitor's role is to continuously evaluate the positioning quality of the GNSS. In case of very poor positioning accuracy (quality below 2 in Table 5.1) or a catastrophic failure (e.g., power supply unavailable), the monitor will instantly switch the information received from the UKF to the one received from the virtual sensor. The output state parameters are combined with a failure tag (1/0) to inform this status to the decision system so that a degraded condition and proper action taken.

5.4 Decision-Based DDT Fallback Strategy

The FO positioning system provides information on the vehicle's position and the existence of a failure to the decision system of the control architecture depicted in Figure 5.2. In this section, the fallback strategy, which includes both the trajectory planner and the collision-avoidance subsystems, will be detailed.

5.4.1 Trajectory Planning

In normal operation, a fixed route is planned off-line based on Bezier and feasible curvatures generation procedure (see Section 4.3.1). The velocities are limited considering the curvatures along the route defining bounds for lateral and longitudinal accelerations bearing in mind the passenger comfort [279].

In case of failure, a DDT fallback strategy starts, and the trajectory planned is modified to achieve a degraded driving mode. The velocity is instantly reduced to a degraded value, to avoid lateral displacements in vehicle motion control while dead-reckoning is performed and maintained until the vehicle is located over a safe-parking spot, where the vehicle stops. The path is not modified until a safe-parking space is available.

The strategy for a degraded velocity (${v_x}^{degr}$) is depicted in Figure 5.4a. After the failure, a start distance (d_{start}) is defined to reduce the speed at degraded deceleration (${a_x}^{degr}$),

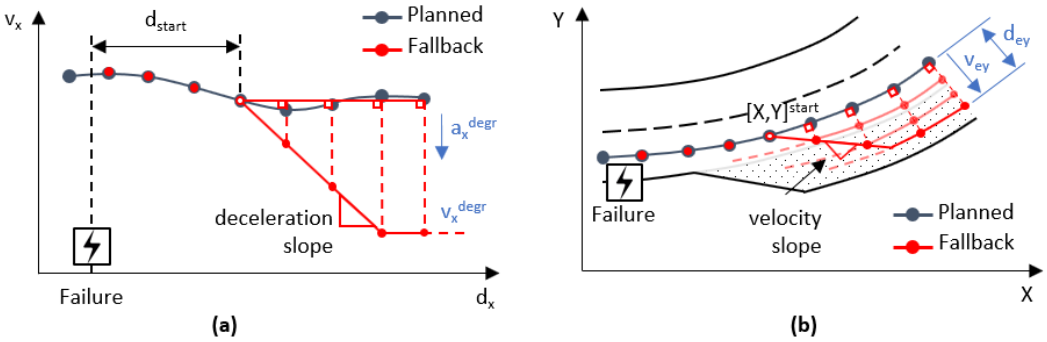

Figure 5.4 Real-time trajectory planning for (a) velocity and (b) path.

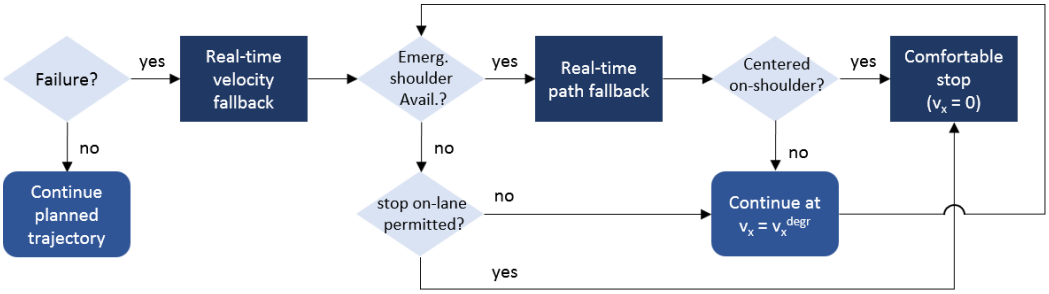

Figure 5.5 Flowchart on real-time trajectory planning

as a sudden reduction could affect negatively speed tracking, producing undesirable and uncomfortable responses. The same procedure is repeated to stop once the vehicle is located over the emergency shoulder.

The strategy for a degraded path is presented in Figure 5.4b. After the failure, the planned path is maintained until a safe-parking place becomes available ($[X, Y]^{start}$), at this point, the planned route is moved perpendicularly based on a predefined lateral velocity (v_{ey}) to a proper distance in the emergency shoulder (d_{ey}).

The degraded path reference is estimated to displace laterally from the original route faster than the vehicle's capabilities, therefore the absolute value of the lateral deviation increases and decreases during the lane-change maneuver. The d_{ey} magnitude helps to predict when the vehicle goes out the main route ($d_{ey} > 0.64$ m) and afterward is located enough on the emergency shoulder ($d_{ey} < 0.16$ m), finally permitting reduction of the degraded velocity to zero. A flowchart of the real-time trajectory planning is depicted in Figure 5.5. The practicability of this methodology is discussed in Section 5.5.4.1.

5.4.2 MPC-based Collision Avoidance

In both normal and degraded operation, the automated vehicle will implement a Rear-End Collision Avoidance (RECA) system using the data provided by FO positioning and the detection of the objects on-path provided by the perception system.

The Model Predictive Control (MPC) approach is based on a previous case study in

Section 4.6.1, however, this time is implemented to generate a speed profile to be followed by a low-level tracker, attempting to maintain a safe relative distance (d_r) and velocity (v_r) from objects ahead on-route.

A point-mass **vehicle model** is considered longitudinal motion description as in Equations 4.16 and 4.20. The problem formulation is solved at each time step with a prediction horizon defined as $i, i+1, ..., i+N_{s_u}$ and presented in Section 4.3.2.1 (see Equations 4.5a-f).

The differential states $x = [v_x,\ d_r,\ v_r]$ are optimized in the entire prediction horizon (N_x). The speed reference (v_x^{ref}) is defined by the speed planner introduced in Section 5.4.1. The relative distance reference (d_r^{ref}) is defined by the switching line of transitional tracking design described in Section 4.3.3.4, considering as constraints [d_r^{min}, d_r^{max}] as [5 m, 20 m]. The relative speed reference (v_r^{ref}) is defined as 0.

The state weighting matrix $Q_w = \text{diag}(q_{v_x}, q_{d_r}, q_{v_r})$ changes according to the $d_r - v_r$ diagram (see Section 4.3.3.4) as mentioned in a previous case study in Section 4.6, which determines the operation mode to perform *cruise*, *speed*, *headway* or *too-close* control in case of object detection on driving path.

The maximum deceleration allowed changes also with the operation mode, being this an important value to properly perform a speed track. Constraints are considered to maintain properly a safe distance from objects ahead as 5 m $< d_r <$ 50 m.

5.4.3 MPC-based Trajectory Tracking

The trajectory tracking is inspired by the MPC strategy described on a previous case study in Section 4.5.1, however, this time the model implemented in MPC is defined only by the *kinematic model-based approach* (see Section 5.3.1) with additional equations for jerk (j_x) and lateral deviation (e_y) to constraint it and assure an accurate lane-keeping. Consequently, the **vehicle model** is defined by Equations 4.8, 4.10a and 4.16.

The differential states $x_i = [X,Y,\psi,v_x,e_y]_i^T$ and control inputs $u_i = [\Delta\delta,j_x]_i^T$ are considered in the problem optimization for a horizon N_x. The speed profile is defined by the RECA system when an object ahead is present, in other cases this reference comes from the planned trajectory as well as those for lateral vehicle motion control. The obtained control inputs u_i are integrated to reproduce the steering and pedal position as actuation signals for the vehicle interface.

The differential states and control input weights for optimization are intuitively defined as $Q_w = \text{diag}([1\ 1\ 25\ 1])$ and $R_w = \text{diag}([10\ 10])$, respectively, giving more importance to the vehicle orientation over the route.

Constraints are defined for both differential states $x_i = [\delta, v_x, a_x, e_y]_i^T$ as [$\pm$ 0.68 rad, v_x^{ref},a_x^{ref},e_y^{ref}]; and control inputs $u_i = [\Delta\delta, j_x]_i^T$ as $\pm$ [1 rad/s, 1 m/s^3]. In this sense, v_x^{ref} is the speed profile, $a_x^{l,r,ref}$ depends to the longitudinal operation mode defined in Section 5.4.2 (although a comfortable acceleration is fixed at 0.2 m/s^2 to ensure comfort). The **road limits** $e_y^{l,ref}$ and $e_y^{r,ref}$ are the left and right lateral deviation, respectively, according to the current e_y. Path constraints are described as in Figure 5.6.

The ACADO Toolkit(see Section 4.3.2; Figure 4.6) is employed to solve the MPC problem both in RECA system and trajectory tracking. A continuous output Implicit Runge–Kutta integrator of second-order simulates the system integration step in both cases. The N_x is parametrized to obtain 10 elements with a constant time step of 0.5 s.

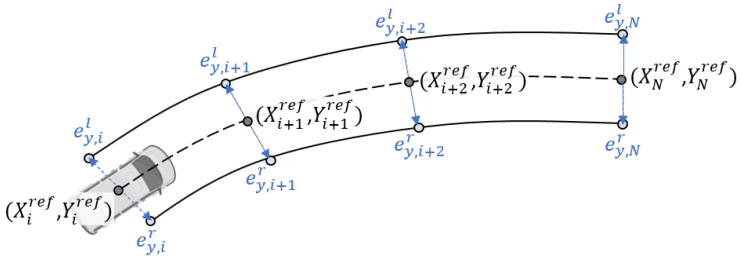

Figure 5.6 Path borders as constraints based on e_y

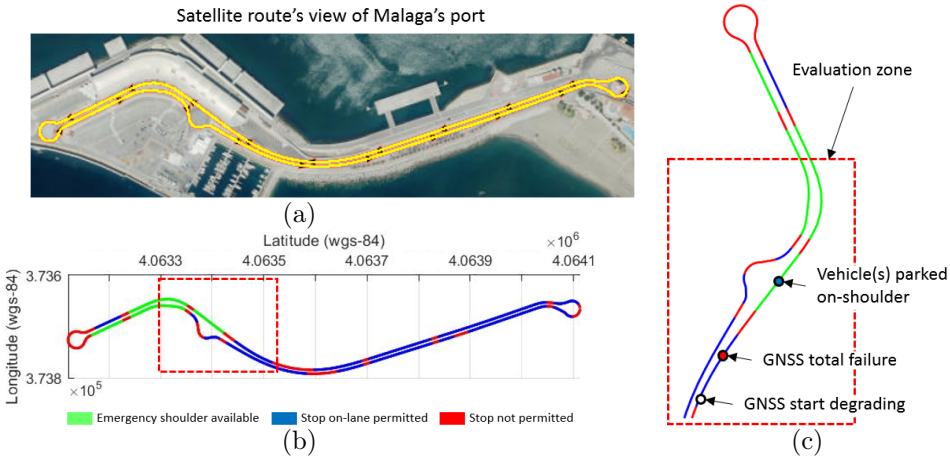

Figure 5.7 Realistic environment for DDT fallback testing. (a) Satellite's view of urban route, (b) permitted and non-permitted stops in case of total positioning failure, and (c) evaluation zone for test case study

5.5 Case Study: Relevant-Performance Position Failure

In this section, the case study to evaluate the proposed FO approach is presented. First, the test scenario is defined based on a route in a real urban scenario. Secondly, the test platform to perform the decision-based DDT fallback strategy is detailed. Thirdly, the parameters considered from the database, decision, and control systems are mentioned. Finally, the results are thoroughly analyzed.

5.5.1 Realistic Scenario

The realistic scenario considered to validate the proposed approach is a highly automated driving bus to carry passengers at the port of Malaga city (Spain), which was previously depicted in Figure 3.4c and is now detailed in Figure 5.7.

The selected test route covers a challenging environment which is part of the AutoDrive Project[28], with static objects in addition to difficult vehicle motion maneuvers as round-abouts, merging streets and intersections, as seen in Figure 5.7a. The Trajectory planning procedure has been previously described through a case study in Section 4.4.

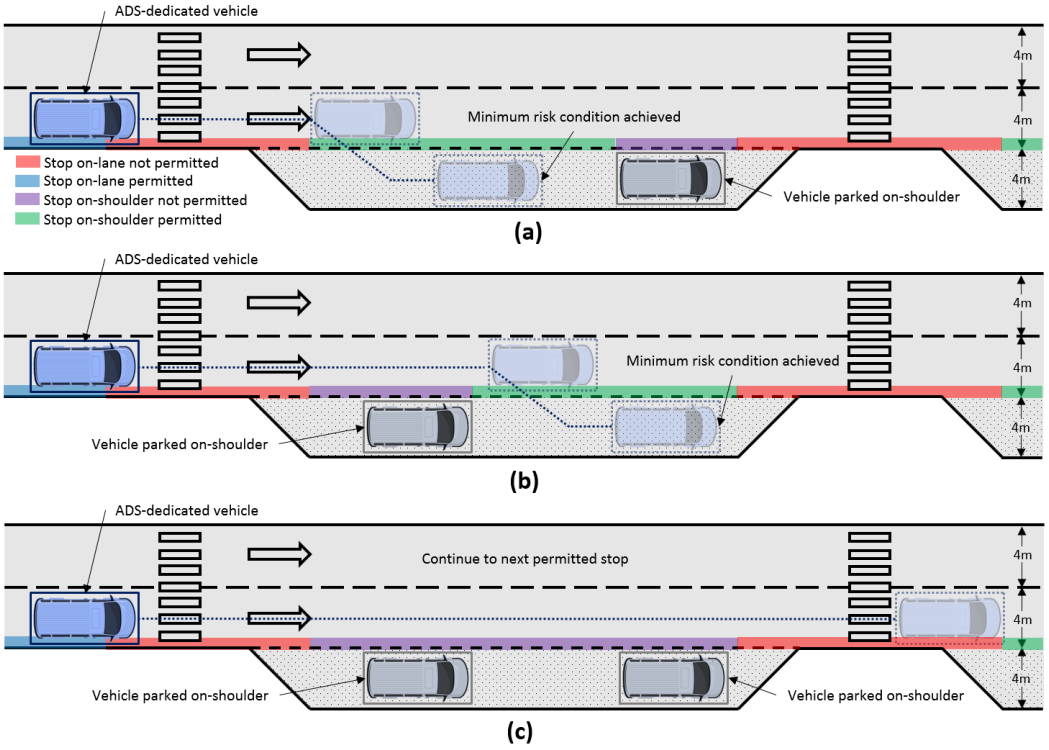

Figure 5.8 DDT fallback strategy response under three different scenarios. A minimum risk condition is achieved (a) before and (b) after an object parked on shoulder. A next permitted stop necessary due to (c) no space available on shoulder

In case of system failures, the ADS must respond without driver intervention to achieve a minimal risk condition bringing the vehicle to a safe state. In this sense, permitted and non-permitted stops are showed in Figure 5.7b avoiding to instantly stop.

The test case analyzed in this work is delimited to the evaluation zone depicted in Figure 5.7c. The failure to be studied is the possible malfunction of the GNSS position receiver (which is a vital part of the ADS), which starts degrading up to total failure and a DDT fallback strategy must be activated by the ADS.

As an additional issue, the case is considered in which the emergency shoulder cannot be used, as another vehicle is already parked, requiring driving of a long distance to the next permitted stop while performing dead reckoning. Three different failure scenarios are analyzed, as shown in Figure 5.8.

When a failure of the GNSS occurs, the relative distance required to perform a safe-parking (${d_r}^{req}$) is calculated constantly before to initiate the maneuver as presented in the Equation (5.4). If the d_r^{req} is lower than d_r from and object and the available emergency shoulder longitude, then the lane-change maneuver initiates to achieve a minimal risk condition, parking the vehicle on the emergency shoulder. Moreover, the first one of the two terms in the right-hand side of Equation (5.4) can be employed to estimate a stop

on-lane if permitted. On the contrary, the vehicle continues to the next permitted stop.

$$d_r^{req} = v_x\left(\frac{v_x}{a_x^{degr}} + t^{delay} + t^{timeout}\right) + \frac{d_{ey} - e_y}{v_{ey}} \tag{5.4}$$

where t^{delay} and t^{out} are additional times considered to complete the lane-change maneuver being conservative. The t^{delay} is stated as 0.5 s and related to actuation devices and vehicle's inertia that retard the final stopping time. The t^{out} is defined as 1 s considering a required time for the vehicle to be located enough on the emergency shoulder before totally stop.

This case study has been implemented in a simulation environment. This allows the introduction of degrading behavior in the perception system and evaluating the proposed fallback strategies with minimal risk before future implementation.

5.5.2 Test Platform: A Vehicle Simulation Model

A standard electric bus has been selected as the test platform for the case study scenario. The technical specifications of this test vehicle are detailed in Table 3.3. This way, the test platform has been modeled in Dynacar simulator as described in Section 3.3.2.

Moreover, the sensors have been simulated from the data obtained from the Dynacar model, introducing measurement errors to simulate degraded scenarios. The exteroceptive sensors can cover 360° around the vehicle, reaching a maximum radius of 60 m for object detection. The speed profile provided by the RECA system is considered when objects are detected ahead instead of references from the real-time planner. In the GNSS sensor case, which is the development focus, a random Gaussian noise associated with the quality signal of the GNSS+INS interface is added around the nominal state parameter obtained from the simulated test platform. The random noise values are introduced considering the quality of the signal to be simulated, as in real commercial devices as shown in Table 5.1.

This way, a 4-m road width is considered, so that the road borders are placed at 2 m of lateral distance from the center-lane (X, Y). The lateral distances are estimated from the vehicle's position to the left (e_y^l) and right (e_y^r) borders.

5.5.3 Technical Parameters

To test the proposed approaches, the following parameter values have been applied.

The noise covariances for the UKF have been calculated as suggested by [273], the process noise covariance matrix (Q_n=diag($[q_X, q_Y]^T$)) is defined assuming the standard deviation of parameters from the test vehicle circulating in normal conditions helps to determine Q_n. The measurement noise covariance matrix (R_n=diag($[q_y, q_{v_y}, q_\psi, q_r]$)^T) is selected by taking into account the accuracy of commercially available acquisition devices. The Q_n and R_n are depicted in Table 5.1.

The FO positioning system requires the estimation of cornering stiffness coefficients. As detailed in Section 5.3.2, a set of open-loop tests is carried out to determine the steady-state circular driving behavior[34], obtaining a set of data that can be used to create a cornering stiffness map.

For that purpose, the open-loop tests must cover the entire range of v_x and δ for the test platform detailed in Section 5.5. Hence, the δ has been modified from -0.5 to 0.5 rad, in 0.1 rad steps, while the v_x have taken the values of 0.5, 1, 2, 3, 4, 5 m/s.

Table 5.1 Process and measurement covariances in UKF.

Position Covariances					Inertial Covariances			
Parameter	**Quality**	Q_n	R_n	**Unit**	**Parameter**	Q_n	R_n	**Unit**
	5		1.41e-2	m	q_y	1.26e-2	2.78e-2	m
	4		2.83e-1	m	q_{v_y}	1.26e-4	2.78e-4	m/s
q_{XY}	3	1e-3	4.24e-1	m	q_ψ	2.70e-1	1.70e-1	rad/s
	2		1.13	m	q_r	2.70e-3	1.7e-3	rad/s^2

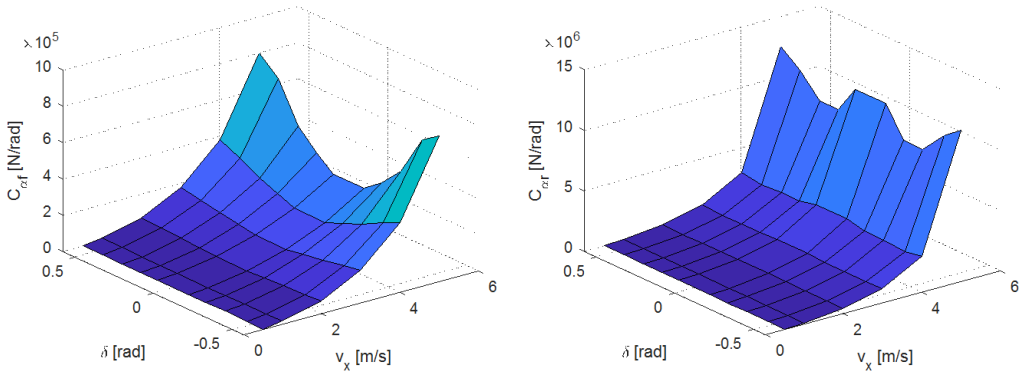

(a) (b)

Figure 5.9 (a) Front and (b) rear cornering stiffness estimation

The resulting cornering stiffness map is shown in Figure 5.9. From this map, intermediate values required by the FO positioning system are estimated using interpolation.

In the case of the real-time trajectory planner, the start distance d_{start}, longitudinal velocity and deceleration in degraded mode are fixed to 5 m, 1.5 m/s and 0.2 m/s^2, respectively, while (v_{ey} and d_{ey}) are fixed for the case study proposed to 0.2 m/s and 4 m, respectively.

5.5.4 Decision-Based DDT Fallback Verification Tests

In this section, the most relevant results associated with the proposed FO positioning system and defined fall-back strategies are analyzed. Moreover, the effect on passenger comfort is also evaluated.

5.5.4.1 Fail-Operational System Analysis

The robustness of the control architecture is evaluated here performing complete laps on the test circuit. Figure 5.7a-b shows the route defined for the evaluation of the FO positioning system based on UKF. This trajectory is executed using the architecture proposed in Section 5.2. Four different scenarios with distinct GNSS positioning qualities (from 2 to 5, see measurement noises in Table 5.1) are proposed.

In each simulation, the positioning data gave by the raw GNSS-INS sensor (with Gaussian noise), the output of the UKF filter, and the real position of the vehicle are measured

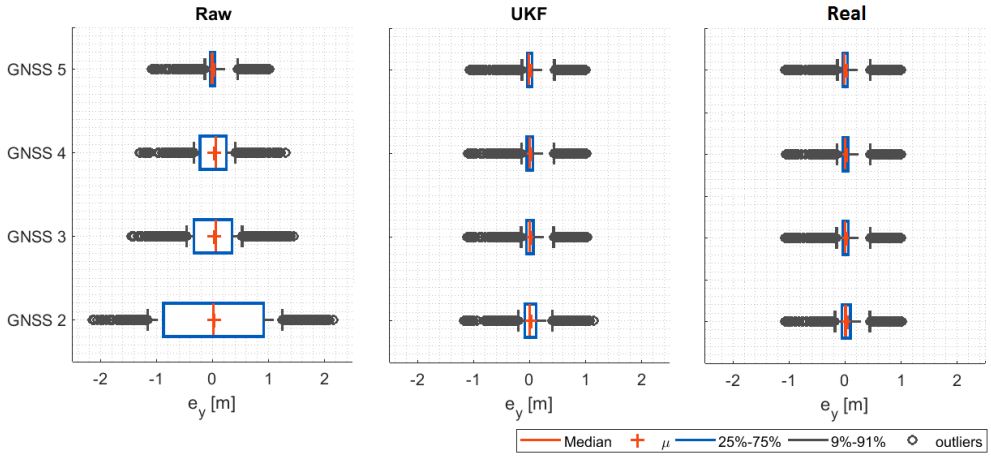

Figure 5.10 Lateral deviation under different GNSS positioning quality

and compared with the trajectory reference, to calculate the lateral deviation (e_y).

The signal quality results are shown in Figure 5.10, where the statistic distribution of e_y is calculated considering the raw GNSS-INS sensor data (raw), the UKF filter output (UKF), and the real position of the vehicle (real).

From the results, the decrease in GNSS signal quality increases significantly the lateral deviation if the raw data will be used (raw case). This could be fatal in an automated vehicle operation such as the one analyzed. Moreover, the errors could introduce instability in the controllers, depending on the nature of the noise. This emphasizes the need for providing robust solutions to positioning measurements in automated vehicles.

Results also demonstrate the positive performance of the proposed UKF approach (UKF case), which can reduce in more than 90% errors associated with e_y in the poorest quality condition (GNSS 2). This demonstrates the validity of the proposed approach. Also, the level of performance achieved using UKF is showed in ADS-dedicated vehicles (real case).

5.5.4.2 DDT Fallback Strategy Analysis

In this section, the proposed fallback strategy performance is evaluated in the three different scenarios depicted in Figure 5.8: stopping before a parked vehicle, after a parked vehicle, and continuing to a next permitted stop due to no space availability.

In all three scenarios, the same GNSS failure sequence will be evaluated, as depicted in Figure 5.7c). At the beginning of the test, the GNSS system has a higher signal quality, sequentially reducing it until a total failure exists. At that point, the fallback strategy will have to take on the control of the automated bus and lead it to a minimum risk position using the data provided by the virtual positioning controller.

Figure 5.11 indicates, for each scenario, the fallback sequence carried out. In the first row, the point at which the failure occurs (the same in three cases) is depicted. In the second one, the activation of the degraded condition is shown, in which the speed of the vehicle is reduced. Then, when a free parking spot is activated, the lane-changing maneuver is activated, to finally brake and stop. The black lines represent the road borders, the green

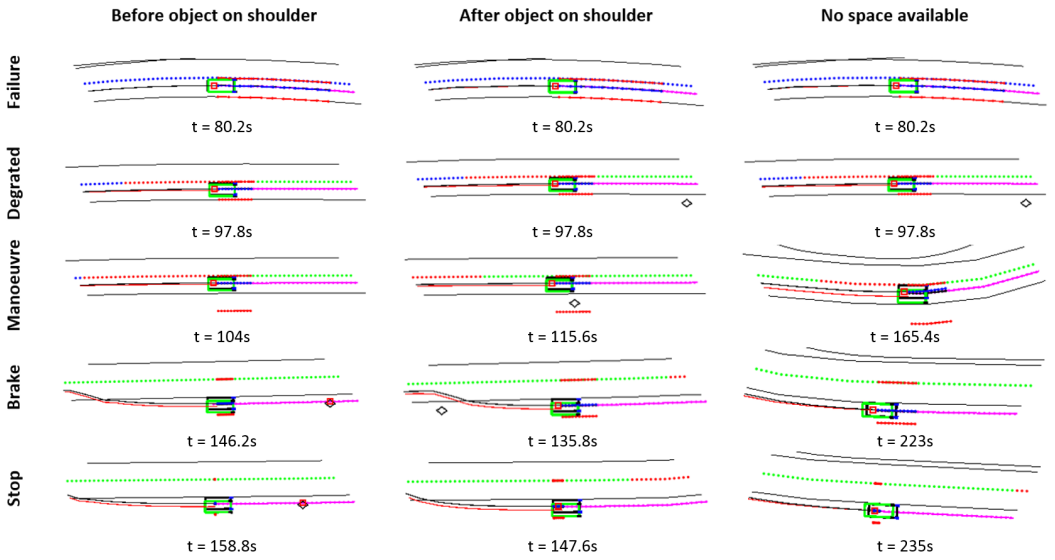

Figure 5.11 DDT fallback strategy under different use cases

dotted line is the central line of the road, while the red and violet lines are the executed and calculated trajectories.

The performance data in the three scenarios are shown in Figure 5.12. In this graph, the vertical dashed lines define the starting points of the failure, degraded, maneuver, and brake phases (stop is considered the end of the graph). Moreover, four main performance indicators are analyzed for each scenario. In the first row (v_x) the longitudinal speed reference given by the trajectory planner (*Reference*) and the real speed of the vehicle (*Ego-vehicle*) is depicted. In the second one (d_x), the longitudinal distance to the nearest object (parked vehicle) (*ObjectDistance*) and to the next emergency shoulder (*SpaceAvailable*) is shown. These distances are calculated with the position of these items in the planned trajectory. Also, the longitudinal distance required for performing the lane-change maneuver is shown (*SpaceRequired*). This calculation is detailed in the Equation (5.4). In the third row, the time evolution of the lateral deviation e_y for the planned trajectory is shown, considering the raw data provided by the GNSS system (which fails) (*raw*), the output of the UKF (*UKF*) and the real position of the vehicle (*real*). Finally, the computational cost of the high and low-level controllers is shown.

From these graphs, several conclusions can be drawn. First, the robustness of the proposed UKF-based position estimator is demonstrated in all scenarios. If e_y is analyzed, it can be noted that the effect of GNSS quality degradation directly affects the noise of the positioning system, which causes important e_y errors (up to 1 m). However, as previously analyzed, the use of the proposed UKF-based estimator reduces the effect substantially.

Second, the proposed FO Positioning System proves an effective approach in a total failure case. When total failure happens (black vertical dashed line), the data provided by the GNSS remains constant and no longer can be used to estimate the position. At this point, the Positioning Monitor of the FO positioning system switches to the Virtual Positioning Controller, entering degraded mode while making use of the odometer and the

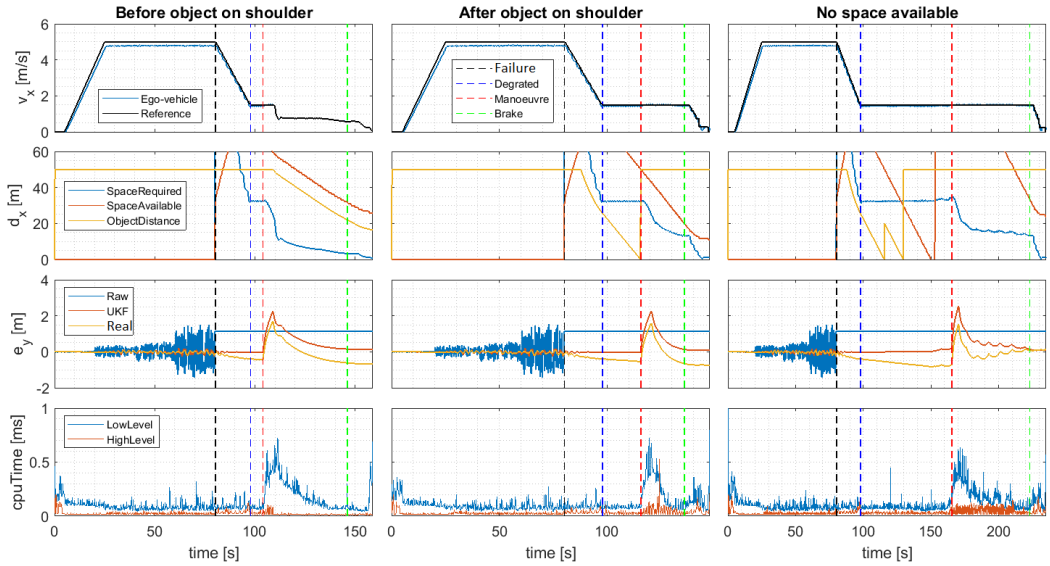

Figure 5.12 DDT fallback response due GNSS total failure after degraded position

steering wheel to estimate the position of the vehicle. Due to the nature of the selected sensors, estimation errors in e_y graphs will accumulate in time (see *real*), creating a drift. This effect is better seen in the third scenario, in which the nearest emergency shoulder is not available (is full) and therefore, the vehicle needs to move to the next one, operating more time in degraded mode. Hence, the degraded mode is intended to be used in emergencies for limited amounts of time or small distances, which is a valid assumption in urban environments such as the ones analyzed in the case study.

Third, the longitudinal speed (v_x) and distance (d_x) show that the proposed fallback strategy performs properly using the data provided by the FO positioning system. When the failure occurs (black vertical dashed line), the vehicle reduced its speed to 1.5 m/s in all cases, entering a degraded state (blue vertical dashed line) once constant speed is achieved.

In this state, the trajectory planner searches for available spaces on the next emergency shoulder. For that purpose, the planner calculates required space for emergency parking maneuver (*SpaceRequired*) which depends on current v_x and compares it with the distance to nearest object/vehicle parked (*ObjectDistance*) and available emergency shoulder distance (*SpaceAvailable*). Only if both are higher than the required distance to maneuver, the trajectory planner modifies the original route to start the lane-change maneuver. The object detection distance limit is 50 m and the emergency shoulder-distance limit detection is 60 m, hence higher distances are limited to the maximum value.

The first scenario (parking before an object/vehicle on a shoulder), is the simplest one. It can be seen that when the degraded state is activated (97 s), the required space is less than the available shoulder distance, and the distance to the next vehicle, activating the lane-change maneuver (which implies a peak in e_y due to the lateral reference change) and moving through the shoulder until the maneuver has been completed. In the second

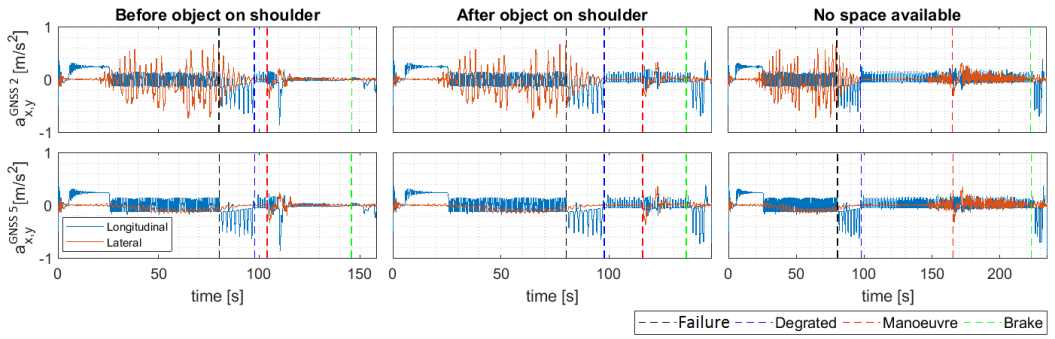

Figure 5.13 Longitudinal and lateral accelerations in DDT fallback strategy

scenario (parking after an object/vehicle in a shoulder), the degraded state is activated at the same time, but in this case, the emergency shoulder is still available, but a vehicle is already parked and the relative distance to it is too low to maneuver. Hence, the vehicle continues moving until the parked vehicle is surpassed (115 s). At this point, 50 m of emergency shoulder remains, which is more than the space required for the maneuver. In the third scenario (no space), there are two vehicles parked on the emergency shoulder. Hence, when the degraded state is activated, the distance to the first vehicle, and then, to the second, is detected (the vehicle change is shown as a peak at time 115 s). When the second vehicle is surpassed, however, the remaining shoulder-distance is not enough to maneuver safely, and the vehicle continues moving to the next emergency shoulder.

5.5.4.3 Passenger Comfort Analysis

As mentioned in Section 4.2, comfort is a key issue when considering automated driving solutions. Traditionally, comfort has been related to the magnitude of the lateral and longitudinal accelerations, being higher ones less comfortable for passengers. Threshold values for driving comfort have been pointed out in Table 4.1.

Figure 5.13 shows the lateral and longitudinal accelerations associated with the three scenarios analyzed in the previous section. Two situations are considered, the first row depicts the acceleration results with an existent degraded GNSS quality (level 2) when the failure happens. The second situation considers the case with optimal quality (level 5).

As can be seen, even before the failure, differences in lateral acceleration are important due to the noise that GNSS presents in lower qualities. Lateral accelerations are an order of magnitude higher in these cases, resulting in more uncomfortable driving. Therefore, sensor quality directly can affect passenger comfort.

The longitudinal acceleration is not affected in this case, due to the odometry will be used to estimate it. When failure occurs, similar behavior is achieved. However, the vehicle speed and accelerations are reduced when the positioning monitor switches to the virtual positioning sensor.

5.6 Conclusion

Although the research and development in automated driving have considerably helped the implementation of higher SAE automation levels, current control architectures rely on the driver as a backup in case of system failures. Moreover, hardware redundancy is the usual action plan to ensure FO systems, as few software solutions exist in the literature.

This chapter targets the issue of a vehicle bringing itself to a safe state in degraded mode after a major failure in the position receiver. Instead of a progressive deceleration on the current lane, the system focuses on seeking a permitted space on the route, performing a lane-change maneuver to the emergency shoulder, and then executes a safe stop.

The proposed FO control architecture includes basic ADS features to achieve a minimal risk condition along a route, according to a realistic case study presented for bus shuttling services as: FO positioning system, real-time trajectory planner, collision-avoidance system, and vehicle motion controller.

The FO positioning system comprises a UKF to improve the vehicle location due to lack of quality in the position receiver, an issue very common in urban scenarios where the satellite line-of-sight would be constantly obstructed. A virtual sensor switches on by a positioning monitor in case of total failure in the position sensor is detected, then a DDT fallback strategy is possible performing dead reckoning with database information. A previous cornering stiffness estimation through open-loop tests provides useful information for the vehicle model employed.

The real-time trajectory planner is capable of comfortably slow-down the speed profile after the failure, expecting an available and permitted space to perform a lane-change maneuver and safely locating the vehicle on the emergency shoulder. The benefits of having an object parked in advance are considered, hence the available space to initiate the parking maneuver is contrasted constantly with a required space calculation. A RECA system is activated at all times adapting the speed profile to remain a safe distance to objects ahead.

Both the collision-avoidance system and the vehicle motion controller are based on MPC. It is possible to optimize the trajectory bearing in mind safety and comfort in maneuvers. The vehicle motion controller includes a lateral position restriction aiming to improve the lane-keeping performance, being possible to enhance it on one side when lane-change maneuvers are required avoiding that the vehicle goes out the road boundaries.

Chapter Six
Conclusions

This chapter encloses this Ph.D. Thesis report with the concluding remarks of the presented State-of-the-Art review, methods for validation in automated driving, techniques for safety and comfort in vehicle motion, and a proposal for dynamic driving task fallback. Furthermore, the future work that can be derived from the accomplished goals is described.

6.1 Concluding Remarks

Intelligent transportation systems are increasingly aiding drivers to reduce mostly monotonous tasks. In inter-urban scenarios, systems have become safer and more efficient, due to the development of Advanced Driving Assistance Systems such as Cruise Control (CC), Adaptive CC (ACC), Lane Keeping Assistance (LKA), and lately, Traffic Jam Assistant (TJA), which keeps the vehicle on the driving path while ensures a safe distance concerning any preceding objects. In urban scenarios, systems like Automatic Emergency Braking (AEB), automated parking, and pedestrian or blind angle vehicle detection are also contributing towards safety in populated areas, relieving significantly the work from driving professionals (e.g. bus drivers), and achieving higher efficiency in operations. Nevertheless, three main challenges remain including 1) a direct relationship between vehicle dynamics and Automated Driving Systems (ADS) is not evident in current validation procedures, being this essential for virtual testing in automated driving, 2) comfort should not be considered in the decision system alone (e.g. trajectory planning) if robustness in trajectory tracking solutions is considered as a target, 3) a fail-operational architecture is required to maintain the ADS operative in case of relevant-performance failures.

This Ph.D. Thesis proposes solutions to the previous challenges seeking the obtention of high-quality results performing a system development life cycle, for verification and validation of both Advanced Driving Assistance Systems (ADAS) and ADS, while fostering the development of driving functionalities relying on virtual testings. In this sense, the following contributions are derived from the present work: 1) the proposal of a novel validation method for both vehicle simulation models and ADAS functionalities based on virtual testings, 2) the exploration of novel trajectory planning and tracking strategies considering thresholds for a more comfortable and safe Dynamic Driving Task (DDT) execution, and 3) the verification of a fail-operational (FO) strategy to achieve a minimal risk condition based on position degradation. These contributions are summarized next.

Regarding the first main contribution, a two-step methodology is proposed to validate not only the vehicle and its actuation models under simulation environments but also automated driving functionalities through technical safety testings. For that purpose, first,

a set of open-loop tests are proposed, which allow tuning models for the actuation devices, longitudinal and lateral dynamics. Second, the developed model allows testing ADS functionalities in a set of closed-loop tests based on driving scenarios. To illustrate this approach, two case studies based on automated vehicles of considerable dissimilar sizes are proposed: an Renault Twizy and a Irizar i2e bus. In both case studies, the vehicle models and actuation systems are firstly validated using real data. Results show that actuation dynamics have a significant effect that must be considered, as they could importantly affect the development using virtual testings. Secondly, a TJA functionality is tested. The lane support system keeps the vehicle on lane along the tests ensuring safety. Regarding Renault Twizy's case study, the consideration of lateral acceleration allows the Speed Assist System (SAS) to adapt the longitudinal velocity while avoiding collisions with preceding objects ensuring safety and comfort. Regarding the Irizar i2e's case study, the consideration of road gradients allows testing the SAS on critical driving scenarios for heavy-duty passenger vehicles. Subjective (face-validity analysis) and objective (statistical analysis) validation approaches assess the behavior between experiments and simulations. The proposed validation procedure enables to tune reliable simulated test platforms and automated driving strategies in simulation environments, reducing the time on real test implementations. Moreover, the proposed procedure is evaluated considering non-faulted automated driving scenarios and use cases, as a standardized practice presented in ISO/PAS 21448: Safety of the intended functionality.

Considering the second main contribution, safety and comfort on different methods for vehicle motion planning and control in automated driving have been proposed. On one hand, a trajectory planning approach has been proposed to tackle the reference generation problem for both path and velocity considering driving safety (e.g. collision checking with static infrastructure in path planning, and legal limitation in speed planning) and comfort (e.g. lateral and longitudinal acceleration thresholds in trajectory planning). On the other hand, an MPC-based set of trajectory tracking controllers that consider both path and velocity tracking have been proposed. These consider both driving comfort (e.g. acceleration and jerk threshold limits) and safety (e.g. path and speed tracking accuracy, physical limits in both vehicle and actuation systems) by the introduction of related constraints. Moreover, a model blending approach has been proposed to further increase the operational range of the trajectory tracking controllers. The proposed approaches have been used in two case studies. In a first case study, Bézier curves generation is employed for path planning using information from global planners based on JOSM. In a second case study, the use of the lateral acceleration as opposed to the speed is proposed as the switching condition to blend vehicle models within an MPC-based trajectory tracking control. As tire forces are the critical factor for the validity of the kinematic/dynamic models, the lateral acceleration is considered as a variable with direct relation to these forces, allowing for increasing the overall performance of the blended approach. The results of the method presented show that the proposed blending approaches based on lateral acceleration provide a relative improvement of 15% in terms of lateral deviation, in contrast to the method based on speed proposed in the literature. In a third case study, object and event detection and response algorithms were proposed and implemented within an MPC-based speed tracking control. As in urban environments, the compromise between safety and comfort is always present depending of road actors behavior located on driving surroundings, the changing nature of traffic lights and dynamic objects were assessed. The comparison between time-to-red-light and time-to-traffic-light values allows braking comfortably, or continuing at current speed

as enough time is available, respecting the red light status at all times. When objects are crossing on path, comfort braking is performed when safety is not a primary issue. In the latter case, the increase of threshold limits enables emergency brakings to avoid impacts.

Finally, regarding the third area, research and development in automated driving have considerably helped the implementation of higher SAE automation levels, current control architectures rely on the driver as a backup in case of system failures. Moreover, hardware redundancy is the usual action plan to ensure FO systems, as few software solutions exist in the literature. The issue of a vehicle bringing itself to a safe state in degraded mode after a major failure in the position receiver is assessed, instead of a progressive deceleration on the current lane, the system focuses on seeking a permitted space on the route, performing a lane-change maneuver to the emergency shoulder, and then executes a safe stop. A proposed FO control architecture includes basic ADS features to achieve a minimal risk condition along a route, according to a realistic case study presented for bus shuttling services as: FO positioning system, real-time trajectory planner, collision-avoidance system, and vehicle motion controller. The injection of electric/electronic malfunctions is considered within the system development life cycle using simulations, considering the safety verification process mentioned in the standard ISO 26262: Functional safety.

This Ph.D. Thesis was aligned within the goals of AutoDrive Project, which received funding from ECSEL Joint Undertaking under grant agreement No. 737469 and support from the European union's Horizon 2020 Research and Innovation Programme. The development covers 2017-2020 spanning the advancement of this work.

6.2 Research Perspective and Future Works

The developments presented in this Ph.D. Thesis covers urban driving assist applications as key development paths for urban mobility vehicles defined by the European Technology Platform [15]. Moreover, the obtained outputs fulfills the expected results from AutoDrive Project[28]. In this sense, as the presented solutions lay the foundations of driving automation systems among SAE level 2-4, future developments may use this Ph.D. Thesis as a solid starting point to strengthen the current systems with new functionalities, including an expansion of the operational design domain, considering same approaches of robustness, reliability, and scalability, such as:

- **Validation in Automated Driving:** Due to the limited time of this project, some of the verified automated driving functionalities such as vehicle-models-blending trajectory tracking, traffic light response, and positioning fallback strategies, still require to complete the validation process using real testing platforms. Moreover, as statistical validation methods provide the strength to perform objective evaluations, other techniques to generate more reliable interval confidences such as heteroscedastic and non-stationary gaussian process regressions can be employed as more robust methods to noisy experimental data. Futhermore, a conversion of the two-step method to an online validation technique, would considerably improve the proposed approach. On one hand, allowing a credibility estimation of the vehicle dynamics model during run time. On other hand, enabling a parallel evaluation of several decision-making scenarios for a safer and more comfortable driving.

- **Safety and Comfort in Vehicle Motion:** The achievement of ODD enhancements

towards a highly automated driving, is only possible combining the functionalities presented in this work with more complex ones, this provides the ADS an increased versatility to execute more DDT subtasks in urban scenarios, including: 1) an improved real-time path planning, assessing collisions with surrounding objects and/or infrastructure to perform: lane-changing, overtaking maneuvers, accurate docking (for carrying passenger or charging stations); 2) a consideration of the road actors' intention using the perception system data, improving the current on/off-path object verification to an extrapolation of the velocity and heading of objects, this enables the ADS to respond in advance to future behaviors, 3) a cooperative adaptive cruise control for urban driving, making the ADS capable to negotiate with other road actors on intersections and roundabouts. 4) the improvement of trajectory planning and traking executions after manual to automated driving mode trasitions, allowing the ADS to follow to perform reliable lane-keeping maneuvers when high lateral deviations exists.

- **Dynamic Driving Task Fallback:** The redundancy of systems both from hardware and software represents the key to achieve a fully FO ADS. Therefore, the proposed FO architecture and DDT Fallback strategy would be improved with other positioning methods, as using lane detections from perception components (e.g. stereo cameras or LiDARs), allowing the ADS to keep the vehicle on path when satellite positioning fails due to urban sight-of-line obstructions. Moreover, novel DDT fallback approaches can be developed from typical relevant-performance failures on driving scenarios, including, object and event acquisition, vehicle-to-x communications, drive by-wire actuation.

REFERENCES

[1] S. international, "Taxonomy and definitions for terms related to driving automation systems for on-road motor vehicles," *SAE International,(J3016)*, 2018.

[2] M. Viehof and H. Winner, "Research methodology for a new validation concept in vehicle dynamics," *Automotive and Engine Technology*, vol. 3, no. 1-2, pp. 21–27, 2018.

[3] D. González, J. Pérez, V. Milanés, and F. Nashashibi, "A review of motion planning techniques for automated vehicles," *IEEE Transactions on Intelligent Transportation Systems*, vol. 17, no. 4, pp. 1135–1145, 2015.

[4] A. Eskandarian, C. Wu, and C. Sun, "Research advances and challenges of autonomous and connected ground vehicles," *IEEE Transactions on Intelligent Transportation Systems*, 2019.

[5] D. Watzenig and M. Horn, "Introduction to automated driving," in *Automated Driving*, pp. 3–16, Springer, 2017.

[6] S. Riedmaier, T. Ponn, D. Ludwig, B. Schick, and F. Diermeyer, "Survey on scenario-based safety assessment of automated vehicles," *IEEE Access*, vol. 8, pp. 87456–87477, 2020.

[7] D. González, J. Perez, R. Lattarulo, V. Milanés, and F. Nashashibi, "Continuous curvature planning with obstacle avoidance capabilities in urban scenarios," in *17th International IEEE Conference on Intelligent Transportation Systems (ITSC)*, pp. 1430–1435, IEEE, 2014.

[8] A. Avizienis, J.-C. Laprie, B. Randell, and C. Landwehr, "Basic concepts and taxonomy of dependable and secure computing," *IEEE transactions on dependable and secure computing*, vol. 1, no. 1, pp. 11–33, 2004.

[9] J. Y. Wong, *Theory of ground vehicles*. John Wiley & Sons, 2008.

[10] H. Winner, S. Hakuli, and G. Wolf, *Handbuch Fahrerassistenzsysteme: Grundlagen, Komponenten und Systeme für aktive Sicherheit und Komfort: mit 550 Abbildungen und 45 Tabellen*. Springer-Verlag, 2009.

[11] D. Schramm, M. Hiller, and R. Bardini, "Vehicle dynamics: Modeling and simulation," in *Modeling and Simulation*, pp. XXI, 440, Springer-Verlag Berlin Heidelberg, 2018.

[12] E. Kutluay and H. Winner, "Assessment methodology for validation of vehicle dynamics simulations using double lane change maneuver," in *Proceedings of the 2012 Winter Simulation Conference (WSC)*, pp. 1–12, IEEE, 2012.

[13] B. Houska, H. J. Ferreau, and M. Diehl, "Acado toolkit—an open-source framework for automatic control and dynamic optimization," *Optimal Control Applications and Methods*, vol. 32, no. 3, pp. 298–312, 2011.

[14] P. Fancher and Z. Bareket, "Evaluating headway control using range versus range-rate relationships," *Vehicle System Dynamics*, vol. 23, no. 1, pp. 575–596, 1994.

[15] E. W. Group, "Connectivity and automated driving," 2019.

[16] W. H. Organization, "Global status report on road safety 2018: Summary," tech. rep., World Health Organization, 2018.

[17] I. T. Forum, *Road Safety Annual Report 2019*. 2019.

[18] A. S. Mueller, J. B. Cicchino, and D. S. Zuby, "What humanlike errors do autonomous vehicles need to avoid to maximize safety?," 2020.

[19] P. Office, "The european green deal," Dec 2019.

[20] A. Peters, "A quick shift to electric vehicles could drive the green new deal forward," Jun 2019.

[21] H. Igliński and M. Babiak, "Analysis of the potential of autonomous vehicles in reducing the emissions of greenhouse gases in road transport," *Procedia Engineering*, vol. 192, pp. 353 – 358, 2017. 12th international scientific conference of young scientists on sustainable, modern and safe transport.

[22] S. Smith, J. Bellone, S. Bransfield, A. Ingles, G. Noel, E. Reed, M. Yanagisawa, *et al.*, "Benefits estimation framework for automated vehicle operations.," tech. rep., Department of Transportation, 2015.

[23] C. Sessa, F. Pietroni-ISIS, A. Alessandrini, D. Stam, P. Delle Site, C. Holguin-CTL, M. Flament-ERTICO, and S. Polis, "Results on the on-line delphi survey," *CityMobil2*, vol. 27, 2015.

[24] M. Azad, N. Hoseinzadeh, C. Brakewood, C. R. Cherry, and L. D. Han, "Fully autonomous buses: A literature review and future research directions," *Journal of Advanced Transportation*, vol. 2019, 2019.

[25] P. M. Bosch, F. Becker, H. Becker, and K. W. Axhausen, "Cost-based analysis of autonomous mobility services," *Transport Policy*, vol. 64, pp. 76–91, 2018.

[26] J. M. Lutin, "Not if, but when: autonomous driving and the future of transit," *Journal of Public Transportation*, vol. 21, no. 1, p. 10, 2018.

[27] K. Bimbraw, "Autonomous cars: Past, present and future a review of the developments in the last century, the present scenario and the expected future of autonomous vehicle technology," in *2015 12th international conference on informatics in control, automation and robotics (ICINCO)*, vol. 1, pp. 191–198, IEEE, 2015.

[28] R. Coppola and M. Morisio, "Connected car: technologies, issues, future trends," *ACM Computing Surveys (CSUR)*, vol. 49, no. 3, pp. 1–36, 2016.

[29] K. Cardew, "The automatic steering of vehicles: An experimental system fitted to a ds 19 citroen car," *RRL report; LR 340*, 1970.

[30] Y. Ohshima, "Control system for automatic automobile driving," in *Proc. IFAC Tokyo Symposium on Systems Engineering for Control System Design, 1965*, 1965.

[31] S. Tsugawa, "Automated driving systems: Common ground of automobiles and robots," *International Journal of Humanoid Robotics*, vol. 8, no. 01, pp. 1–12, 2011.

[32] C. Thorpe, M. H. Hebert, T. Kanade, and S. A. Shafer, "Vision and navigation for the carnegie-mellon navlab," *IEEE Transactions on Pattern Analysis and Machine Intelligence*, vol. 10, no. 3, pp. 362–373, 1988.

[33] S. E. Shladover, "Path at 20—history and major milestones," *IEEE Transactions on intelligent transportation systems*, vol. 8, no. 4, pp. 584–592, 2007.

[34] S. Tsugawa, "A history of automated highway systems in japan and future issues," in *2008 IEEE International Conference on Vehicular Electronics and Safety*, pp. 2–3, IEEE, 2008.

[35] J. Hellaker, "Prometheus-strategy," in *Vehicle Electronics in the 90's: Proceedings of the International Congress on Transportation Electronics*, pp. 195–199, IEEE, 1990.

[36] R. Gregg, B. Pessaro, *et al.*, "Vehicle assist and automation (vaa) demonstration evaluation report," tech. rep., Federal Transit Administration, 2016.

[37] S. Tsugawa, "An overview on an automated truck platoon within the energy its project," *IFAC Proceedings Volumes*, vol. 46, no. 21, pp. 41–46, 2013.

[38] A. Zlocki, "Automated driving," *Encyclopedia of Automotive Engineering*, pp. 1–16, 2014.

[39] M. Hughes-Cromwick and M. Dickens, "Public transit increases exposure to automated vehicle technology," 2019.

[40] J. Cregger, E. Machek, P. Cahill, *et al.*, "Transit bus automation market assessment," tech. rep., Federal Transit Administration, 2019.

[41] E. W. Group, "Long distance freight transport," 2019.

[42] C. Call, "Freight and logistics in a multimodal context falcon handbook understanding what influences modal choice," 2017.

[43] J. Spears, J. Lutin, Y. Wang, R. Ke, and S. M. Clancy, "Active safety-collision warning pilot in washington state," tech. rep., 2017.

[44] J. Tor, "Ambitious, university-led effort explores mobility technologies," *Nevada Today*, 2017.

[45] Y. Sugimoto and S. Kuzumaki, "Sip-adus: An update on japanese initiatives for automated driving," in *Road Vehicle Automation 5*, pp. 17–26, Springer, 2019.

[46] R. Threlfall, "2020 autonomous vehicles readiness index," *Klynveld Peat Marwick Goerdeler (KPMG) International*, 2020.

[47] M. A. Schreurs and S. D. Steuwer, "Autonomous driving-political, legal, social, and sustainability dimensions," in *Autonomes Fahren*, pp. 151–173, Springer, 2015.

[48] J. Ainsalu, V. Arffman, M. Bellone, M. Ellner, T. Haapamaki, N. Haavisto, E. Josefson, A. Ismailogullari, B. Lee, O. Madland, *et al.*, "State of the art of automated buses," *Sustainability*, vol. 10, no. 9, p. 3118, 2018.

[49] M. A. Nees, "Acceptance of self-driving cars: An examination of idealized versus realistic portrayals with a self-driving car acceptance scale," in *Proceedings of the Human Factors and Ergonomics Society Annual Meeting*, vol. 60, pp. 1449–1453, SAGE Publications Sage CA: Los Angeles, CA, 2016.

[50] J. Berrada, Z. Christoforou, and F. Leurent, "Which business models for autonomous vehicles," in *ITS Europe*, ITS, 2017.

[51] H. W. Coleman and W. G. Steele, *Experimentation, validation, and uncertainty analysis for engineers*. John Wiley & Sons, 2018.

[52] D. K. Pace, "Modeling and simulation verification and validation challenges," *Johns Hopkins APL Technical Digest*, vol. 25, no. 2, pp. 163–172, 2004.

[53] R. G. Sargent, "Verification and validation of simulation models," *Journal of simulation*, vol. 7, no. 1, pp. 12–24, 2013.

[54] H. Jamson, "Curve negotiation in the leeds driving simulator: the role of driver experience," *Engineering in psychology and cognitive ergonomics*, vol. 3, pp. 351–358, 1999.

[55] A. Hoskins and M. El-Gindy, "Technical report: Literature survey on driving simulator validation studies," *International Journal of Heavy Vehicle Systems*, vol. 13, no. 3, pp. 241–252, 2006.

[56] N. A. Kaptein, J. Theeuwes, and R. Van Der Horst, "Driving simulator validity: Some considerations," *Transportation research record*, vol. 1550, no. 1, pp. 30–36, 1996.

[57] T. D. Gillespie, *Fundamentals of vehicle dynamics*, vol. 400. Society of automotive engineers Warrendale, PA, 1992.

[58] A. Sorniotti, P. Barber, and S. De Pinto, "Path tracking for automated driving: A tutorial on control system formulations and ongoing research," in *Automated driving*, pp. 71–140, Springer, 2017.

[59] M. Althoff, "Commonroad: Vehicle models," *Technische niversität München, Garching*, pp. 1–25, 2017.

[60] J.-B. Tomas-Gabarron, E. Egea-Lopez, and J. Garcia-Haro, "Vehicular trajectory optimization for cooperative collision avoidance at high speeds," *IEEE Transactions on ITS*, vol. 14, no. 4, pp. 1930–1941, 2013.

[61] J. M. Snider *et al.*, "Automatic steering methods for autonomous automobile path tracking," *Tech. Rep. CMU-RITR-09-08*, 2009.

[62] S. Thrun, M. Montemerlo, H. Dahlkamp, D. Stavens, A. Aron, J. Diebel, P. Fong, J. Gale, M. Halpenny, G. Hoffmann, *et al.*, "Stanley: The robot that won the darpa grand challenge," *Journal of field Robotics*, vol. 23, no. 9, pp. 661–692, 2006.

[63] N. H. Amer, H. Zamzuri, K. Hudha, and Z. A. Kadir, "Modelling and control strategies in path tracking control for autonomous ground vehicles: a review of state of the art and challenges," *Journal of intelligent & robotic systems*, vol. 86, no. 2, pp. 225–254, 2017.

[64] R. N. Jazar, *Vehicle dynamics: theory and application*. Springer, 2017.

[65] R. Rajamani, *Vehicle dynamics and control*. Springer Science & Business Media, 2011.

[66] Y. Gao, A. Gray, H. E. Tseng, and F. Borrelli, "A tube-based robust nonlinear predictive control approach to semiautonomous ground vehicles," *Vehicle System Dynamics*, vol. 52, no. 6, pp. 802–823, 2014.

[67] G. Schildbach and F. Borrelli, "Scenario model predictive control for lane change assistance on highways," in *2015 IEEE Intelligent Vehicles Symposium (IV)*, pp. 611–616, IEEE, 2015.

[68] A. Liniger, A. Domahidi, and M. Morari, "Optimization-based autonomous racing of 1: 43 scale rc cars," *Optimal Control Applications and Methods*, vol. 36, no. 5, pp. 628–647, 2015.

[69] J. Levinson, J. Askeland, J. Becker, J. Dolson, D. Held, S. Kammel, J. Z. Kolter, D. Langer, O. Pink, V. Pratt, *et al.*, "Towards fully autonomous driving: Systems and algorithms," in *2011 IEEE Intelligent Vehicles Symposium (IV)*, pp. 163–168, IEEE, 2011.

[70] C. E. Beal and J. C. Gerdes, "Model predictive control for vehicle stabilization at the limits of handling," *IEEE Transactions on Control Systems Technology*, vol. 21, no. 4, pp. 1258–1269, 2012.

[71] G. Tagne, R. Talj, and A. Charara, "Design and comparison of robust nonlinear controllers for the lateral dynamics of intelligent vehicles," *IEEE Transactions on Intelligent Transportation Systems*, vol. 17, no. 3, pp. 796–809, 2015.

[72] K. Kritayakirana and J. C. Gerdes, "Autonomous vehicle control at the limits of handling," *International Journal of Vehicle Autonomous Systems*, vol. 10, no. 4, pp. 271–296, 2012.

[73] T. Besselmann and M. Morari, "Autonomous vehicle steering using explicit lpv-mpc," in *2009 ECC*, pp. 2628–2633, IEEE, 2009.

[74] E. Bertolazzi, F. Biral, and M. Da Lio, "Real-time motion planning for multibody systems," *MSD*, vol. 17, no. 2-3, pp. 119–139, 2007.

[75] H. B. Pacejka and R. S. Sharp, "Shear force development by pneumatic tyres in steady state conditions: a review of modelling aspects," *Vehicle system dynamics*, vol. 20, no. 3-4, pp. 121–175, 1991.

[76] J. C. Dixon and S. of Automotive Engineers, "Tires, suspension, and handling," 1996.

[77] E. Fiala, "Lateral forces on rolling pneumatic tires," *Zeitschrift VDI*, vol. 96, no. 29, pp. 973–979, 1954.

[78] H. B. Pacejka and E. Bakker, "The magic formula tyre model," *Vehicle system dynamics*, vol. 21, no. S1, pp. 1–18, 1992.

[79] H. Dugoff, "Tire performance characteristics affecting vehicle response to steering and braking control inputs. final report," tech. rep., 1969.

[80] M. Marcano, J. A. Matute, R. Lattarulo, E. Martí, and J. Pérez, "Low speed longitudinal control algorithms for automated vehicles in simulation and real platforms," *Complexity*, vol. 2018, 2018.

[81] J. Sarabia, J. A. Matute-Peaspan, A. Zubizarreta, *et al.*, "Caracterización de los sistemas de actuación para vehículos altamente automatizados," 2019.

[82] E. Kutluay, *Development and demonstration of a validation methodology for vehicle lateral dynamics simulation models*. VDI-Verlag Dusseldorf, Germany, 2013.

[83] G. J. Heydinger, W. R. Garrott, J. P. Chrstos, and D. A. Guenther, "A methodology for validating vehicle dynamics simulations," *SAE transactions*, pp. 126–146, 1990.

[84] W. R. Garrott, P. A. Grygier, J. P. Chrstos, G. J. Heydinger, K. Salaani, J. G. Howe, and D. A. Guenther, "Methodology for validating the national advanced driving simulator's vehicle dynamics (nadsdyna)," *SAE transactions*, pp. 882–894, 1997.

[85] H. Coleman and F. Stern, "Uncertainties and cfd code validation," 1997.

[86] W. L. Oberkampf and T. G. Trucano, "Verification and validation in computational fluid dynamics," *Progress in aerospace sciences*, vol. 38, no. 3, pp. 209–272, 2002.

[87] C. Roy and W. Oberkampf, "A complete framework for verification, validation, and uncertainty quantification in scientific computing," in *48th AIAA Aerospace Sciences Meeting Including the New Horizons Forum and Aerospace Exposition*, p. 124, 2010.

[88] K. Massow and I. Radusch, "A rapid prototyping environment for cooperative advanced driver assistance systems," *Journal of Advanced Transportation*, vol. 2018, 2018.

[89] S. Rhode, "Non-stationary gaussian process regression applied in validation of vehicle dynamics models," *Engineering Applications of Artificial Intelligence*, vol. 93, p. 103716, 2020.

[90] J. S. Carson, "Model verification and validation," in *Proceedings of the winter simulation conference*, vol. 1, pp. 52–58, IEEE, 2002.

[91] A. M. Law, "How to build valid and credible simulation models," in *2019 Winter Simulation Conference (WSC)*, pp. 1402–1414, IEEE, 2019.

[92] A. M. Law, *Simulation modeling and analysis*, vol. 5. McGraw-Hill New York, 2015.

[93] D. C. Montgomery, *Design and analysis of experiments*. John wiley & sons, 2017.

[94] C. Urmson, J. Anhalt, D. Bagnell, C. Baker, R. Bittner, M. Clark, J. Dolan, D. Duggins, T. Galatali, C. Geyer, *et al.*, "Autonomous driving in urban environments: Boss and the urban challenge," *Journal of Field Robotics*, vol. 25, no. 8, pp. 425–466, 2008.

[95] J. Hasch, E. Topak, R. Schnabel, T. Zwick, R. Weigel, and C. Waldschmidt, "Millimeter-wave technology for automotive radar sensors in the 77 ghz frequency band," *IEEE Transactions on Microwave Theory and Techniques*, vol. 60, no. 3, pp. 845–860, 2012.

[96] R. H. Rasshofer and K. Gresser, "Automotive radar and lidar systems for next generation driver assistance functions.," *Advances in Radio Science*, vol. 3, 2005.

[97] A. Eskandarian, *Handbook of intelligent vehicles*, vol. 2. Springer, 2012.

[98] E. Marti, M. A. de Miguel, F. Garcia, and J. Perez, "A review of sensor technologies for perception in automated driving," *IEEE Intelligent Transportation Systems Magazine*, vol. 11, no. 4, pp. 94–108, 2019.

[99] E. Kaplan and C. Hegarty, *Understanding GPS: principles and applications*. Artech house, 2005.

[100] K. Abboud, H. A. Omar, and W. Zhuang, "Interworking of dsrc and cellular network technologies for v2x communications: A survey," *IEEE transactions on vehicular technology*, vol. 65, no. 12, pp. 9457–9470, 2016.

[101] Z. MacHardy, A. Khan, K. Obana, and S. Iwashina, "V2x access technologies: Regulation, research, and remaining challenges," *IEEE Communications Surveys & Tutorials*, vol. 20, no. 3, pp. 1858–1877, 2018.

[102] D. Gruyer, V. Magnier, K. Hamdi, L. Claussmann, O. Orfila, and A. Rakotonirainy, "Perception, information processing and modeling: Critical stages for autonomous driving applications," *Annual Reviews in Control*, vol. 44, pp. 323–341, 2017.

[103] F. Alam, R. Mehmood, I. Katib, N. N. Albogami, and A. Albeshri, "Data fusion and iot for smart ubiquitous environments: A survey," *IEEE Access*, vol. 5, pp. 9533–9554, 2017.

[104] J. Van Brummelen, M. O'Brien, D. Gruyer, and H. Najjaran, "Autonomous vehicle perception: The technology of today and tomorrow," *Transportation research part C: emerging technologies*, vol. 89, pp. 384–406, 2018.

[105] S. Kuutti, S. Fallah, K. Katsaros, M. Dianati, F. Mccullough, and A. Mouzakitis, "A survey of the state-of-the-art localization techniques and their potentials for autonomous vehicle applications," *IEEE Internet of Things Journal*, vol. 5, no. 2, pp. 829–846, 2018.

[106] T. Liebig, N. Piatkowski, C. Bockermann, and K. Morik, "Dynamic route planning with real-time traffic predictions," *Information Systems*, vol. 64, pp. 258–265, 2017.

[107] H. Bast, D. Delling, A. Goldberg, M. Müller-Hannemann, T. Pajor, P. Sanders, D. Wagner, and R. F. Werneck, "Route planning in transportation networks," in *Algorithm engineering*, pp. 19–80, Springer, 2016.

[108] B. Paden, M. Čáp, S. Z. Yong, D. Yershov, and E. Frazzoli, "A survey of motion planning and control techniques for self-driving urban vehicles," *IEEE Transactions on intelligent vehicles*, vol. 1, no. 1, pp. 33–55, 2016.

[109] J. Guanetti, Y. Kim, and F. Borrelli, "Control of connected and automated vehicles: State of the art and future challenges," *Annual Reviews in Control*, vol. 45, pp. 18–40, 2018.

[110] R. Isermann, R. Schwarz, and S. Stolzl, "Fault-tolerant drive-by-wire systems," *IEEE Control Systems Magazine*, vol. 22, no. 5, pp. 64–81, 2002.

[111] R. K. Jurgen, "Electronic braking, traction, and stability controls, volume 2," tech. rep., SAE Technical Paper, 2006.

[112] M. Bertoluzzo, P. Bolognesi, O. Bruno, G. Buja, A. Landi, and A. Zuccollo, "Drive-by-wire systems for ground vehicles," in *2004 IEEE International Symposium on Industrial Electronics*, vol. 1, pp. 711–716, IEEE, 2004.

[113] G. Castignani, T. Derrmann, R. Frank, and T. Engel, "Driver behavior profiling using smartphones: A low-cost platform for driver monitoring," *IEEE Intelligent Transportation Systems Magazine*, vol. 7, no. 1, pp. 91–102, 2015.

[114] J. Pérez, V. Milanés, T. De Pedro, and L. Vlacic, "Autonomous driving manoeuvres in urban road traffic environment: a study on roundabouts," *IFAC Proceedings Volumes*, vol. 44, no. 1, pp. 13795–13800, 2011.

[115] P. Junietz, W. Wachenfeld, K. Klonecki, and H. Winner, "Evaluation of different approaches to address safety validation of automated driving," in *2018 21st International Conference on Intelligent Transportation Systems (ITSC)*, pp. 491–496, IEEE, 2018.

[116] S. Kitajima, K. Shimono, J. Tajima, J. Antona-Makoshi, and N. Uchida, "Multi-agent traffic simulations to estimate the impact of automated technologies on safety," *Traffic injury prevention*, vol. 20, no. sup1, pp. S58–S64, 2019.

[117] C. Roesener, M. Harth, H. Weber, J. Josten, and L. Eckstein, "Modelling human driver performance for safety assessment of road vehicle automation," in *2018 21st International Conference on Intelligent Transportation Systems (ITSC)*, pp. 735–741, IEEE, 2018.

[118] M. Saraoglu, A. Morozov, and K. Janschek, "Mobatsim: Model-based autonomous traffic simulation framework for fault-error-failure chain analysis," *IFAC-PapersOnLine*, vol. 52, no. 8, pp. 239–244, 2019.

[119] S. Ulbrich, T. Menzel, A. Reschka, F. Schuldt, and M. Maurer, "Defining and substantiating the terms scene, situation, and scenario for automated driving," in *2015 IEEE 18th International Conference on Intelligent Transportation Systems*, pp. 982–988, IEEE, 2015.

[120] T. Menzel, G. Bagschik, and M. Maurer, "Scenarios for development, test and validation of automated vehicles," in *2018 IEEE Intelligent Vehicles Symposium (IV)*, pp. 1821–1827, IEEE, 2018.

[121] G. Bagschik, T. Menzel, and M. Maurer, "Ontology based scene creation for the development of automated vehicles," in *2018 IEEE Intelligent Vehicles Symposium (IV)*, pp. 1813–1820, IEEE, 2018.

[122] M. Wood, P. Robbel, M. Maass, R. Tebbens, M. Meijs, M. Harb, and P. Schlicht, "Safety first for automated driving," *Online verfügbar unter https://www. daimler. com/documents/innovation/other/safety-first-for-automated-driving. pdf, zuletzt geprüft am*, vol. 19, no. 11, p. 2019, 2019.

[123] J.-A. Bolte, A. Bar, D. Lipinski, and T. Fingscheidt, "Towards corner case detection for autonomous driving," in *2019 IEEE Intelligent Vehicles Symposium (IV)*, pp. 438–445, IEEE, 2019.

[124] W. Huang, K. Wang, Y. Lv, and F. Zhu, "Autonomous vehicles testing methods review," in *2016 IEEE 19th International Conference on Intelligent Transportation Systems (ITSC)*, pp. 163–168, IEEE, 2016.

[125] M. Buhren and B. Yang, "Simulation of automotive radar target lists using a novel approach of object representation," in *2006 IEEE Intelligent Vehicles Symposium*, pp. 314–319, IEEE, 2006.

[126] C. Miquet, "New test method for reproducible real-time tests of adas ecus:"vehicle-in-the-loop" connects real-world vehicles with the virtual world," in *5th International Munich Chassis Symposium 2014*, pp. 575–589, Springer, 2014.

[127] N. Arechiga, "Specifying safety of autonomous vehicles in signal temporal logic," in *2019 IEEE Intelligent Vehicles Symposium (IV)*, pp. 58–63, IEEE, 2019.

[128] S. Shalev-Shwartz, S. Shammah, and A. Shashua, "On a formal model of safe and scalable self-driving cars," *arXiv preprint arXiv:1708.06374*, 2017.

[129] N. Aréchiga, S. M. Loos, A. Platzer, and B. H. Krogh, "Using theorem provers to guarantee closed-loop system properties," in *2012 American Control Conference (ACC)*, pp. 3573–3580, IEEE, 2012.

[130] H. Täubig, U. Frese, C. Hertzberg, C. Lüth, S. Mohr, E. Vorobev, and D. Walter, "Guaranteeing functional safety: design for provability and computer-aided verification," *Autonomous Robots*, vol. 32, no. 3, pp. 303–331, 2012.

[131] M. Althoff and J. M. Dolan, "Online verification of automated road vehicles using reachability analysis," *IEEE Transactions on Robotics*, vol. 30, no. 4, pp. 903–918, 2014.

[132] B. Johnson, F. Havlak, H. Kress-Gazit, and M. Campbell, "Experimental evaluation and formal analysis of high-level tasks with dynamic obstacle anticipation on a full-sized autonomous vehicle," *Journal of Field Robotics*, vol. 34, no. 5, pp. 897–911, 2017.

[133] N. Kalra and S. M. Paddock, "Driving to safety: How many miles of driving would it take to demonstrate autonomous vehicle reliability?," *Transportation Research Part A: Policy and Practice*, vol. 94, pp. 182–193, 2016.

[134] N. Kalra, *Challenges and approaches to realizing autonomous vehicle safety*. RAND, 2017.

[135] W. H. K. Wachenfeld, *How stochastic can help to introduce automated driving*. PhD thesis, Technische Universität Darmstadt, 2017.

[136] C. Wang and H. Winner, "Overcoming challenges of validation automated driving and identification of critical scenarios," in *2019 IEEE Intelligent Transportation Systems Conference (ITSC)*, pp. 2639–2644, IEEE, 2019.

[137] J. Ibañez-Guzman, C. Laugier, J.-D. Yoder, and S. Thrun, "Autonomous driving: Context and state-of-the-art," 2012.

[138] C. Katrakazas, M. Quddus, W.-H. Chen, and L. Deka, "Real-time motion planning methods for autonomous on-road driving: State-of-the-art and future research directions," *Transportation Research Part C: Emerging Technologies*, vol. 60, pp. 416–442, 2015.

[139] M. Pivtoraiko, R. A. Knepper, and A. Kelly, "Differentially constrained mobile robot motion planning in state lattices," *Journal of Field Robotics*, vol. 26, no. 3, pp. 308–333, 2009.

[140] A. Artuñedo, J. Villagra, and J. Godoy, "Real-time motion planning approach for automated driving in urban environments," *IEEE Access*, vol. 7, pp. 180039–180053, 2019.

[141] E. W. Dijkstra *et al.*, "A note on two problems in connexion with graphs," *Numerische mathematik*, vol. 1, no. 1, pp. 269–271, 1959.

[142] R. Arnay, N. Morales, A. Morell, J. Hernandez-Aceituno, D. Perea, J. T. Toledo, A. Hamilton, J. J. Sanchez-Medina, and L. Acosta, "Safe and reliable path planning for the autonomous vehicle verdino," *IEEE Intelligent Transportation Systems Magazine*, vol. 8, no. 2, pp. 22–32, 2016.

[143] A. Bacha, C. Bauman, R. Faruque, M. Fleming, C. Terwelp, C. Reinholtz, D. Hong, A. Wicks, T. Alberi, D. Anderson, *et al.*, "Odin: Team victortango's entry in the darpa urban challenge," *Journal of field Robotics*, vol. 25, no. 8, pp. 467–492, 2008.

[144] Q. Li, Z. Zeng, B. Yang, and T. Zhang, "Hierarchical route planning based on taxi gps-trajectories," in *2009 17th International Conference on Geoinformatics*, pp. 1–5, IEEE, 2009.

[145] P. E. Hart, N. J. Nilsson, and B. Raphael, "A formal basis for the heuristic determination of minimum cost paths," *IEEE transactions on Systems Science and Cybernetics*, vol. 4, no. 2, pp. 100–107, 1968.

[146] M. Likhachev, D. I. Ferguson, G. J. Gordon, A. Stentz, and S. Thrun, "Anytime dynamic a*: An anytime, replanning algorithm.," in *ICAPS*, vol. 5, pp. 262–271, 2005.

[147] D. Dolgov, S. Thrun, M. Montemerlo, and J. Diebel, "Path planning for autonomous vehicles in unknown semi-structured environments," *The International Journal of Robotics Research*, vol. 29, no. 5, pp. 485–501, 2010.

[148] T. M. Howard and A. Kelly, "Optimal rough terrain trajectory generation for wheeled mobile robots," *The International Journal of Robotics Research*, vol. 26, no. 2, pp. 141–166, 2007.

[149] J. Ziegler and C. Stiller, "Spatiotemporal state lattices for fast trajectory planning in dynamic on-road driving scenarios," in *2009 IEEE/RSJ International Conference on Intelligent Robots and Systems*, pp. 1879–1884, IEEE, 2009.

[150] M. McNaughton, C. Urmson, J. M. Dolan, and J.-W. Lee, "Motion planning for autonomous driving with a conformal spatiotemporal lattice," in *2011 IEEE International Conference on Robotics and Automation*, pp. 4889–4895, IEEE, 2011.

[151] W. Xu, J. Wei, J. M. Dolan, H. Zhao, and H. Zha, "A real-time motion planner with trajectory optimization for autonomous vehicles," in *2012 IEEE International Conference on Robotics and Automation*, pp. 2061–2067, IEEE, 2012.

[152] T. Gu, J. M. Dolan, and J.-W. Lee, "Automated tactical maneuver discovery, reasoning and trajectory planning for autonomous driving," in *2016 IEEE/RSJ International Conference on Intelligent Robots and Systems (IROS)*, pp. 5474–5480, IEEE, 2016.

[153] X. Li, Z. Sun, D. Cao, Z. He, and Q. Zhu, "Real-time trajectory planning for autonomous urban driving: Framework, algorithms, and verifications," *IEEE/ASME Transactions on mechatronics*, vol. 21, no. 2, pp. 740–753, 2015.

[154] M. Likhachev and D. Ferguson, "Planning long dynamically feasible maneuvers for autonomous vehicles," *The International Journal of Robotics Research*, vol. 28, no. 8, pp. 933–945, 2009.

[155] S. M. LaValle and J. J. Kuffner Jr, "Randomized kinodynamic planning," *The international journal of robotics research*, vol. 20, no. 5, pp. 378–400, 2001.

[156] L. Claussmann, M. Revilloud, D. Gruyer, and S. Glaser, "A review of motion planning for highway autonomous driving," *IEEE Transactions on Intelligent Transportation Systems*, vol. 21, no. 5, pp. 1826–1848, 2019.

[157] Y. Kuwata, J. Teo, G. Fiore, S. Karaman, E. Frazzoli, and J. P. How, "Real-time motion planning with applications to autonomous urban driving," *IEEE Transactions on control systems technology*, vol. 17, no. 5, pp. 1105–1118, 2009.

[158] S. Karaman and E. Frazzoli, "Sampling-based algorithms for optimal motion planning," *The international journal of robotics research*, vol. 30, no. 7, pp. 846–894, 2011.

[159] A. Perez, R. Platt, G. Konidaris, L. Kaelbling, and T. Lozano-Perez, "Lqr-rrt*: Optimal sampling-based motion planning with automatically derived extension heuristics," in *2012 IEEE International Conference on Robotics and Automation*, pp. 2537–2542, IEEE, 2012.

[160] J. D. Gammell, S. S. Srinivasa, and T. D. Barfoot, "Informed rrt*: Optimal sampling-based path planning focused via direct sampling of an admissible ellipsoidal heuristic," in *2014 IEEE/RSJ International Conference on Intelligent Robots and Systems*, pp. 2997–3004, IEEE, 2014.

[161] R. R. Radaelli, C. Badue, M. A. Gonçalves, T. Oliveira-Santos, and A. F. De Souza, "A motion planner for car-like robots based on rapidly-exploring random trees," in *Ibero-American Conference on Artificial Intelligence*, pp. 469–480, Springer, 2014.

[162] M. Du, T. Mei, H. Liang, J. Chen, R. Huang, and P. Zhao, "Drivers' visual behavior-guided rrt motion planner for autonomous on-road driving," *Sensors*, vol. 16, no. 1, p. 102, 2016.

[163] L. E. Dubins, "On curves of minimal length with a constraint on average curvature, and with prescribed initial and terminal positions and tangents," *American Journal of mathematics*, vol. 79, no. 3, pp. 497–516, 1957.

[164] H. Mouhagir, R. Talj, V. Cherfaoui, F. Aioun, and F. Guillemard, "Integrating safety distances with trajectory planning by modifying the occupancy grid for autonomous vehicle navigation," in *2016 IEEE 19th International Conference on Intelligent Transportation Systems (ITSC)*, pp. 1114–1119, IEEE, 2016.

[165] M. Arbitmann, U. Stähli, M. Schorn, and R. Isermann, "Method and device for performing a collision avoidance maneuver," June 26 2012. US Patent 8,209,090.

[166] R. Lattarulo, L. González, E. Martí, J. Matute, M. Marcano, and J. Pérez, "Urban motion planning framework based on n-bézier curves considering comfort and safety," *Journal of Advanced Transportation*, vol. 2018, 2018.

[167] C. Badue, R. Guidolini, R. V. Carneiro, P. Azevedo, V. B. Cardoso, A. Forechi, L. Jesus, R. Berriel, T. M. Paixão, F. Mutz, *et al.*, "Self-driving cars: A survey," *Expert Systems with Applications*, p. 113816, 2020.

[168] T. Gu, J. Snider, J. M. Dolan, and J.-w. Lee, "Focused trajectory planning for autonomous on-road driving," in *2013 IEEE Intelligent Vehicles Symposium (IV)*, pp. 547–552, IEEE, 2013.

[169] J. Ziegler, P. Bender, M. Schreiber, H. Lategahn, T. Strauss, C. Stiller, T. Dang, U. Franke, N. Appenrodt, C. G. Keller, *et al.*, "Making bertha drive—an autonomous journey on a historic route," *IEEE Intelligent transportation systems magazine*, vol. 6, no. 2, pp. 8–20, 2014.

[170] J. Choi, "Kinodynamic motion planning for autonomous vehicles," *International Journal of Advanced Robotic Systems*, vol. 11, no. 6, p. 90, 2014.

[171] R. A. Lattarulo Arias, "Validation of trajectory planning strategies for automated driving under cooperative, urban, and interurban scenarios.," 2019.

[172] E. D. Dickmanns and B. D. Mysliwetz, "Recursive 3-d road and relative ego-state recognition," *IEEE Transactions on Pattern Analysis & Machine Intelligence*, no. 2, pp. 199–213, 1992.

[173] C. J. Taylor, J. Košecká, R. Blasi, and J. Malik, "A comparative study of vision-based lateral control strategies for autonomous highway driving," *The International Journal of Robotics Research*, vol. 18, no. 5, pp. 442–453, 1999.

[174] W. Wang, J. Xi, C. Liu, and X. Li, "Human-centered feed-forward control of a vehicle steering system based on a driver's path-following characteristics," *IEEE transactions on intelligent transportation systems*, vol. 18, no. 6, pp. 1440–1453, 2016.

[175] D. Yang, B. Jacobson, M. Jonasson, and T. J. Gordon, "Closed-loop controller for post-impact vehicle dynamics using individual wheel braking and front axle steering," *International Journal of Vehicle Autonomous Systems*, vol. 12, no. 2, pp. 158–179, 2014.

[176] A. Benine-Neto, S. Scalzi, S. Mammar, and M. Netto, "Dynamic controller for lane keeping and obstacle avoidance assistance system," in *13th International IEEE Conference on Intelligent Transportation Systems*, pp. 1363–1368, IEEE, 2010.

[177] Y. Kanayama, Y. Kimura, F. Miyazaki, and T. Noguchi, "A stable tracking control method for an autonomous mobile robot," in *Proceedings., IEEE International Conference on Robotics and Automation*, pp. 384–389, IEEE, 1990.

[178] Z.-P. JIANGdagger and H. Nijmeijer, "Tracking control of mobile robots: A case study in backstepping," *Automatica*, vol. 33, no. 7, pp. 1393–1399, 1997.

[179] B. d'Andréa Novel, G. Campion, and G. Bastin, "Control of nonholonomic wheeled mobile robots by state feedback linearization," *The International journal of robotics research*, vol. 14, no. 6, pp. 543–559, 1995.

[180] O. Sename, P. Gaspar, and J. Bokor, *Robust control and linear parameter varying approaches: application to vehicle dynamics*, vol. 437. Springer, 2013.

[181] A. Rupp and M. Stolz, "Survey on control schemes for automated driving on highways," in *Automated driving*, pp. 43–69, Springer, 2017.

[182] J. Pérez, V. Milanés, and E. Onieva, "Cascade architecture for lateral control in autonomous vehicles," *IEEE Transactions on Intelligent Transportation Systems*, vol. 12, no. 1, pp. 73–82, 2011.

[183] J. Pérez, V. Milanés, J. Godoy, J. Villagra, and E. Onieva, "Cooperative controllers for highways based on human experience," *Expert Systems with Applications*, vol. 40, no. 4, pp. 1024–1033, 2013.

[184] J. E. Naranjo, C. Gonzalez, R. Garcia, and T. De Pedro, "Lane-change fuzzy control in autonomous vehicles for the overtaking maneuver," *IEEE Transactions on Intelligent Transportation Systems*, vol. 9, no. 3, pp. 438–450, 2008.

[185] E. Onieva, J. E. Naranjo, V. Milanés, J. Alonso, R. García, and J. Pérez, "Automatic lateral control for unmanned vehicles via genetic algorithms," *Applied Soft Computing*, vol. 11, no. 1, pp. 1303–1309, 2011.

[186] C. Hu, R. Wang, F. Yan, and N. Chen, "Should the desired heading in path following of autonomous vehicles be the tangent direction of the desired path?," *IEEE Transactions on Intelligent Transportation Systems*, vol. 16, no. 6, pp. 3084–3094, 2015.

[187] S. Dixit, S. Fallah, U. Montanaro, M. Dianati, A. Stevens, F. Mccullough, and A. Mouzakitis, "Trajectory planning and tracking for autonomous overtaking: State-of-the-art and future prospects," *Annual Reviews in Control*, vol. 45, pp. 76–86, 2018.

[188] L. S. Pontryagin, *Mathematical theory of optimal processes*. Routledge, 2018.

[189] Y. Tassa, N. Mansard, and E. Todorov, "Control-limited differential dynamic programming," in *2014 IEEE International Conference on Robotics and Automation (ICRA)*, pp. 1168–1175, IEEE, 2014.

[190] F. N. Martins, W. C. Celeste, R. Carelli, M. Sarcinelli-Filho, and T. F. Bastos-Filho, "An adaptive dynamic controller for autonomous mobile robot trajectory tracking," *Control Engineering Practice*, vol. 16, no. 11, pp. 1354–1363, 2008.

[191] P. S. Pratama, J. H. Jeong, S. K. Jeong, H. K. Kim, H. S. Kim, T. K. Yeu, S. Hong, and S. B. Kim, "Adaptive backstepping control design for trajectory tracking of automatic guided vehicles," in *AETA 2015: Recent Advances in Electrical Engineering and Related Sciences*, pp. 589–602, Springer, 2016.

[192] X. Li, Z. Wang, J. Zhu, and Q. Chen, "Adaptive tracking control for wheeled mobile robots with unknown skidding," in *2015 IEEE Conference on Control Applications (CCA)*, pp. 1674–1679, IEEE, 2015.

[193] N. Hovakimyan and C. Cao, *L1 Adaptive Control Theory: Guaranteed Robustness with Fast Adaptation*. SIAM, 2010.

[194] C. Wu, X. Guo, B. Yang, X. Pei, and S. Guo, "Hydraulic retarder torque control for heavy duty vehicle longitudinal control," *International Journal of Heavy Vehicle Systems*, vol. 26, no. 6, pp. 854–871, 2019.

[195] A. T. Azar and Q. Zhu, *Advances and applications in sliding mode control systems*. Springer, 2015.

[196] H. Aithal and S. Janardhanan, "Trajectory tracking of two wheeled mobile robot using higher order sliding mode control," in *2013 International Conference on Control, Computing, Communication and Materials (ICCCCM)*, pp. 1–4, IEEE, 2013.

[197] J.-Y. Wang and M. Tomizuka, "Gain-scheduled h_∞ loop-shaping controller for automated guidance of tractor-semitrailer combination vehicles," in *Proceedings of the 2000 American Control Conference. ACC (IEEE Cat. No. 00CH36334)*, vol. 3, pp. 2033–2037, IEEE, 2000.

[198] J. B. Rawlings and D. Q. Mayne, *Model predictive control: Theory and design*. Nob Hill Pub., 2009.

[199] S. Li, K. Li, R. Rajamani, and J. Wang, "Model predictive multi-objective vehicular adaptive cruise control," *IEEE Transactions on Control Systems Technology*, vol. 19, no. 3, pp. 556–566, 2010.

[200] P. Shakouri, A. Ordys, and M. R. Askari, "Adaptive cruise control with stop&go function using the state-dependent nonlinear model predictive control approach," *ISA transactions*, vol. 51, no. 5, pp. 622–631, 2012.

[201] S. Di Cairano, H. E. Tseng, D. Bernardini, and A. Bemporad, "Vehicle yaw stability control by coordinated active front steering and differential braking in the tire sideslip angles domain," *IEEE Transactions on Control Systems Technology*, vol. 21, no. 4, pp. 1236–1248, 2012.

[202] H. Park and J. C. Gerdes, "Optimal tire force allocation for trajectory tracking with an over-actuated vehicle," in *2015 IEEE Intelligent Vehicles Symposium (IV)*, pp. 1032–1037, IEEE, 2015.

[203] P. Falcone, F. Borrelli, H. E. Tseng, J. Asgari, and D. Hrovat, "Linear time-varying model predictive control and its application to active steering systems: Stability analysis and experimental validation," *International Journal of Robust and Nonlinear Control: IFAC-Affiliated Journal*, vol. 18, no. 8, pp. 862–875, 2008.

[204] M. Diehl, H. J. Ferreau, and N. Haverbeke, "Efficient numerical methods for nonlinear mpc and moving horizon estimation," in *Nonlinear model predictive control*, pp. 391–417, Springer, 2009.

[205] P. Falcone, M. Tufo, F. Borrelli, J. Asgari, and H. E. Tseng, "A linear time varying model predictive control approach to the integrated vehicle dynamics control problem in autonomous systems," in *2007 46th IEEE Conference on Decision and Control*, pp. 2980–2985, IEEE, 2007.

[206] A. Ollero and O. Amidi, "Predictive path tracking of mobile robots. application to the cmu navlab," in *Proceedings of 5th International Conference on Advanced Robotics, Robots in Unstructured Environments, ICAR*, vol. 91, pp. 1081–1086, 1991.

[207] G. V. Raffo, G. K. Gomes, J. E. Normey-Rico, C. R. Kelber, and L. B. Becker, "A predictive controller for autonomous vehicle path tracking," *IEEE transactions on intelligent transportation systems*, vol. 10, no. 1, pp. 92–102, 2009.

[208] M. Brown, J. Funke, S. Erlien, and J. C. Gerdes, "Safe driving envelopes for path tracking in autonomous vehicles," *Control Engineering Practice*, vol. 61, pp. 307–316, 2017.

[209] E. Kim, J. Kim, and M. Sunwoo, "Model predictive control strategy for smooth path tracking of autonomous vehicles with steering actuator dynamics," *International Journal of Automotive Technology*, vol. 15, no. 7, pp. 1155–1164, 2014.

[210] P. Falcone, F. Borrelli, J. Asgari, H. E. Tseng, and D. Hrovat, "Predictive active steering control for autonomous vehicle systems," *IEEE Transactions on control systems technology*, vol. 15, no. 3, pp. 566–580, 2007.

[211] S.-H. Lee and C. C. Chung, "Multilevel approximate model predictive control and its application to autonomous vehicle active steering," in *52nd IEEE Conference on Decision and Control*, pp. 5746–5751, IEEE, 2013.

[212] J. Kong, M. Pfeiffer, G. Schildbach, and F. Borrelli, "Kinematic and dynamic vehicle models for autonomous driving control design," in *2015 IEEE Intelligent Vehicles Symposium (IV)*, pp. 1094–1099, IEEE, 2015.

[213] P. Polack, F. Altché, B. d'Andréa Novel, and A. de La Fortelle, "The kinematic bicycle model: A consistent model for planning feasible trajectories for autonomous vehicles?," in *2017 IEEE Intelligent Vehicles Symposium (IV)*, pp. 812–818, IEEE, 2017.

[214] C. Gold, D. Damböck, L. Lorenz, and K. Bengler, ""take over!" how long does it take to get the driver back into the loop?," in *Proceedings of the human factors and ergonomics society annual meeting*, vol. 57, pp. 1938–1942, Sage Publications Sage CA: Los Angeles, CA, 2013.

[215] J. Radlmayr, C. Gold, L. Lorenz, M. Farid, and K. Bengler, "How traffic situations and non-driving related tasks affect the take-over quality in highly automated driving," in *Proceedings of the human factors and ergonomics society annual meeting*, vol. 58, pp. 2063–2067, Sage Publications Sage CA: Los Angeles, CA, 2014.

[216] M. Marcano, S. Díaz, J. Pérez, and E. Irigoyen, "A review of shared control for automated vehicles: Theory and applications," *IEEE Transactions on Human-Machine Systems*, pp. 1–17, 2020.

[217] K. Zeeb, A. Buchner, and M. Schrauf, "Is take-over time all that matters? the impact of visual-cognitive load on driver take-over quality after conditionally automated driving," *Accident Analysis & Prevention*, vol. 92, pp. 230–239, 2016.

[218] Y. Emzivat, J. Ibanez-Guzman, P. Martinet, and O. H. Roux, "Dynamic driving task fallback for an automated driving system whose ability to monitor the driving environment has been compromised," in *2017 IEEE Intelligent Vehicles Symposium (IV)*, pp. 1841–1847, IEEE, 2017.

[219] J. Yu and F. Luo, "Fallback strategy for level 4+ automated driving system," in *2019 IEEE Intelligent Transportation Systems Conference (ITSC)*, pp. 156–162, IEEE, 2019.

[220] C. Fernandez, D. Fernandez-Llorca, and M. A. Sotelo, "A hybrid vision-map method for urban road detection," *Journal of Advanced Transportation*, vol. 2017, 2017.

[221] W. Xue, B. Yang, T. Kaizuka, and K. Nakano, "A fallback approach for an automated vehicle encountering sensor failure in monitoring environment," in *2018 IEEE Intelligent Vehicles Symposium (IV)*, pp. 1807–1812, IEEE, 2018.

[222] W. Xue, R. Zheng, B. Yang, Z. Wang, T. Kaizuka, and K. Nakano, "An adaptive model predictive approach for automated vehicle control in fallback procedure based on virtual vehicle scheme," *Journal of Intelligent and Connected Vehicles*, 2019.

[223] S. Grubmüller, G. Stettinger, M. Á. Sotelo, and D. Watzenig, "Fault-tolerant environmental perception architecture for robust automated driving," in *2019 IEEE International Conference on Connected Vehicles and Expo (ICCVE)*, pp. 1–6, IEEE, 2019.

[224] J. Kabzan, M. d. l. I. Valls, V. Reijgwart, H. F. C. Hendrikx, C. Ehmke, M. Prajapat, A. Bühler, N. Gosala, M. Gupta, R. Sivanesan, *et al.*, "Amz driverless: The full autonomous racing system," *arXiv preprint arXiv:1905.05150*, 2019.

[225] M. Ruf, J. R. Ziehn, D. Willersinn, B. Rosenhahny, J. Beyerer, and H. Gotzig, "Global trajectory optimization on multilane roads," in *2015 IEEE 18th International Conference on Intelligent Transportation Systems*, pp. 1908–1914, IEEE, 2015.

[226] L. Svensson, L. Masson, N. Mohan, E. Ward, A. P. Brenden, L. Feng, and M. Törngren, "Safe stop trajectory planning for highly automated vehicles: an optimal control problem formulation," in *2018 IEEE Intelligent Vehicles Symposium (IV)*, pp. 517–522, IEEE, 2018.

[227] J.-w. Lee, N. K. Moshchuk, and S.-K. Chen, "Lane centering fail-safe control using differential braking," Mar. 11 2014. US Patent 8,670,903.

[228] A. Tengg and M. Stolz, "A safety gateway for autonomous driving demonstrator vehicles," in *2020 IEEE 92nd Vehicular Technology Conference*, pp. 1–8, IEEE, 2020.

[229] S. R. Venkita, B. Boulkroune, A. Mishra, and E. van Nunen, "A fault tolerant lateral control strategy for an autonomous four wheel driven electric vehicle," in *2020 IEEE Intelligent Vehicles Symposium (IV)*, IEEE, 2020.

[230] U. P. Mudalige, "Fail-safe speed profiles for cooperative autonomous vehicles," Mar. 18 2014. US Patent 8,676,466.

[231] N. An, J. Mittag, and H. Hartenstein, "Designing fail-safe and traffic efficient 802.11 p-based rear-end collision avoidance," in *2014 IEEE Vehicular Networking Conference (VNC)*, pp. 9–16, IEEE, 2014.

[232] A. Kohn, M. Käßmeyer, R. Schneider, A. Roger, C. Stellwag, and A. Herkersdorf, "Fail-operational in safety-related automotive multi-core systems," in *10th IEEE International Symposium on Industrial Embedded Systems (SIES)*, pp. 1–4, IEEE, 2015.

[233] M. Campbell, M. Egerstedt, J. P. How, and R. M. Murray, "Autonomous driving in urban environments: approaches, lessons and challenges," *Philosophical Transactions of the Royal Society A: Mathematical, Physical and Engineering Sciences*, vol. 368, no. 1928, pp. 4649–4672, 2010.

[234] W. L. Oberkampf and C. J. Roy, *Verification and validation in scientific computing*. Cambridge University Press, 2010.

[235] E. Kutluay and H. Winner, "Validation of vehicle dynamics simulation models–a review," *Vehicle System Dynamics*, vol. 52, no. 2, pp. 186–200, 2014.

[236] R. Pastorino, D. Dopico, E. Sanjurjo, and M. Á. Naya, "Validation of a multibody model for an x-by-wire vehicle prototype through field testing," in *Proceedings of the Multibody Dynamics 2011, ECCOMAS Thematic Conference*, pp. 144–145, 2011.

[237] H. Ansoff and R. Hayes, "Roles of models in corporation decision making," *Operational Research*, vol. 72, 1973.

[238] G. J. Heydinger, M. Salaani, W. Garrott, and P. Grygier, "Vehicle dynamics modelling for the national advanced driving simulator," *Proceedings of the institution of mechanical engineers, part D: journal of automobile engineering*, vol. 216, no. 4, pp. 307–318, 2002.

[239] J. P. Chrstos and P. A. Grygier, "Experimental testing of a 1994 ford taurus for nadsdyna validation," *SAE transactions*, pp. 895–908, 1997.

[240] R. Pastorino, E. Sanjurjo, A. Luaces, M. A. Naya, W. Desmet, and J. Cuadrado, "Validation of a real-time multibody model for an x-by-wire vehicle prototype through field testing," *Journal of Computational and Nonlinear Dynamics*, vol. 10, no. 3, 2015.

[241] W. Pan and Y. E. Papelis, "Real-time dynamic simulation of vehicles with electronic stability control: modelling and validation," *International Journal of Vehicle Systems Modelling and Testing*, vol. 1, no. 1-3, pp. 143–167, 2005.

[242] K.-U. Henning and O. Sawodny, "Vehicle dynamics modelling and validation for online applications and controller synthesis," *Mechatronics*, vol. 39, pp. 113–126, 2016.

[243] M. Batra, J. McPhee, and N. L. Azad, "Parameter identification for a longitudinal dynamics model based on road tests of an electric vehicle," in *International Design Engineering Technical Conferences and Computers and Information in Engineering Conference*, vol. 50138, p. V003T01A026, American Society of Mechanical Engineers, 2016.

[244] A. Pena, I. Iglesias, J. Valera, and A. Martin, "Development and validation of dynacar rt software, a new integrated solution for design of electric and hybrid vehicles," *EVS26 Los Angeles*, vol. 26, pp. 1–7, 2012.

[245] A. Daniel, "Suspension design for uniti, a lightweight urban electric vehicle," 2018.

[246] J. C. Gerdes and J. K. Hedrick, "Brake system modeling for simulation and control," 1999.

[247] A. Kiruthika, A. A. Rajan, and P. Rajalakshmi, "Mathematical modelling and speed control of a sensored brushless dc motor using intelligent controller," in *2013 IEEE international conference on emerging trends in computing, communication and nanotechnology (ICECCN)*, pp. 211–216, IEEE, 2013.

[248] J. Xie, F. Nashashibi, M. Parent, and O. G. Favrot, "A real-time robust global localization for autonomous mobile robots in large environments," in *2010 11th International Conference on Control Automation Robotics & Vision*, pp. 1397–1402, IEEE, 2010.

[249] J. Schmid, M. Schneider, A. Höß, and B. Schuller, "A comparison of ai-based throughput prediction for cellular vehicle-to-server communication," in *2019 15th International Wireless Communications & Mobile Computing Conference (IWCMC)*, pp. 471–476, IEEE, 2019.

[250] C. Fernández, J. Muñoz-Bulnes, D. Fernández-Llorca, I. Parra, I. Garcia-Daza, R. Izquierdo, and M. Á. Sotelo, "High-level interpretation of urban road maps fusing deep learning-based pixelwise scene segmentation and digital navigation maps," *Journal of Advanced Transportation*, vol. 2018, 2018.

[251] R. Q. Mínguez, I. P. Alonso, D. Fernández-Llorca, and M. Á. Sotelo, "Pedestrian path, pose, and intention prediction through gaussian process dynamical models and pedestrian activity recognition," *IEEE Transactions on Intelligent Transportation Systems*, vol. 20, no. 5, pp. 1803–1814, 2018.

[252] R. Izquierdo, A. Quintanar, I. Parra, D. Fernández-Llorca, and M. Sotelo, "The prevention dataset: a novel benchmark for prediction of vehicles intentions," in *2019 IEEE Intelligent Transportation Systems Conference (ITSC)*, pp. 3114–3121, IEEE, 2019.

[253] A. Hernández, S. Woo, H. Corrales, I. Parra, E. Kim, D. Llorca, and M. Sotelo, "3d-deep: 3-dimensional deep-learning based on elevation patterns forroad scene interpretation," *arXiv preprint arXiv:2009.00330*, 2020.

[254] O. Kirovskii and V. Gorelov, "Driver assistance systems: analysis, tests and the safety case. iso 26262 and iso pas 21448," in *IOP Conference Series: Materials Science and Engineering*, vol. 534, p. 012019, IOP Publishing, 2019.

[255] S. McLaughlin, J. Hankey, and T. Dingus, "Driver measurement: methods and applications," in *International Conference on Engineering Psychology and Cognitive Ergonomics*, pp. 404–413, Springer, 2009.

[256] V. Punzo, M. T. Borzacchiello, and B. Ciuffo, "Estimation of vehicle trajectories from observed discrete positions and next-generation simulation program (ngsim) data," in *TRB 88 annual meeting. Washington DC, USA*, pp. 11–15, Citeseer, 2009.

[257] B. C. Fabien, "dsoa: The implementation of a dynamic system optimization algorithm," *Optimal Control Applications and Methods*, vol. 31, no. 3, pp. 231–247, 2010.

[258] L. L. Simon, Z. K. Nagy, and K. Hungerbuehler, "Swelling constrained control of an industrial batch reactor using a dedicated nmpc environment: Optcon," in *Nonlinear model predictive control*, pp. 531–539, Springer, 2009.

[259] A. Romanenko, N. Pedrosa, J. Leal, and L. Santos, "A linux based nonlinear model predictive control framework," *II Seminario de Aplicaciones Industriales de Control Avanzado*, p. 229, 2007.

[260] A. Carvalho, S. Lefévre, G. Schildbach, J. Kong, and F. Borrelli, "Automated driving: The role of forecasts and uncertainty—a control perspective," *European Journal of Control*, vol. 24, pp. 14–32, 2015.

[261] M. A. Sotelo, "Lateral control strategy for autonomous steering of ackerman-like vehicles," *Robotics and Autonomous Systems*, vol. 45, no. 3-4, pp. 223–233, 2003.

[262] R. Ritschel, F. Schrödel, J. Hädrich, and J. Jäkel, "Nonlinear model predictive path-following control for highly automated driving," *IFAC-PapersOnLine*, vol. 52, no. 8, pp. 350–355, 2019.

[263] A. M. Carvalho, *Predictive Control under Uncertainty for Safe Autonomous Driving: Integrating Data-Driven Forecasts with Control Design*. PhD thesis, UC Berkeley, 2016.

[264] C. Sierra, E. Tseng, A. Jain, and H. Peng, "Cornering stiffness estimation based on vehicle lateral dynamics," *Vehicle System Dynamics*, vol. 44, no. sup1, pp. 24–38, 2006.

[265] O. Marques, *Practical image and video processing using MATLAB*. John Wiley & Sons, 2011.

[266] M. Alonso Raposo, B. Ciuffo, F. Ardente, J. Aurambout, G. Baldini, R. Braun, and I. Vandecasteele, "The future of road transport—implications of automated, connected, low-carbon and shared mobility," *Publications Office of the European Union, Luxembourg*, 2019.

[267] D. F. Llorca, V. Milanés, I. P. Alonso, M. Gavilán, I. G. Daza, J. Pérez, and M. Á. Sotelo, "Autonomous pedestrian collision avoidance using a fuzzy steering controller," *IEEE Transactions on Intelligent Transportation Systems*, vol. 12, no. 2, pp. 390–401, 2011.

[268] N. Bernini, M. Bertozzi, L. Castangia, M. Patander, and M. Sabbatelli, "Real-time obstacle detection using stereo vision for autonomous ground vehicles: A survey," in *17th International IEEE Conference on Intelligent Transportation Systems (ITSC)*, pp. 873–878, IEEE, 2014.

[269] A. B. Hillel, R. Lerner, D. Levi, and G. Raz, "Recent progress in road and lane detection: a survey," *Machine vision and applications*, vol. 25, no. 3, pp. 727–745, 2014.

[270] V. Milanés, J. E. Naranjo, C. González, J. Alonso, and T. de Pedro, "Autonomous vehicle based in cooperative gps and inertial systems," *Robotica*, vol. 26, no. 5, p. 627–633, 2008.

[271] H. Guan, W. Yan, Y. Yu, L. Zhong, and D. Li, "Robust traffic-sign detection and classification using mobile lidar data with digital images," *IEEE Journal of Selected Topics in Applied Earth Observations and Remote Sensing*, vol. 11, no. 5, pp. 1715–1724, 2018.

[272] F. Castanedo, "A review of data fusion techniques," *The Scientific World Journal*, vol. 2013, 2013.

[273] P. Balzer, T. Trautmann, and O. Michler, "Epe and speed adaptive extended kalman filter for vehicle position and attitude estimation with low cost gnss and imu sensors," in *2014 11th International Conference on Informatics in Control, Automation and Robotics (ICINCO)*, vol. 1, pp. 649–656, IEEE, 2014.

[274] F. De Ponte Müller, "Survey on ranging sensors and cooperative techniques for relative positioning of vehicles," *Sensors*, vol. 17, no. 2, 2017.

[275] S. Shladover and R. Bishop, "Road transport automation as a public-private enterprise," *White Paper*, vol. 1, pp. 14–15, 2015.

[276] E. Thorn, S. C. Kimmel, M. Chaka, B. A. Hamilton, *et al.*, "A framework for automated driving system testable cases and scenarios," tech. rep., United States. Department of Transportation. National Highway Traffic Safety . . . , 2018.

[277] L.-Y. Hsu and T.-L. Chen, "Vehicle dynamic prediction systems with on-line identification of vehicle parameters and road conditions," *Sensors*, vol. 12, no. 11, pp. 15778–15800, 2012.

[278] G. Welch, G. Bishop, *et al.*, "An introduction to the kalman filter," 1995.

[279] J. Villagra, V. Milanés, J. Pérez, and J. Godoy, "Smooth path and speed planning for an automated public transport vehicle," *Robotics and Autonomous Systems*, vol. 60, no. 2, pp. 252–265, 2012.